

Lincoln University Digital Thesis

Copyright Statement

The digital copy of this thesis is protected by the Copyright Act 1994 (New Zealand).

This thesis may be consulted by you, provided you comply with the provisions of the Act and the following conditions of use:

- you will use the copy only for the purposes of research or private study
- you will recognise the author's right to be identified as the author of the thesis and due acknowledgement will be made to the author where appropriate
- you will obtain the author's permission before publishing any material from the thesis.

Two reduction methods to simplify complex ODE mathematical models of biological networks and a case study: The G1/S checkpoint/DNA-damage signal transduction pathways

A thesis
submitted in partial fulfilment
of the requirements for the Degree of
Doctor of Philosophy in Computer Science

at
Lincoln University
by
Mutaz Khazaaleh

Lincoln University

2018

Abstract of a thesis submitted in partial fulfilment of the requirements for the Degree of Doctor of Philosophy in Computer Science

Two reduction methods to simplify complex ODE mathematical models of biological networks and a case study: The G1/S checkpoint/DNA-damage signal transduction pathways

by

Mutaz Khazaaleh

Model reduction is a hot topic in studies of biological systems. By reducing the complexity of detailed models through finding important elements, developing multi-level models and keeping the soul (biological meaning) of the model, model reduction can help answer many important questions raised about these systems.

This thesis addressed several issues related to complex systems, complexity, biological systems complexity and the different reduction methods used to simplify biological models. It gives a brief review of the biological background of the regulation of the cell cycle and proposes two reduction methods to simplify the corresponding complex ODE mathematical models. The first method is based on a hierarchical representation and lumping approach, and the Second method uses a time windows for identifying active and inactive periods of a system and logical models.

For the purpose of the current study, biological network model reduction is defined as any method designed to reproduce the original model through a set of smaller models that collectively produce the same behaviour as the original model. It does this, by reducing one or more dimensions of the biological network model's complexity (*i.e., reducing the number of species, number of reactions or model run time*).

In the first reduction method, based on hierarchical representation and a lumping approach, we used G1/S checkpoint pathway as a case study to present this reduction method. This consisted of two parts; the first part reorganised the biological network as a hierarchy (levels) based on the protein binding relations, and this allowed us to model the biological network with different levels of abstraction. The

second part applied different levels (level 1, 2, 3) of lumping the species together depending on the level of the hierarchy.

We propose and simulate the reduced models for level-1, level-2 and level-3 of lumping for the G1/S checkpoint pathway and evaluate the biological plausibility of the proposed method by comparing the results with the original (ODE) model of Iwamoto et al. (2011). The results of the G1/S checkpoint pathway with or without DNA-damage for reduced models of level-1, level-2 and level-3 of lumping have agreed and are consistent with the original model results and with biological experiments Iwamoto et al. (2011). Therefore, the reduced model (level-1) can be used to evaluate the effects of DNA damage on G1 progression. It is suggested that the proposed method is suitable to reduce complex biological networks. Moreover, the reduced model is more efficient to run and generate solutions than the original ODE model.

In second reduction method we used time windows and logical models. Time windows were used to identify regions of slow activity such as gene expression, fast activity such as protein signalling and no activity. In general, most knowledge about regulatory and signalling networks is of a qualitative nature, which allows these networks to be represented by logical models, where the state of a molecule is either 0 (inactive) or 1 (active). These simpler models have many advantages, such as ; they do not require kinetic parameters and are able to capture the essential behaviour of a network; however, they are not able to reproduce detailed time courses for the concentration levels of molecules.

Nowadays, however, experiments yield more and more quantitative data, so many quantitative models have been built and most of these models are very complex. An obvious question, therefore, is how to reduce complex quantitative models so they can be used to explain and predict the outcome of these experiments.

Here, we present a way of reducing complex quantitative models into logical (Boolean) models, where the use of time windows allows a reduction in time complexity and logical representation allows to do so without kinetic parameters in the model. The method is standardised and can readily be applied to complex quantitative models. Moreover, we discuss and generalise existing theoretical results on the relations between the Boolean and continuous models. As a case study, a continuous ODE model is reduced into a logical model describing the G1/S checkpoint with and without DNA damage. We discuss how this model can explain and predict the G1/S checkpoint behaviour with DNA damage, including oscillations for some molecules and the cell fate. This shows the reduced model is still useful for obtaining biological insights and is easier to run and analyse.

This new method greatly helps to simplify complex quantitative models into simpler models and can facilitate the interactions between the modelling and the experiments. Moreover, it helps researchers

and those who build models to focus on understanding and representing system behaviour rather than on determining the values for the kinetic parameters.

While the analysis presented was in terms of biological networks, it should be noted that the specific example used was chosen to explain our two reduction methods. However, the two methods used could be more generally applied to the reduction of ODEs of biological systems and, even more generally, to most complex systems. Relaxing the struggle with the complexity of mathematical models is possible and the proposed reduction methods have the potential to make an impact across many fields of biomedical research.

Keywords: Biological systems, biological networks, complexity, model reduction, hierarchy of protein complex formation (abstraction), Ordinary Differential Equations (ODEs), time windows, Boolean model, G1/S checkpoint, DNA damage.

Acknowledgements

First of all, all praise and thanks are due to Allah, the Almighty, having made everything possible by giving me strength and patience to accomplish this work. I must acknowledge and thank the Almighty Allah for blessing and grace.

I would like to thank my supervisor, Professor Sandhya Samarasinghe, for the opportunity to undertake this thesis, and for her expert guidance and support in all aspects and stages of research. Without her supervision this research would not have been possible. I would like to thank my co-supervisor, Professor Don Kulasiri, for his expert help and support.

To the staff at Lincoln University, thank you. This University offered me services and all the facilities I needed during my PhD thesis. The staff were very friendly and helpful. Special thanks also go to Caitriona Cameron at Teaching and Learning Services.

I would like to thank Mom and Dad. Thanks for your love and support. And for teaching me to finish what I start.

In addition, I want to direct many thanks to my brothers, sisters and friends, especially Professor Abdel-Rahman Abu-Melhim, for their continuous encouragement and support. Last but not least, great thanks go to my wife, for her love, patience, interest in my work and support. I would like to include my beautiful children (Karam, Jood, Hala, Seraj and Murad) in this acknowledgement. Finally, I dedicate this work to my father, who is a great man.

Thank you all!

Mutaz Khazaaleh

July, 2018

Table of Contents

Abstract	ii
Acknowledgements	v
Table of Contents	vi
List of Tables	x
List of Figures	xii
Abbreviations	xvi
Chapter 1 Introduction	1
1.1 General Introduction	1
1.2 Overview	3
1.3 Goals and Objectives	4
1.4 Thesis Structure	8
Chapter 2 Literature Review	9
2.1 Complex Systems and Complexity	9
2.2 Model Reduction	10
2.3 Complexity of Biological Networks	14
2.4 Mathematical Models of Biological Systems	20
2.4.1 Ordinary Differential Equations (ODEs)	23
2.4.2 Delay Differential Equations (DDEs).....	23
2.4.3 Partial Differential Equations (PDEs).....	23
2.4.4 Agent-based Models (ABMs)	23
2.4.5 Stochastic Differential Equations (SDEs).....	24
2.5 Reduction Methods for Biological Systems	25
2.6 Summary of the Chapter.....	32
Chapter 3 Biological Background	35
3.1 The Cell: General Review	35
3.2 The Cell Cycle	38
3.2.1 Regulation of the Cell Cycle	41
3.2.2 DNA Damage and Cancer	44
3.2.3 G1/S Checkpoint.....	45
3.2.3.1 G1/S Checkpoint without DNA Damage	45
3.2.3.2 G1/S Checkpoint with DNA Damage	46
3.3 G1/S Checkpoint Modelling	47
3.4 The DNA Damage Signalling Pathway and Whole Cell Cycle Regulation (Integrated Between G1/S and G2/M) Model Iwamoto et al. (2011).....	51
Chapter 4 Model Reduction Based on a Hierarchical Representation and Lumping	58
4.1 The DNA Damage Signalling Pathway Integrated with G1/S Checkpoint Pathway as the Base Model	58
4.2 Methodology	64

4.2.1	Understand the Protein Interactions Involved in the Biological Network.....	64
4.2.2	Representing the Biological Network as a Hierarchical Representation	65
4.2.3	Determine the Key Elements in the Biological Network and Find the Number of Acceptable Key Elements that can be Lumped (AKEL)	66
4.2.4	Introduce Different Levels of Lumping Formation.....	66
4.2.4.1	Determine the Lumps at each Level.....	66
4.2.4.2	Rewrite the Equations	70
4.3	Model Reduction Method	72
4.3.1	Understand the Protein Interactions Involved in the Base Model	72
4.3.2	Representing the Biological Network as a Hierarchical Representation	79
4.3.3	Determine the Key Elements in the Biological Network and Find the Number of Acceptable Key Elements that can be Lumped (AKEL)	82
4.3.4	Introduce Different Levels of Lumping Formation	84
4.3.4.1	Determine the Lumps at Each Level	84
4.3.4.2	Rewrite the Equations	90
Chapter 5 Results and Discussion		92
5.1	Element Behaviour	92
5.1.1	Comparison of the Reduced Model (level-1) with the Base Model.....	92
5.1.1.1	Reduced Model (level-1) Simulation without DNA Damage	92
5.1.1.2	Reduced Model (level-1) Simulation with DNA Damage.....	105
5.1.2	Comparison of the Reduced Model (level-2) with the Base Model.....	108
5.1.2.1	Reduced Model (level-2) Simulation without DNA Damage	108
5.1.2.2	Reduced Model (level-2) Simulation with DNA Damage.....	111
5.1.3	Comparison of the Reduced Model (level-3) with the Base Model.....	113
5.1.3.1	Reduced Model (level-3) Simulation without DNA Damage	113
5.1.3.2	Reduced Model (level-3) Simulation with DNA Damage.....	116
5.2	Evaluation Reduced Model using the Root Mean Squared Error (RMSE) and the Root Mean Squared Percentage Error (RMSPE)	118
5.3	Comparison of the Reduced models (level-1), (level-2) and (level-3) with the Base Model from a Computational Viewpoint	127
5.4	Summary of the Chapter.....	130
Chapter 6 Using Time Windows and Logical Representation to Reduce the G1/S Checkpoint Pathway with the DNA Damage		131
6.1	Summary	131
6.2	Introduction and Literature Review	132
6.3	Research Methodology.....	135
6.3.1	Understand the Protein Interactions Involved in the System.....	135
6.3.2	Divide the Dynamics of the System into Time Windows (Active Time Windows, Steady or Frozen Time Windows)	135
6.3.3	Determine the Key Elements in Each Active Time Window	136
6.3.4	Building Logical Model for each Active Time Window	138
6.4	Results and Discussion	140
6.5	Conclusions	143
Chapter 7 Conclusions and Future Directions.....		144
7.1	General Overview	144
7.2	Contributions	145

7.3	Future Directions	147
7.4	Conclusions	147

Appendix A Initial conditions, kinetic parameters and mass balance equations of the ODE mathematical model for the DNA damage signalling pathway and whole cell cycle regulation149

A.1	Initial conditions of the mathematical model (Iwamoto et al., 2011).....	149
A.2	Kinetic parameters of the ODE mathematical model (Iwamoto et al., 2011)	150
A.3	Mass balance equations of the ODE mathematical model (Iwamoto et al., 2011).....	151

Appendix B Initial conditions, kinetic parameters and mass balance equations of the ODE mathematical model for the DNA damage signalling pathway and G1/S checkpoint used as the basis for the current study153

B.1	Initial conditions of the mathematical model used as the basis for the current study.....	153
B.2	Kinetic parameters of the ODE mathematical model used as the basis for the current study.....	154
B.3	Biochemical meaning of the kinetic parameters of the G1/S base model	155
B.4	Mass balance equations of the ODE mathematical model used as the basis for the current study.....	158

Appendix C Initial conditions, lump nodes, partial elements, kinetic parameters and mass balance equations of the reduced model (level-1)159

C.1	Initial conditions of the reduced model (level-1)	159
C.2	Lump node composition of the reduced model (level-1)	159
C.3	Initial conditions of the reduced model (level-1) for partial elements.....	160
C.4	Kinetic parameters of the reduced model (level-1).....	160
C.5	Mass balance equations of the reduced model (level-1)	161

Appendix D Initial conditions, lump nodes, partial elements, kinetic parameters and mass balance equations of the reduced model (level-2)162

D.1	Initial conditions of the reduced model (level-2)	162
D.2	Lump node composition of the reduced model (level-2)	162
D.3	Initial conditions of the reduced model (level-2) for partial elements.....	163
D.4	Kinetic parameters of the reduced model (level-2).....	163
D.5	Mass balance equations of the reduced model (level-2)	164

Appendix E Initial conditions, lump nodes, partial elements, kinetic parameters and mass balance equations of the reduced model (level-3)165

E.1	Initial conditions of the reduced model (level-3)	165
E.2	Lump node composition of the reduced model (level-3)	165
E.3	Initial conditions of the reduced model (level-3) for partial elements.....	166
E.4	Kinetic parameters of the reduced model (level-3).....	166
E.5	Mass balance equations of the reduced model (level-3)	167

Appendix F All time courses of the reduced model (level-1) elements168

F.1	All time courses of the reduced model (level-1) elements without DNA damage vs the base model	168
F.2	All time courses of the reduced model (level-1) elements with different levels of DNA damage	172
Appendix G All time courses of the reduced model (level-2) elements.....		178
G.1	All time courses of the reduced model (level-2) elements without DNA damage vs the base model	178
G.2	All time courses of the reduced model (level-2) elements with different levels of DNA damage	182
Appendix H All time courses of the reduced model (level-3) elements.....		188
H.1	All time courses of the reduced model (level-3) elements without DNA damage vs the base model	188
H.2	All time courses of the reduced model (level-3) elements with different levels of DNA damage	191
Appendix I ODEs, Initial conditions and logical equations of the reduced model (R1) (used for time slicing and logical modelling).....		196
I.1	ODEs of the reduced model (R1)	196
I.2	Initial conditions of the reduced model (R1)	196
I.3	Logical equations of the reduced model (R1)	197
Appendix J ODEs, Initial conditions and logical equations of the reduced model (R2) (used for time slicing and logical modelling).....		198
J.1	ODEs of the reduced model (R2)	198
J.2	Initial conditions of the reduced model (R2)	198
J.3	Logical equations of the reduced model (R2)	199
References		200

List of Tables

Table 2.1	Summary of the classes of reduction methods	12
Table 2.2	Categories of the reduction methods.....	30
Table 2.3	Reduction methods and titles of some related article	31
Table 2.4	Number of links to the well-know reduction methods (Google , 15th May 2017)	32
Table 3.1	Summary features of prokaryotic and eukaryotic cells	37
Table 3.2	Summary of the major cell cycle regulatory proteins	43
Table 3.3	Articles related to G1/S checkpoint modelling	48
Table 3.4	Limitations of G1/S checkpoint models.....	50
Table 4.1	Changes in the model equations	60
Table 4.2	The biochemical meaning of kinetic parameters in an interaction map and the effect on the species of the base model.....	74
Table 4.3	The rank $R(Y_i)$ and the level $L(Y_i)$ for all proteins included in the base model	79
Table 4.4	Functions of key elements in the base model	82
Table 4.5	The concentration for each lump at $t=0$, reduced model level-1.....	90
Table 4.6	Partial concentration of every species included in the lump at $t=0$, reduced model level-1	90
Table 5.1	Reduced model (level-1) evaluation without DNA damage by using the root mean squared error (RMSE) and the root mean squared percentage error (RMSPE)	119
Table 5.2	Reduced model (level-2) evaluation without DNA damage by using the root mean squared error (RMSE) and the root mean squared percentage error (RMSPE).....	120
Table 5.3	Reduced model (level-3) evaluation without DNA damage by using the root mean squared error (RMSE) and the root mean squared percentage error (RMSPE).....	121
Table 5.4	CycE/Cdk2-P values from the base model, the reduced model (level-1), the reduced model (level-2) and the reduced model (level-3) simulation with low DNA damage..	122
Table 5.5	CycE/Cdk2-P values from the base model, the reduced model (level-1), the reduced model (level-2) and the reduced model (level-3) simulation with medium DNA damage	122
Table 5.6	CycE/Cdk2-P values from the base model, the reduced model (level-1), the reduced model (level-2) and the reduced model (level-3) simulation with high DNA damage	122
Table 5.7	CycE/Cdk2-P values from the base model, the reduced model (level-1), the reduced model (level-2) and the reduced model (level-3) simulation with excess DNA damage	123
Table 5.8	p21 values from the base model, the reduced model (level-1), the reduced model (level-2) and the reduced model (level-3) simulation with low DNA damage	123
Table 5.9	p21 values from the base model, the reduced model (level-1), the reduced model (level-2) and the reduced model (level-3) simulation with medium DNA damage....	123
Table 5.10	p21 values from the base model, the reduced model (level-1), the reduced model (level-2) and the reduced model (level-3) simulation with high DNA damage	123
Table 5.11	p21 values from the base model, the reduced model (level-1), the reduced model (level-2) and the reduced model (level-3) simulation with excess DNA damage.....	124
Table 5.12	E2F values from the base model, the reduced model (level-1), the reduced model (level-2) and the reduced model (level-3) simulation with low DNA damage	124
Table 5.13	E2F values from the base model, the reduced model (level-1), the reduced model (level-2) and the reduced model (level-3) simulation with medium DNA damage....	124
Table 5.14	E2F values from the base model, the reduced model (level-1), the reduced model (level-2) and the reduced model (level-3) simulation with high DNA damage	124
Table 5.15	E2F values from the base model, the reduced model (level-1), the reduced model (level-2) and the reduced model (level-3) simulation with excess DNA damage.....	125

Table 5.16	p21/CycE/Cdk2-P values from the base model, the reduced model (level-1), the reduced model (level-2) and the reduced model (level-3) simulation with low DNA damage	125
Table 5.17	p21/CycE/Cdk2-P values from the base model, the reduced model (level-1), the reduced model (level-2) and the reduced model (level-3) simulation with medium DNA damage	125
Table 5.18	p21/CycE/Cdk2-P values from the base model, the reduced model (level-1), the reduced model (level-2) and the reduced model (level-3) simulation with high DNA damage	125
Table 5.19	p21/CycE/Cdk2-P values from the base model, the reduced model (level-1), the reduced model (level-2) and the reduced model (level-3) simulation with excess DNA damage	126
Table 5.20	p53 values from the base model, the reduced model (level-1), the reduced model (level-2) and the reduced model (level-3) simulation with low DNA damage	126
Table 5.21	p53 values from the base model, the reduced model (level-1), the reduced model (level-2) and the reduced model (level-3) simulation with medium DNA damage.....	126
Table 5.22	p53 values from the base model, the reduced model (level-1), the reduced model (level-2) and the reduced model (level-3) simulation with high DNA damage	126
Table 5.23	p53 values from the base model, the reduced model (level-1), the reduced model (level-2) and the reduced model (level-3) simulation with excess DNA damage.....	127
Table 5.24	Simplification achieved by the reduced models (level1), (level-2) and (level-3), in comparison to the ODE base model.....	127
Table 5.25	Simplifying the percentages in the number of nodes of the reduced models (level1), (level-2) and (level-3) vs. the ODE base model.....	127
Table 5.26	Efficiency the reduced model (level-1), (level-2) and (level-3) run time vs. the ODE base model run time.....	128
Table 5.27	General comparison between the base model and reduced models (level-1, 2 and 3).....	128
Table 6.1	G1/S checkpoint protein behaviour with and without DNA damage in multiple time windows.....	137

List of Figures

Figure 2.1	Network of EWS-FLI1 effects on proliferation and apoptosis	16
Figure 2.2	Large scale of the molecular system	16
Figure 2.3	Cloud topology in the human PIN.....	17
Figure 2.4	Map of some protein - protein interactions of the SCF ubiquitin ligase and other proteins	18
Figure 2.5	The p53-Mdm2 subsystem related to DNA repair	19
Figure 2.6	Interaction between systems biology and mathematical modelling	21
Figure 2.7	Refining models of biological networks.....	22
Figure 2.8	Number of links to they well-know reduction methods on Google	32
Figure 2.9	Dimensions of biological network model complexity	33
Figure 3.1	Differences between prokaryotes and eukaryotes.	36
Figure 3.2	DNA structure.	38
Figure 3.3	Cell cycle phases	39
Figure 3.4	The Inter-phase stages	40
Figure 3.5	Cell cycle checkpoints	42
Figure 3.6	p53: simplified mode of action	44
Figure 3.7	The Transcription factor E2F.....	46
Figure 3.8	The G1/S checkpoint pathway involving the DNA damage signal transduction pathway	47
Figure 3.9	Diagram of key regulators in the Iwamoto et al. model (2011)	52
Figure 3.10	G1/S and S/G2 transitions	53
Figure 3.11	G2/M and M/G1 transitions and the DNA damage signalling pathway	54
Figure 3.12	Time courses of several cell cycle regulators from a simulation run using the Iwamoto model 2011 without DNA damage	55
Figure 3.13	Time courses of several cell cycle regulators from a simulation run using the Iwamoto model 2011 with different levels of DNA damage (a) low-damage where $DDS = 0.002$ (b) medium-damage where $DDS = 0.004$ (c) high-damage where $DDS = 0.008$ and (d) excess-damage where $DDS = 0.016$	56
Figure 4.1	G1/S transitions and DNA damage signalling pathway	59
Figure 4.2	Time courses of some chemical species in the G1/S phase without DNA damage from a simulation run using the base model	62
Figure 4.3	Time courses of p21 in the G1/S phase with and without DNA damage from a simulation run using the base model	63
Figure 4.4	Time courses of p53 in the G1/S phase with and without DNA damage from a simulation run using the base model	63
Figure 4.5	(a) Multiple levels of protein complex formation map graph G; (b), Adjacency matrix A for graph G, L vector for node level and S vector for node status	67
Figure 4.6	Examples of joint protein in a protein complex formation map graph	68
Figure 4.7	G1/S transitions and DNA damage signalling pathway base model.....	73
Figure 4.8	Statistics of interaction types on the base model	74
Figure 4.9	Protein concentration flow diagram.....	75
Figure 4.10	Balancing feedback loop between Chk1 and Chk1-P	76
Figure 4.11	Balancing feedback loop between Cdc25A and Cdc25A-P	76
Figure 4.12	Unbalancing feedback	77
Figure 4.13	Unbalancing feedback with five species.....	78
Figure 4.14	Unbalancing feedback with seven species	78
Figure 4.15	Feedback to regulate the concentration of CycD, CycD/Cdk4, p27/CycD/Cdk4 and p21/CycD/Cdk4.....	79
Figure 4.16	Hierarchical interactions map for the base model.....	81

Figure 4.17	Key elements, joint proteins and key regulator proteins in a hierarchical interaction map for the base model	83
Figure 4.18	Adjacency matrix A for the base model, graph G	86
Figure 4.19	Vector L for node level for the base model graph.....	86
Figure 4.20	Vector S for node status for the base model graph	86
Figure 4.21	Network level-1 lumping	87
Figure 4.22	Network level-2 lumping	88
Figure 4.23	Network level-3 lumping	89
Figure 5.1	Comparison between the concentration history for F1 (CycD + CycD/Cdk4) in the base model and F1' lump in the reduced model (level-1)	93
Figure 5.2	Comparison between the concentration history for F2 (CycE + CycE/Cdk2) in the base model and F2' lump in the reduced model (level-1)	93
Figure 5.3	Comparison between the concentration history for Y8 (CycE/Cdk2-P) in the base model and Y8' (CycE/Cdk2-P) in the reduced model (level-1).....	94
Figure 5.4	Comparison between the concentration history for F3 (CycA + CycA/Cdk2) in the base model and F3' lump in the reduced model (level-1)	94
Figure 5.5	Comparison between the concentration history for Y10 (CycA/Cdk2-P) in the base model and Y10' (CycA/Cdk2-P) in the reduced model (level-1)	95
Figure 5.6	Comparison between the concentration history for Y11 (p27) in the base model and Y11' (p27) in the reduced model (level-1).....	95
Figure 5.7	Comparison between the concentration history for Y12 (p27/CycD/CDK4) in the base model and Y12' (p27/CycD/CDK4) in the reduced model (level-1)	96
Figure 5.8	Comparison between the concentration history for Y13 (p27/CycE/Cdk2-P) in the base model and Y13' (p27/CycE/Cdk2-P) in the reduced model (level-1)	96
Figure 5.9	Comparison between the concentration history for Y14 (p27/CycA/Cdk2-P) in the base model and Y14' (p27/CycA/Cdk2-P) in the reduced model (level-1)	97
Figure 5.10	Comparison between the concentration history for Y15 (p21) in the base model and Y15' (p21) in the reduced model (level-1).....	97
Figure 5.11	Comparison between the concentration history for Y16 (p21/CycD/CDK4) in the base model and Y16'(p21/CycD/CDK4) in the reduced model (level-1).....	98
Figure 5.12	Comparison between the concentration history for Y17 (p21/CycE/Cdk2-P) in the base model and Y17' (p21/CycE/Cdk2-P) in the reduced model (level-1)	98
Figure 5.13	Comparison between the concentration history for Y18 (p21/CycA/Cdk2-P) in the base model and Y18' (p21/CycA/Cdk2-P) in the reduced model (level-1)	99
Figure 5.14	Comparison between the concentration history for Y19 (p16) in the base model and Y19' (p16) in the reduced model (level-1).....	99
Figure 5.15	Comparison between the concentration history for Y20 (Rb/E2F) in the base model and Y20' (Rb/E2F) in the reduced model (level-1)	100
Figure 5.16	Comparison between the concentration history for Y21 (Rb-PP/E2F) in the base model and Y21'(Rb-PP/E2F) in the reduced model (level-1).....	100
Figure 5.17	Comparison between the concentration history for Y22 (E2F) in the base model and Y22' (E2F) in the reduced model (level-1)	101
Figure 5.18	Comparison between the concentration history for F4 (Rb-PPP + Rb) in the base model and F4' lump in the reduced model (level-1)	101
Figure 5.19	Comparison between the concentration history for Y25 (p53) in the base model and Y25' (p53) in the reduced model (level-1).....	102
Figure 5.20	Comparison between the concentration history for Y26 (Mdm2) in the base model and Y26' (Mdm2) in the reduced model (level-1)	102
Figure 5.21	Comparison between the concentration history for Y27 (ATM/ATR) in the base model and Y27' (ATM/ATR) in the reduced model (level-1)	102
Figure 5.22	Comparison between the concentration history for F5 (Cdc25A + Cdc25A-P) in the base model and F5' lump in the reduced model (level-1).....	103
Figure 5.23	Comparison between the concentration history for F6 (Chk1 + Chk1-P) in the base model and F6' lump in the reduced model (level-1)	103

Figure 5.24	Comparison between the concentration history for Y32 (NF-Y) in the base model and Y32' (NF-Y) in the reduced model (level-1).....	104
Figure 5.25	Comparison between the concentration history for F7 (B-Myb + B-Myb-P) in the base model and F7' lump in the reduced model (level-1)	104
Figure 5.26	Comparison between the concentration history for Im in the base model and Im' lump in the reduced model (level-1)	105
Figure 5.27	Time course of p21 resulting from the reduced model (level-1) runs with different levels of DNA damage.....	106
Figure 5.28	Time course of p53 resulting from the reduced model (level-1) runs with different levels of DNA damage.....	106
Figure 5.29	Time course of F2(CycE + CycE/Cdk2) lump resulting from the reduced model (level-1) runs with different levels of DNA damage	107
Figure 5.30	Time course of CycE/Cdk2-P resulting from the reduced model (level-1) runs with different levels of DNA damage.....	107
Figure 5.31	Comparison between the concentration history for F8 (CycD + CycD/Cdk4 + p21/CycD/Cdk4) in the base model and F8' lump in the reduced model (level-2)	108
Figure 5.32	Comparison between the concentration history for F9 (Rb-PPP + Rb + Rb-PP/E2F) in the base model and F9' lump in the reduced model (level-2)	109
Figure 5.33	Comparison between the concentration history for F2 (CycE + CycE/Cdk2) in the base model and F2' lump in the reduced model (level-2)	109
Figure 5.34	Comparison between the concentration history for Y8 (CycE/Cdk2-P) in the base model and Y8'(CycE/Cdk2-P) in the reduced model (level-2)	110
Figure 5.35	Compare between the concentration history for Y22 (E2F) in the base model and Y22'(E2F) in the reduced model (level-2)	110
Figure 5.36	Comparison between the concentration history for Y25 (p53) in the base model and Y25'(p53) in the reduced model (level-2).....	110
Figure 5.37	Time course of p21 resulting from the reduced model (level-2) runs with different levels of DNA damage.....	111
Figure 5.38	Time course of p53 resulting from the reduced model (level-2) runs with different levels of DNA damage.....	112
Figure 5.39	Time course of F2 (CycE + CycE/Cdk2) lump resulting from the reduced model (level-2) runs with different levels of DNA damage	112
Figure 5.40	Time course of CycE/Cdk2-P resulting from the reduced model (level-2) runs with different levels of DNA damage.....	113
Figure 5.41	Comparison between the concentration history for F10 (CycA + CycA/Cdk2 + p27/CycA/Cdk2-P + p21/CycA/Cdk2-P) in the base model and F10' lump in the reduced model (level-3).....	114
Figure 5.42	Comparison between the concentration history for F2 (CycE + CycE/Cdk2) in the base model and F2' lump in the reduced model (level-3)	114
Figure 5.43	Comparison between the concentration history for Y8 (CycE/Cdk2-P) in the base model and Y8'(CycE/Cdk2-P) in the reduced model (level-3)	115
Figure 5.44	Comparison between the concentration history for Y22 (E2F) in the base model and Y22' (E2F) in the reduced model (level-3)	115
Figure 5.45	Comparison between the concentration history for Y15 (p21) in the base model and Y15' (p21) in the reduced model (level-3).....	116
Figure 5.46	Time course of p21 resulting from the reduced model (level-3) runs with different levels of DNA damage.....	116
Figure 5.47	Time course of p53 resulting from the reduced model (level-3) runs with different levels of DNA damage.....	117
Figure 5.48	Time course of F2 (CycE + CycE/Cdk2) lump resulting from the reduced model (level-3) runs with different levels of DNA damage	117
Figure 5.49	Time course of CycE/Cdk2-P resulting from the reduced model (level-3) runs with different levels of DNA damage.....	118

Figure 5.50	Network reduction: (a) Base model (b) Reduced model (level-1) (c) Reduced model (level-2) (d) Reduced model (level-3) of the original network	129
Figure 6.1	Interaction graph, logical model and logical equations of protein network examples (a) Interaction graph: The nodes (Y1, Y2 ... Y6) in the graph represent proteins, and the edges represent interactions. Blue arrows represent activations and red bar arrows inhibitions. (b) Logic-based representation of a logical model for the interaction graph given in (a). (c) Equations of a logical model for the interaction graph given in (a).	134
Figure 6.2	Behaviour on multiple time windows.....	136
Figure 6.3	Regulatory graph for the reduced model (R1) for time window A	138
Figure 6.4	Regulatory graph for the reduced model (R2) for time window C	139
Figure 6.5	Logic-based graph for the reduced model (R1)	139
Figure 6.6	Logic-based graph for the reduced model (R2)	140
Figure 6.7	Simulation results of the reduced model (R1) without DNA damage (green: active, red: inactive)	141
Figure 6.8	Simulation results of the reduced model (R1) with DNA damage (green: active, red: inactive)	141
Figure 6.9	Simulation results of the reduced model (R2) without DNA damage (green: active, red: inactive)	142
Figure 6.10	Simulation results of the reduced model (R2) with DNA damage (green: active, red: inactive)	143

Abbreviations

Acceptable **K**ey **E**lements number that can be **L**umped (AKEL)

Agent-**B**ased **M**odels (ABMs)

Cdk **A**ctivating **K**inase (CAK)

Computational **S**ingular **P**erturbation (CSP)

Coupled **D**ifferential **E**quations (CDEs)

Cyclin **D**ependent **K**inases (CDKs)

Cyclin-dependent **K**inase **I**nhibitor (CKI)

Delay **D**ifferential **E**quations (DDEs)

Deoxyribonucleic **A**cid (DNA)

DN**A** **D**amage **S**ignal (DDS)

Dominant **S**ystem (DS)

Fuzzy **C**ognitive **M**aps (FCMs)

Geometric **S**ingular **P**erturbation **M**ethod (GSPM)

Intrinsic **L**ow **D**imensional **M**anifold (ILD M)

Ordinary **D**ifferential **E**quations (ODEs)

Partial **D**ifferential **E**quations (PDEs)

Proportional **I**ntegral **D**erivative (PID)

Protein-**P**rotein **I**nteraction (PPI)

Pseudo **S**tady **S**tate **H**ypothesis (PSSH)

Quasi-**E**quilibrium (QE)

Quasi **E**quilibrium **A**pproximation (QEA)

Quasi **S**tationarity **E**quations (QSE)

Quasi-**S**tady **S**tate (QSS)

Quasi-**S**tady **S**tate **A**pproximation (QSSA)

Rao-**B**lackwellised **P**article **F**ilters (RBPF)

Rapid **E**quilibrium **A**pproximation (REA)

Recurrent **N**eural **N**etworks (RNNs)

Retinoblastoma (Rb)

Root **M**ean **S**quared **E**rror (RMSE)

Root **M**ean **S**quared **P**ercentage **E**rror (RMSPE)

Simulation Error Minimisation Connectivity Method (SEMCM)

Simulation Error Minimisation with the Principal Component Analysis of matrix F (SEM-PCAF)

Stochastic Differential Equations (SDEs)

Transcription Factor (E2F)

Visual Basic (VB)

Visual Basic for Applications (VBA)

Chapter 1

Introduction

Our world is full of complex systems and they are around us all the time. This prediction agrees with the famous words of Stephen Hawking, “I think the next century will be the century of complexity.” He said this on January 23, 2000 (San Jose Mercury News) in his ‘millennium’ interview. To better understand and control complex systems we need to develop and use new reduction methods. Reduction methods are used to minimise the level of complexity through different ways. First, to reduce a complex system to a simple mathematical model; and, secondly, to reduce the mathematical model into an even simpler mathematical model that achieves the goal of finding a solution faster and more easily and at a lower cost.

Romeo and Juliet is a play written in 200 pages; to know the details we need to read the whole book but if you need to know the main idea you can describe the story in just two lines. “Romeo and Juliet is a tragedy written by William Shakespeare. Romeo and Juliet is a play about star-crossed teenage lovers from two prominent families at war with one another.” Any story can be represented in different levels of detail to simplify it. The same idea can be applied to biological networks. We propose two reduction approaches to represent biological networks with different levels of detail (abstraction). The first approach is based on a hierarchical representation and lumping approach; and the second approach is through the use of time windows and logical models.

In Section 1.1 of this chapter, general introduction, in Section 1.2, we provided an overview of the context of the thesis, in Section 1.3, we discuss the goals and objectives of this thesis; and, in Section 1.4, we show the thesis structure.

1.1 General Introduction

Biological systems are very complex and consist a large number of components that interact with each other in the cell. Mathematical models are used to describe biological phenomena. All these models aim to understand the biology behind different diseases or effects of different cellular perturbations or stresses. Most of the models that have been built to understand regulatory networks were ODE mathematical models and most of these models were complex and needed kinetic information for molecules and that was not easily gathered. Simplifying the complex ODE mathematical models can lead to better understanding and control of these systems. Mathematical modelling of biological research is necessary and useful. Researchers use it to analyse cellular networks or to invent strategies for controlling cellular dynamics which might be considered the cornerstone of development of

therapeutic medical applications. A mathematical model is basically a systematic analysis of a biological system that empowers quantitative predicting. Many scholars (such as: Endy & Brent, 2001; Hasty et al., 2001; Rao & Arkin, 2001; Kitano, 2002; Neves & Iyengar, 2002; Weston & Hood, 2004; You, 2004; Alves et al., 2006; Kholodenko, 2006; Ideker et al., 2006) have studied the combination of computing power and developed numerical methods to conduct the analysis of complex cellular networks dynamics and model simulation.

Mathematical models simulating biological systems that are used include: ordinary differential equations (ODEs), delay differential equations (DDEs), partial differential equations (PDEs), agent-based models (ABMs), and stochastic differential equations (SDEs). Ordinary differential equations are the most common type of equations used for biological networks modeling. But, most of these models have high dimensional complexity (contain large numbers of species and reactions) and nonlinear behaviour. For this reason, many methods for model reduction are needed to simplify complex models. The behaviour of the reduced model should be like the behaviour of the original model.

There are several techniques of model reduction in use with biochemical reaction network models to reduce their complexity. Quasi-steady state approximation (QSSA) is the most famous approach of model reduction used with biochemical kinetics (Bodenstein, 1913). This idea was later used to produce the classical Michaelis Menten formula (Michaelis and Menten, 1913). More development and improvement were achieved on this method to be the basic tool to analyse the behaviour of chemical reaction mechanisms and kinetics (Semenoff, 1939; Christiansen, 1953; Helfferich, 1989; Segel and Slemrod, 1989). Another approach to model reduction is the geometric singular perturbation method (GSPM). This is useful when the models have slow and fast variables. This approach works based on the assumption that when the model contains fast and slow variables, and the slow variables control the fast variables, so we can remove the fast variables from the model (Tikhonov, 1952; Fenichel, 1979; Jones, 1995).

Another common approach of model reduction is quasi-equilibrium approximation (QEA) or the rapid equilibrium approximation (REA). The first appearance of this idea was in 1973 by Vasiliev and his colleagues (Vasiliev et al., 1973). Later, many studies provided further explanation and clarification of the approach as an approach for model reduction (Volpert and Khudyaev, 1985; Schnell and Maini, 2002; Lee and Othmer, 2010; Noel et al., 2012). Another trend in the reduction is applied to chemical reaction models based on the concept of a limiting step. Many researchers studied and extended the idea of limiting step (see Johnston, 1966; Boyd, 1978; Murdoch, 1981). Recently, a general theory of static and dynamic limitations for linear multi-scale networks was developed by Gorban and other researchers (Gorban and Radulescu, 2008; Gorban et al., 2010).

The lumping technique was studied by Wei and Kuo (1969). Many researchers have developed and applied the lumping technique in many chemical reaction problems; see Genyuan (1984); Li and Rabitz (1989); Li and Rabitz (1990); Li and Rabitz (1991); Li et al. (1994); Dokoumetzidis and Aarons (2009).

Another reduction method was proposed by Radulescu and his colleagues (2012). They suggested some essential ideas such as dominance and limitation, for greater understanding of dynamical and computational biological systems (Radulescu et al., 2012). The methods of averaging approximation and invariant manifolds proved their effectiveness in reducing the asymptotic dynamics of chemical reaction networks with clear time-scale separation. Many studies have provided further explanation on how to calculate invariant manifolds. According to Gorban and Karlin (2005), the slow mode dynamics are carried by invariant manifold that results from the relaxation of fast variables. For more information see Roussel and Fraser (1991); Gorban and Karlin (2003); Krauskopf et al. (2005).

Several other methods have also been used for reducing chemical reactions networks. For instance, Noel and his colleagues (2012) reduced and hybridised networks of biochemical reactions using the Litvinov-Maslov correspondence principle. They applied this method on a cell cycle oscillator model. Lam and Goussis (1994) implemented a singular computational perturbation. Maas and Pope (1992; 1994) used an intrinsic low dimensional manifold to exploit the interval between timescales of models' various processes and variables. Rao and other researchers proposed a Kron reduction of the weighted Laplacian matrix. The method is based on a variety of reversible and irreversible enzyme kinetic rate laws (Rao et al., 2014). Radulescu and his colleagues (2015) reduced the model based on tropical geometry and analysis that combines graphical approaches, semi-quantitative reasoning and symbolic manipulation. Further studies of model reduction with examples of application from systems biology can be found in Petzold and Zhu (1999); Gorban et al., (2004); Nagy and Turányi (2009); Gay et al. (2010); Anderson et al. (2011); Karadeniz et al. (2012); Kutumova et al. (2013); Ishizaki et al. (2014); Kooshkbaghi et al. (2014); West et al. (2015); and Sun and Medvedovic (2016).

1.2 Overview

This thesis addresses several subjects related to complex systems, complexity, biological systems complexity, and different reduction methods used to simplify biological models and proposes two reduction methods. All these aspects are described in this thesis. The subjects studied in this thesis can be summarised as follows:

First, we review some issues and facts about complex systems, model reduction, complexity of biological networks, and then reduction methods that are used to reduce the mathematical models of biological systems. In this review we show that biological systems, in general, are complex and, so to better understand biological systems, scientists have used mathematical models, but the results from

these mathematical models for biological systems shows that these models are complex . To address this challenge, new model reduction techniques are required. In this chapter we look into the modelling process in general. We also discuss different methods for model reduction (based on the approach, advantages, disadvantages and examples).

Secondly, any researcher from the computer science field who has little or no knowledge about biology, specifically, the cell and regulation of cell cycle, can build a good biological background from this thesis (Chapter 3), which gives a brief review of the biological background, including that of a cell: general review, cell cycle, regulation of cell cycle, (DNA damage and cancer) and the details of the G1/S checkpoint and models.

Thirdly, we proposed a new method based on a hierarchical representation and lumping approach to reduce protein-protein interaction (PPI) networks. This new method can be applied to reduce complex systems. We used the G1/S checkpoint pathway integrated with DNA damage pathways as a case study to evaluate the efficiency of this method.

Fourthly, we validated the reduced model output with the base model, firstly, by comparing model element behaviour and secondly, by comparing results and the Root Mean Squared Error (RMSE) and the Root Mean Squared Percentage Error (RMSPE) to be sure that the reduced model is accurate and applicable for answering a specific set of questions. Furthermore, we show from a computational view that the reduced model is more efficient in running the system and generating solutions than the Ordinary Differential Equations (ODEs) base model. From a biological view, we show the advantages of the new reduction method and how these advantages can help treat diseases, especially cancer.

Fifthly, we offered another method to aid in model reduction and applied it to the behaviour of the G1/S checkpoint with and without DNA damage. In particular, we focused on simplifying the time dimension by dividing the G1/S checkpoint pathway into time windows (active time windows and steady or frozen time windows where there is no activity in the system). Then, the active time windows are represented by logical models to aid in model reduction.

Finally, we provide conclusions and outcomes from this research and discuss directions for future work. The main conclusion is that easing the struggle with the complexity of mathematical models is possible through effective model reduction as proposed in this thesis.

1.3 Goals and Objectives

Our world is complex. Social, biological, economic, weather, communication and information systems all comprise a large number of interacting entities that give rise to complex behaviour. Complexity research is a novel research field devoted to dealing with issues such as understanding the roots of

complex phenomenology observable in our world, measuring complexity, modelling complex systems and model reduction methods.

Over the last two decades, research in bioinformatics moved from the analysis of genomic sequence to the study and analysis of intracellular signalling networks (protein-protein interactions, transport, expression of proteins and RNA, etc.). This huge data explosion in biology increased the size and complexity of mathematical models of intracellular signalling networks. Furthermore, the uncertainty in model structure and, especially, model parameters has become a further complicating factor. To meet these two challenges of complexity and uncertainty, abstracting reduced or simple models from complex models is a central area of investigation within systems studies, including biology and medicine.

As we mentioned previously, the real world contains a huge number of complex systems, one of these systems is biological networks. A common example of complex biological networks is the protein interaction networks in cells. Better understanding of protein interactions is useful for the treatment of diseases such as cancer.

Several computational models have been proposed to help us understand protein interaction networks, but these models have the aforementioned limitations. An effective reduced network in contrast has fewer complexes, reactions, variables and parameters compared to full (original) networks, and yet the behaviour of a preselected set of significant elements in the reduced network resembles that of the original network. Moreover, the reduced network largely retains the structure and kinetics of the original model.

Mathematical modelling of biological research is necessary and useful. Researchers use it to analyse cellular networks or to invent strategies for controlling cellular dynamics which might be considered the cornerstone of development of therapeutic medical applications. A mathematical model is, basically a systematic analysis of a biological system that empowers quantitative predicting. Many scholars (such as: Endy & Brent, 2001; Hasty et al., 2001; Rao & Arkin, 2001; Kitano, 2002; Neves & Iyengar, 2002; Weston & Hood, 2004; You, 2004; Alves et al., 2006; Kholodenko, 2006; Ideker et al., 2006) have studied the combination of computing power and developed numerical methods to conduct the analysis of complex cellular networks dynamics and model simulation.

Dynamical models of biochemical reaction networks are composed of a reaction graph (structure) and equations (dynamics). The reaction graph contains nodes representing the species and vertices representing the reactions where reaction vertices are labelled with kinetic parameters. Most dynamical models of biochemical reaction networks use Ordinary Differential Equations (ODEs).

Model reduction is a key concept for modelling a biological process at different levels of abstraction or for developing multi-scale models in systems biology. Most model reduction approaches work as follows: identify critical parts (components or interactions) in the model, identify noncritical parts (components or interactions) in the model, describe critical parts with precision in the reduced model, while noncritical parts can be simplified. There exist several classical approaches for model reduction (Computational Singular Perturbation (CSP), Intrinsic Low Dimensional Manifold (ILDM), Lumping and Graphical Reduction Methods, Symmetry Reduction Methods and Tropical Analysis Reduction Methods). In recent years, many reduction methods have been investigated (Clarke, 1992; Maas & Pope, 1992; Lam & Goussis, 1994; Maas & Pope, 1994; Clarke et al., 1996; Gorban & Karlin, 2005; Feret et al., 2009; Gorban et al., 2010; Noel et al., 2011; Radulescu et al., 2012; Rao et al., 2013; Sunday et al., 2013; Rao et al., 2014; Radulescu et al., 2015).

Simplifying dynamic models for large and complex biological networks by incorporating the proposed reduced techniques will help us building a comprehensive biological network and gaining a greater understanding of the emerging properties of cellular activities. There are many reduction methods but a fully formal method that exploited the hierarchical orders for large volumes of biological network models are missing. Known reduction methods often face difficulties when applied to complex systems. These difficulties can be summarized as follows:

1. The reduced mathematical model is still either too large or too complex to be useful.
2. The reduced mathematical model still requires a parameter that depends on the original model.
3. The simpler model cannot answer all the questions that the original model can.
4. The reduced mathematical model cannot describe the complex behaviour.
5. Some reduction methods have extra computational costs to find new parameter values to run the reduced model.
6. The reduced model does not have enough accuracy to be useful and reliable.
7. Most reduction methods do not provide multi-level of abstraction (zoom in, zoom out).
8. Most reduction methods have been applied on small networks containing two or three nodes with a limited number of interactions.

All these indicate the need for developing reduction methods for mathematical models that are applicable to large networks of biochemical interactions.

This research aims to provide an overview of complex systems, modelling and model reduction. The research touches on several topics of traditional and current research in complexity science. The

reader will learn concepts of complexity and deal with real examples as they will learn how to measure and characterise complex features in natural systems. These notions are increasingly in demand to approach complex problems in many different fields of study, including economics, biology, social science, chemistry and climatology.

Further, this research will suggest new reduction approaches to achieve general and specific goals. The general goal is to suggest two reduction approaches that can be used to allow for better mathematical models of complex systems. The specific goal is to use the suggested reduction approaches to simplify mathematical models of biological networks and simulate a reduced model that makes it easier to achieve results and analyse the results and analyse all possible scenarios, while providing better understanding of biological networks that can help find better treatments for diseases, especially cancer. Furthermore, it allows the combination of separate and existing mathematical models into a comprehensive master model (for example, the cell cycle and apoptosis (cell death)).

This thesis proposes two reduction methods. Firstly, a reduction method is proposed to produce a model of biological networks that simplifies cell signalling pathways into different level of abstraction (zoom in, zoom out) and simulate it using the G1/S checkpoint pathway integrated with DNA damage as a case study. It then, validates the new reduction method by comparing several numerically simulated time course histories for the levels of individual biochemical species with the base model output. Furthermore, we validate the new reduction method by finding the Root Mean Squared Error (RMSE) and the Root Mean Squared Percentage Error (RMSPE) to be sure that the reduced model is useful for the intended purpose of the pathways and is applicable to answering a specific set of questions. Secondly, another reduction method is proposed to find a reduced model using time windows and a logical model approach and demonstrate its application to G1/S checkpoint pathway integrated with DNA damage pathways. Therefore, this thesis has the following objectives:

1. To explore relevant aspects of two reduction methods and identify potential improvements in the design process and then propose new reduction methods through reviewing the theory.
2. To build a good biological background to help researchers who do not have much knowledge of regulation of cell cycle.
3. To develop a new reduction method to simplify biological signalling networks based on a hierarchical representation and lumping approach by simplifying the base model into different levels of abstraction (zoom in, zoom out).
4. To apply the new reduction method to G1/S checkpoint pathway integrated with DNA damage pathways.
5. To simulate the reduced model at different levels of abstraction.

6. To validate the reduced model with results from the base model and the available experimental evidence and data, to evaluate the reduction method.
7. To propose a new (second) reduction method to simplify complex ODE mathematical models for biological signalling networks based on time windows and logical models.
8. To present the proposed reduction methods as promising approaches for reducing all biological networks.

In conclusion, behind each complex system there is a network that defines the interactions between its components. We will never understand complex systems unless we map and understand the networks behind them. Proposing simplified dynamic models for large and complex biological networks using new and reduced techniques could allow us to build comprehensive biological networks. This will help researchers to understand the emerging properties of cellular activities better. Hierarchical modelling is important when there is the need to zoom in and out of several levels of complexity. Critical elements identification is an important issue in systems biology.

In our research we introduce two reduction approaches to reduce complex systems; especially complex protein interaction networks. The first approach allows critical elements identification and produces hierarchies of models, and the second approach allows us to get rid of the kinetic parameters in a system. The reduced models have less complexity, reactions, variables and parameters compared to the base model and, yet the behaviour of a pre-selected set of significant species in the reduced model resembles that of the base model. The reduced models have improved our understanding of the dynamics of the G1/S checkpoint pathway integrated with a DNA damage pathways network indicating that relaxing the struggle with the complexity of mathematical models is possible.

1.4 Thesis Structure

This thesis is set out in seven chapters, with this chapter (Chapter 1) providing an overview, the goals and objectives of this thesis, an overview of the thesis structure. Chapter 2 is the literature review: this gives a review of complex systems and biological reduction methods needed to drive this research. Chapter 3 reviews the biological background of cell cycle and provides an overview summary of the original model of Iwamoto (2011) for G1/S checkpoint pathway incorporating DNA damage pathways the base model used as the basis for the current research. Chapter 4 provides the first reduction method based on a hierarchical representation and lumping approach. Chapter 5 provides the results and a discussion on the first reduction method. Chapter 6 provides the second reduction method based on time windows and logical models, and also the results and a discussion on this method. Chapter 7 gives concluding discussion about the scientific contributions and future work.

Chapter 2

Literature Review

“I think the next century will be the century of complexity”

Stephen Hawking

What Stephen Hawking said two decades ago is, indeed, a fact nowadays. To help with understanding complexity this study addresses complex systems and complexity, the complexity of biological networks, mathematical models of biological systems, reduction techniques, in general and biological systems reduction techniques in particular.

Section 2.1 offers an overview of complex systems and complexity; Section 2.2 discusses model reduction methods; Section 2.3 focuses on the complexity of biological networks; Section 2.4 gives a review of mathematical models for biological systems; Section 2.5 gives an overview of reduction methods for biological systems; and Section 2.6 provides a summary of the chapter.

2.1 Complex Systems and Complexity

Complexity features include uncertainty, ambiguity, inconsistency, multiple players or participants with different information, experience, influential factors and relationships, ill-posed definitions, and multiple dimensions. Problems, including some or all of these properties, are considered complex and dynamic. Real life problems (social, political, economic, biological and ecological problems) share some of these properties.

To understand real life problems and make decisions we need to study and manage the computational systems of these problems. In other words, to identify knowledge about the complex and dynamic human-nature interactions, which are experimental, we need to integrate them into a comprehensive model that simulates system behaviour to aid decisions making. This study attempts to produce an approach to tackle complex real-life model problems and examine their efficacy/usefulness in addressing one such problem.

Complex systems are difficult systems to model with a large number of nonlinear interacting components which, under selective pressure, demonstrate hierarchical self-organisation. They intersect with science (biology, medicine, physics, chemistry and engineering), the human brain system, the immune networks, financial markets, telecommunication systems, distribution networks,

biological systems, neural networks, reaction-diffusion systems, ecological networks and sociological systems.

Complex systems have been defined by several researchers from various disciplines. In biology Weng and his research team (1999) defined complex systems as systems that are difficult to understand and verify in design or function. In physics Gallagher and his colleagues (1999) referred to complex systems as having system properties that may not be fully explained by understanding its components. Likewise, Goldenfeld and Kadanoff (1999) said complex systems are highly structured and varied. Rind (1999) said that a complex system is a system that involves multiple interactions between many different components found in a domain. Mayes (2012) differentiated between a complex system and its mathematical model, saying that the first is “any system composed of a large number of components and interactions that is not traceable by analysis,” while the complex mathematical model is “a large system of coupled equations which are either too complex or too large to admit a sufficiently useful model or solution.”

According to Bar-Yam (2000) the modern study of complex systems has three interrelated approaches: how interactions give rise to behaviour patterns; the space of possibilities; and the formation of complex systems via pattern formation and evolution.

Difficulties in complexity are apparent, as Gorban and Yablonsky (2013) mentioned in measuring complexity, model reduction and invariant manifolds, traces, criteria, interpretation of experiments and modelling classes. Measuring complexity was tackled by Monshizadeh (2013), who said that it is measured by its dynamic order, that is, the number of state components in a state space representation of the system.

Mathematical language is used in describing natural phenomena in physical sciences in terms of models based on equations. This allows for logical reasoning over the representation of physical entities involved in the phenomenon and accounts for the experimental observations.

2.2 Model Reduction

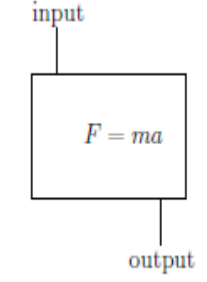
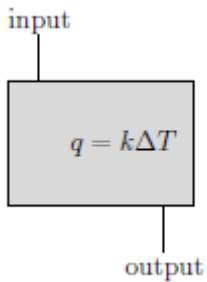
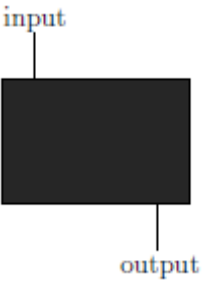
This section discusses system reduction methods, advantages, disadvantages and developments. Successful simple models rely on the important properties of large dynamical systems. In pursuing the optimal level of complexity that captures the salient features of the phenomenon, the middle out modelling becomes the art of the modeller. Over time, trying to reduce model complexity leads to the development of model reduction techniques.

Zinovyev (2014) said the first step to fight against complexity is by dimension reduction. Reducing the number of variables makes data extraction easier. In the same respect Radulescu and his colleagues

(2015) mentioned that model reduction is a way to avoid computational difficulties by replacing large-scale models with smaller scale models that are easier to analyse. And Mayes (2012) defined model reduction as a process of simplifying a mathematical system in order to obtain solutions. He classified reduction methods into three categories (as illustrated in Table 2.1):

1. The white-box reduction method is a direct result of the philosophy of methodological reductionism. It assumes that adequate explanations about behaviour may be achieved by focusing on one or a few lower levels of analysis (*e.g., focusing on genes as the primary cause of behaviour*). This explains individual behaviour by interpreting the properties of parts, which are often studied in isolation (Wimsatt, 1980). In this approach, a system is reduced and modelled using a bottom-up approach; although this approach proves to be effective, it has faced two difficulties: the volume of the internal complexity and the appearance of emergent phenomena. Prigogine and Stengers (1997) evaluated this approach and said it is no longer valid for science. According to the authors, the problem of irreversibility, instability, and time may not be explained by the reductionist approach. This approach may be considered the best example of mathematical modelling for simple systems, but it fails to explain complex systems because it ignores the interactions between the parts in different levels of the organisation behaviour (Wimsatt, 1980).
2. The grey-box reduction method is used with real systems to control the system better (it uses a combination of white-box reduction and black-box reduction methods).
3. The black-box reduction method or the holism reduction philosophy is used with complex systems (only the system's overall behaviour is of interest in this method and no attention is paid to the components or inner processes). The behaviour in the holistic approach of a complex system may not be fully understood on its own on the basis of a complete understanding of the constituent parts; it must be studied as a whole system. The holism approach was briefly described in Aristotle's *Metaphysics* with the phrase "the whole is more than the sum of its parts." Examples of nearly-holistic approaches include neural networks, proportional integral derivative (PID) control, fuzzy logic, knowledge based systems, and any other expert system that depends on human experience. The holistic approach is implemented by reducing these examples because their details are important. However, for large systems the approach is used in the field of biological science mainly because of their true emergent behaviours such as consciousness and life.

Table 2.1 Summary of the classes of reduction methods

No	Class	Reduction Philosophies	Approach	Explanation by graph
1	White-box reduction methods	Methodological reductionism	A system reduced to its smallest parts and modelled using a bottom-up approach	
2	Grey-box reduction methods	Model-based methods	Uses a combination of the white-box reduction method and the black-box reduction method	
3	Black-box reduction methods	Holism	Only the system's overall behaviour is of interest, and the components and the inner processes are not of interest	

For example, large biochemical model dynamics may be reduced to produce a simpler model called a dominant sub system (Gorban & Radulescu, 2008; Radulescu et al., 2008; Gorban et al., 2010); this dominant sub system contains fewer parameters and is easier to analyse. The notion of dominance, which is a natural mathematical framework to capture multiple asymptotic relations, uses change in scale to transform nonlinear systems into discontinuous piecewise linear systems. It is motivated by applications from mathematical physics and systems of polynomial equations, as in tropical geometry (Sturmfels, 2002). The linear system involves switching between several different systems (modes). Dominance was used by Litvinov and Maslov (1996) to obtain simpler models from larger models that have multiple separated timescales and are assembled into hybrid models. The model reduction problems in a high order dynamics system can be summed up as finding a simpler lower order models for the system in a way that the reduced order model approximates relatively well the behaviour of the original model. Moreover, it is important to preserve certain desired properties of the original

model in the reduced order model (Monshizadeh, 2013). Choosing the dominant sub-system relies on comparing the time scales of the large model. The quasi-equilibrium (QE) and the quasi-steady state (QSS) approximations presented by Gorban et al. (2010) led to dominance and generated reduced models. But time scales and dominant sub-systems may change during the dynamics and may go through sharp transitions into nonlinear systems. The existence of transitions refers to a well-adapted hybrid, discrete or continuous structure for the description of the dynamics of large nonlinear systems with multiple time scales (Crudu et al., 2009; Noel et al., 2010; Noel et al., 2011).

Model order reduction techniques may be categorised into two groups: balanced truncation schemes and moment matching based methods. The former was introduced by Mullis and Roberts (1976) and the latter appeared in control system studies (Moore, 1981 and Pernebo & Silverman, 1982). The balanced scheme transforms the system into a balanced form, and then a reduced order model is obtained by truncation. According to Moore (1981), the most important technique is the Lyapunov balanced truncation, whose main idea is to transform the system into an equivalent system representation in which the states that are easy (difficult) to reach are also easy (difficult) to observe. Other balancing types include: stochastic and positive real balancing proposed by Desai and Pal (1984); bounded real balancing proposed by Opdenacker and Jonckheere (1988); and frequency weighted balancing proposed by Enns (1984); Lin and Chiu (1992); Zhou (1995) and Wang et al. (1999).

The other category of model reduction is formed based on moment matching by the Krylov method and this led to the moment matching model reduction techniques (e.g. Sorensen, 1992; Feldman & Freund, 1995; Grimme, 1997; Jaimoukha & Kasenally, 1997). Many scholars base their research on this category, such as Feldman and Freund (1995), Grimme (1997) and Jaimoukha and Kasenally (1997). Developing methods for model reduction by switching systems dynamics are scarce, as far as the researcher of the current study knows, such as the studies of Gao et al. (2006); Shaker and Wisniewski (2011) and Birouche et al. (2012).

Monshizadeh (2013) developed two model reduction approaches for networks and multi-agent systems reduction of the dynamic order of the individual agents and reduction of the size of the communication graph. The first approach adopted bounded real balancing to reduce certain network dynamics in a way that preserves stability or synchronicity with the original system. An priori model reduction error bound was established to compare the behaviour of the original network to the reduced order model; the interconnection structure of the network remains the same in this technique. The second approach focused on the interconnection structure and, in particular, the size of the underlying communication graph. The model reduction technique proposed was based on clustering the vertices (agents) of the underlying communication graph by means of suitable graph partitions. The inevitable challenge was to preserve the spatial structure of the network, which was accounted for in the proposed model reduction method, and the reduced size model realised as a

multi-agent system is defined on a new graph with a reduced number of vertices. An explicit formula for the H2-norm of the error system was obtained by comparing the input-output behaviours of the original model and the reduced size model, in the case of choosing the clusters using “almost equitable partitions” of the graph. However, the major drawback of balanced truncation reduction is the probable collapse of the spatial structure of the network by the direct application of classical model reduction tools.

In the reduced size model, the main structure to be maintained is the network typology. Imura (2012) and Ishizaki et al. (2012) conducted studies on a clustering-based algorithm proposed as an asymptotically stable networks.

When the reductionism approach proved to be inadequate and incomplete in dealing with complex systems, individual-based modelling emerged to bridge this gap (see Judson, 1994). Individual-based modelling is a strategy that focuses on modelling the individual and the interactions with other individuals. The individual’s behaviour may be represented by the rules and group behaviour or the social organisations are viewed as emerging from the interactions among individuals. Kauffman (1976) introduced an early explanation for using individual based models as surrogates to experimentally investigating complex biological systems.

Finally, it is important to mention what Zinovyev (2014) said: “Wild complexity behaviour that may not be reduced to a relatively simple view or may not be self-averaged may only be observed and reproduced by engineering more or less complex models of their behaviour.”

2.3 Complexity of Biological Networks

The term "complex" refers to the difficulty in understanding or verifying a component in terms of its design or function, or both. The complexity of a certain system is defined or decided by the number of components, the connections between the components, the nonlinearity of mathematical equations, the nesting degree, data structure and type, significant behaviours and abstraction problems. Miller and Page (2009) linked complexity with self-organisation and emergence, while others correlated it with the dimensionality and size. Complex system emerged as a special field in the mathematical and physical sciences. To understand complex systems, simple interactions (e.g., signalling) are studied first and then new complex levels are added (Weng et al., 1999). Complex systems depend on the occurrence of events in time space, and then they modify themselves accordingly.

Many human diseases such as cancer, diabetes and neural disorders, occur due to erroneous function or malfunction of signalling components. A single component malfunction does not often cause complexity, but multiple or total effects of malfunctioning can cause complexity. Understanding the function of individual components within the system helps in understanding anomalies in signalling

that cause pathophysiology; such understanding may also provide a clear molecular prospect of human interaction with the surroundings (Weng et al., 1999).

In exploring complexity of biological systems, we face a challenge that arises from the systems' ability to respond to different types of signals. The determinants of a complex biological system include the dynamic assembly, translocation, degradation and chemical reactions channelling, all of which occur simultaneously. Biochemical reaction processes include feedback loops, which present nonlinear properties such as disorder, bifurcation and complex disturbance wave etc (McNeil & Walls, 1974; Nitzan et al., 1974; Matheson et al., 1975; Lee et al., 1993; Roesky et al., 1993). Barillot et al. (2012), Calzone et al. (2012) and Wagner (2013) connected biological systems complexity with its validity and evolution history.

Österlund (2014) stated that biological systems should be studied systemically in order to understand the behaviour of cells. For example, the central nervous system and the ganglia of the peripheral nervous system comprise neurons that may connect to form neural networks. There are a huge number of neurons (100 billion) in our brain, and each neuron can have over 100 synapses coupled with other neurons; this huge number of the neurons and synapses causes complexity of the neural network and modelling becomes intractable (Koch & Laurent, 1999).

Complex biological systems include many different processes, such as metabolism, cell growth and cell division, as in the case of cancer. The complexity of these processes emerges from the interactions components, such as genes, proteins and metabolites (Sauer et al., 2007). For instance, Barillot and his colleagues (2012) discussed this in "*Computational Systems Biology of Cancer*". Zinovyev (2014) said that in order to understand cancer, one must understand the disease mechanism by understanding cell cycle (the process by which individual cells divide into two cells), death, motility, and the survival immune and angiogenesis mechanisms, as well as DNA repair and replication. For example, if the cell DNA changes, it may transfer to become a tumour cell; this infected cell grows faster than a normal one and the change occurs at the cell and tissue levels (Castiglione et al., 2014). Immunity is considered a complex system; it operates with complex self-regulatory networks, emergent attributes and nonlinear dynamics. Ideker and his colleagues (2001) said that the term "emergent" is applicable to biological systems as it explains the emergence of a complex structure from simple interactions of components. In the same way, Weng and his colleagues (1999) said that complexity arises from the connections between the components and the spatial correlations between them.

Sengupta (2011) said that biological systems are complex, holistic, unbalanced and thermodynamically open, in addition to being emergent and self-organising; hence, the normal analysis tools may not be used to address this complexity. Biological systems evolved from emergent mechanisms that "interact with themselves and produce themselves from themselves" (Sengupta, 2011).

Stoll and his colleagues (2013) presented an example of the biological network complexity "EWS-FLI1 effects on proliferation and apoptosis" as illustrated in Figure 2.1.

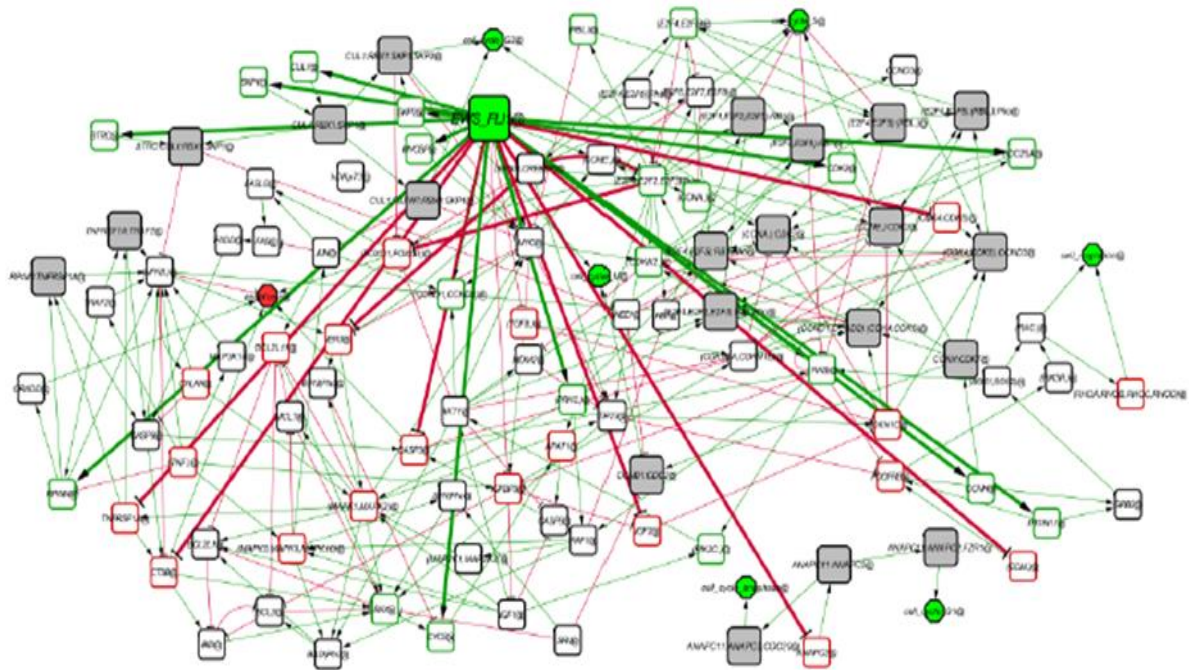


Figure 2.1 Network of EWS-FLI1 effects on proliferation and apoptosis (Stoll et al., 2013)

A second example has been provided by Kitano (2004); who illustrated the typically large scale of molecular systems as seen in the human Protein Interaction Network (PIN) in Figure 2.2.

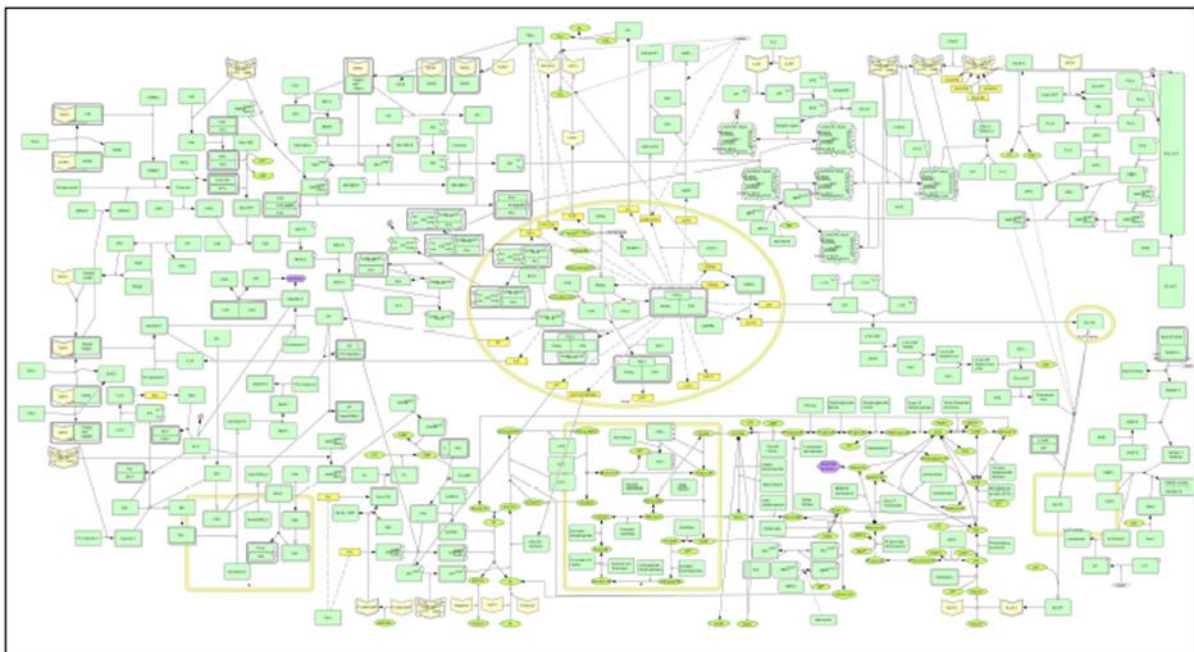


Figure 2.2 Large scale of the molecular system (Kitano, 2004)

A third example was provided by Takeshi Hase and his research team (2009) who illustrated human Protein Interaction Network (PIN)s topology and its statistical properties. They found that a human PIN structure was based on the number of high-degree and middle-degree nodes. Figure 2.3 illustrates the example.

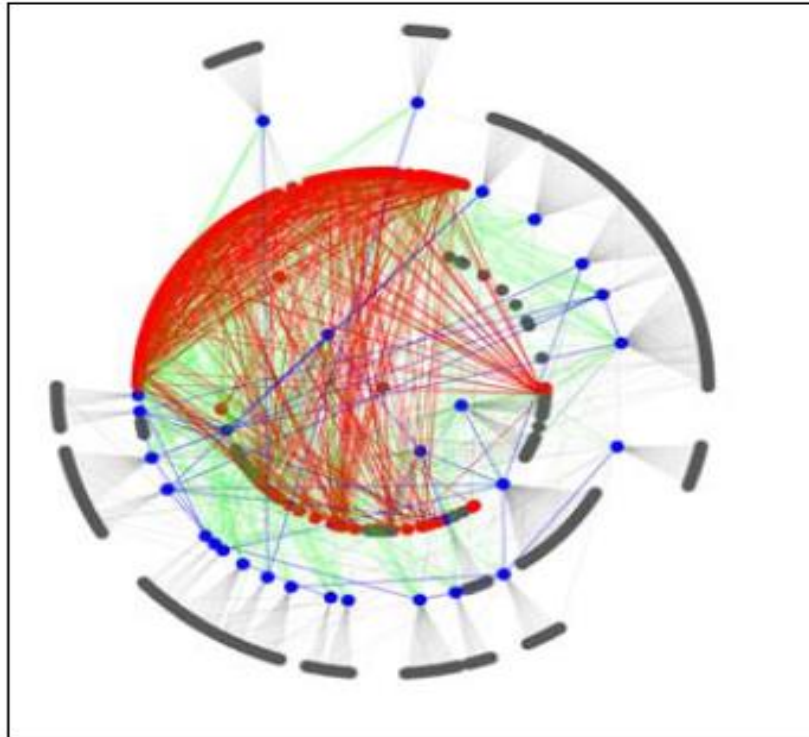


Figure 2.3 Cloud topology in the human PIN (Hase et al., 2009)

A complex network of protein interactions in the cell is the main characteristic of these interactions. Some idea of the complexity of protein interactions networks can be gained from Figure 2.4, which represents a map of some protein - protein interactions of the SCF ubiquitin ligase and other proteins (Alberts et al., 2010).

These networks interactions may involve tens of thousands of multi-dimensional protein complexes and tens of millions of protein sequences derived from the nucleotide sequences of genes. To increase our understanding of cells, researchers have proposed new methods to simulate these biological networks. Specifically, computer-based bioinformatics tools are being combined with modern experimental technologies to allow thousands of proteins to be investigated in a single set of experiments. Proteomics studies focus on the large scale analysis of proteins (Alberts et al., 2010).

Other manifestations of complexity in protein interactions include the fact that a typical protein in a human cell may interact with between five and 15 different molecules (Alberts et al., 2010).

To understand any function in cell cycle, we should draw the interactions in a diagram as a map (Kohn, 1999). The most popular method used to represent protein – protein interactions is through a protein interaction map; this is a graphical representation method.

Each protein is represented by an oval shape or box with arrows connecting the proteins that interact with each other. This aims to describe all the binding interactions between thousands of distinct proteins in a cell; this method is useful for small number of proteins, but when hundreds or thousands of proteins are represented on the same map, the network graph becomes bewilderingly complicated (Alberts et al., 2010). Much more useful is to divide the map into small subsections with a few proteins of interest. This leads us to the principle of abstraction and multiple levels in the organisation of proteins.

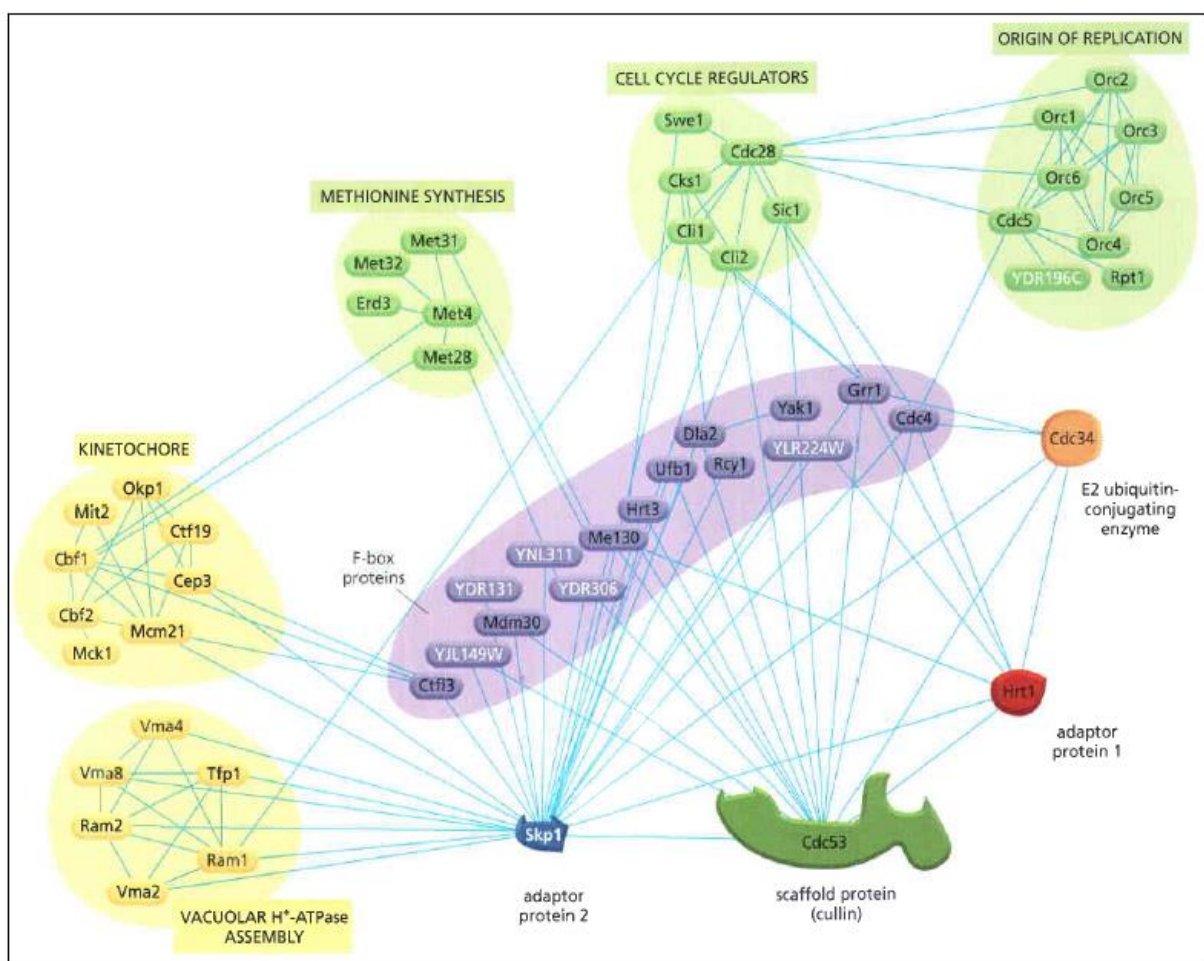


Figure 2.4 Map of some protein - protein interactions of the SCF ubiquitin ligase and other proteins (Alberts et al., 2010).

Kohn (1999) presents several reasons for using molecular interaction maps. Firstly, it is often difficult to keep in mind all the known interactions. Secondly, the maps can suggest new interpretations or questions for experimentation. Thirdly, the act of preparing a molecular interaction map imposes a

discipline of logic and critique in the formulation of functional models. Finally, the diagram convention provides a shorthand for recording complicated findings or hypotheses.

Figure 2.5 shows another example of the complexity of protein interaction networks. The p53-Mdm2 subsystem related to DNA repair. The figure shows the remarkable richness of p53 interconnections and the diversity of functionally determinant p53 modifications. Eleven phosphorylation or acetylation sites (or groups of sites) for which functionality has been determined are shown. If all these could occur independently, there would be 2000 possible modification states for the p53 monomers (Kohn, 1999). Kohn (1999) suggested that the molecular components are grouped in putative subsystems according to mutual interactions or functional coherence.

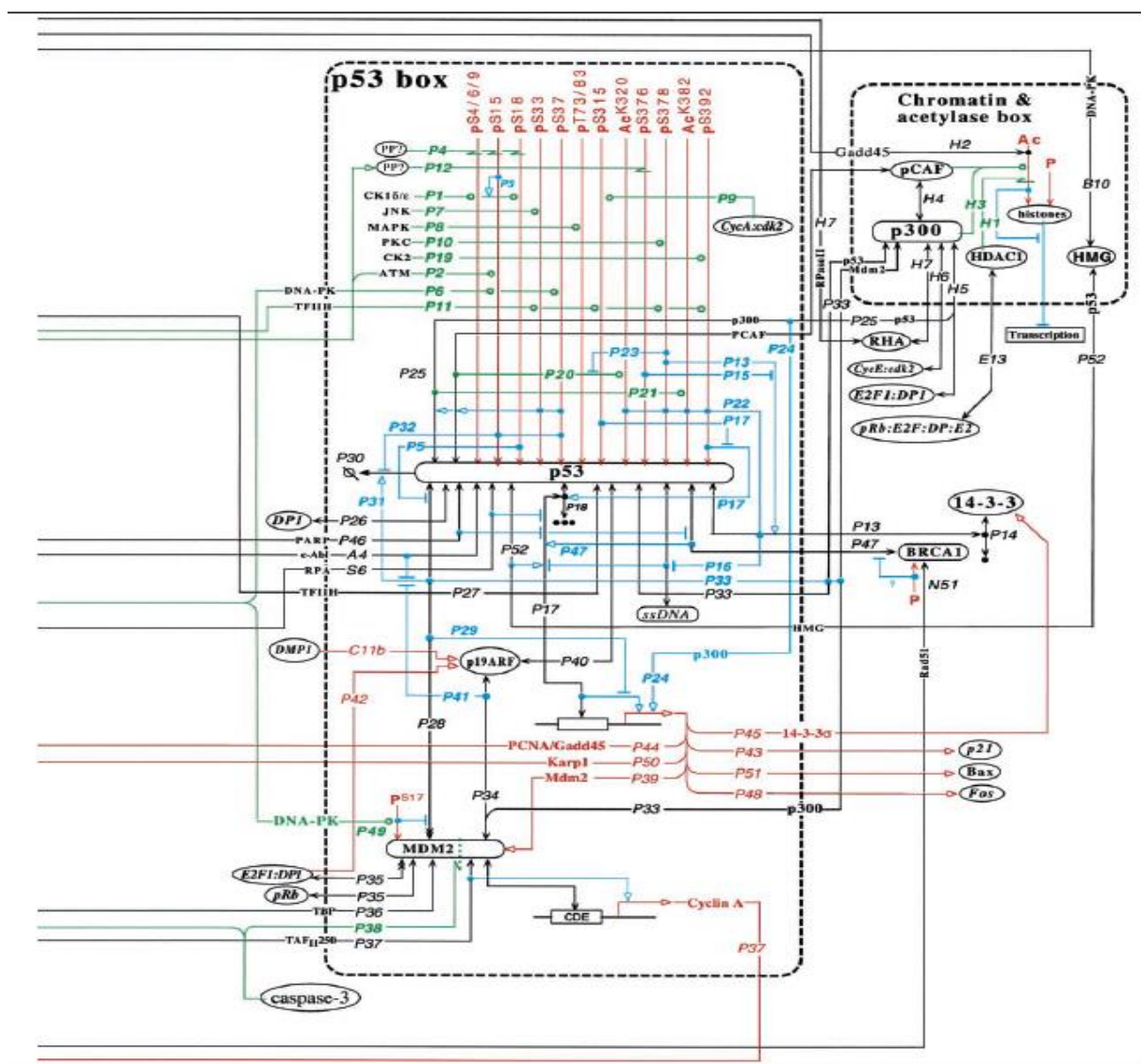


Figure 2.5 The p53-Mdm2 subsystem related to DNA repair (Kohn, 1999)

2.4 Mathematical Models of Biological Systems

The main aim of biological research is to understand the principles of organisation and functioning of biological systems, diseases or cellular disorders and the stresses that influence biology. A greater understanding of biological systems behaviour can be gained through a comprehensive biological model describing the many mechanisms and pathways of the cell (*e.g. a phenotype of an organism*). The model concept in molecular biology is well-recognised. For certain biological systems complexity is obvious by the difficulty in predicting the outcomes of disorders. The microscopic structure in biological systems is hard to recognise, so noticing system behaviour signifies a functional complexity within molecular components and interactions. Hence, imaginary models connecting macro and microscopic behaviour continue to be found. Biological models may be formulated and analysed by mathematical approaches, which serve as an inspecting eye and allow for logical viewing of unobservable molecular mechanisms by their macroscopic signs assuming adherence to basic laws that govern molecular interactions. Mathematical models, combined with experimental data from gene expression, protein abundance, metabolite concentration, or other biological parameters, are used when working with the complex biological networks.

Systems biology is a recently expanding research field and was led by scientists need to study the interactions of components (Yuan et al. 2008). Stelling (2004) said that model developments and experiments broadly enhanced our understanding of complex biological networks. These developments led to a large amount of data, including transcriptomics, proteomics and metabolomics. Biological systems functionality is not explained only by the common laws of biophysics and biochemistry, although they are fundamental for constructing biological models; molecular biology scientists are also confronted with the challenge of connecting basic laws of nature to biologically complex organisations.

System properties on a genomic level of a system are captured and described by biological networks; the process is illustrated in the Figure 2.6. Defining the components of genes and gene products of the system is undertaken by the genome, and small molecules, such as metabolites or metal ions, are also considered components of the system. Models may be structured by the data obtained from genes functionality, product and pathway knowledge and literature. This procedure was called systems biology bottom-up approach by Palsson (2006); and transferring transcriptomics, proteomics and metabolomics data into biological knowledge or conclusions obtained from mathematical models was called a top-down approach.

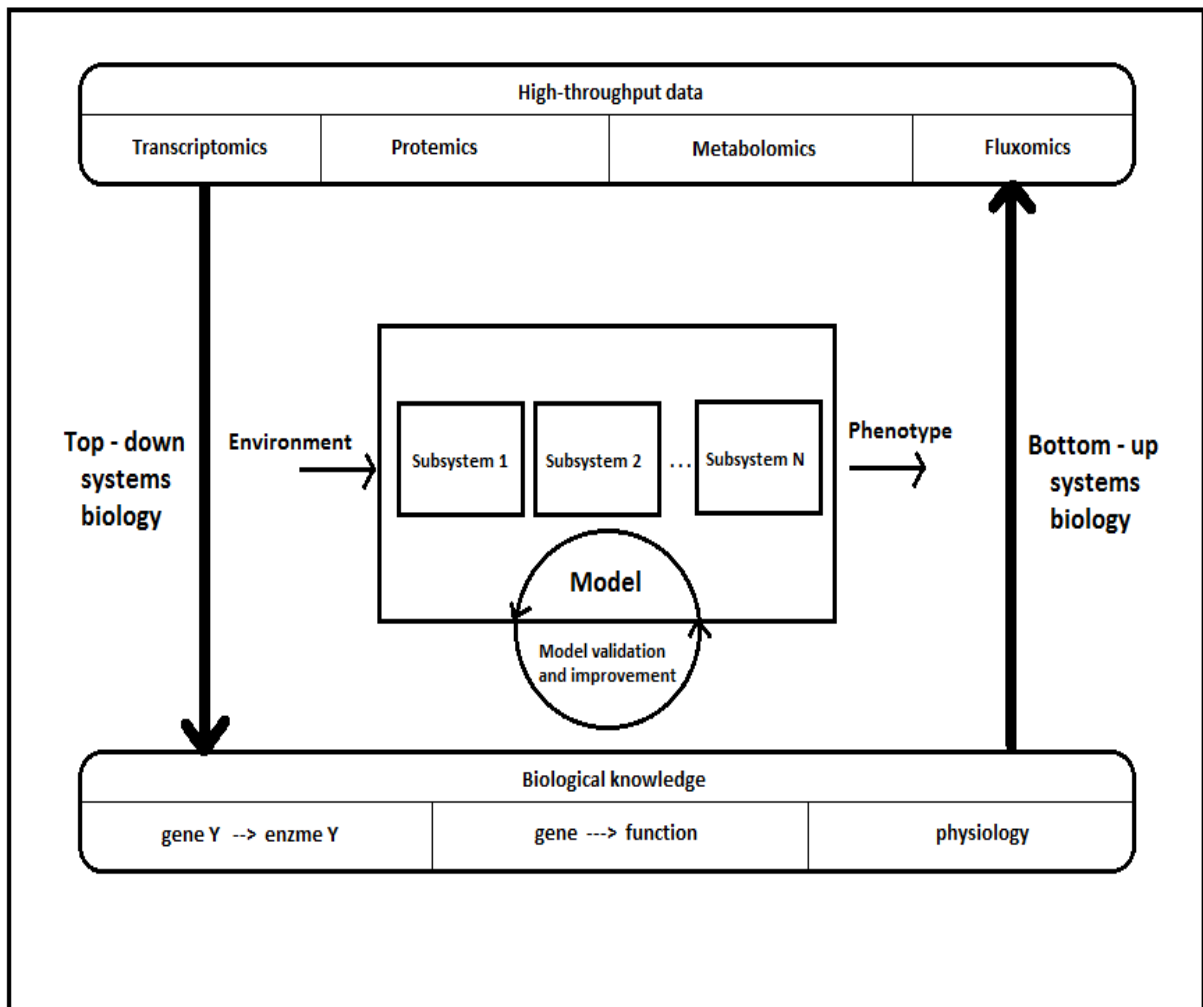


Figure 2.6 Interaction between systems biology and mathematical modelling

Mathematical modelling of biological research is necessary and useful. Researchers use it to analyse cellular networks or to invent strategies for controlling cellular dynamics which might be considered the cornerstone of development of therapeutic medical applications. A mathematical model is, basically a systematic analysis of a biological system that empowers quantitative predicting. Many scholars (such as: Endy & Brent, 2001; Hasty et al., 2001; Rao & Arkin, 2001; Kitano, 2002; Neves & Iyengar, 2002; Weston & Hood, 2004; You, 2004; Alves, 2006; Kholodenko, 2006; Ideker et al., 2006) have studied the combination of computing power and developed numerical methods to conduct the analysis of complex cellular networks dynamics and model simulation. Their studies explained the use of mathematical modelling to understand complex biological systems where prediction on its own was not sufficient. Although mathematical modelling proved beneficial for basic and applied biological modeling, many challenges were encountered by researchers in structuring and analyzing; when biological modelling was accompanied by assumptions on behalf of the modeller's goals. Lack of detailed, quantitative biological information is a challenge faced by modeller's.

The types of mathematical modelling are various and are widely used. In the next sections of this chapter, kinetic models that represent systems of coupled chemical reactions are discussed. Further, construction of mathematical models of complex cellular networks is illustrated, mathematical representations used to describe cellular networks are highlighted and common methods of analysing of modelling outcomes are discussed.

A set of ordinary differential equations that describes the dynamics of metabolites in a reaction network comprise the kinetic models of biochemical reaction networks. Complex biological networks involve many enzyme-catalysed processes with non-linear kinetics and intricate stoichiometric and regulatory interactions between enzymes. As a result, their mathematical models include sets of coupled rational differential equations of high-dimension, and to analyse them maximum computational efforts are required.

Previous experimental data, when compared with system simulation results, validate models. Model simulations give optimal flux distribution, which may be compared with the measured flux distributions or phenotypic data, such as growth rate, glucose uptake rate, product formation rate, etc. (Pramanik & Keasling, 1997; Price et al., 2004). Modelling is a process to improve the model until it reaches good agreement with experiments.

Construction of models of biological systems reactions passes through the steps of construction, validation and refinement, it is a repetition process as illustrated in Figure 2.7. The steps are then repeated until the model reaches an adequate equivalent level (Lee et al., 2007).

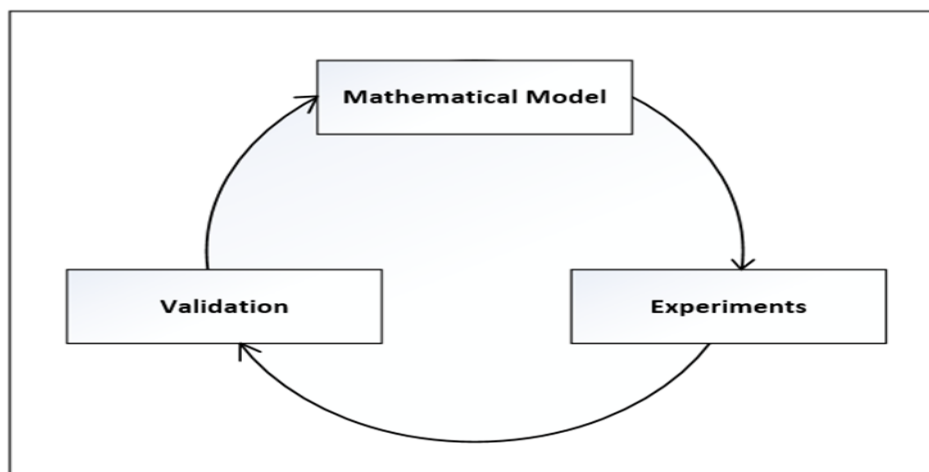


Figure 2.7 Refining models of biological networks

Mathematical models simulating biological systems that are used include: ordinary differential equations (ODEs), delay differential equations (DDEs), partial differential equations (PDEs), agent-based models (ABMs), and stochastic differential equations (SDEs). Biological modelling examples are

provided in the discussion to help understand the dynamics of cell regulation; these models and examples are discussed briefly in the following sections:

2.4.1 Ordinary Differential Equations (ODEs)

Ordinary differential equations are the most common type of equations used for biological networks modeling. They have been applied in studying reaction kinetics and other physical phenomena. Mathematical analyses of ODE systems are suited to limited dimensional dynamical systems and they are relatively simple compared with the other types, and their computational simulation solutions are efficient (Kim et al., 2009).

2.4.2 Delay Differential Equations (DDEs)

Delay differential equations are unlimited dimensional dynamical systems and they need more computational and analytical complexity; however, their advantages are unique. DDE systems are simple, except for their time delays. DDE models explain the effects of these delays on the biological processes; their complexity is a little bit harder to simulate than the ODEs. The evaluation of DDEs has decreased to recording the history of all populations through the simulation. The slight increase in DDEs computational complexity expands the collection of the phenomena widely (Kim et al., 2009).

2.4.3 Partial Differential Equations (PDEs)

Partial differential equations are more complex compared with DDE and ODE. This type is implemented in age structured and spatio-temporal biological models. Age structured models explain individual cells or member's advancement by a scheduled development process. Age structured models offer an internal modelling frame for organisms over time, because an organism's behaviours depends on the level of maturity and development. This type is considered the most powerful mathematical modelling approach, although it requires more computational processes than the other types mentioned (Kim et al., 2009).

2.4.4 Agent-based Models (ABMs)

This type addresses unique and discrete agents, such as individual cells and molecules. ABMs explain biological interactions probabilistic or stochastic uncertainty within large populations. An individual cell in a stochastic model changes the state or the location with a certain probability and accounts for its agent's movement in space. Computational complexity of ABM is typically huge. An individual simulation of this model can take a long time to process, up to several days. ABMs should be simulated several times to achieve the overall average behaviour of the systems (Kim et al., 2009).

2.4.5 Stochastic Differential Equations (SDEs)

If models were arranged on a straight line, the stochastic differential equations model would be mediating them in terms of complexity. This model resembles ODEs in its formula, except that its values are random. It works on populations rather than individual agents. This model can explain noise, random walks and irregular events, it is used in finance, mathematics, chemistry and physics (Kim et al., 2009).

After having discussed the models of ODEs, DDEs, PDEs, ABMs and SDEs the question of "which modeling approach is more appropriate?" arises. The answer to this question relies on the organisational interactions involved, among other issues.

The most efficient modelling method of biological complexity is ODE; it does not require a large amount of computational work. This approach is suitable and effective when delayed feedback, spatial distributions of the cell or probabilistic events are not what the network rely on but, if networks rely on delayed feedback, then the DDE is a better choice.

When cells and molecules were studied, the best approach would be PDE for the cells that do not efficiently blend or confine themselves over long durations; also, when gradual changes of behaviour occurs because of maturity or age, PDEs are the solution. SDEs add stochasticity to differential equations and they are more complex computationally.

ABMs usage has recently increased as, at present it offers the most complex framework of mathematical modeling. It combines all spatial and temporal dynamics elements, probabilistic events, and individual diversity within populations, but it requires focused computational algorithms, so it is considered impractical for statistical analyses. ABMs reproduce the complexity of biological systems and thus help reduce financial cost of the experiments due to silicon usage rather than experimenting with living organisms. By doing so, experimental studies are transferred from wet laboratories into computer laboratories, even though they do not replace other modelling types. This is because they fail to reduce biological systems complexity, while hybrid methods that combine ABMs and differential equations are efficient in capturing the biological network features without adding extra unnecessary details.

Predicting the most suitable mathematical and computational paradigm is very difficult. To understand a biological system deeply, all the previous types should be consulted. But this is not reasonable; instead, once each type's abilities and limitations are understood then the type that determines accurately the system's essential dynamics without adding unnecessary complexity is selected.

2.5 Reduction Methods for Biological Systems

Interest in complex models and datasets of biological systems has increased recently. The issue of simplifying them to control/manage their behaviour is important (Zinovyev, 2014). Complex spatial and temporal behaviour of molecular systems may be reproduced by a small dynamic model that includes tens of variables. If a comprehensive description is required for high productivity data, the dynamic model is rendered ineffective (Danos et al., 2007).

In biochemical reaction networks researchers use ordinary differential equations (ODEs) models to describe the dynamic behaviour of the system. Most of these models have high dimensional complexity (contain large numbers of species and reactions) and nonlinear behaviour. For this reason, many methods for model reduction are needed to simplify complex models. The behaviour of the reduced model should be like the behaviour of the original model.

In this section, many approaches of model reduction are addressed. There are several techniques of model reduction in use with biochemical reaction network models to reduce their complexity.

Quasi-steady state approximation (QSSA) is the most famous approach of model reduction used with biochemical kinetics. The pseudo steady state hypothesis (PSSH) is another name for this approach. In 1913, Bodeustein proposed the main idea of the quasi-steady state approximation (Bodenstein, 1913). This idea was later used to produce the classical Michaelis Menten formula (Michaelis and Menten, 1913). More development and improvement were achieved on this method to be the basic tool to analyse the behaviour of chemical reaction mechanisms and kinetics (Semenoff, 1939; Christiansen, 1953; Helfferich, 1989). In 1983, Segel and Slemrod elaborated the quasi-steady state assumption method in the case of perturbation (Segel and Slemrod, 1989). The QSSA idea may be summarised as follows: if an intermediate species in the model has not changed considerably with time or the difference between the rates of production and consumption is small then; the model may be reduced.

Another approach to model reduction is the geometric singular perturbation method (GSPM). This is useful when the models have slow and fast variables. This approach works based on the assumption that when the model contains fast and slow variables, and the slow variables control the fast variables, so we can remove the fast variables from the model (Tikhonov, 1952; Fenichel, 1979; Jones, 1995).

Another common approach of model reduction is quasi-equilibrium approximation (QEA) or the rapid equilibrium approximation (REA). The first appearance of this idea was in 1973 by Vasiliev and his colleagues (Vasiliev et al., 1973). Later, many studies provided further explanation and clarification of the approach as an approach for model reduction (Volpert and Khudyaev, 1985; Lee and Othmer, 2010; Noel et al., 2012).

The quasi-equilibrium approximation approach has two formulations. The first is based on equilibration of fast reactions; while the second, is based on the conditional entropy maximum (thermodynamic approach). To know more see Schnell and Maini (2002). In the Schnell and Maini study the quasi-equilibrium approximation was applied to a kinetic model of a single enzyme substrate reaction.

Another trend in the reduction is applied to chemical reaction models based on the concept of a limiting step. A limiting step is defined as "A rate-controlling (rate-determining or rate limiting) step in a reaction occurring by a composite reaction sequence is an elementary reaction, the rate constant for which exerts a strong effect stronger than that of any other rate constant on the overall rate" (Gorban & Radulescu, 2008). In a limiting step reduction approach, we focus more on a rate constant that effects the overall rate more significantly than all other rate constants. Many of researchers studied and extended the idea of limiting step (see Johnston, 1966; Boyd, 1978; Murdoch, 1981). Recently, a general theory of static and dynamic limitations for linear multi-scale networks was developed by Gorban and other researchers (Gorban and Radulescu, 2008; Gorban et al., 2010).

In 1963, Kruskal defined the idea of "asymptotology" as "the art of handling applied mathematical systems in limiting cases" (Kruskal, 1963). This idea plays an important role in model reduction, and it produced the quasi-equilibrium asymptotic (QE) and the quasi-steady state asymptotic (QSS) approaches, the most common approaches for model reduction. They worked on the separation of small and large terms in the model whereby the small terms can be removed from the model in some cases.

Asymptotology simplifies biological systems in several methods. According to Zinovyev (2014) asymptotic method simplifies model equations and makes them more traceable; determines a model's parameters and their relation to the parameters of the complete model; breaks down model complexity into simple models and matches every biological observation with the possible asymptotic model dynamics; predicts the varying methods between different asymptotic behavioural modes and finally, decides whether a mathematical model is complex, or it is merely complication.

Recently, based on static and dynamic limitation in multi-scale reaction networks, a new technique was proposed to reduce complex chemical networks. The complex network and the reduced network have the same behaviour (Gorban and Radulescu, 2008; Gorban et al., 2010). The reduced network or what is called the dominant system (DS) is defined as "a minimal dynamic system." Sometimes the DS is considered a sub-system of the original system but in other times it is not because it may include new reactions.

Radulescu and his colleagues (2008) proposed three techniques to reduce the NF- κ B pathway model when they wrote about robust simplifications of multi-scale biochemical networks. In the first technique, they used a reduction algorithm based on a generalised method of a limiting step to simplify linear kinetic models. In the second technique, they used a reduction algorithm based on dominant solutions of quasi-stationarity equations (QSE) to simplify nonlinear kinetic models. In the last technique, they used a reduction algorithm based on combining the ideas of quasi-stationarity and averaging to simplify oscillating kinetic models.

Castiglione and his colleagues (2014) stressed the importance of multi-scale modelling of biological systems to resolve the challenges of large amount of measurements required in modern biology. The importance of these manifests when developing comprehensive computational and mathematical models for a system with different spatial and time scales. For instance, they used multi-scale modelling on the immune system.

In another study, Rao and other researchers proposed a Kron reduction of the weighted Laplacian matrix, which describes the graph structure of the complexes and network reactions. The method is based on a variety of reversible and irreversible enzyme kinetic rate laws. It uses a stepwise reduction in the number of complexes from the left- and right-hand sides of the reactions and maintains the behaviour of the original model. The method was applied to a yeast glycolysis model and a rat liver fatty acid beta-oxidation model. The difference between metabolite concentrations in the reduced and the full model was 8% and 7.5%, respectively, for the two cases. The number of species in the yeast model was reduced from 12 to 7, and the number of species in the rat-liver beta-oxidation model was reduced from 42 to 29 (Rao et al., 2014).

Another reduction approach has been proposed and used to reduce the kinetic models of the nuclear factor kappa B network (NF- κ B). In this approach, the algorithm uses the speed coefficients to eliminate fast variables. To know more about this approach, see West et al. (2015). Kooshkbaghi and his colleagues proposed a systematic technique for eliminating non-important species from the model based on the relative contribution of each elementary reaction to the total entropy production (Kooshkbaghi et al., 2014). Further studies of model reduction with examples of application from systems biology can be found in Petzold and Zhu (1999); Gay et al. (2010); Anderson et al. (2011); Karadeniz et al. (2012); and Ishizaki et al. (2014).

Gorban and his colleagues (2004) produced two reduction methods. For slow manifolds, they produced invariant grids for computing approximations. To describe the network of monomolecular reactions they produced a reduction system of equations if the kinetic constants were well-separated. These two methods are correlated with quite abstract mathematics such as tropical algebras and model tropicalisation, or with dominant system notions in dynamical systems (Gorban et al., 2004).

Another reduction method was proposed by Radulescu and his colleagues (2012). They suggested some essential ideas such as dominance and limitation, for greater understanding of dynamical and computational biological systems (Radulescu et al., 2012). The methods of averaging approximation and invariant manifolds proved their effectiveness in reducing the asymptotic dynamics of chemical reaction networks with clear time-scale separation. Many studies have provided further explanation on how to calculate invariant manifolds. According to Gorban and Karlin (2005), the slow mode dynamics are carried by invariant manifold that results from the relaxation of fast variables. For more information see Roussel and Fraser (1991); Gorban and Karlin (2003); Krauskopf et al. (2005).

Kutumova and his colleagues (2013) proposed a new method for model composition. It was based on reducing several models to the same level of complexity and then combining them together. They defined a model of minimal complexity as the simplest model that may be obtained from a complex model, by using a group of model reduction techniques that can approximate the experimental data. The method was tested on two models describing cell fate decisions between NF- κ B mediated cell survival and apoptosis. The reduced model proved to lead to the same dynamical behaviour of observable measures and to the same predictions as the complex model. The newly composed model summarised several experimental datasets. These datasets calibrated the original models separately, but they had dynamical features that allowed formulating new verifiable predictions.

Several other methods have also been used for reducing chemical reactions networks. For instance, Noel and his colleagues (2012) reduced and hybridised networks of biochemical reactions using the Litvinov-Maslov correspondence principle. They applied this method on a cell cycle oscillator model. Lam and Goussis (1994) implemented a singular computational perturbation. Maas and Pope (1992; 1994) used an intrinsic low dimensional manifold to exploit the interval between timescales of models' various processes and variables.

The lumping technique was studied by Wei and Kuo (1969). This technique works based on combining reagents into quasi-components for reducing the system size in monomolecular and pseudo monomolecular systems (Wei and Kuo, 1969). Many researchers have developed and applied the lumping technique in many chemical reaction problems; see Genyuan (1984); Li and Rabitz (1989); Li and Rabitz (1990); Li and Rabitz (1991); Li et al. (1994); Dokoumetzidis and Aarons (2009).

Another reduction method was proposed by Nagy and Turányi (2009). They developed a new species reduction method called the simulation error minimisation connectivity method (SEMCM). The method works according to SEM-CM and the principal component analysis of matrix F with simulation error minimisation (SEM-PCAF). These processes present an efficient way to eliminate redundant species and reactions from large chemical reaction systems.

Another reduction model method for computational biology was presented by Radulescu and his colleagues (2015). This method was inspired by tropical geometry and analysis that combines graphical approaches, semi-quantitative reasoning and symbolic manipulation, but does not explain the combination method of one-scale approximations to obtain a multi-scale approximation that is valid for both fast and slow time scales.

In a recent study, Sun and Medvedovic (2016) used the Rao-Blackwellised particle filters (RBPF) decomposition methods technique to reduce the dimensions of the dynamic model and improve estimation accuracy. Some familiar parameters and structure of the system were used as a priori knowledge and incorporated into a dynamic model. Consequently, the two researchers decomposed the whole dynamic model into sub-set network modules, and then applied different estimation approaches. They used experimental data of the JAK-STAT pathway and synthetic data generated from the repressilator model as a case study.

Model reduction approaches presented in this chapter can be divided into four main categories as shown in Table 2.2.

Table 2.2 Categories of the reduction methods

Method	Refers to	How it works	Suitable for	Advantage	Disadvantage
Timescale exploitation	Methods that use large differences in reaction rates that can occur within a biochemical system.	Divides the system into fast and slow components. After an initial transient period, the fast portions settle for the remainder of the operation of the network.	Singular perturbation, intrinsic low dimensional, singular computational perturbation, stiff and nonlinear systems.	Maintains species biological meaning.	May fail in justifying reduction due to short time-scale separation. Computationally expensive if slow/fast partitioning is not known.
Optimization and sensitivity analysis	Methods that obtain the lowest possible dimensional model, where an error metric stays at an acceptable level	Either it measures the sensitivity degree to perturbations and uses it to guide a reduction, or it employs an iterative optimisation procedure.	Very high dimensional, stiff and nonlinear systems.	Maintains species biological meaning, highly algorithmic and computationally efficient for small systems, common procedures implement well in software packages.	Highly computationally expensive for large systems. May be impossible to achieve convincing sensitivity analysis
Lumping	Methods that constructs a reduced state-variables system corresponding to sub-sets of original species	By two approaches: proper lumping (each original species corresponds to one, at most, lumped state) and improper lumping (each original species corresponds to one or more lumped state)	Very high dimensional, stiff and nonlinear systems.	Common in reduction of chemical kinetic systems. Algorithmic approaches. Biological meaning is maintained.	Computationally expensive for large systems. Better reduction is achieved by nonlinear and/or improper lumping techniques, but this may lead to loss of biological meaning.
Singular value decomposition	Singular value decomposition.	Approximates the matrix via one of a lower rank.	Balanced truncation that reduces the model and preserves the input-output relationship.	Controls theoretical description. Fits systems pharmacology. Highly algorithmic. Potential automation in a straightforward manner. May be a priori error bound.	Biological meaning is lost, only inputs and outputs preserve meaning. Standard approach exists for linear models – but generalisations for nonlinear systems exist. Highly computationally expensive for large systems.

Table 2.3 shows some articles that explain and use different reduction methods.

Table 2.3 Reduction methods and title of some related articles

Reduction Method	Based on	Title	Author
Numerical Methods	Computational singular perturbation (CSP)	The CSP method for simplifying kinetics.	(Lam & Goussis, 1994)
	Intrinsic low dimensional manifold (ILDM)	Simplifying chemical kinetics: intrinsic low-dimensional manifolds in composition space. Laminar flame calculations using simplified chemical kinetics based on intrinsic low-dimensional manifolds. Invariant manifolds for physical and chemical kinetics. Asymptotology of chemical reaction networks.	(Maas & Pope, 1992) (Maas & Pope, 1994) (Gorban & Karlin, 2005) (Gorban et al., 2010)
Formal Methods	Lumping and graphical reduction methods	General method for simplifying chemical networks while preserving overall stoichiometry in reduced mechanisms. Internal coarse-graining of molecular systems. Reduction of dynamical biochemical reaction networks in computational biology. A graph-theoretical approach for the analysis and model reduction of complex-balanced chemical reaction networks. A model reduction method for biochemical reaction networks.	(Clarke, 1992) (Feret et al., 2009) (Radulescu et al., 2012) (Rao et al., 2013) (Rao et al., 2014)
	Symmetry	Exploiting symmetry in temporal logic model checking. Noisy dynamic simulations in the presence of symmetry: data alignment and model reduction	(Clarke et al., 1996) (Sunday et al., 2013)
	Tropical analysis	Tropical geometries and dynamics of biochemical networks application to hybrid cell cycle models. Model reduction of biochemical reactions networks by tropical analysis methods.	(Noel et al., 2011) (Radulescu et al., 2015)

To find out which approach to model reduction is the most popular, we searched Google. Table 2.4 shows the number of links to every reduction method.

Table 2.4 Number of links to the well-known reduction method. (From Google as of 15th May 2017)

Reduction Method	# of Links in Google
“Quasi–steady state”	461,000
“Pseudo–steady state”	108,000
“Quasi–equilibrium”	255,000
“Geometric singular perturbation”	13,500
“Singular perturbation”	574,000
“Invariant manifold”	61,400
“Rate-limiting step”	712,000

As shown in Figure 2.8, the “rate-limiting step” has the largest number of links and the “geometric singular perturbation” has the smallest number of links.

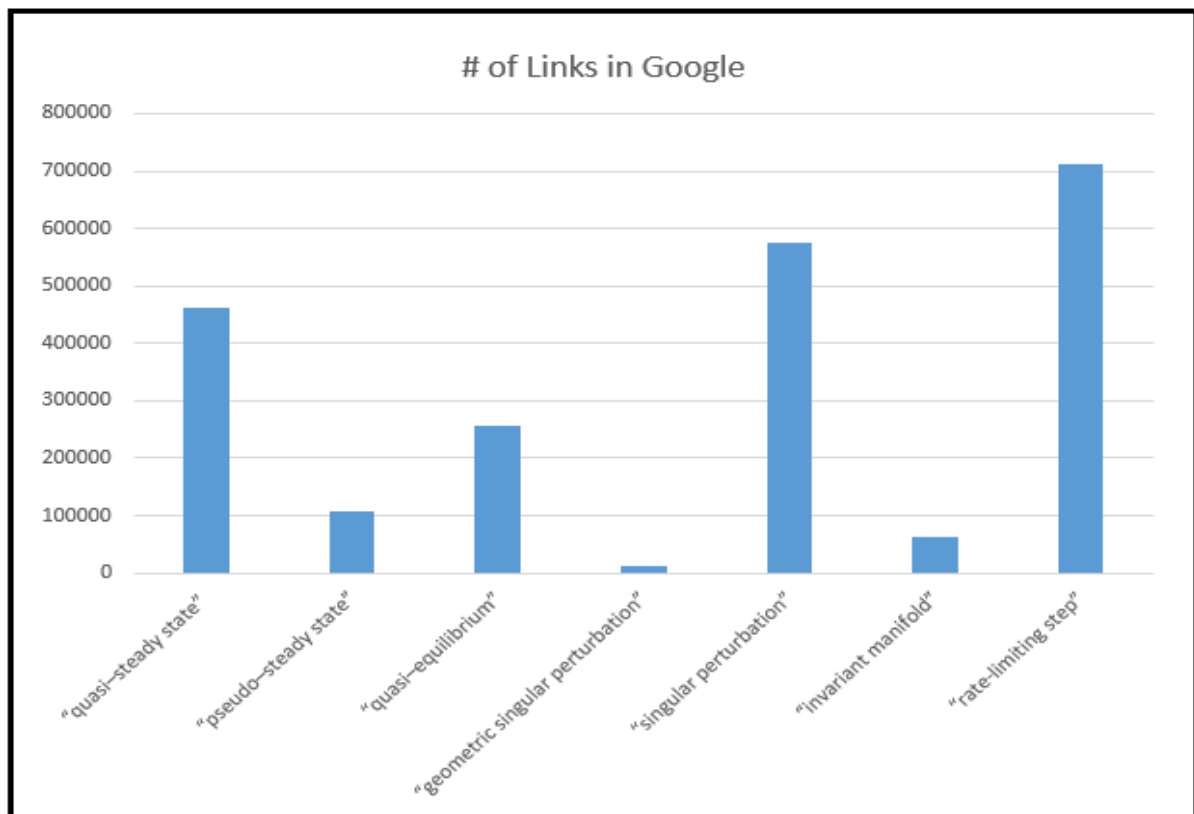


Figure 2.8 Number of links to the well-known reduction methods on Google

2.6 Summary of the Chapter

As shown in Figure 2.9, there are three dimensions of complexity in biological network models: number of species, number of interactions and model run time. If we want to reduce biological network models, we need to reduce one or more dimensions of model complexity. We can reduce the number of species by removing noise from the model (the ineffective elements) or using lumping. Another

trend was to reduce number of species by their similarity of behaviour. Moreover, reducing the number of species led to a reduction in the number of interactions by default.

Some researchers reduced the number of interactions by paying attention to the issue of fast and slow interactions, as mentioned in Section 2.5. Also, if we want to reduce the model run time we should look at the model as a play and the species as actors on the stage. The play consists of several scenes. Often each scene contains a limited number of actors (under the lights) and not all of them. The same idea is applicable to the model, it divides the model run time into time slices or windows and then two options emerge: the first option; is to remove the time windows that are not active or have little activities (steady window), and keep the time windows where most of the activities are. The second option, finds a sub-model for every time window that contains only the active species that play an active role at that time.

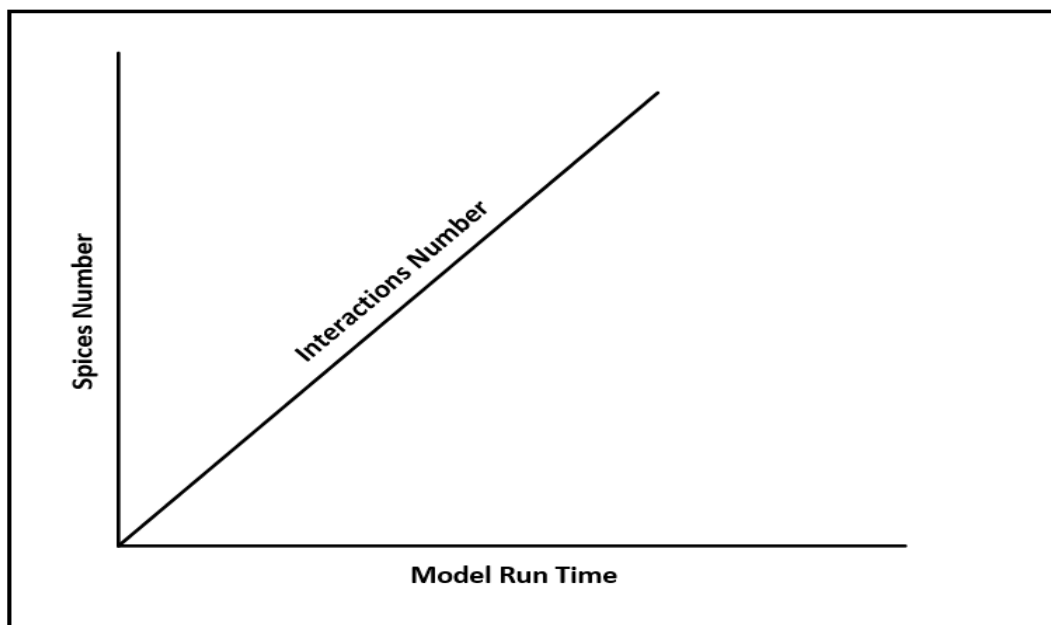


Figure 2.9 Dimensions of biological network model complexity

Another trend in reduction is reducing the model mathematically, as mentioned in Section 2.5. It is more effective with linear systems; however, most biological systems are nonlinear.

Another reduction can be obtained by converting the biological model from the ODE form to a Boolean form and use special software that converts the status of the species through time (active 1, inactive 0) into a continuous curve by knowing the highest and lowest concentration a species can reach.

Finally, we can combine more than one idea; for example, incorporating the idea of reducing the number of species by lumping using time windows or merging the idea of using time windows with the

idea of converting the model from an ODE to a Boolean form. All previous trends depend mainly on our deep understanding of biological systems and the dynamics in which they operate.

For the purpose of the current study, the biological network model reduction is defined as any method designed to decompose the original model into smaller models that produce the same behaviour as the original model, by reducing one or more dimensions of biological network model complexity (reduce the number of species, reduce the number of reactions or reduce the model run time).

As seen in Section 2.5, there are many reduction methods but a fully formal method for systems with orders of magnitude larger volume of variables is missing.

An overview of the reduction methods in Section 2.5 yielded the following conclusions:

- The literature review demonstrated the existence of a wide range of reduction methods.
- Methods of model reduction have no "one size fits all."
- Many of the methods are computerised, but it is the modeller's responsibility to select the best method based on the research question.
- The purpose of using a certain model determines its appropriateness, such as simulation time or speed.
- Model reduction methods may produce significant reductions and still maintain accuracy.

All these previous conclusions indicate the need for developing reduction methods for mathematical models that are applicable to large networks of biochemical interactions.

This research proposes two reduction methods to simplify the corresponding complex ODE mathematical models. The first reduction method based on a hierarchical representation and lumping approach to reduce protein-protein interaction (PPI) networks provides possibility to zoom in and out several levels of complexity which is attractive for analysing biological networks. So, this makes it unique compared to the existing reduction methods. And the Second reduction method uses a time windows for identifying active and inactive periods of a system and Logical models to further simplify a model. This reduction method is the first method that combined Boolean models and time windows to reduce the complex biological models for promising outcomes. So, this make the second proposed reduction method unique compared to the existing ones.

The proposed reduced techniques will help researchers to build a comprehensive biological network and gain a greater understanding of the emerging properties of cellular activities.

Chapter 3

Biological Background

The previous discussion focused on, but was not limited to, complex systems and the struggle with complexity using reduction techniques. In this chapter we give a brief review of the biological background especially the cell cycle, with more consideration and focus on the G1/S checkpoint and DNA damage pathways as a complex system, to use as a case study to apply a new reduction approach, in Chapter 4.

The biological background is organised as follows: Section 3.1 gives a brief review of a cell general review; Section 3.2 discusses the cell cycle, the regulation of the cell cycle, (DNA damage and cancer) and the G1/S checkpoint; Section 3.3 presents the details of the G1/S checkpoint and models. Section 3.4 discusses the DNA damage signalling pathway and the cell cycle regulation (integrated between G1/S and G2/M) model of Iwamoto et al. (2011).

3.1 The Cell: General Review

The cell is the basic unit of life. It represents the smallest level of a living organism. All organisms are composed of one or more cells. Humans are made up of many millions of cells. Cells exist in bacteria, animals and plants. Many of the basic structures are found inside all types of cells and the way these structures work are, fundamentally, very similar, so the cell is said to be the basic unit of life.

It was in 1839 that cell theory was developed by Matthias Jakob and Theodor Schwann (Vasil, 2008). This word 'cell' means a small room and it comes from the Latin *cellula*. Robert Hooke published a book in 1665 coining this descriptive term for the smallest living biological structure (Gest, 2004).

Since then, cells have been classified into two categories: eukaryotes and prokaryotes (Sagan, 1967) (Figure 3.1). Cells from eukaryotic organisms differ from prokaryotic organisms in a large number of characteristics (Table 3.1). Scientists categorise organisms based on shared characteristics into groups called taxa. "Prokaryotic" is a characteristic of organisms in two taxa: Domain Archaea and Domain Bacteria (Bouman, 2007).

Eukaryotes are cells that contain chromosomes, such as humans, plants and animals. They have a nucleus that stores their genetic information. Prokaryotes are cellular organisms that do not have a real nucleus. The nucleus is the control centre of a cell. It contains the genetic material packed into chromosomes and is associated with other organelles that function in the production of amino acids

and proteins based on what the genetic material dictates. Human cells have 46 chromosomes (23 pairs) (Tjio & Puck, 1958; Nowell & Hungerford, 1960).

Prokaryotes have some genetic material, but it is not the same as in eukaryotes. However, prokaryotes are still able to reproduce. Examples of these cells are bacteria and blue-green algae.

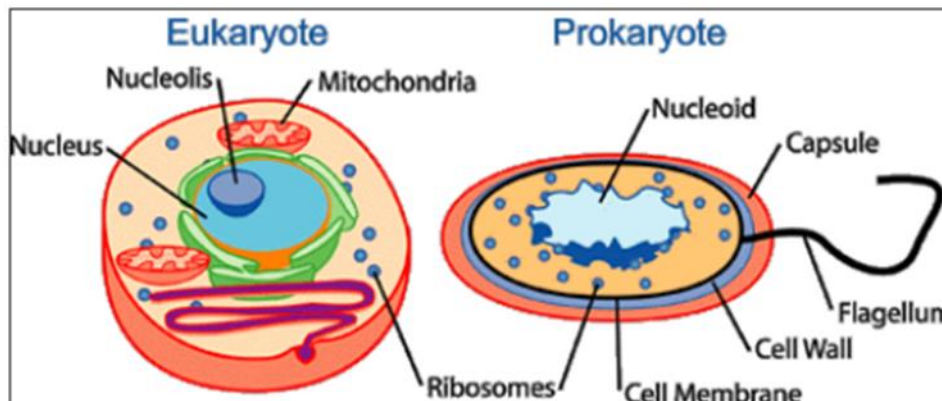


Figure 3.1 Differences between prokaryotes and eukaryotes. Source: NCBI (National Centre for Biotechnology Information) www.ncbi.nlm.nih.gov

The hereditary material in humans is deoxyribonucleic acid (DNA) (Calladine & Drew, 1997). DNA is the same in every cell of the human body and most DNA is located in the cell nucleus (where it is called nuclear DNA), but a small amount of DNA can also be found in the mitochondria (where it is called mitochondrial DNA or mtDNA).

The information in DNA is stored as a code made up of four chemical bases: cytosine (C), adenine (A), thymine (T) and guanine (G). Human DNA consists of about three billion bases, and more than 99 percent of these bases are the same in all people. These bases determine the information available for building and maintaining an organism as their sequence is like the way in which letters of the alphabet appear in a certain order to form words and sentences (Popovici, 2010).

DNA bases pair up with each other, A with T and C with G, to form units called base pairs. Each base is also attached to a sugar molecule and a phosphate molecule. Together, a base, sugar, and phosphate is called a nucleotide (Figure 3.2). Nucleotides are arranged in two long strands that form a spiral called a double helix. The structure of the double helix is somewhat like a ladder, with the base pairs forming the ladder rungs and the sugar and phosphate molecules forming the vertical sidepieces of the ladder. An important property of DNA is that it can replicate, make copies of itself. Each strand of DNA in the double helix can serve as a pattern for duplicating the sequence of bases. This is a critical point when cells divide because each new cell needs to have an exact copy of the DNA present in the old cell.

Table 3.1 Summary features of prokaryotic and eukaryotic cells (Bouman, 2007)

Comparison of archaea, bacteria and eukaryotic cells			
Characteristic	Archaea	Bacteria	Eukaryotes
Nucleus	Absent in all	Absent	Present in all
Free organelles bound with phospholipid membranes	Absent in all	Present in a few	Present, include ER, Golgi bodies, lysosomes, mitochondria, and chloroplasts
Glycocalyx	Present	Present as organised capsule or unorganised slime layer	Present, surround some animal cells
Motility	Present in some	Present in some	Some have complex undulating flagella and cilia composed of a "9+2" arrangement of microtubules; others move with amoeboid action using pseudopodia
Flagella	Some have flagella, each composed of basal body, hook, and filament; flagella rotate	Some have flagella, each composed of basal body, hook, and filament; flagella rotate	Present in some
Cilia	Absent in all	Absent in all	Present in some
Fimbriae or pili	Present in some	Present in some	Absent in all
Hami	Present in some	Absent in all	Absent in all
Cell wall	Present in most, lack peptidoglycan	Present in most, composed of peptidoglycan	Present in plants, algae, and fungi
Cytoplasmic membrane	Present in all	Present in all	Present in all
Cytosol	Present in all	Present in all	Present in all
Inclusions	Present in most	Present in most	Present in some
Endospores	Absent in all	Present in some	Absent in all
Ribosomes	Small (70S)	Small (70S)	Large (80S) in cytosol and on ER, smaller (70S) in mitochondria and chloroplasts
Chromosomes	Commonly single and circular	Commonly single and circular	Linear and more than one chromosome per cell

The most important characteristic of a cell is that it can reproduce by dividing. If cells did not reproduce, no living thing would continue to live. Cell division is the process by which cells duplicate and replace themselves and this process is called the cell cycle.

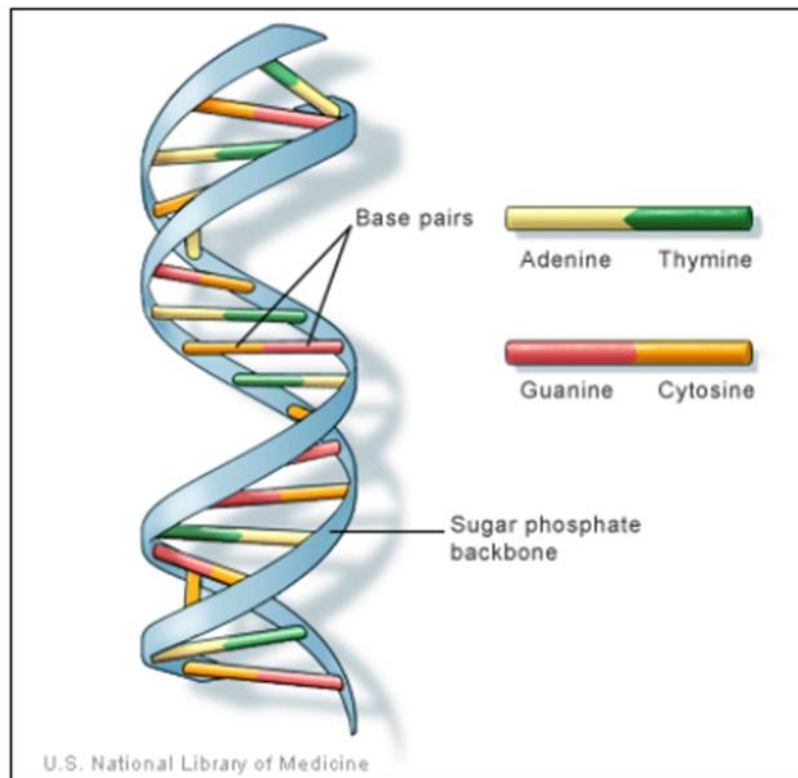


Figure 3.2 DNA structure. Source: NIH (U.S. National Library of Medicine) <http://www.nlm.nih.gov>

3.2 The Cell Cycle

All organisms on this planet start their life from one single cell. Reproduction and growth are most important characteristics of cells, indeed of all living organisms. All cells propagate by dividing into two new cells, with each original cell giving rise to two daughter cells each time they divide. These newly formed daughter cells can themselves grow and divide, this is called cell cycle.

The cell cycle is the way to produce two daughter cells by causing a cell to divide and duplicate (replication) (Behl & Ziegler, 2014). Eukaryotic cells, such as human cells, take approximately 24 hours to divide (Wille et al., 1984).

There are three phases in which a cell goes through in cell division. These three phases are: interphase, mitosis and cytokinesis (Alberts et al., 2010) (Figure 3.3).

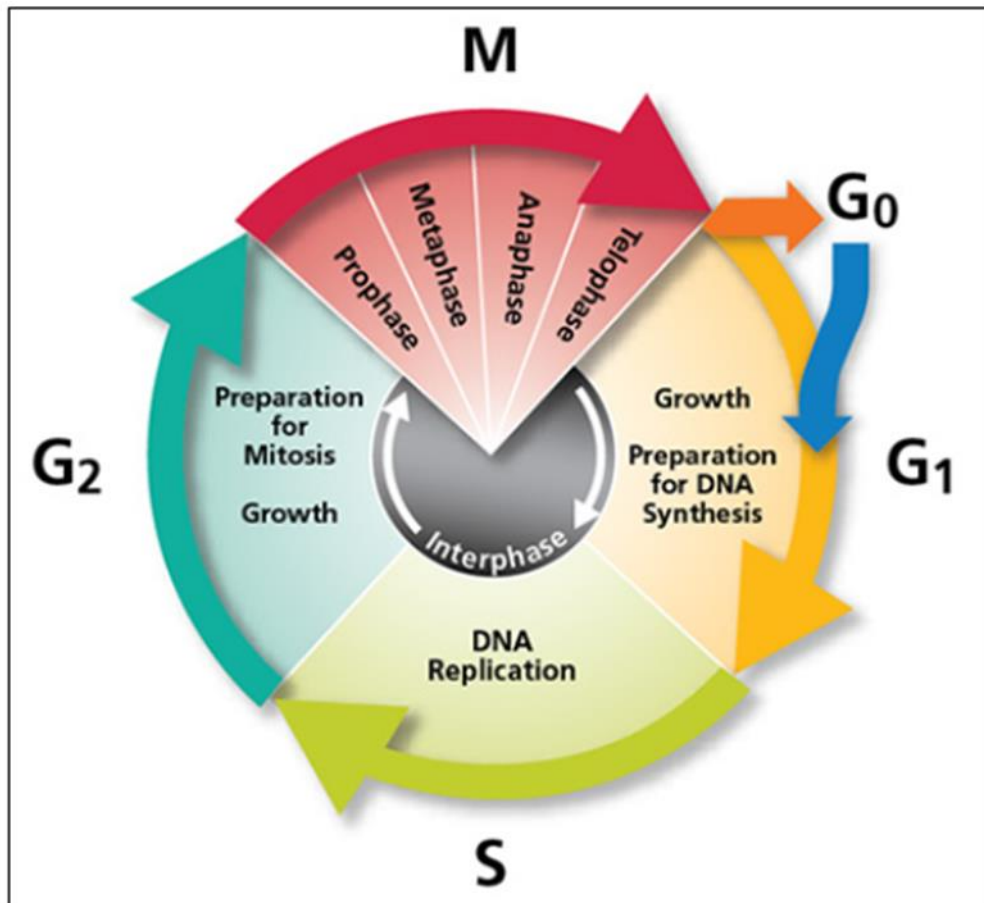


Figure 3.3 Cell cycle phases Source: DB Bioscience

[http:// www.bdbiosciences.com](http://www.bdbiosciences.com)

Inter-phase is the longest phase of the cell cycle. It is known as the resting phase, which is completely misleading, as it is during this time of normal metabolic activity that the cell performs all its normal functions, beginning with growth and development.

The inter-phase is divided into three stages (Alberts et al., 2010):

I. G1 Phase (Gap 1 phase): A period of normal metabolic activity – the number of cell organelles increases to normal levels and the volume of the cytoplasm also increases, eventually reaching a mature size. A cell can remain in this phase indefinitely. Its length can vary greatly depending on external conditions and extracellular signals from other cells. If extracellular conditions are unfavourable, for example, cells delay their progress through G1 and may even enter a specialised resting state known as G0 (G zero), in which they can remain for days, weeks or even years before resuming proliferation. If the cell undergoes division, the substrates required during S phase are also synthesised.

II. S Phase: (S for DNA synthesis) The DNA and chromosomes replicate. The cell is now committed to division.

III. G2 Phase: Structures directly involved with mitosis are formed. The new DNA is checked for errors and the substances that will be needed during mitosis are synthesised.

Mitosis only involves the division of the nucleus into two identical nuclei. It is divided into five stages (Alberts et al., 2010) see (Figure 3.4):

I. Prophase: In this stage, the chromatin condenses into chromosomes by dehydrating and coiling. The nucleolus and nuclear envelope then disappear and the centriole (animal cells only) divides into two centrosomes, which move apart, creating the spindle.

II. Prometaphase: The nuclear membrane breaks apart, and the spindle starts to interact with the chromosomes.

III. Metaphase: The chromosomes are moved to the equator of the cell and the centromeres attach to the spindle fibres, so the sister chromatids line up in the centre of the cell.

IV. Anaphase: The centromeres of each chromosome divide and are pulled apart by the contraction of the spindle fibres; thus, moving the chromosomes to opposite poles of the cell.

V. Telophase: The chromosomes reach the poles. After that the spindle disappears and the chromosomes return to their functional chromatin state by rehydrating and uncoiling. A new nuclear envelope begins to form around the chromosomes at each end of the cell, each with its own nucleolus.

Mitosis is followed by cytokinesis in which the cytoplasm is divided into two daughter cells, which are roughly equal in size (Alberts et al., 2010).

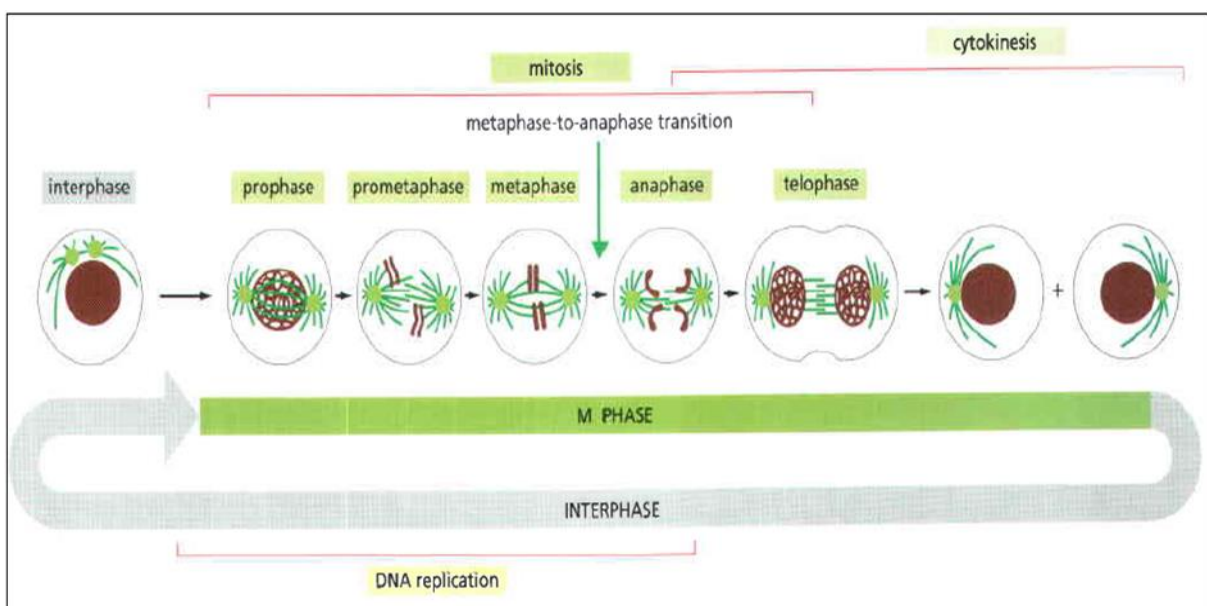


Figure 3.4 The Inter-phase stages (Alberts et al., 2010)

3.2.1 Regulation of the cell cycle

The regulation of cell cycle is a hot topic for bioinformatics researchers although many details of the cycle are already known. The cell cycle control system was still a black box until the 1980s with the identification of the key proteins of the control system. This goes along with the realisation that they are distinct from proteins that perform the processes of DNA replication, chromosome segregation, and so on (Alberts et al., 2010).

The regulation of the cell cycle, or what is called the cell cycle control system, has several points in the cell cycle, called checkpoints, at which the cycle can be arrested if previous events have not been completed.

Cell cycle checkpoints are control mechanisms that ensure the fidelity of cell division in eukaryotic cells. These checkpoints verify whether the processes at each phase of the cell cycle have been accurately completed before it progresses into the next phase.

Checkpoints are complex signal transduction pathways that serve as control points to regulate the order of events in the cell cycle and integrate cell cycle progression with DNA repair (Hartwell & Weinert, 1989).

There are three checkpoints at which the cell cycle is regulated to ensure the cells are ready to proceed through the process of division (Saltman, 2005): the G1/S, G2/M and M checkpoints see Figure 3.5.

During G1, cells check whether their environment favours proliferation and whether their genome is ready to be replicated (G1/S checkpoint).

Before undergoing chromosome condensation and nuclear division, cells have to be sure that their DNA is fully replicated and undamaged (G2/M checkpoint). However, separation of sister chromatids during anaphase should take place only when all chromosomes are attached to the bipolar mitotic spindle via their kinetochores. The spindle checkpoint guarantees this dependence (M checkpoint) (Novak et al., 2002).

The cell cycle is controlled by a collection of proteins interacting with each other, called cyclins and cyclin dependent kinases. Checkpoints in the cell cycle are responsible for the supervision but the key protagonists in cell cycle control are the proteins, such as p53 and RB (Behl & Ziegler, 2014). Table 3.2 contains a summary of the major cell cycle regulatory proteins.

In each checkpoint, there is an important protein; in the G1/S and G2/M checkpoints, p53 plays an important role in triggering the control mechanisms. It can be activated by damaged DNA, such as like that caused by radiation or chemicals. When the concentration of p53 increases, that makes the

protein perform its function of binding to particular DNA sequences and activates the expression (transcription) of adjacent genes; these genes control cells to stay alive or die or, even inhibit cell division.

The cell adjusts the concentration of its p53 protein by the rate at which it is degraded rather than that at which it is made. This process is called ubiquitin mediated proteolysis. It works by adding a small peptide (ubiquitin) to the p53 protein to degrade it. The most important factor in enzyme participation in labelling p53 with ubiquitin is the MDM2 protein (Momand et al., 2000).

The process between p53 and MDM2 is called a feedback loop. The MDM2 protein binds to p53, which causes the degradation of p53. This lowers the concentration of p53 and reduces transcription of the MDM2 gene, closing the feedback loop and allowing p53 levels to rise again.

Two classes (cyclin-dependent kinases (CDKs) and cyclins) determine a cell's progression through the cell cycle (Nigg, 1995). Cyclins form the regulatory subunits and CDKs the catalytic subunits of an

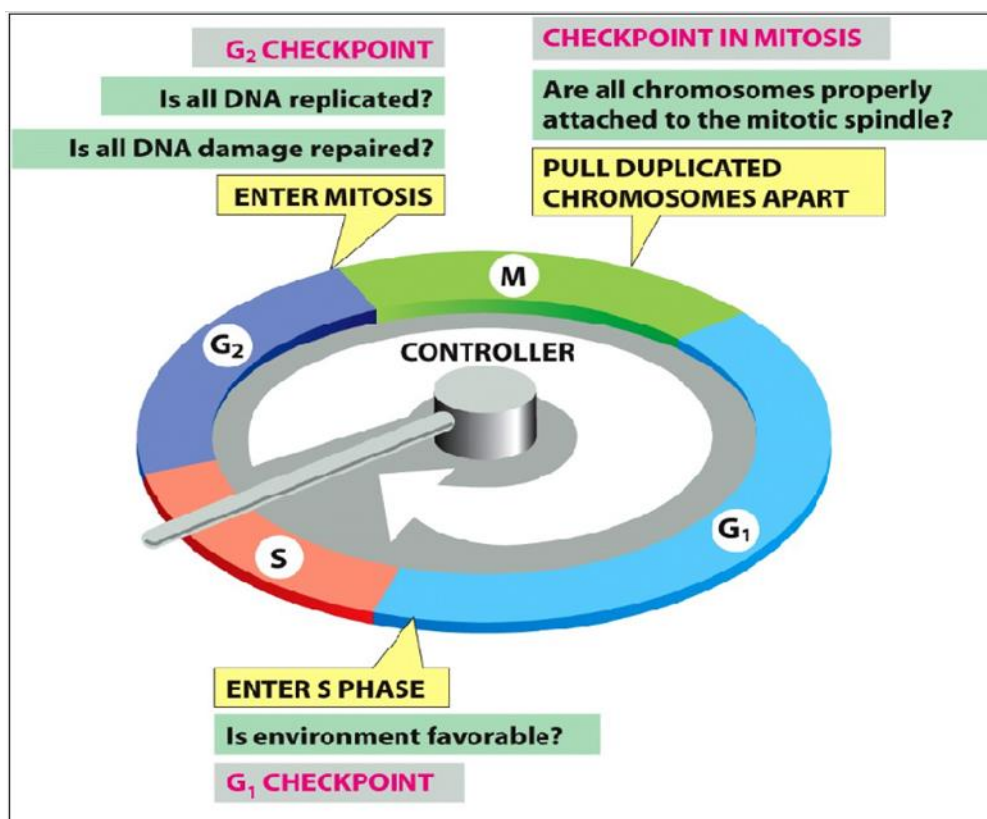


Figure 3.5 Cell cycle checkpoints (Alberts et al., 2013)

activated heterodimer; cyclins have no catalytic activity and CDKs are inactive in the absence of a partner cyclin. When activated by a bound cyclin, CDKs perform a common biochemical reaction, called phosphorylation, which activates or inactivates target proteins to orchestrate a coordinated entry into

the next phase of the cell cycle. Different cyclin-CDK combinations determine the downstream proteins targeted. CDKs are constitutively expressed in cells whereas cyclins are synthesised at specific stages of the cell cycle in response to various molecular signals (Kumar et al., 2009).

In Section 3.2.3 the G1/S checkpoint and pathway of interacting proteins will be discussed in detail.

Table 3.2 Summary of the major cell cycle regulatory proteins (Alberts et al., 2010)

General Name	Functions and Comments
Protein kinases and protein phosphatases that modify Cdks	
Cdk-activating kinase (CAK)	Phosphorylates an activating site in Cdks
Wee1 kinase	Phosphorylates Inhibitory sites in Cdks, primarily involved in suppressing Cdk1 activity before mitosis
Cdk25 phosphatase	Removes inhibitory phosphates from Cdks; three family members (Cdc25A, B, C) in mammals; primarily involved in controlling Cdk1 activation at the onset of mitosis
Cdk inhibitor proteins (CKIs)	
Sic1 (budding yeas)	Suppresses Cdk1 activity in G1; phosphorylation by Cdk1 at the end of G1 triggers its destruction
p27 (mammals)	Suppresses G1/S-Cdk and S-Cdk activities in G1; helps cells withdraw from cell cycle when they terminally differentiate; phosphorylation by Cdk2 triggers its ubiquitylation by SCF
p21 (mammals)	Suppresses G1/S-Cdk and S-Cdk activities following DNA damage
p16 (mammals)	Suppresses G1-Cdk activity in G1; frequently inactivated in cancer
Ubiquitin ligases and their activators	
APC/C	Catalyses ubiquitylation of regulatory proteins involved primarily in exit from mitosis, including securin and S- and M-cyclins; regulated by association with activating subunits
Cdc20	APC/C- activating subunit in all cells; triggers initial activation of APC/C at metaphase-to-anaphase transition; stimulated by M-Cdk activity
Cdh1	APC/C- activating subunit that maintains APC/C activity after anaphase and throughout G1; inhibited by Cdk activity
SCF	Catalyses ubiquitylation of regulatory involved in G1 control, including some CKIs (Sic1 in budding yeast, p27 in mammals); phosphorylation of target protein usually required for this activity

3.2.2 DNA Damage and Cancer

Mistakes in the DNA transferred from the mother cell to the daughter cells can cause cancer (Behl & Ziegler, 2014). If the DNA is damaged by radiation or chemicals, then the progression through G1 and G2 is delayed by braking mechanisms at the corresponding checkpoints. Delays at these checkpoints provide time for the damaged DNA to be repaired, after which the cell cycle brakes are released and cell cycle progression resumes (Alberts et al., 2010).

The two main proteins that control cell cycle are p53 and the retinoblastoma (Rb); therefore, p53 and Rb are key tumour suppressor proteins (Behl & Ziegler, 2014).

p53 is involved in several pivotal signaling pathways, its specificity being governed by its interaction with other cellular proteins. Most importantly, p53 acts as a transcription factor inducing the expression of genes that mediate the arrest of growth, DNA repair and apoptosis (cell death) as shown in Figure 3.6. The G1 checkpoint is accomplished by p53 trans-activating the CKI (cyclin-dependent kinase inhibitor), protein p21 that blocks G1/S-CDK complexes (Tokino & Nakamura, 2000; Vogelstein et al., 2000; Vousden & Lu, 2002). Moreover, it has been shown that p53 takes direct part in the repair of double strand breaks by controlling the fidelity of the recombination processes and, thus exhibits functions counteracting carcinogenesis beyond cell cycle checkpoint control (Bertrand et al., 2004; Gatz & Wiesmüller, 2006).

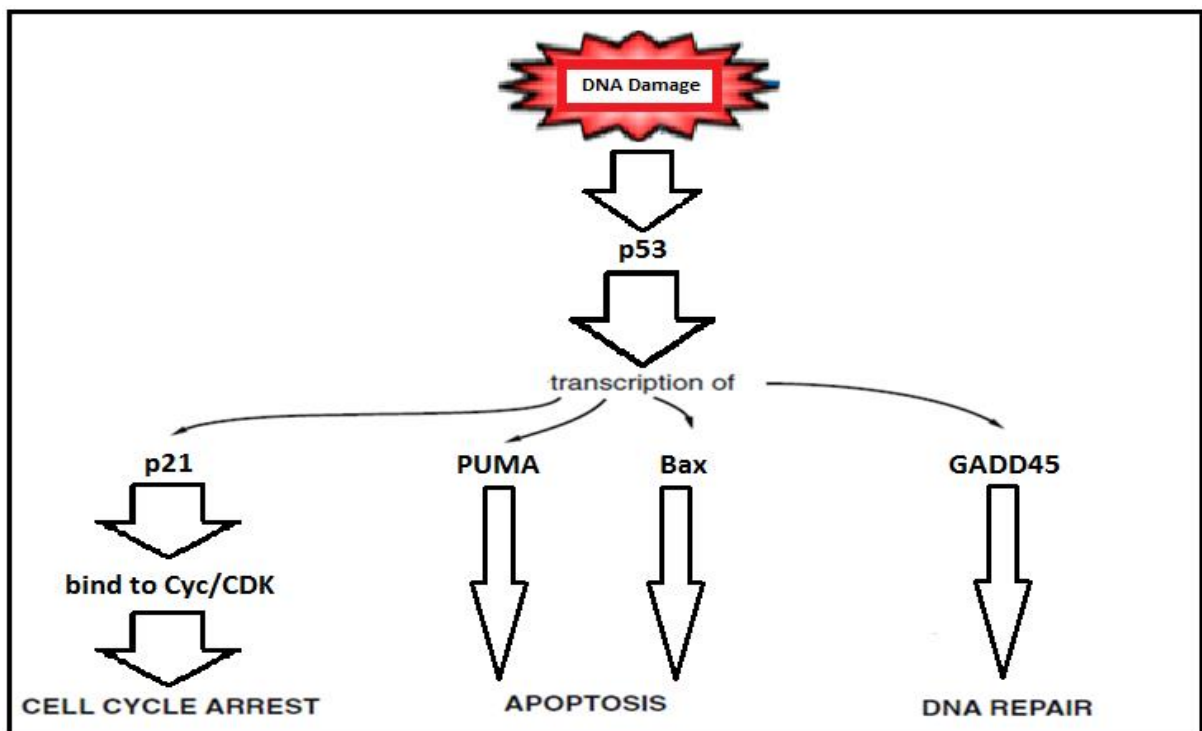


Figure 3.6 p53: simplified mode of action

3.2.3 G1/S checkpoint

Cell cycle progression is controlled not only by extracellular mitogens but also by other extracellular and intracellular mechanisms. The most important influence is DNA damage, which can occur as a result of exposure to certain chemicals, radiation or spontaneous chemical reactions during DNA replication. It is important that the cell repairs damaged DNA before attempting to duplicate or segregate it. The regulators of the cell cycle can readily detect DNA damage and arrest the cycle at either of the two checkpoints, G1/S and G2/M.

The main purpose of G1/S is to ensure the fidelity of the genome for the initiation of DNA replication. The transcription factor, E2F plays a main role in the completion of the G1/S transition and initiation of DNA replication through promoting the activation of CycE and CycA. The E2F protein is produced when the phosphorylation of the retinoblastoma protein (Rb) releases E2F, as shown in Figure 3.7 (Lundberg & Weinberg, 1998; Obaya & Sedivy, 2002; Sherr & Roberts, 2004; Satyanarayana & Kaldis, 2009).

3.2.3.1 G1/S Checkpoint without DNA Damage

In normal cell proliferation, when the cell cycle is in the early stages of the G1 phase, CycD synthesis is triggered through proliferation signal triggers. The essential function of CycD is to bind with CDK4/6 to initiate the phosphorylation of Rb to produce the hypophosphorylated form of Rb-PP/E2F; the complex protein CycD/CDK4/6, also plays a role in keeping CycE/CDK2 in an active form through two processes: first, by competing with CycE/CDK2 for binding with free p27 (a CDK inhibitor) to form the complex, p27/CycD/CDK4/6; and secondly by sequestering p27 from p27/CycE/CDK2 (Obaya & Sedivy, 2002; Sherr & Roberts, 2004; Satyanarayana & Kaldis, 2009).

CycE/CDK2 activation is the main reason for further hyperphosphorylation of Rb-pp/E2F resulting in the dissociation of Rb-PPPP from E2F; thus, releasing E2F. CDK2 and CDK4/6 release E2F through hypophosphorylating Rb. The increased concentration of E2F promotes the synthesis of CycE in the mid to late G1 phase, which facilitates the binding between CycE and CDK2 to form more of CycE/CDK2. This results in further freeing of E2F; thus, establishing a positive feedback loop between E2F and CycE; The increased concentrations of E2F and CycE move the cell from the G1/S checkpoint to the S phase (Satyanarayana & Kaldis, 2009).

The lowering of the CycD concentration occurs in mid G1 phase, which enhances the release of p27 bound to CycD/CDK4/6. The free p27 gets bound to the new complexes, CycE/CDK2, CycA/CDK2. p27 can inhibit the activity of CycE/CDK2 or CycA/CDK2, but the large amount of activated CycE/CDK2 can cause p27 degradation by phosphorylating it when p27 binds to CycE/CDK2. E2F enhances CycA

expression at the G1/S transition with a high concentration of CycA in the S phase (Obaya & Sedivy, 2002; Coqueret, 2003; Satyanarayana & Kaldis, 2009).

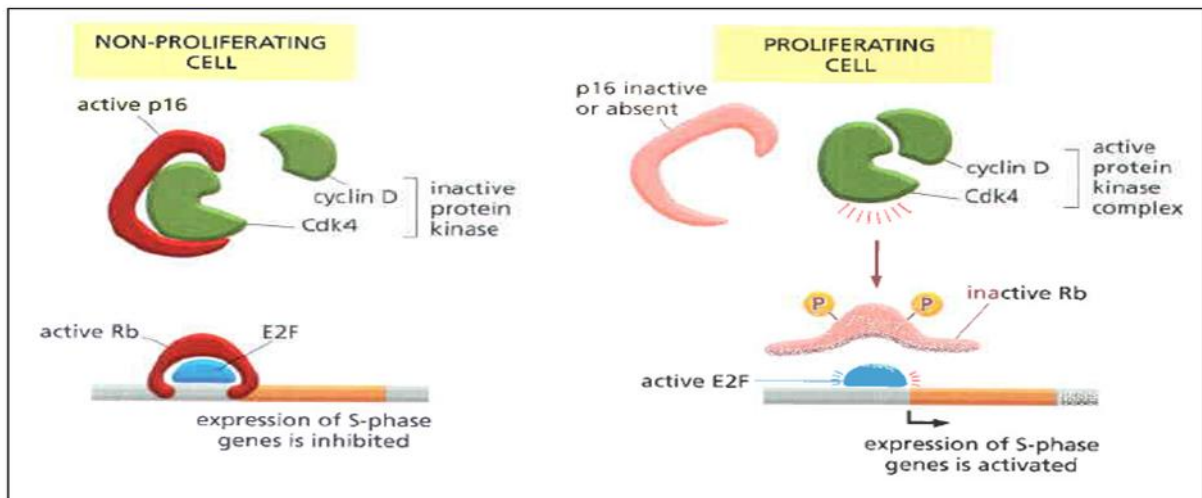


Figure 3.7 The Transcription factor E2F (Alberts et al., 2010)

3.2.3.2 G1/S Checkpoint with DNA Damage

The highest threat to genome integrity is DNA damage. If DNA damage has occurred, then p53 is released from its inhibitor, Mdm2 promoting the activation of p53 as a transcription factor to regulate the transcription of a large number of genes required for different purposes, including damage recovery or cell death process (see Figure 3.8) (Li & Ho, 1998; Lahav et al., 2004; Ciliberto et al., 2005; Harris & Levine, 2005; Geva-Zatorsky et al., 2006).

There are some proteins that can prevent cell cycle progression in G1. DNA damage leads to p53 activation that induces p21 (Yu et al., 1999). The role of p21 is to inhibit the activity of CDK to affect the cell cycle arrest through inhibition of the phosphorylation of Rb that keeps E2F inactive (Campisi & Fabrizio, 2007).

The loss of CycE/CDK2 inhibits the release of E2F and, consequently, the synthesis of CycE and CycA, which are essential steps in the progression to the S phase (Dulic et al., 1994). This stops the cell cycle progressing and activates the cell cycle repair pathway in order to provide enough time for cells to repair their DNA damage. With the removal of DNA damage, the negative feedback loop of p53 and Mdm2 is fully restored and p53 returns to a low level. The decrease in p53 reduces the level of p21, which releases complexes CycE/CDK2 and CycA/CDK2 and makes the cell cycle return to its normal condition (Ling et al., 2013).

The p16-Rb pathway usually occurs, secondary to the engagement of the p53 and p21 pathways in the senescence induced cell growth arrest (Stein et al. 1999; Jacobs & de Lange, 2004; Campisi & Fabrizio, 2007).

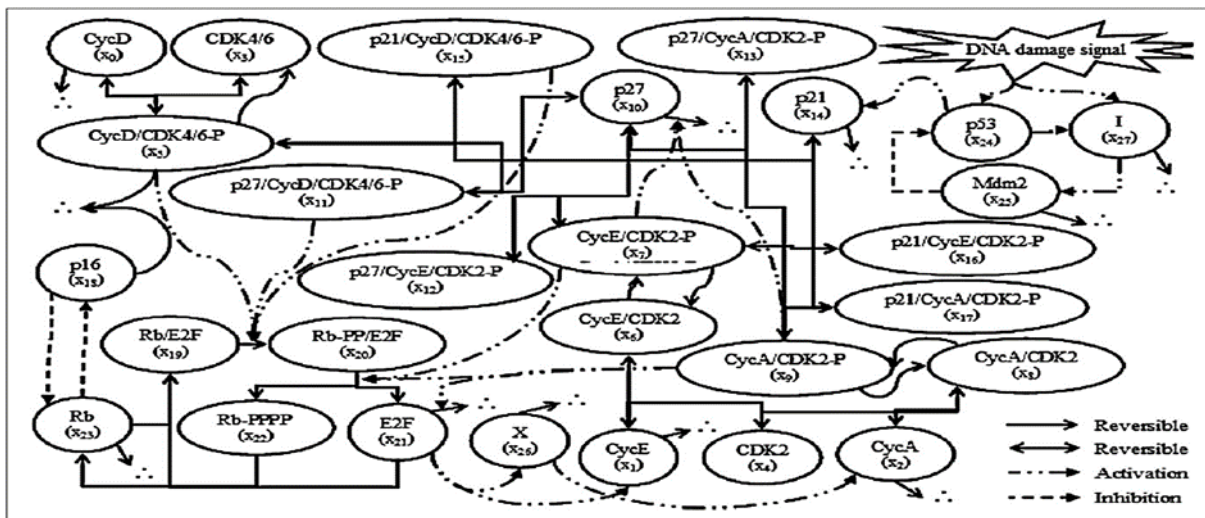


Figure 3.8 The G1/S checkpoint pathway involving the DNA damage signal transduction pathway (Ling et al., 2013)

3.3 G1/S checkpoint Modelling

Many computational approaches and models have been proposed to study biological networks. These have examined molecular pathways and complex interactions at many levels of biological information: proteins, protein function, pathways and protein interaction networks to understand how they work together. For this, continuous, discrete, hybrid, and stochastic methods have been proposed. The most common approach to accurately modeling the temporal dynamics of networks is ordinary differential equations (ODE).

The following is a review of the models used to simulate the G1/S checkpoint.

There are several types of models that have been developed to represent the G1/S checkpoint that involve protein to protein interactions. These types are mathematical, Boolean, petri net and hybrid models (see Table 3.3).

The first mathematical model was proposed by Hatzimanikatis and his colleagues in 1995. This model not only simulates the qualitative consequences on cell cycle regulation of over expression of cyclin E, E2F, and of RB deregulation in agreement with experiment, but it also suggests strategies for the rational manipulation of the cell cycle based on bifurcation analysis (Hatzimanikatis et al., 1995).

In 1997, Obeyesekere and his colleagues developed a mathematical model for the regulation of the G1 phase of Rb+/+ and Rb-/- mouse embryonic fibroblasts and an osteosarcoma cell line. This model focused on the regulation of progression through the G1 phase of the mammalian cell cycle that involved cdk4/cyclin D, cdk2/cyclin E, E2F and RB (Obeyesekere et al., 1997).

Many mathematical models have been proposed from 1997 until now (Kohn, 1998; Aguda & Tang, 1999; M. N. Obeyesekere et al., 1999; V Hatzimanikatis et al., 1999; Qu et al., 2003; Tashima et al., 2003, 2004; Novak & Tyson, 2004; Iwamoto et al., 2006, 2008; Haberichter et al., 2007; Tashima et al., 2008; Ling et al., 2010; Iwamoto et al., 2011; Zhao et al., 2012).

Table 3.3 Articles related to G1/S checkpoint modelling

No	Article Title	Model Type	Year
1	A mathematical model for the G1/S transition of the mammalian cell cycle	ODEs	1995
2	A mathematical model of the regulation of the G1 phase of Rb+/+ and Rb-/- mouse embryonic fibroblasts and an osteosarcoma cell line	ODEs	1997
3	Functional capabilities of molecular network components controlling the mammalian G1/S cell cycle phase transition	ODEs	1998
4	The kinetic origins of the restriction point in the mammalian cell cycle	ODEs	1999
5	A model of cell cycle behaviour dominated by kinetics of a pathway stimulated by growth factors	ODEs	1999
6	A mathematical description of regulation of the G1-S transition of the mammalian cell cycle	ODEs	1999
7	Regulation of the mammalian cell cycle: a model of the G1-to-S transition	ODEs	2003
8	Kinetics behaviour of G1-to-S cell cycle phase transition model	ODEs	2003
9	Simulation for detailed mathematical model of G1-to-S cell cycle phase transition	ODEs	2004
10	A model for restriction point control of the mammalian cell cycle	ODEs	2004
11	Mathematical modelling of G1/S phase in the cell cycle with involving the p53/Mdm2 network	ODEs	2006
12	A systems biology dynamical model of mammalian G1 cell cycle progression	Coupled Differential Equations (CDEs)	2007
13	Mathematical modeling and sensitivity analysis of G1/S phase in the cell cycle including the DNA-damage signal transduction pathway	ODEs	2008
14	Prediction of key factor controlling G1/S phase in the mammalian cell cycle using system analysis	ODEs	2008
15	Robustness of G1/S checkpoint pathways in cell cycle regulation based on probability of DNA-damaged cells passing as healthy cells	ODEs	2010
16	Mathematical modeling of cell cycle regulation in response to DNA damage: exploring mechanisms of cell-fate determination	ODEs	2011

17	Computational modeling of signaling pathways mediating cell cycle checkpoint control and apoptotic responses to ionizing radiation-induced DNA damage	ODEs	2012
18	Dynamical analysis of a generic Boolean model for the control of the mammalian cell cycle	Logical	2006
19	A Computational model of mammalian cell cycle using Petri nets	Petri Net	2002
20	Modeling the cell cycle: From deterministic models to hybrid systems	Hybrid	2011
21	A hybrid model of mammalian cell cycle regulation	Hybrid	2011
22	Hybrid models of the cell cycle molecular machinery	Hybrid	2012
23	Hybrid Petri nets for modeling the eukaryotic cell cycle	Hybrid Petri Nets	2013
24	Petri net modelling of oscillatory processes in the activation of cell cycle proteins	Petri Net	2013
25	Petri net based modelling and simulation of p16-Cdk4/6-Rb pathway	Petri Net	2013
26	Novel recurrent neural network for modelling biological networks: Oscillatory p53 interaction dynamics	Recurrent Neural Network	2013

Most models are based on ODEs; however, the critical limitations of ODE models are the difficulties in kinetic parameter estimation and numerical solutions to a large number of equations, making them more suited to smaller systems.

In the study by Adrien Faure and his colleagues (2006), they suggested a Boolean model for the control of the mammalian cell cycle. Fauré et al. (2006) used a logical model to understand the behaviour of complex biological regulatory networks. The critical limitation of Boolean models is that they can fail show complex behaviours, such as oscillations.

Considering the amount of information available from biological research, hybrid and petri net models have been proposed to understand the interactions governing biological networks. In 2002, a computational model of the mammalian cell cycle using petri nets was published by Kotani, Yoshioka and Konagaya (Kotani et al., 2002). The limitation of petri net modelling is that it can only obtain qualitative analyses of system behaviours with time being implicit in the firing of the transitions (Ling et al., 2013b).

However, since 2002, new hybrid and petri net models have been published (Alfieri et al., 2011; Singhania et al., 2011; Noel et al., 2012; Cetin et al., 2013; Herajy et al., 2013; Sugii et al., 2013). These types of models are still new and have not yet been fully explored.

Ling et al. (2013) introduced a novel recurrent artificial neural network (RNN) model capable of handling a large number of molecular interactions and quantifying the temporal dynamics and emergent systems properties. The models were just applied to the p53-Mdm2 oscillation system, a crucial component of the DNA damage response pathways activated by a damage signal (Ling et al., 2013b). This model converts an ODE system into a powerful recurrent network with attractive features.

In the model above, Ling et al. (2013b) modelled the power of recurrent neural networks (RNN) to accurately mimic and parameterise biological networks through the attractive features of continuous processing in neurons with forward and feedback loops and incremental weight updates. The novel recurrent neural network (RNN) model (Ling et al., 2013b) was applied to a small system with three proteins, but its potential for larger systems was revealed in the extension of their model to represent G1/S pathway through modularisation with RNN (Samarasinghe and Ling, 2017).

As mentioned earlier, all previous models have limitations (those relevant to G1/S are shown in Table 3.4 as G1/S is the focus of this thesis but these apply to other aspects of cell cycle as well). For this reason, a new modelling approaches and new reduction methods are needed, in particular, to reduce the mathematical models based on ordinary differential equation (ODE). These modelling approaches and new reduction methods are used to overcome the limitations of the ODE models and other models and to produce simple and still efficient dynamic models. These models can, therefore, handle a large number of molecular interactions, easily estimate parameters from data, quantify temporal dynamics and emergent systems properties, achieve abstraction in the representations of proteins through different levels of organisation of protein complexes and be adaptive.

Table 3.4 Limitations of G1/S checkpoint models

Model Type	Limitations
Mathematical Ordinary Differential Equations (ODE) Model	Difficulty in kinetic parameter estimation and numerical solution of a large number of equations.
Logical Models	Cannot show the complex behaviours, such as oscillations.
Hybrid Petri Nets Model	This type of models is still new and has not yet been fully explored.
Novel Recurrent Neural Network (RNN) Model (Ling et al., 2013b)	only applied to a small system with three proteins.

3.4 The DNA Damage Signalling Pathway and Whole Cell Cycle Regulation (Integrated Between G1/S and G2/M) Model Iwamoto et al. (2011)

Understanding protein interactions in this study involves understanding system dynamics in the G1/S regulation of signal transduction. This involves protein-protein interactions, with the focus on complex proteins and the movement from level to level in protein-protein interactions presentation (abstraction), which is the first step in simulating the G1/S checkpoint process.

Deriving a formal abstraction for the system (G1/S checkpoint) is the crucial step in developing this research. It includes the definition of all system elements: components of the system and the form of molecular interactions in the network, as described in the section on the G1/S checkpoint (Section 3.2.3).

To explain how to produce the structure of the network based on the chemical reactions of the G1/S checkpoint, we take Iwamoto et al. (2011) proposed model for the G1/S checkpoint system as an example. Iwamoto et al. (2011) presented a novel model of the DNA damage signalling pathway and whole cell cycle regulation (integrated between G1/S and G2/M) and explored the effect of p53 oscillation on cell fate selection. The PhD research described in this thesis uses a base model for G1/S transitions and DNA damage signalling pathway extracted from Iwamoto et al. (2011) model as a case study. For this reason we discuss the Iwamoto et al. (2011) model in detail.

Iwamoto et al. (2011) presented a novel model for the DNA damage signaling pathway and whole cell cycle regulation (integrated between G1/S and G2/M) and explored the effect of p53 oscillation on cell fate decisions.

The Iwamoto et al. (2011) model, as shown in Figure 3.9, shows the reaction scheme of the proposed model that integrated the G1/S model, the G2/M model, and the DNA damage signaling pathway. The model consists of 54 dependent variables and 137 kinetic parameters (see Appendix A). Both the initial conditions and kinetic parameters in the Iwamoto et al. (2011) model were estimated based on values described in previous works (Lev Bar-Or et al., 2000; Tashima et al., 2006; Iwamoto et al., 2008).

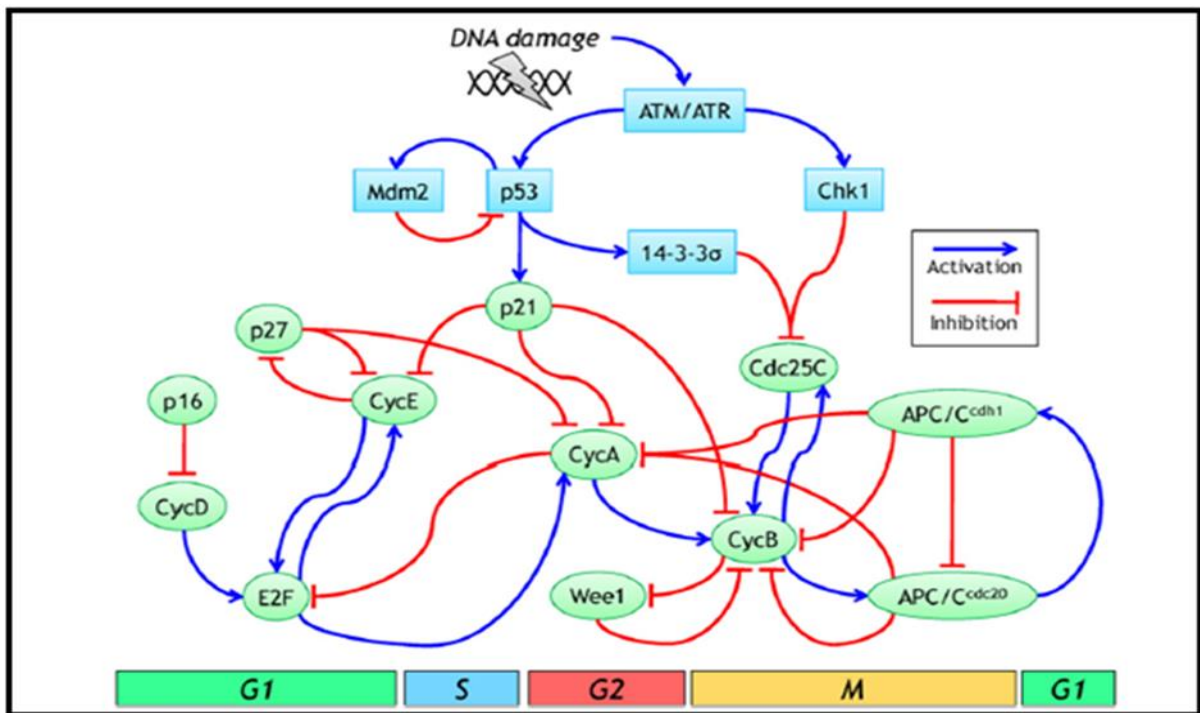


Figure 3.9 Diagram of key regulators in the Iwamoto et al. model (2011)

The scenario explaining the Iwamoto et al. (2011) model of the DNA damage signalling pathway and whole cell cycle regulation follows as:

In G1/S and S/G2 transitions the E2F (transcription factor) plays a central role in DNA replication and is repressed by the binding of Rb (retinoblastoma protein) in G1. In the normal cell, CycD is synthesised, and G1 progression is initiated. The activated binary complex CycD/Cdk4 is formed when CycD binds to Cdk4. The CycD/Cdk4 complex phosphorylates Rb bound to E2F, which becomes the hypophosphorylated form (Rb-PP). Furthermore, the hyperphosphorylated form (Rb-PPP) occurs when the Rb-PP phosphorylated by both CycE/Cdk2 and CycA/Cdk2. Rb-PPP disassociates from Rb-PP/E2F and E2F is activated. The transcriptional activation of CycE, CycA, Cdc25A are activated by E2F, and this is required for DNA replication (Helin, 1998). CycE binds to separate inactive Cdk2 molecules to form an inactivate complex, iCycE/Cdk2 and CycA binds to separate inactive Cdk2 molecules to form an inactivate complex, iCycA/Cdk2. Activated binary complexes aCycE/Cdk2 and aCycA/Cdk2 form after Cdc25A dephosphorylates and activates iCycE/Cdk2 and iCycA/Cdk2. The further dissociation of Rb-PPP and E2F and concomitant the activation of E2F is the result of phosphorylation of Rb-PP by both aCycE/Cdk2 and aCycA/Cdk2. The positive feedback loop between two types of Cyc/Cdk complexes and Rb/E2F complexes plays an essential role in the G1 progression. Initiating DNA replication and driving the progression to the S phase happens after sufficient expressions of both E2F and aCycE/Cdk2 (Matsumura et al., 2003; Woo and Poon, 2003). After completing DNA replication during the S phase, aCycA/Cdk2 promotes the degradation of E2F that reduces the synthesis of CycE and the formation of aCycE/Cdk2, which causes the progression to the G2 phase (Xu et al., 1994).

Regulating G1/S progression is dependent on three Cdk inhibitors (CKIs), p16, p21, and p27. p16 inhibits the activation of CycD/Cdk4, and both p21 and p27 repress aCycE/Cdk2 and aCycA/Cdk2 (Parry et al., 1995; LaBaer et al., 1997), as shown in Figure 3.10.

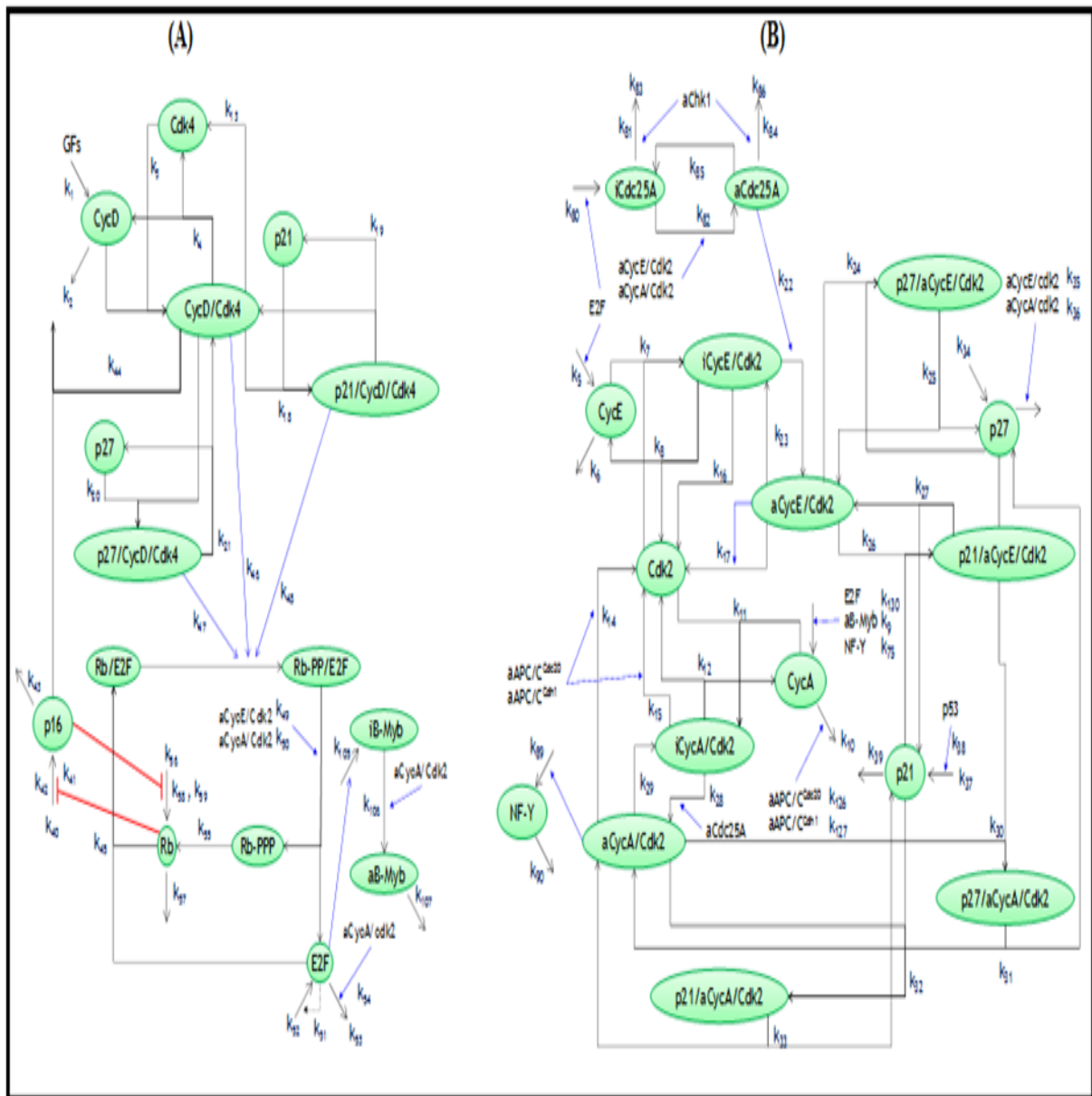


Figure 3.10 G1/S and S/G2 transitions (Iwamoto et al., 2011)

In G2/M and M/G1 transitions shown in Figure 3.11, the transcriptional activation of CycB is induced through the active transcription factor NF-Y that is activated by aCycA/Cdk2 from the late S phase to the G2 phase (Chae et al., 2004). CycB binds to Cdk1 and forms an inactivated complex, iCycB/Cdk1. Although the iCycB/Cdk1 is dephosphorylated by Cdc25C to become the activated complex aCycB/Cdk1, aCycB/Cdk1 is continuously phosphorylated and inactivated by Wee1. The aCycB/Cdk1 complex has a nuclear export signal, unlike CycD/Cdk4, CycE/Cdk2, and CycA/Cdk2; therefore, it localises to the cytoplasm in G2 phase (aCycB/Cdk1_{cyto}) (Takizawa and Morgan, 2000). Then it drives

the progression to the M phase where chromosome condensation is caused by aCycA/Cdk2 (Furuno et al., 1999; Gong et al., 2007). In M phase, aCycB/Cdk1_{cyto} transport to the nucleus (aCycB/Cdk1_{nuc}) mediated by CycB, followed by chromosome condensation and nuclear breakdown (Li et al., 1997; Kong et al., 2000). After that, APC/C^{cdc20} is formed when the anaphase promoting complex/cyclosome (APC/C) binds to Cdc20, followed by the activation of aCycB/Cdk1_{nuc}, and forms activated APC/C^{cdc20}. The degradation of securin, CycA, and CycB promoted by activate APC/C^{cdc20} induces several reactions to exit from M (Castro et al., 2005). The degradation of CycA inactivates aCycA/Cdk2 and the degradation of CycB inactivates aCycB/Cdk1_{nuc} that activates APC/C^{cdh1}. Activated APC/C^{cdh1} promotes degradation of CycA and that inactivates aCycA/Cdk2, degradation of CycB that inactivates aCycB/Cdk1_{nuc}, and the degradation of Cdc20 that inactivates APC/C^{cdc20}. APC/C^{cdc20} and APC/C^{cdh1} both induce the exit from the M phase by a sufficient decline in aCycB/Cdk1_{nuc}, which marks the completion of cell cycle progression (Xu and Chang, 2007).

The kinase activity of both aCycA/Cdk2 and aCycB/Cdk1 is inhibited by binding to p21 when the DNA damage occurs that blocks the activation of APC/C^{cdc20} (LaBaer et al., 1997), as shown in Figures 3.10 (B) and 3.10 (A).

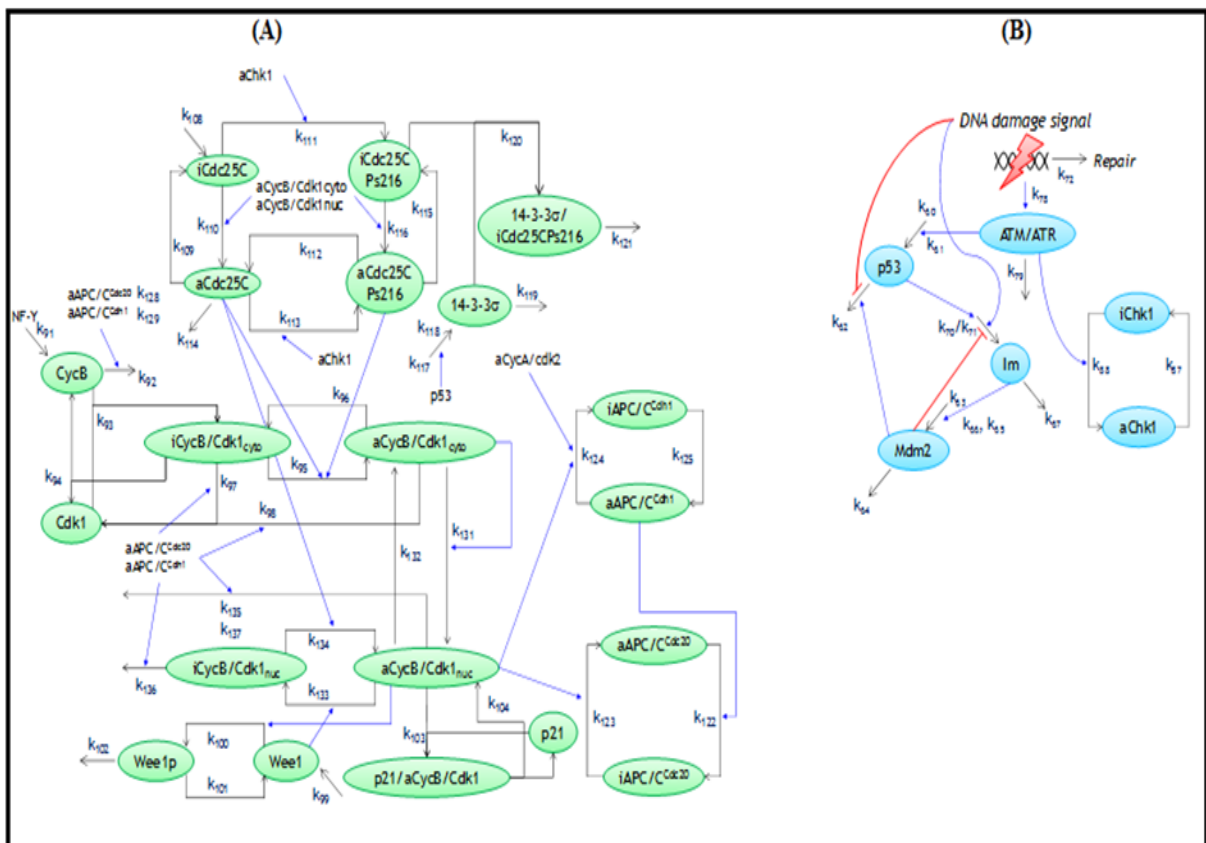


Figure 3.11 G2/M and M/G1 transitions and the DNA damage signalling pathway

(Iwamoto et al., 2011)

In the DNA damage signalling pathway, when DNA is damaged, both ATM and ATR (ATM/ATR) are activated by DNA damage signal transduction (Figure 3.11 (B)). The activated ATM/ATR phosphorylates and activates both p53 and Chk1. Transcriptional activation of Mdm2, p21, and 14-3-3 σ happens through activated p53. There is a negative feedback loop between p53 and Mdm2 so the activated form of Mdm2 promotes degradation of p53. That negativity feedback produces oscillatory dynamic behaviours for both p53 and Mdm2 (Lev Bar-Or et al., 2000; Batchelor et al., 2008).

The activities of aCycE/Cdk2, aCycA/Cdk2 and CycB/Cdk1 are inhibited by the binding of p21, which induces G1 arrest and G2 arrest, respectively. Cdc25C is exported to the cytoplasm after being phosphorylated by Chk1 by 14-3-3 σ that inhibits the activation of CycB/Cdk1, and G2 arrest is induced as shown in Figure 3.11 (B).

In the Iwamoto et al. model (2011) every 189 timesteps correspond to an hour in real time and 24.82 hours is the time required for one cell cycle, which approximately equal to about 24 hours, the time required for one cell cycle in normal mammalian cells. They employed the XPPAUT software (Ermentrout, 2002) to simulate the model and they used a single independent variable “DNA damage signal (DDS)” to represent DNA damage. First, they ran the model without DNA damage (DDS = 0) to calculate the time course of several cell cycle regulators, total CycE (tCycE), total CycA (tCycA), total CycB (tCycB), aCycE/Cdk2, p27, and APC/Ccdc20. The results shown in Figure 3.12 were in good agreement with experimentally observed data.

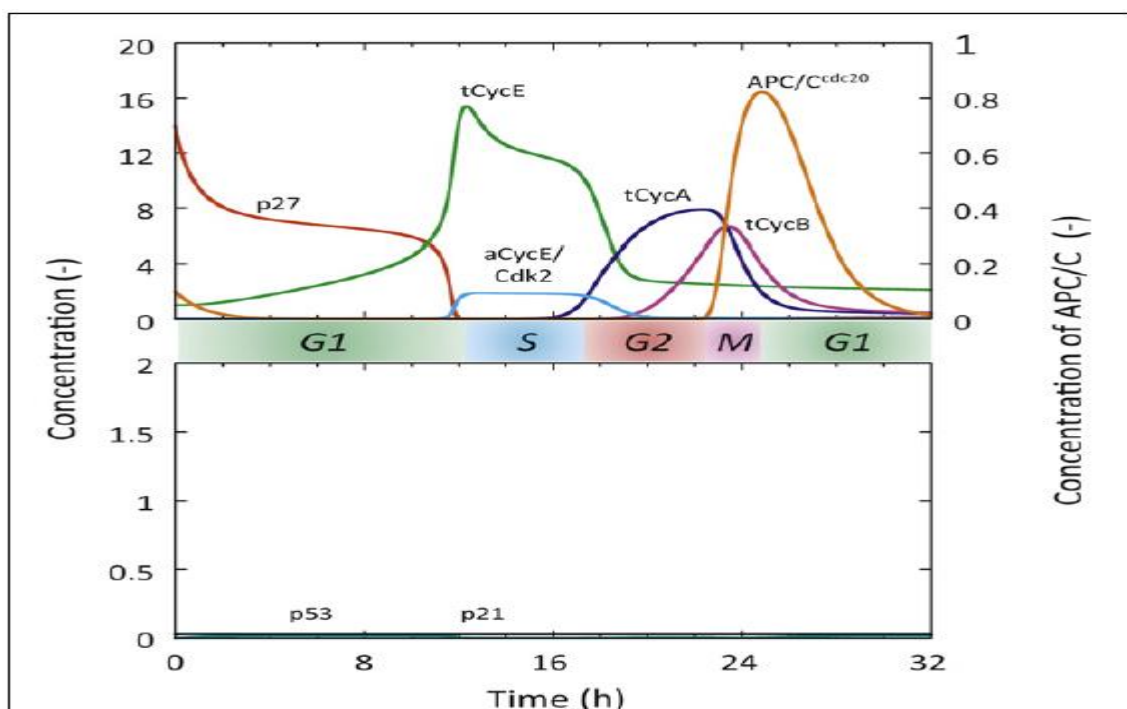


Figure 3.12 Time courses of several cell cycle regulators from a simulation run using the Iwamoto model 2011 without DNA damage (Iwamoto et al., 2011)

Secondly, they ran the model with four levels of DNA damage $DDS = 0.002$ (low-damage), $DDS = 0.004$ (medium-damage), $DDS = 0.008$ (high-damage), and $DDS = 0.016$ (excess-damage). The results (Figure 3.13) have shown good agreement with experimentally observed data.

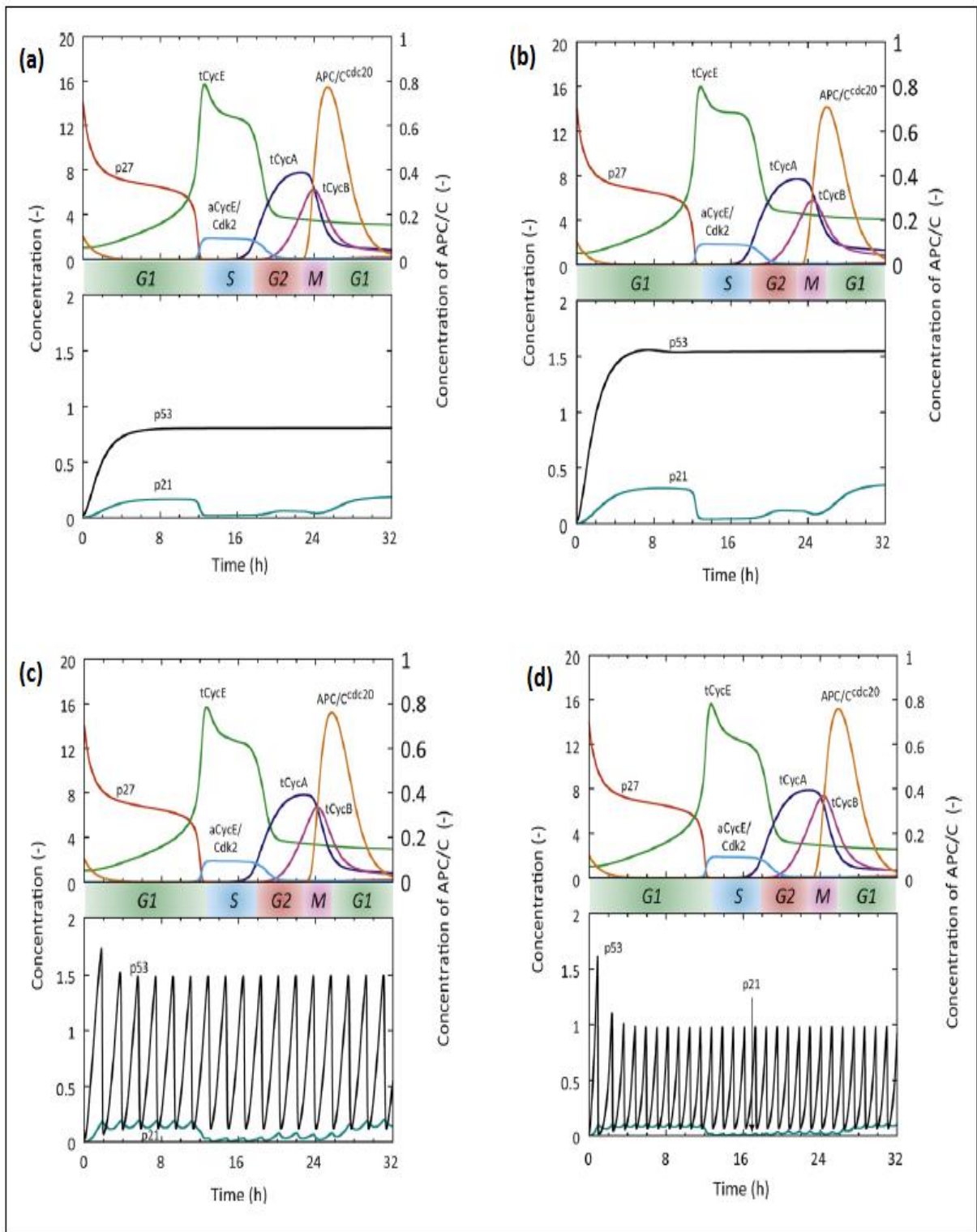


Figure 3.13 Time courses of several cell cycle regulators from a simulation run using the Iwamoto model 2011 with different levels of DNA damage: (a) low-damage where, $DDS = 0.002$ (b) medium-damage where, $DDS = 0.004$ (c) high-damage where, $DDS = 0.008$ and (d) excess-damage where, $DDS = 0.016$ (Iwamoto et al., 2011)

In this chapter we have given a brief review of biological background, especially the cell cycle, with greater consideration and focus on the G1/S checkpoint pathway and DNA damage pathways as a complex systems. The biological background have given through four sections: Section 3.1 given a brief review of a cell general review; Section 3.2 discussed the cell cycle, the regulation of the cell cycle, (DNA damage and cancer) and the G1/S checkpoint; Section 3.3 presented the details of the G1/S checkpoint and models. Section 3.4 discussed the DNA damage signalling pathway and the cell cycle regulation (integrated between G1/S and G2/M) model of Iwamoto et al. (2011).

In the next chapter we extract the base model for our research from the Iwamoto 2011 model and we validate the base model to be sure it is useful and, we discuss a new reduction approach and we apply this approach to the base model to prove the efficiency for this reduction approach.

Chapter 4

Model Reduction Method Based on a Hierarchy Representation and Lumping

The previous discussions have focused on a brief review of the biological background. In this chapter the base model was extracted from the Iwamoto model 2011 then, we propose a method to simplify biological networks based on hierarchical representation and lumping. We use the base model that present in Section 4.1 (G1/S checkpoint pathway and DNA damage pathways model) as a complex system as a case study to apply our new reduction approach.

This chapter is organised as follows: Section 4.1 presents the base model; Section 4.2 presents the methodology; Section 4.3 presents the application of the model reduction method.

4.1 DNA Damage Signalling Pathway Integrated with the G1/S Checkpoint Pathway as the Base Model

After we had looked back at previous reports (Lev Bar-Or et al., 2000; Tashima et al., 2004; Tashima et al., 2006; Iwamoto et al., 2008) and read in the Iwamoto et al. (2011) paper about the DNA damage signalling pathway and whole cell cycle regulation, we extracted a base model from Iwamoto et al. (2011) a novel model that presented the DNA damage signalling pathway integrated with G1/S checkpoint pathway as shown in Figure 4.1.

The model consisted of 35 dependent variables and 92 kinetic parameters (see Appendix B). Both initial conditions and kinetic parameters in the our model were estimated based on values described in previous reports (Lev Bar-Or et al., 2000; Tashima et al., 2006; Iwamoto et al., 2008; Iwamoto et al., 2011).

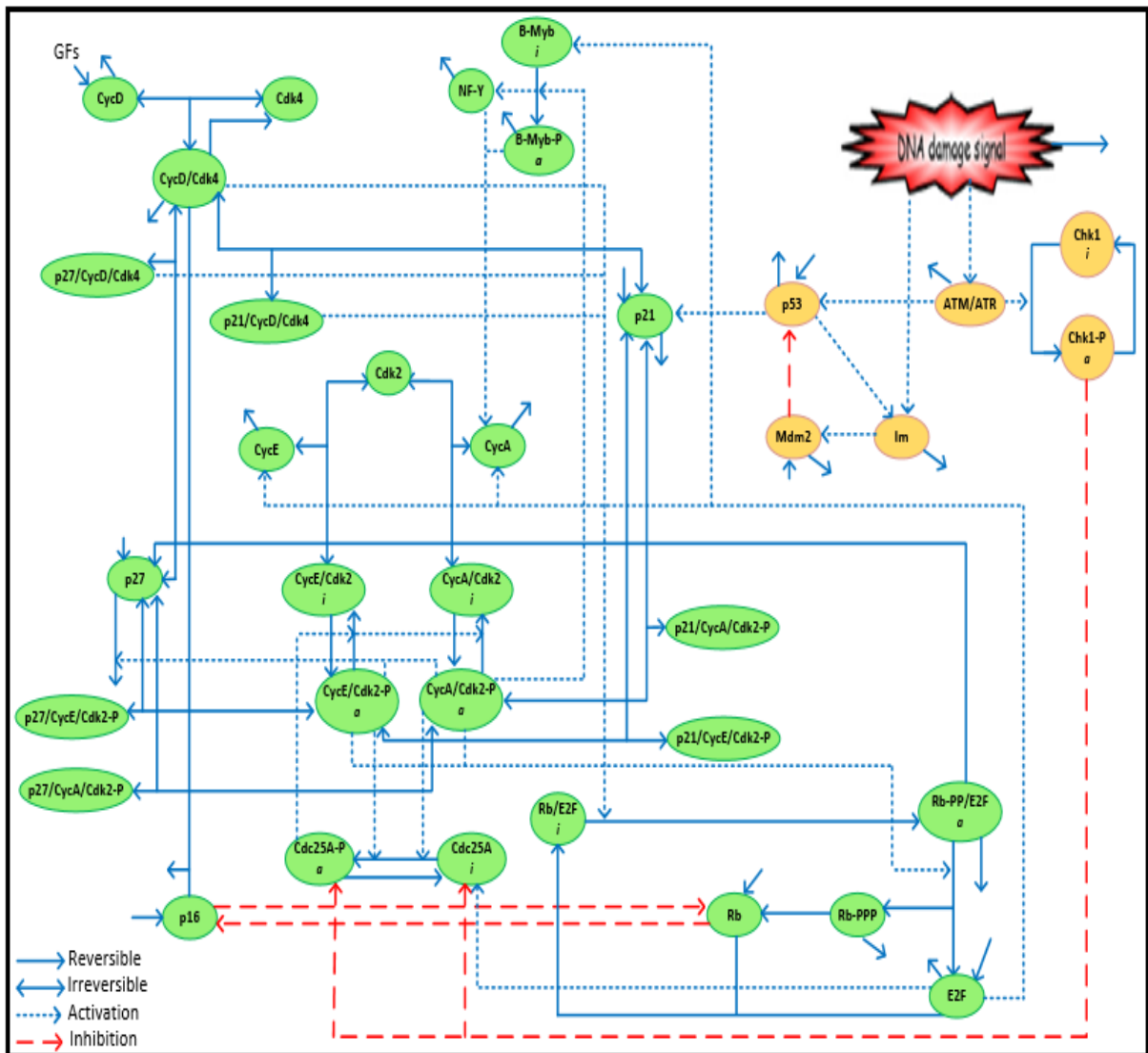


Figure 4.1 G1/S transitions and DNA damage signalling pathway

In our model, in the normal cell, G1/S CycD is synthesised and G1 progression is initiated. The activated binary complex CycD/Cdk4, forms when CycD binds to Cdk4. The CycD/Cdk4 complex phosphorylates Rb bound to E2F, which generates the hypophosphorylated form, Rb-PP. Furthermore, the hyperphosphorylated form (Rb-PPP) is generated when Rb-PP is phosphorylated by both CycE/Cdk2 and CycA/Cdk2. Rb-PPP disassociates from Rb-PP/E2F and E2F is activated. The transcription of CycE, CycA, Cdc25A is activated by E2F, and this is required for DNA replication. CycE binds to inactive Cdk2 molecules to form the inactive complex, CycE/Cdk2, and CycA binds to inactive Cdk2 molecules to form the inactive complex, CycA/Cdk2 (Iwamoto et al., 2011; Alberts et al., 2015). Activated binary complexes, CycE/Cdk2-p and CycA/Cdk2-p, form after Cdc25A dephosphorylates and activates the corresponding inactive complexes. The further dissociation of Rb-PPP and E2F and the concomitant activation of E2F is the result of phosphorylation of Rb-PP by both CycE/Cdk2-p and CycA/Cdk2-p. The positive feedback loop between the two types of Cyc/Cdk complexes and the Rb/E2F complex plays an essential role in G1 progression. Initiating DNA replication and driving the progression to the S phase

happen by sufficient expression of both E2F and CycE/Cdk2-p. After completing DNA replication during S phase, CycA/Cdk2-p promotes the degradation of E2F that reduces the synthesis of CycE and the formation of CycE/Cdk2-p, which causes progression to the G2 phase. Regulation of G1/S progression depends on three Cdk inhibitors (CKIs), p16, p21, and p27. p16 inhibits the activation of CycD/Cdk4, and both p21 and p27 repress CycE/Cdk2-p and CycA/Cdk2-p (Iwamoto et al., 2011; Alberts et al., 2015), as shown in Figure 4.1.

When DNA is damaged, various protein kinases are recruited to the site of the damage and initiate a signalling pathway that causes cell-cycle arrest. The first kinase at the damage site is ATM/ATR, depending on the type of damage. Additional protein kinases, called Chk1 and Chk2, are then recruited and activated, resulting in the phosphorylation of the gene regulatory protein, p53. Mdm2 normally binds to p53 and promotes its ubiquitylation and destruction in proteasomes. Phosphorylation of p53 blocks its binding to Mdm2; as a result, p53 accumulates to high levels and stimulates the transcription of the gene that encodes for the CKI protein, p21. p21 binds and inactivates G1/S-Cdk and S-Cdk complexes, arresting the cell in G1 (Iwamoto et al., 2011; Alberts et al., 2015).

We edit the equations to make the model suitable to represent the DNA damage signalling pathway integrated only with G1/S checkpoint pathway; the changes are shown in Table 4.1.

Table 4.1 Changes in the model equations

No	Equation	Term removed	Reason
1	dY ₃ /td CycA	K9Y ₄₁ Y ₄₁ = aB-Myb	(1.a) The initial value of aB-Myb equals zero and its form from activates iB-Myb which the initial value equals zero, iB-Myb synthesis induces by E2F which the initial value equals zero (Iwamoto et al., 2011). So, the effect of this term is closed to zero through the G1/S.
		K75Y ₃₂ Y ₃₂ = NF-Y	(1.b) The initial value of NF-Y equals zero and it activated at the late S phase to G2 phase by aCycA/Cdk2 (Chae et al., 2004).
		K126Y ₄₉ Y ₄₉ = aAPC/C ^{cdc20}	(1.c) aAPC/C ^{cdc20} it's form at the anaphase and activates by aCycB/Cdk1 _{nuc} after forming from complex/cyclosome (APC/C) binds to Cdc20 to form APC/C ^{cdc20} (Castro et al., 2005)
		K127Y ₅₁ Y ₅₁ = aAPC/C ^{cdh1}	(1.d) aAPC/C ^{cdh1} activates when the degradation of CycA and CycB inactivates aCycA/Cdk2 and aCycB/Cdk1 _{nuc} at the late M phase (Xu and Chang, 2007).

2	dY ₅ /dt CDK2	K14Y ₁₀ (Y ₄₉ + Y ₅₁) Y ₄₉ = aAPC/C ^{cdc20} Y ₅₁ = aAPC/C ^{cdh1}	(2.a) for reason (1.c) and (1.d)
		K15Y ₉ (Y ₄₉ + Y ₅₁) Y ₄₉ = aAPC/C ^{cdc20} Y ₅₁ = aAPC/C ^{cdh1}	(2.b) for reason (1.c) and (1.d)
3	dY ₉ /dt iCycA/CDK2	K15(Y ₄₉ + Y ₅₁) Y ₄₉ = aAPC/C ^{cdc20} Y ₅₁ = aAPC/C ^{cdh1}	(3.a) for reason (1.c) and (1.d)
4	dY ₁₀ /dt aCycA/CDK 2	K14Y ₁₀ (Y ₄₉ + Y ₅₁) Y ₄₉ = aAPC/C ^{cdc20} Y ₅₁ = aAPC/C ^{cdh1}	(4.a) for reason (1.c) and (1.d)
5	dY ₁₅ /dt p21	K104Y ₃₉ Y ₃₉ = p21/CycB/Cdk1	(5.a) p21/CycB/Cdk1 forms at late S phase when p21 bind to aCycB/Cdk1 (Takizawa and Morgan, 2000).
		K103Y ₅₃ Y ₅₃ = aCycB/Cdk1 _{nuc}	(5.b) aCycB/Cdk1 _{nuc} forms in M phase (Li et al., 1997; Kong et al., 2000)

After the base model for our research is ready we calculated the timesteps required for G1/S, which were approximately equal to 12.32 hours (Ohtsubo et al., 1995) in real time, where every 189 timesteps corresponds to an hour and that means we need approximately 2330 time steps to simulate G1/S.

To evaluate the base model we simulated it with and without DNA damage, and we compared the base model results with the Iwamoto model 2011 to be sure the base model was useful for a particular purpose and was applicable to answering a specific set of questions. We used Microsoft Excel spreadsheets with Visual Basic for Applications (VBA) to simulate the base model and from the simulation we analysed the results.

VBA is Microsoft's macro language for applications built on top of the windows operating system. VBA is based on the visual basic (VB) language. VBA is a fully featured language that has all the aspects of a modern computer language. Modelling with VBA provides maximum effectiveness in the simulation of biological systems. Excel VBA provides many helpful features, such as: spreadsheets for data input and output, VBA development environment, dataset analysis tools (graphs and tables, etc.) and statistical functions for summarising data and results (Botchkarev, 2015; Rossetti, 2015).

First, we ran the base model without DNA damage ($DDS = 0$) to calculate the time course of several cell cycle regulators. The results shown in Figure 4.2 are in good agreement with the original model results (Figure 3.12) that accordingly Iwamoto et al. (2011) followed experimentally observed data.

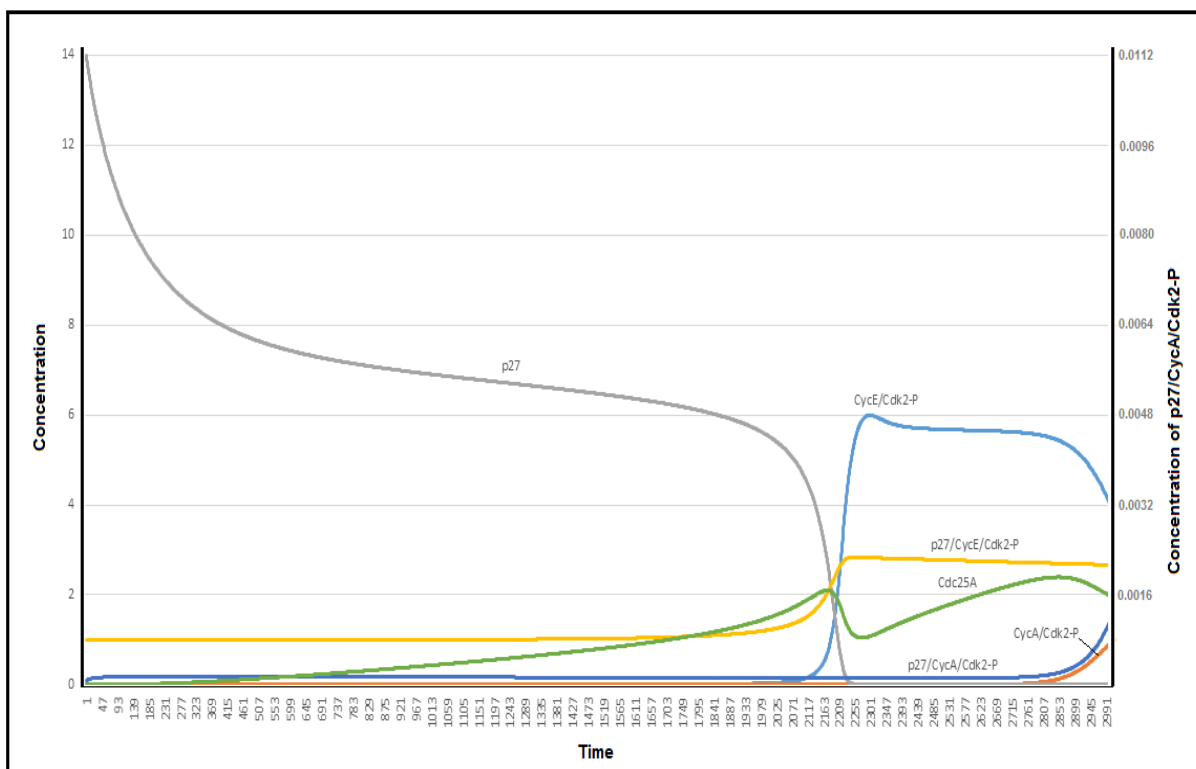


Figure 4.2 Time courses of some chemical species in the G1/S phase without DNA damage from a simulation run using the base model

Secondly, we ran the base model with four levels of DNA damage $DDS = 0.002$ (low-damage), $DDS = 0.004$ (medium-damage), $DDS = 0.008$ (high-damage), and $DDS = 0.016$ (excess-damage). The results were in good agreement with the original model that was already in agreement with experimentally observed data.

If no DNA damage has occurred, the p21 and p53 are stay in stead and low level, as shown in Figures 4.3 and 4.4. DNA damage leads to p53 activation that induces p21 (Yu et al., 1999). The role of p21 is to inhibit the activity of CDK to effect cell cycle arrest through inhibition of phosphorylation of Rb to keep E2F inactive (Campisi & Fabrizio, 2007).

With the removal of DNA-damage, the negative feedback loop of p53 and Mdm2 is fully restored and p53 returns to a low level. The decrease in p53 reduces the level of p21, which releases the complexes of CycE/CDK2 and CycA/CDK2 (Ling et al., 2013) as shown in Figures 4.3 and 4.4 when $DDS=0.004$.

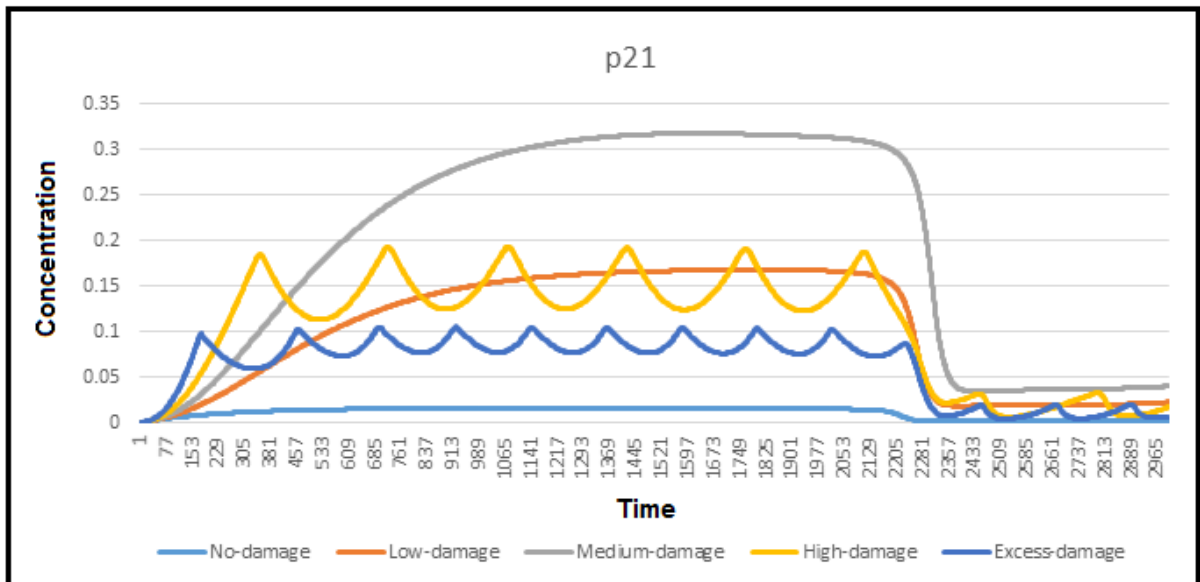


Figure 4.3 Time courses of p21 in the G1/S phase with and without DNA damage from a simulation run using the base model

For the high DNA-damage in $DDS=0.008$, the time courses of p21 and p53 in the G1/S phase are shown in Figures 4.3 and 4.4. The activated p53 showed oscillation, which was in agreement with experimental observations by Lev Bar-Or et al. (2000), Lahav et al. (2004) and Geva-Zatorsky et al. (2006). When DNA was damaged, the DNA-damage signal sequentially activates p53 and Mdm2. The activated p53 also can promote the synthesis of p21, which plays the role of CDK inhibitor. Since p21 binds to both CycE/CDK2-P and CycA/CDK2-P to inhibits the phosphorylation of Rb, the activation of E2F is delayed here as well.

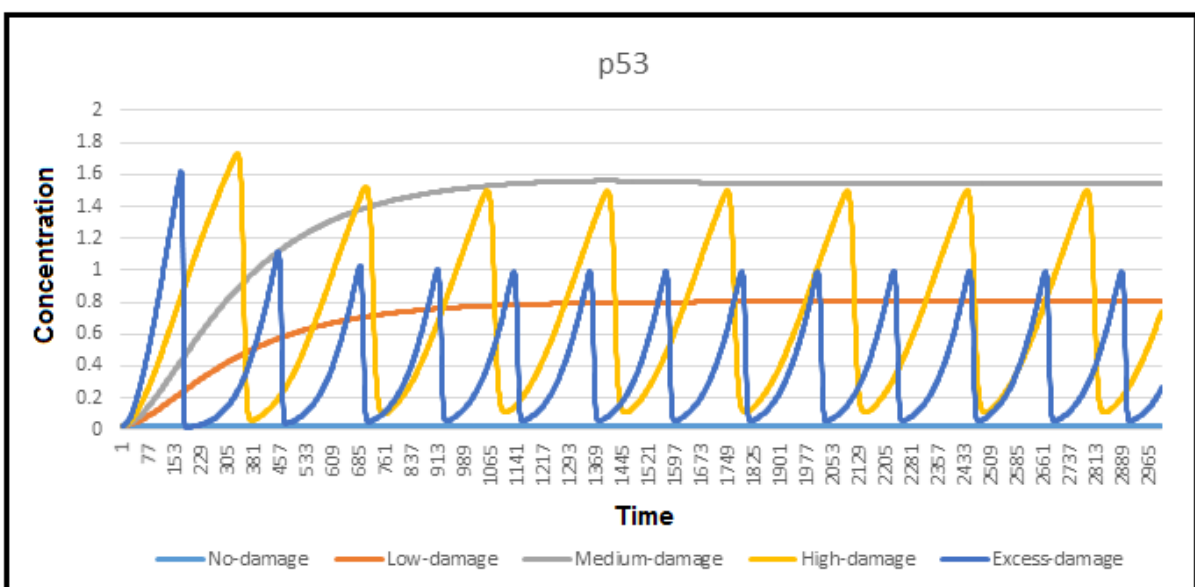


Figure 4.4 Time courses of p53 in the G1/S phase with and without DNA damage from a simulation run using the base model

4.2 The Methodology

Reducing the model of a biological network to a simpler one using a reduction method in this research involves the following tasks: (i) Understanding the protein interactions involved in the biological network; (ii) Representing the biological network as a hierarchical representation; (iii) Determining the key elements in the biological network and finding the acceptable key element numbers that can be lumped (AKEL); and (iv) Introducing different levels of lump formation. This task is divided into two sub-tasks: first, determining the lumps at each level; and secondly, rewriting the equations.

4.2.1 Understand the Protein Interactions Involved in the Biological Network

Understanding protein interactions in this study involves understanding the systems dynamics in the biological network regulation of signal transduction; this involves protein-protein interactions with a focus on complex proteins and the movements from level to level in the presentation of protein-protein interactions.

Deriving a formal abstraction of the system is the crucial first step in a model reduction process. It includes definition of all aspects of the system: components of the system and the form of molecular interactions in the network.

In a general form; suppose a system consists of n chemical species with concentrations Y_1, Y_2, \dots, Y_n participating in the reactions. The rate of change of concentration of all participating chemical species can be written as:

$$\frac{dY_i}{dt} = f_i(Y_1, Y_2, \dots, Y_n) \rightarrow Y_i(t + \Delta t) = Y_i(t) + \int_{\Delta t} f_i(Y_1, Y_2, \dots, Y_n) dt \quad (4.1)$$

When dt becomes very small (from Taylor series expansion) disregarding higher order terms, the new state of the system after a small time increment, Δt , can be rewritten as:

$$Y_i(t + \Delta t) = Y_i(t) + f_i(Y_1, Y_2, \dots, Y_n)\Delta t \quad (4.2)$$

where Y_i is the node output, f_i is the activation function of node i , f_i describes how Y_i values change with time as a function of its current state and inputs, and can be described by nonlinear equations.

4.2.2 Representing the Biological Network as a Hierarchical Representation

The second step is to convert the biological network from a flat to a hierarchical representation to allow different levels of lumping (many levels of abstraction) zoom in and zoom out. Drawing the interactions in the biological network as a hierarchical map helps us visually decide which elements can be lumped together and to figure out directly which equations combine together efficiently.

The nature of the system is its hierarchical structure. This means that the lower level entities form the components of the higher level entities and there is a part-whole relationship between the lower and higher levels of the system. As a result, from this hierarchy, there is a reduction that can be done between each higher and lower levels with different levels of reduction.

The most important characteristic of a biological network is that it contains complex proteins. A complex protein is the result of a protein binding to another protein or molecules of another substance. Individual proteins can participate in the formation of a variety of different protein complexes. Different complexes perform different functions, and the same complex can perform very different functions that depend on a variety of factors.

In any biological network; there are many forms of protein complexes that are divided into different levels. The division process depends on the number of molecules within each kind and the binding relations between these proteins to create complex proteins in the upper level of a biological network. This division method can be applied to represent all biological protein networks. The general rule to calculate the level number of proteins $L(Y_i)$ is as in Eq. (4.3).

$$L(Y_i) = R(Y_i) - 1 \quad (4.3)$$

where $R(Y_i)$ the rank of protein complex formation as in Eq. (4.4).

$$R(Y_i) = \# \text{ Number of single protien in } Y_i \text{ specie} \quad (4.4)$$

In level 0 we put all single proteins. Level 1 contains double complex proteins, which represents two single proteins binding together. Level 2 contains triple complex proteins, which represents three single proteins binding together. Level 3 contains quadruple complex proteins, which represents four single proteins binding together and so on.

The steps to convert a flat biological network into a hierarchical biological network are as follows:

1. Determine the rank of protein complex formation $R(Y_i)$ as in Eq. 4.4, such as single $R(Y_i) = 1$, double $R(Y_i) = 2$... etc.

2. Find the protein complex formation level $L(Y_i)$ in the map, as in Eq. 4.3, based on the rank of protein complex formation $R(Y_i)$.
3. Draw the species into levels.
4. Add the interactions between species.

4.2.3 Determine the Key Elements in the Biological Network and Find the Acceptable Key Elements Number that Can be Lumped (AKEL)

Any biological network has key elements that, mark the start of the process, the completion of a process progression, specific imbalances or the occurrence of a particular disease. For this reason, these key elements need to be kept out of the lumping process as much as possible to maintain the biological meaning of the model; the reduced model thus produced is useful for a particular purpose and is applicable to answering a specific set of questions.

This reduction method enables keeping key elements out of the lumping process or to lump key elements with other elements, but the percentage of the key elements lumped must not exceed 10% of key elements in the system. We suggested 10% in this reduction method to be sure the reduced model still contains 90% of the key elements.

To find the acceptable number of key elements that can be lumped (AKEL) is as in Eq. (4.5).

$$AKEL = \text{Number of key elements} * \frac{1}{10} \quad (4.5)$$

4.2.4 Introduce Different Levels of Lump Formation

This task is divided into two sub-tasks: first, determine the lumps at each level; and, secondly, rewrite the equations.

4.2.4.1 Determine the Lumps at Each Level

In this step, we must apply a graph partition process. The graph partition process is defined as partitioning a Graph, G into smaller components with specific properties.

Consider a Graph $G = (V, E)$, where V denotes the set of n vertices and E the set of edges. Partition V into k parts (sub-sets), F_1, F_2, \dots, F_k , such that the parts are disjointed.

We need to convert the graph into a matrix. For a given Graph G; and its adjacency matrix; A as shown in Figure 4.5 A and B, the rows of the matrix represent the childrens and the columns represent the parents.

An entry A_{ij} implies an edge between nodes Y_i and Y_j , where each entry of A_{ij} , represents the degree of parent Y_j node to Y_i node. To find A_{ij} is as Eq. (4.6).

$$A_{ij} = \begin{cases} L(Y_j) - L(Y_i) & , \text{iff } Y_j \text{ node is the parent of } Y_i \text{ node} \\ 0 & , \text{ otherwise} \end{cases} \quad (4.6)$$

Two more arrays are needed: Array L needs to contain the level number of all nodes in the protein complex formation map graph. Another array, S needs to contain the status of all nodes in the protein complex formation map graph, where S_i find as Eq. (4.7) as shown in Figure 4.5a and b.

$$S_i = \begin{cases} -1 & , \text{for joint node or key regulator node} \\ 1 & , \text{for a key node} \\ 0 & , \text{for other nodes} \end{cases} \quad (4.7)$$

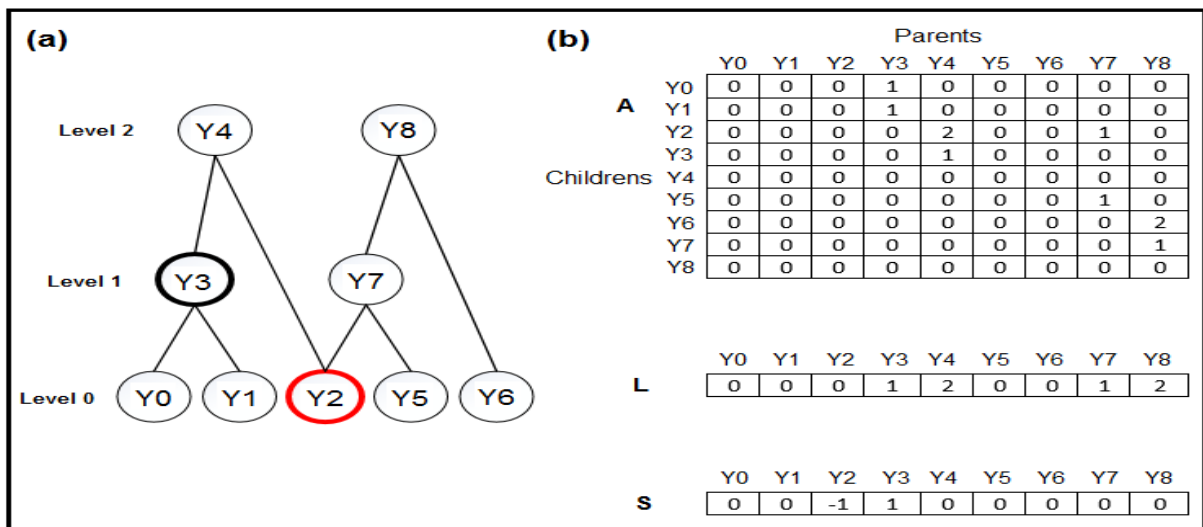


Figure 4.5 (a) Multiple levels of protein complex formation map Graph G; (b) Adjacency matrix A for Graph G, L vector for node level and S vector for node status

In the lumping process, it is important that there is no overlap in scope between different lumps. This overlap could result in duplicated representations or missing interactions regarding responsibility and activity. Such an overlap could also cause confusion about the biological network reduction. For this reason, we must take care of joint proteins and key regulator proteins. A protein is called a joint protein if it has a two parents or more, as shown in Figure 4.6 a and, b where, protein Y2 is a joint protein.

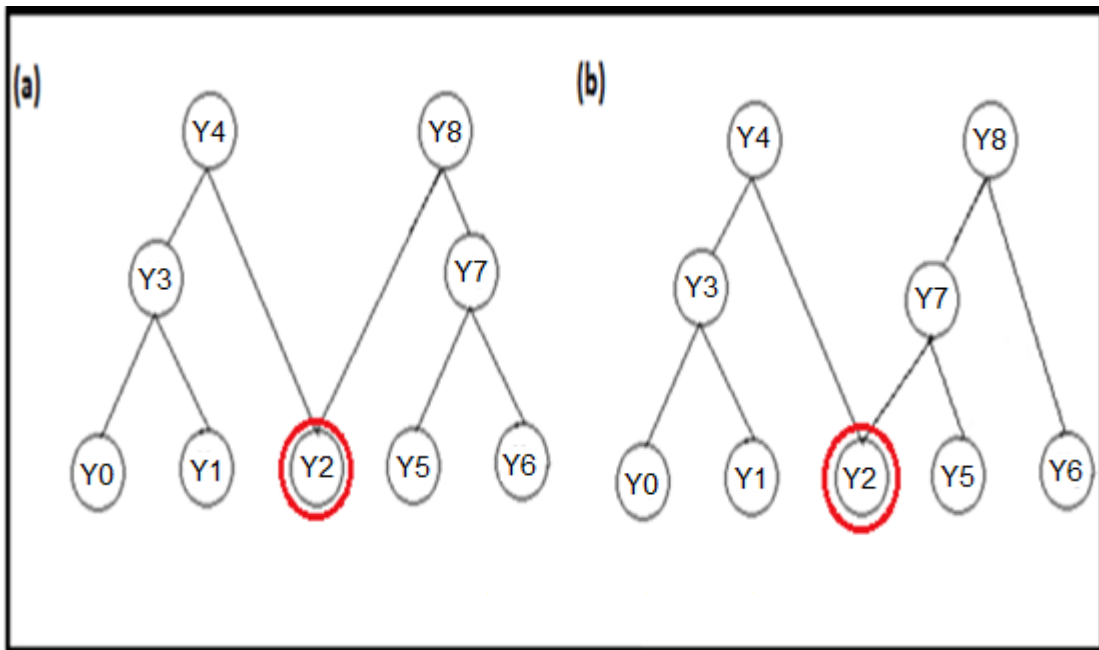


Figure 4.6 Examples of joint proteins in a protein complex formation map graph

Furthermore, in the cell cycle, the progress of the cycle is regulated by a family of protein kinases called cyclin-dependent kinases (Cdks) Cdk1, Cdk2, Cdk4 ... etc., which function to turn specific proteins on and off at appropriate times in the cell cycle. For this reason, these are called key regulator proteins. Joint proteins and the key regulator proteins are kept out of the lumping process to maintain the biological meaning of the model.

The algorithm to partition multiple levels of the protein complex formation map into k parts (sub-sets) to determine the lumps at each level is as follows:

```

NKEL = 0      'Number of key elements lumps

Insert the level number of abstraction

For each node in this level
{ IF node is key node:
  { IF NKEL < AKEL
    { Create lump set
      Insert node to the set
      NKEL = NKEL + 1
      Take all children's of this node and call Test_Node for each node
    }
  }
}

Else
{ Create lump set
  Insert node to the set
  Take all children's of this node and call Test_Node for each node
}
}

Test_Node(node)
{ IF node is key node:
  IF NKEL < AKEL
  { Insert node to the set
    NKEL = NKEL + 1
  }
  Take all children's of this node and call Test_Node for each node
}

Else IF node is not (joint node OR key regulator node):
  Insert node to the set
}

Else IF node is lump
  Insert lump to the set
  Check if the lump in another set Then join the two set in one set
}

```

4.2.4.2 Rewrite the Equations

The lumping process reflects the differential equations for the model (optimise). The optimisation process considers the initial conditions (concentration of all lumps at $t=0$), the kinetic parameters and the mass balance equations of the ODE mathematical model. Many steps are needed to optimise the ordinary differential equations (ODEs) to be suitable for the reduced model after lumping.

1. Find the concentration for each lump at $t=0$; as follows:

$$F_j = \sum_{i=0}^n Y_i \quad \text{where } Y_i \in F_j, t = 0 \quad (4.8)$$

2. Find the partial concentration for every species included in the lump at $t=0$; as follows:

$$Y_{iP} = \frac{Y_i}{F_j} \quad \text{where } Y_i \in F_j, t = 0 \quad (4.9)$$

3. Write the equation for the rate change of concentration of each lump (merge (U) the equations of the species included in the lump); as follows:

$$\frac{dF_i}{dt} =_{\cup} \frac{dY_i}{dt} \quad \text{where } Y_i \in F_j \quad (4.10)$$

4. Simplify the equation by handling each term as in the following cases:

- i. A kinetic parameter term that is not related to any species; keeps its value the same with a new name.

For example: $K1$ in the original model becomes $B1$.

- ii. A kinetic parameter term that relates to one species but is not included in any lump; keeps its value the same with a new name.

For example: $K1Y5$ in the original model becomes $B1Y5$.

- iii. A kinetic parameter term K_n that is related to one species Y_i included in a lump; changes its value into a new value with a new name B_n , calculated as follows:

$$B_n = K_n * Y_{iP} \quad \text{where } Y_i \in F_j \quad (4.11)$$

Then rewrite the term with the new kinetic parameter related to the lump.

For example: $K1Y5$, where $Y5 \in F1$, become $B1F1$, where $B1=K1*Y5P$.

- iv. A kinetic parameter term that is related to two species not included in any lump; keeps the same value in a new name.

For example: $K1Y1Y5$ becomes $B1Y1Y5$.

- v. A kinetic parameter term that is related to two species one of which is included in a lump; changes into a new value with a new name, calculated as follows:

$$Bn = Kn * YiP \quad \text{where } Yi \in Fj \quad (4.12)$$

Then rewrite the term with the new kinetic parameter related to the lump.

For example: $K1Y5Y3$, where $Y5 \in F1$ become $B1F1Y3$, where $B1=K1*Y5P$.

- vi. A kinetic parameter term that is related to two species when both are included in a one lump; changes into a new value with a new name, calculated as follows:

$$Bn = Kn * YiP * YmP \quad \text{where } Yi, Ym \in Fj \quad (4.13)$$

Then rewrite the term with the new kinetic parameter related to the lump.

For example: $K1Y5Y3$, where $Y5, Y3 \in F1$ become $B1F1$, where $B1=K1*Y5P*Y3P$.

- vii. A kinetic parameter term that is related to two species. Each species included in a different lump; changes into a new value with a new name, calculated as follows:

$$Bn = Kn * YiP * YmP \quad \text{where } Yi \in Fj, Ym \in Fs \quad (4.14)$$

Then rewrite the term with the new kinetic parameter related to the lump.

For example: $K1Y5Y3$, where $Y5 \in F1$, $Y3 \in F2$ become $B1F1F2$, where $B1=K1*Y5P*Y3P$.

Note: In the next level of lumping every lump is manipulated as a species.

5. Replace the new formula of the term with the old one wherever it is found in the equations.
6. Simplify the lump equations by deleting or replacing the opposite terms (positive and negative) as in the following cases:
 - a. The term contains a kinetic parameter related to the lump only. Delete the opposite terms (positive and negative).
For example: $B3F1 - B3F1$ delete the two terms.
 - b. The term contains a kinetic parameter related to the lump and a species. Replace the opposite terms (positive and negative) with one term, as follows:

$$B_n * Y_i * F_j - B_n * Y_i * F_j \text{ replace with } B_n * dY_i * F_j \quad (4.15)$$

where $dY_i = Y_i(t) - Y_i(t-1)$, t as timestep

For example: $B3Y5F1 - B3Y5F1$ Replace with $B3dY5F1$.

Note: we use eight decimal digits for parameter values for greater accuracy.

4.3 Model Reduction Method

In the previous section, we described the steps to simplify biological networks in general. In this section, we apply the method to clarify the steps involved. We use the base model that was presented in Section 4.1 (G1/S checkpoint pathway and DNA damage pathways model) as a complex systems to case study to apply our new reduction approach.

4.3.1 Understand the Protein Interactions Involved in the Base Model

Understanding protein interactions involves understanding system dynamics in the G1/S checkpoint pathway and the DNA damage pathway base model. It involves protein-protein interactions where the focus on complex proteins is considered the first step in the model reduction process.

The system and the form of molecular interactions in the network are described in the section on the base model (Section 4.1).

The base model, as shown in Figure 4.7, shows the reaction scheme of the proposed model, which integrated the G1/S model and the DNA damage-signalling pathway. The model consists of 35 dependent variables and 92 kinetic parameters (see Appendix B).

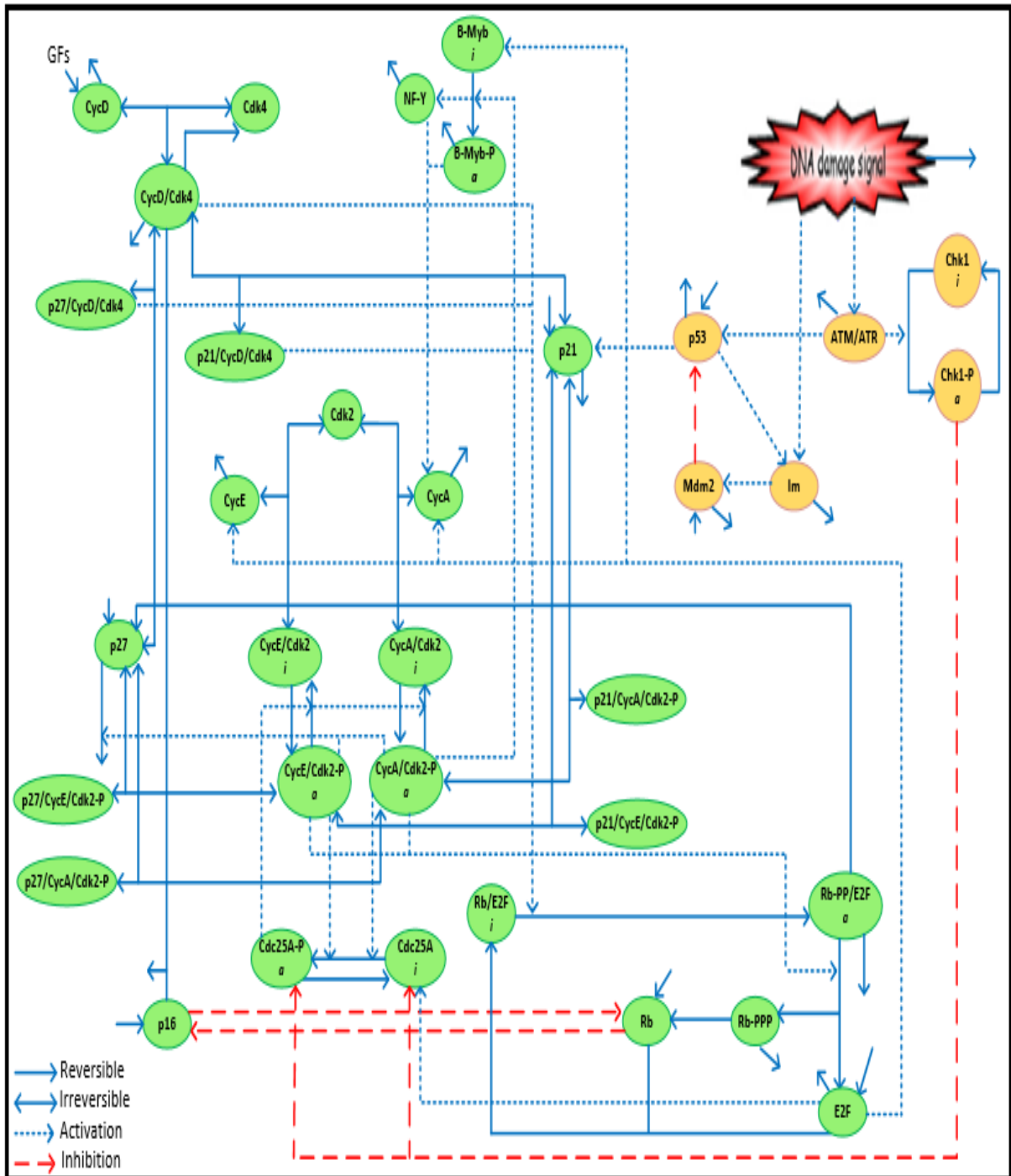


Figure 4.7 G1/S transitions and DNA damage signalling pathway base model

As shown in Figure 4.7, the interactions number 88 between the G1/S elements. These interactions have 11 associations, 10 disassociations, 8 phosphorylation, 6 de-phosphorylation, 11 syntheses, 13 degradations, 24 activations and 5 inhibitions. These statistics of interaction types in the base model are shown in Figure 4.8.

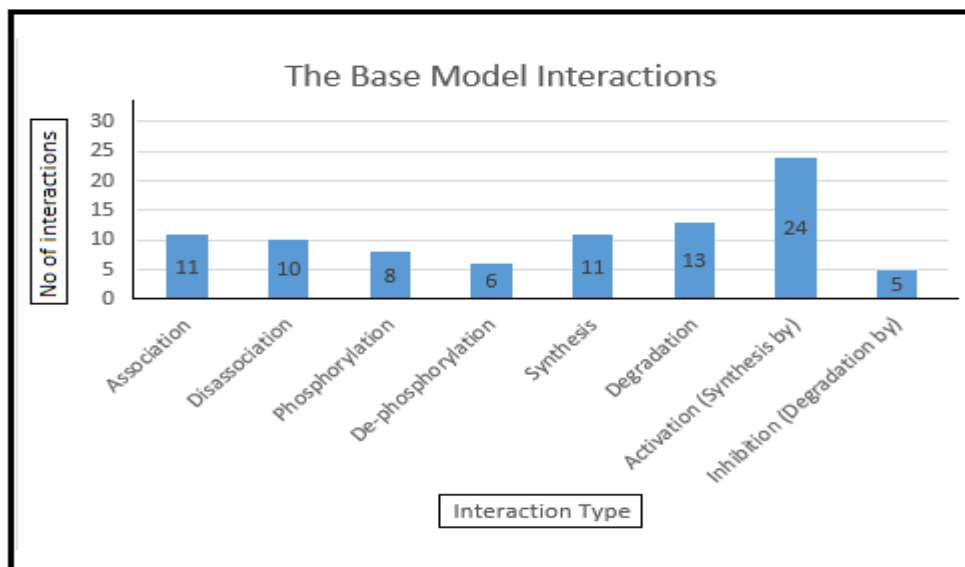


Figure 4.8 Statistics of interaction types on the base model

Table 4.2 shows the biochemical meaning of the kinetic parameters in the interactions map and the effect on the species in the base model. In general, approximately 27% of the interactions are independent interactions for proteins (synthesis and degradation), 40% of the interactions depend on binding and unbinding relations (association, disassociation, phosphorylation and de-phosphorylation), and 33% of the interactions do not depend on binding and unbinding relations (activation and inhibition).

Table 4.2 The biochemical meaning of kinetic parameters in an interactions map and the effect on the species of the base model

No.	Arrow	Meaning	Effect
1	→	Synthesis	Increase
2	←	Degradation	Decrease
4	→	Association	Decrease/Increase
5	→	Dissociation rate	Decrease/Increase
6	→	Phosphorylation rate	Decrease/Increase
7	→	De-phosphorylation rate	Decrease/Increase
8	- - - - ->	Activation	Increase
9	- - - - ->	Inhibition	Decrease

For greater understanding of the dynamics of the G1/S checkpoint pathway and DNA damage pathways base model, we look at the system from another angle (consider the flow and feedback). Proteins concentrations change over time through the interactions (inflow, outflow). The flows are synthesis, degradation, association, disassociation, phosphorylation and de-phosphorylation, activation (synthesis by) and inhibition (degradation by); as shown in Figure 4.9. However, a protein concentration is the present memory of the history of changing flows within the system.

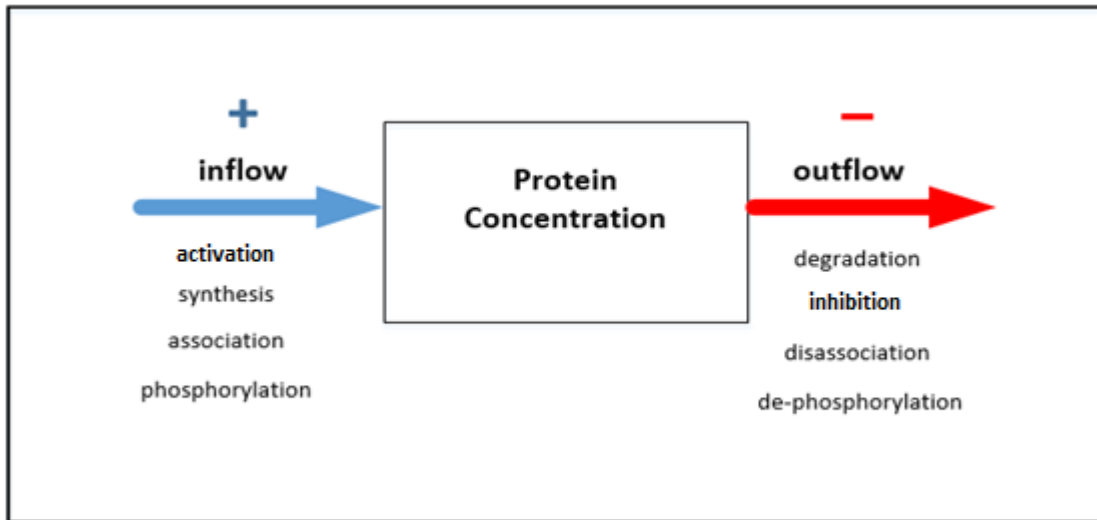


Figure 4.9 Protein concentration flow diagram

In protein networks, the interactions are designed to raise or lower protein concentrations or to keep them within acceptable ranges. As shown in Figure 4.7, G1/S transitions and DNA damage signalling pathway base model is a collection of proteins along with the mechanisms for regulating the levels of the protein concentrations by manipulating flows (a collection of 'feedback processes'); this means the system runs itself by feedback processes. Feedback processes are fundamental to all life and human systems.

Feedback loops can cause protein concentrations to maintain their levels within a range, or grow, or decline. This means the flows into or out of protein are adjusted due to changes in the concentration of the protein itself. Whatever is monitoring the protein concentration level begins a corrective process, adjusting the rates of inflow or outflow (or both), thus changing the protein concentration level. Understanding these feedback processes helps explain the mechanisms of regulation of the G1/S checkpoint and answers these questions: How are biological networks designed to avoid some of the traps/problems that systems with cell interactions have? How do they avoid some extremes and stay within satisfactory bounds without destroying themselves?

As shown in Figure 4.10, a common kind of feedback loop stabilises protein concentration levels, as for example, the relations between Chk1 and Chk1-P. The concentration levels of Chk1 and Chk1-P may

not remain completely fixed but do stay within an acceptable range through phosphorylation and de-phosphorylation interactions. This is known as a balancing feedback.

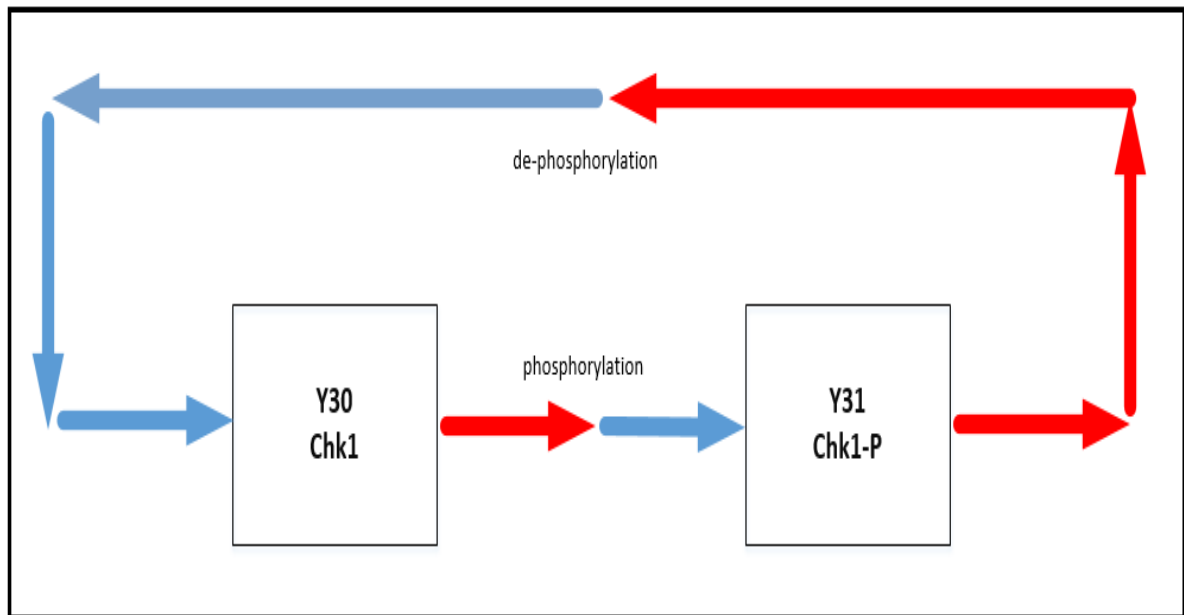


Figure 4.10 Balancing feedback loop between Chk1 and Chk1-P

The relation between Cdc25A and Cdc25A-P is another example of balancing feedback loop in the G1/S checkpoint pathway and DNA damage pathways base model, as shown in Figure 4.11.

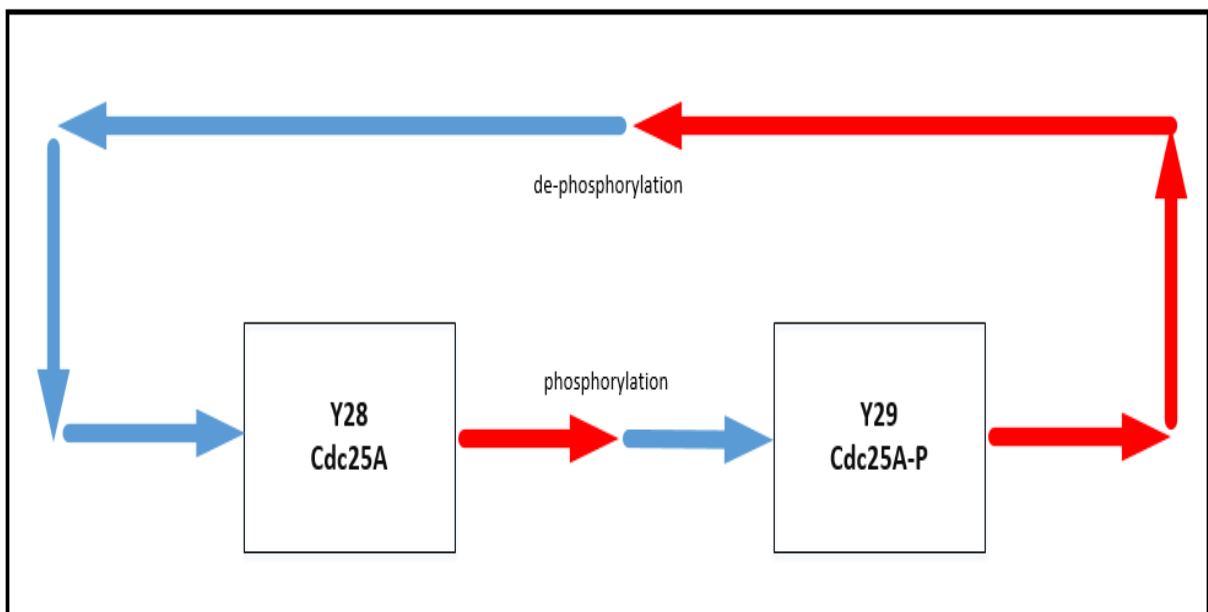


Figure 4.11 Balancing feedback loop between Cdc25A and Cdc25A-P

The second kind of feedback loop is an unbalancing feedback loop that is found wherever a protein concentration can reduce or increase. As shown in Figure 4.12, the feedback includes five proteins (Rb, Rb-PPP, E2F, Rb-PP/E2F and Rb/E2F).

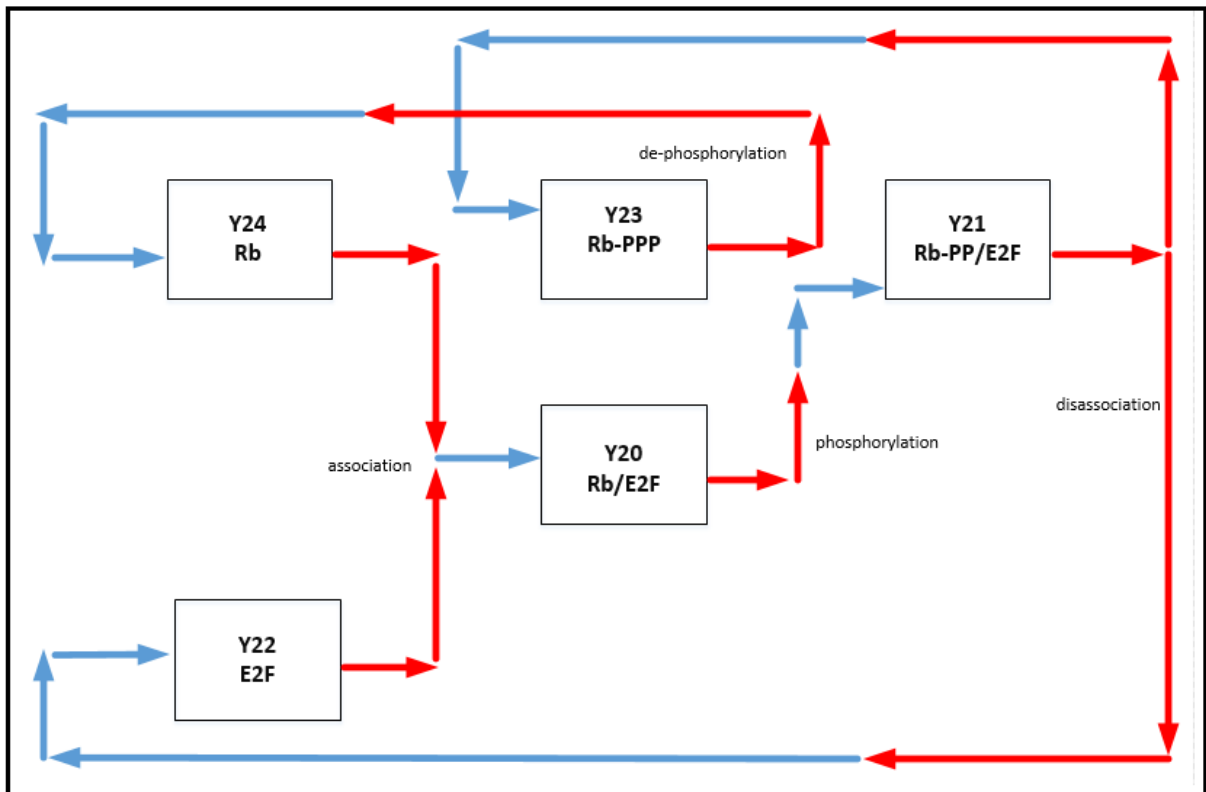


Figure 4.12 Unbalancing feedback

In real systems, feedback loops rarely come in a simple form. Often, they come in multi-level (complex form) and are extended, as shown in Figure 4.13. In this feedback, five proteins are included in the feedback regulation mechanism while, as shown in Figure 4.14, the feedback is extended to include seven proteins in feedback regulation mechanism. This proves two points: first, in understanding all feedbacks in the system it is very important to understand the regulation mechanism in the system and how the system works; secondly, our need to represent the system as a hierarchical representation because the biological system is a multi-level system (hierarchical by nature).

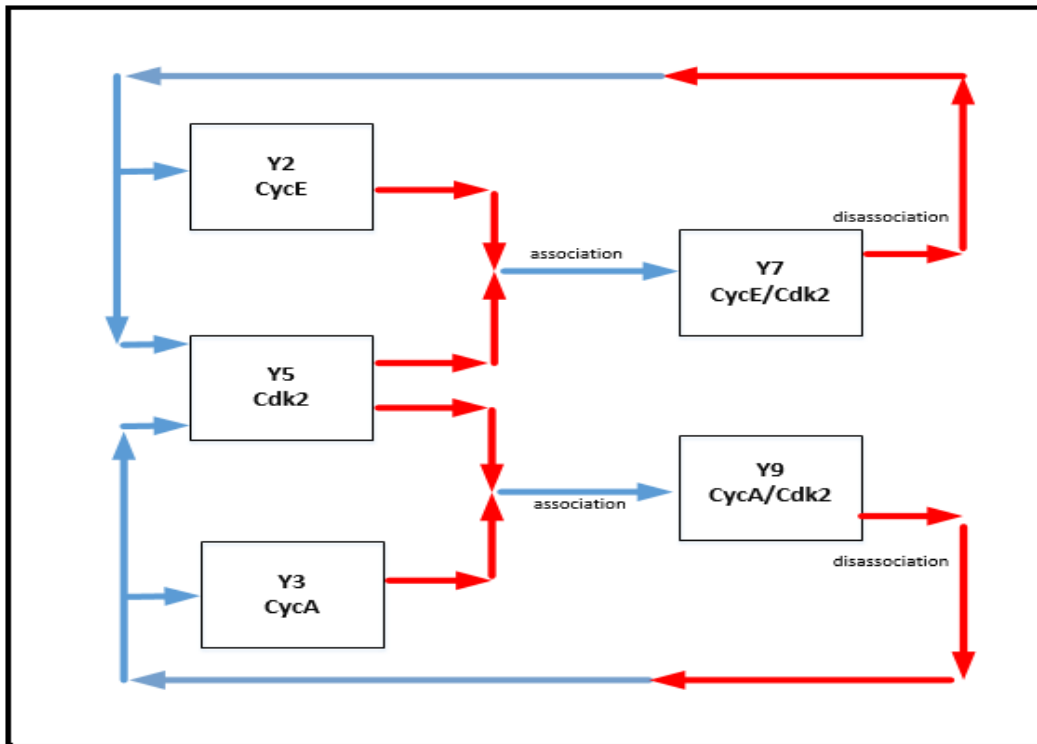


Figure 4.13 Unbalancing feedback with five species

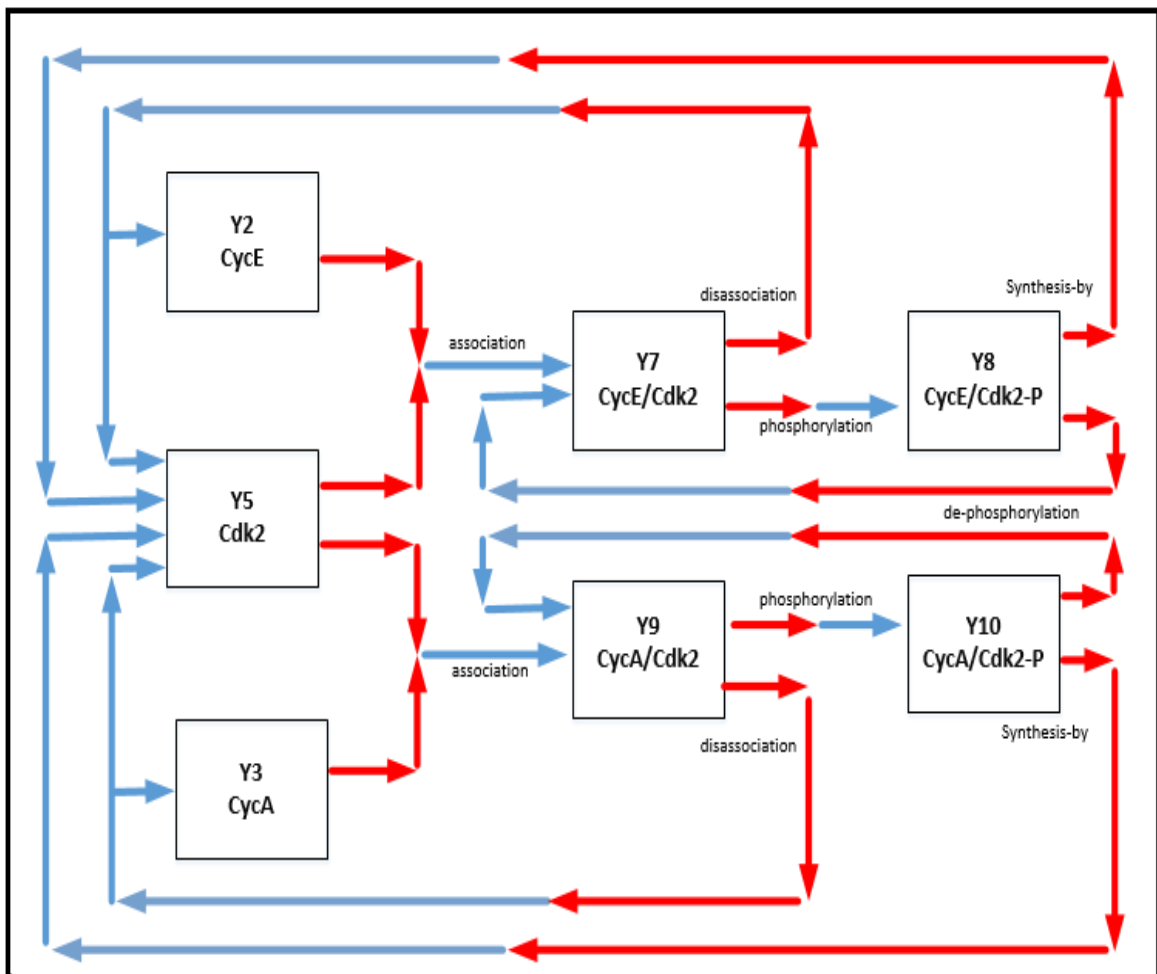


Figure 4.14 Unbalancing feedback with seven species

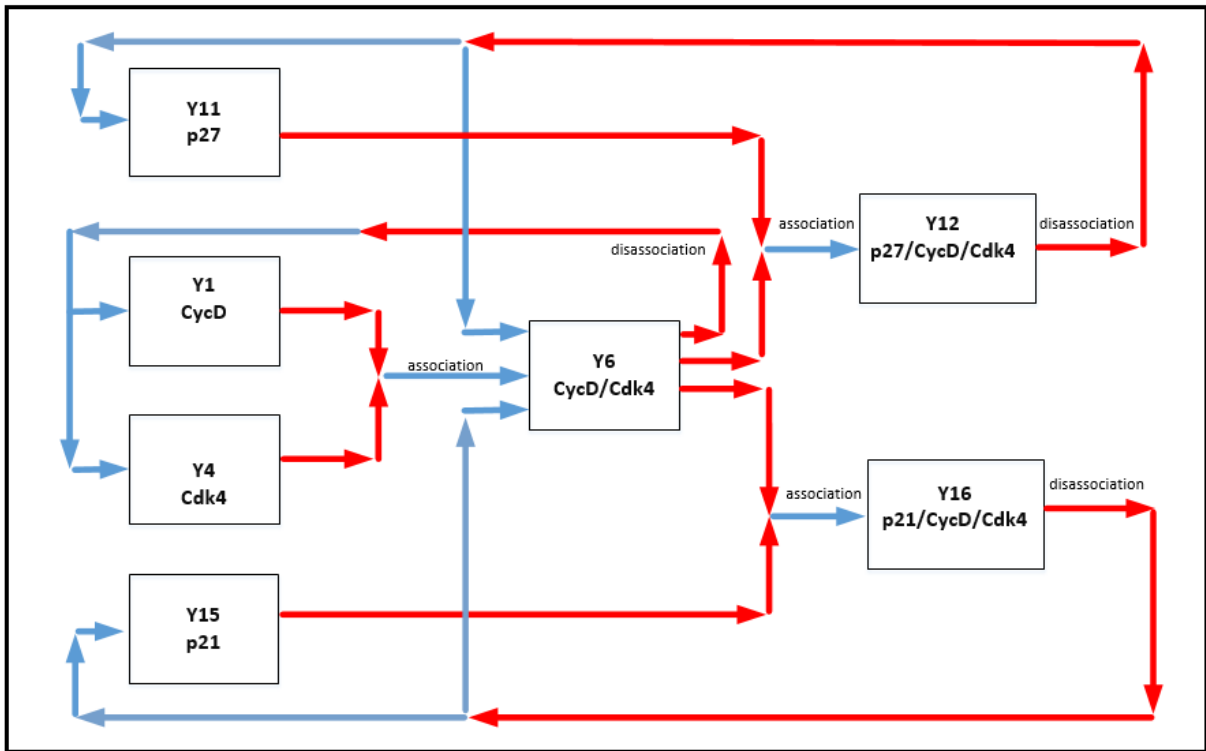


Figure 4.15 Feedback to regulate the concentration of CycD, CycD/Cdk4, p27/CycD/Cdk4 and p21/CycD/Cdk4

In another example from the base model as shown in Figure 4.15, the feedback to regulate the concentration of CycD, CycD/Cdk4, p27/CycD/Cdk4 and p21/CycD/Cdk4 includes seven proteins (CycD, Cdk4, p21, p27, CycD/Cdk4, p27/CycD/Cdk4 and p21/ CycD/Cdk4).

4.3.2 Representing the Biological Network as a Hierarchical Representation

As mentioned in Section 4.2.2, four steps are needed to convert a flat biological network into a hierarchical biological network. Table 4.2 shows the rank $R(Y_i)$ and the level $L(Y_i)$ for all proteins included in the base model. The table is output of step one and two and calculate rank $R(Y_i)$ and the level $L(Y_i)$ by eq. 4.4 and eq. 4.3 respectively.

Table 4.3 The rank $R(Y_i)$ and the level $L(Y_i)$ for all proteins included in the base model

No.	Spice	Protein Name	$R(Y_i)$	$L(Y_i)$
1	Y1	<i>CycD</i>	1	0
2	Y2	<i>CycE</i>	1	0
3	Y3	<i>CycA</i>	1	0
4	Y4	<i>Cdk4</i>	1	0

5	Y5	<i>Cdk2</i>	1	0
6	Y6	<i>CycD/Cdk4</i>	2	1
7	Y7	<i>CycE/Cdk2</i>	2	1
8	Y8	<i>CycE/Cdk2-P</i>	3	2
9	Y9	<i>CycA/Cdk2</i>	2	1
10	Y10	<i>CycA/Cdk2-P</i>	3	2
11	Y11	<i>p27</i>	1	0
12	Y12	<i>p27/CycD/Cdk4</i>	3	2
13	Y13	<i>p27/CycE/Cdk2-P</i>	4	3
14	Y14	<i>p27/CycA/Cdk2-P</i>	4	3
15	Y15	<i>p21</i>	1	0
16	Y16	<i>p21/CycD/Cdk4</i>	3	2
17	Y17	<i>p21/CycE/Cdk2-P</i>	4	3
18	Y18	<i>p21/CycA/Cdk2-P</i>	4	3
19	Y19	<i>p16</i>	1	0
20	Y20	<i>Rb/E2F</i>	2	1
21	Y21	<i>Rb-PP/E2F</i>	3	2
22	Y22	<i>E2F</i>	1	0
23	Y23	<i>Rb-PPP</i>	2	1
24	Y24	<i>Rb</i>	1	0
25	Y25	<i>p53</i>	1	0
26	Y26	<i>Mdm2</i>	1	0
27	Y27	<i>ATM/ATR</i>	1	0
28	Y28	<i>Cdc25A</i>	1	0
29	Y29	<i>Cdc25A-P</i>	2	1
30	Y30	<i>Chk1</i>	1	0
31	Y31	<i>Chk1-P</i>	2	1
32	Y32	<i>NF-Y</i>	1	0
33	Y33	<i>B-Myb</i>	1	0
34	Y34	<i>B-Myb-P</i>	2	1

In Step 3 we draw species into levels and add interactions between species in Step 4, as shown in Figure 4.16.

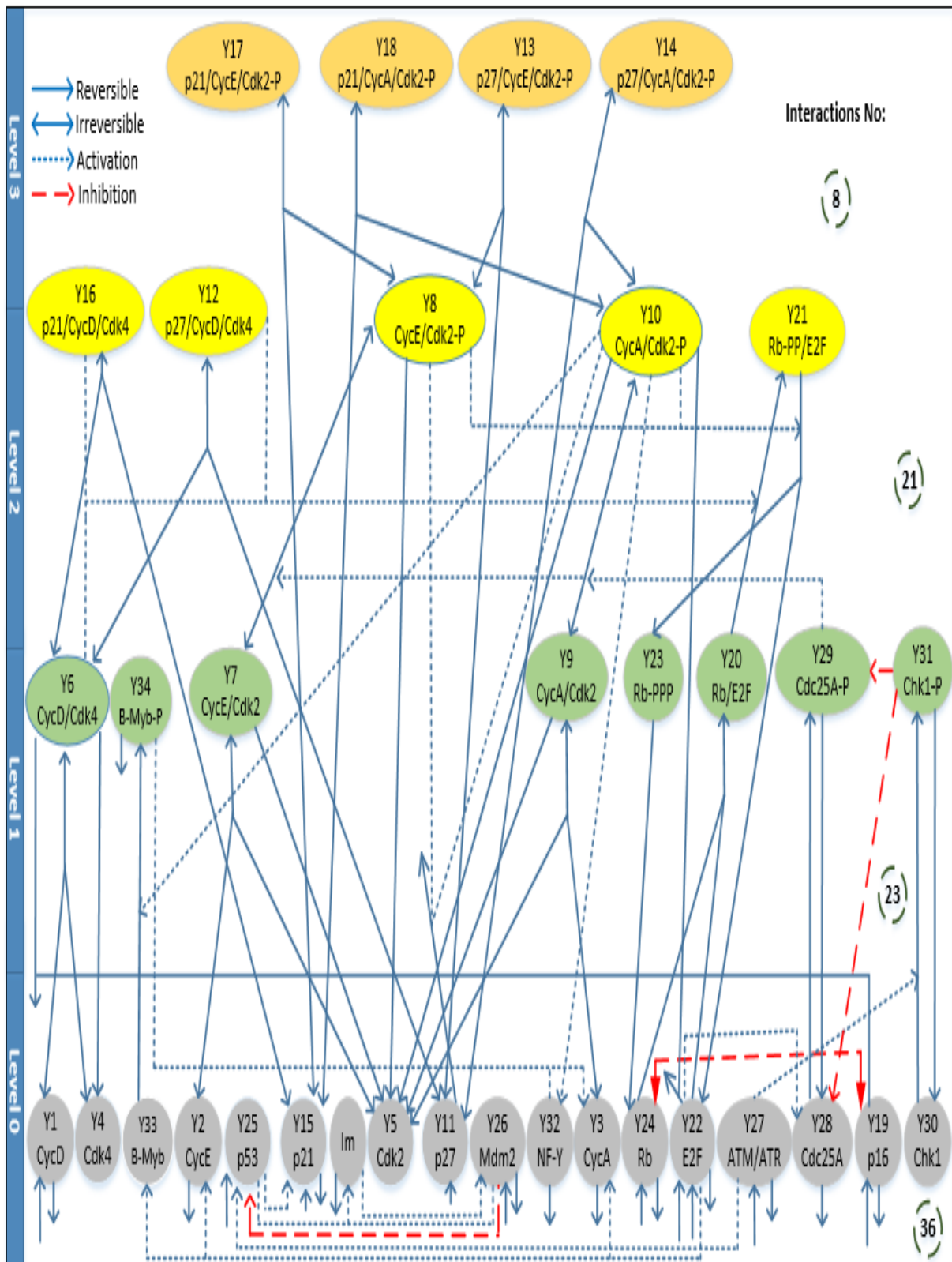


Figure 4.16 Hierarchical interactions map for the base model

4.3.3 Determine the Key Elements in the Biological Network and Find the Number of Acceptable Key Elements that Can be Lumped (AKEL)

In this task, we want to determine the key elements in the base model and calculate the number of key elements that can be lumped. Based on Sections 3.3 and 3.4, the base model contains nine key elements (CycD/Cdk4, CycE/Cdk2-P, CycA/Cdk2-P, p27/CycD/Cdk4, p27/CycE/Cdk2-P, p21/CycE/Cdk2-P, E2F and p53), where each marks a specific point/event or can be used to answer a specific set of questions. These key elements need to be kept out of the lumping process, if possible, to maintain the biological meaning of the model and to be sure that the reduced model is useful. Table 4.4 shows the key elements in the G1/S model and the DNA damage-signalling pathway and their functions.

Table 4.4 Functions of key elements in the base model

No.	Spice	Protein Name	Functions
1	Y6	<i>CycD/Cdk4</i>	There are two functions of CycD/CDK4 complex: 1. To initiate the phosphorylation of Rb bound to E2F to obtain the hypophosphorylated form (Rb-PP/E2F). 2. To keep CycE/CDK2 in active form by (i) Binding with free p27 to form the complex p27/CycD/CDK4. (ii) Isolating p27 from p27/CycE/CDK2.
2	Y8	<i>CycE/Cdk2-P</i>	The activated form of CycE/CDK2-P results in further hypophosphorylation of Rb-PP/E2F to promote dissociation of Rb-PPP and E2F and release E2F.
3	Y10	<i>CycA/Cdk2-P</i>	CycA/CDK2-P drives a negative feedback loop to inhibit the activity of E2F by phosphorylating E2F for its degradation.
4	Y12	<i>p27/CycD/Cdk4</i>	Break cell cycle
5	Y13	<i>p27/CycE/Cdk2-P</i>	Break cell cycle
6	Y15	<i>p21</i>	Plays a role when DNA damage happens, p21 binds to CycE/Cdk2-P and CycA/Cdk2-P, repressing their activity, which induces G1 arrest.
7	Y17	<i>p21/CycE/Cdk2-P</i>	Break cell cycle
8	Y22	<i>E2F</i>	The increase in level of free E2F promotes the synthesis of CycE, which facilitates the association between CycE and Cdk2 to form more of the complex CycE/Cdk2. This results in increases in E2F activity and establishes a positive feedback loop between E2F and CycE.
9	Y25	<i>p53</i>	Plays a role when DNA damage happens, which activates p53 that induces transcriptional activation of Mdm2 and p21.

$$AKEL = 0.9 \approx 1$$

Depending on the value of the variable AKEL, we can lump only one key element, and not more, so that the percentage of key elements lumped is not more than 10%.

4.3.4 Introduce Different Levels of Lump Formation

In this section, we apply two sub-tasks to introduce different levels of lump formation.

4.3.4.1 Determine the Lumps at Each Level

To determine the lumps at each level we converted the graph of hierarchical interactions map to three matrixes:

- a) Adjacency matrix A, as shown in Figure 4.18.
- b) Vector L, as shown in Figure 4.19.
- c) Vector S, as shown in Figure 4.20.

	Y1	Y2	Y3	Y4	Y5	Y6	Y7	Y8	Y9	Y10	Y11	Y12	Y13	Y14	Y15	Y16	Y17	Y18	Y19	Y20	Y21	Y22	Y23	Y24	Y25	Y26	Y27	Y28	Y29	Y30	Y31	Y32	Y33	Y34			
Y1	0	0	0	0	0	1	0	0	0	0	0	0	0	0	0	0	0	0	0	0	0	0	0	0	0	0	0	0	0	0	0	0	0	0	0		
Y2	0	0	0	0	0	0	1	0	0	0	0	0	0	0	0	0	0	0	0	0	0	0	0	0	0	0	0	0	0	0	0	0	0	0	0		
Y3	0	0	0	0	0	0	0	0	1	0	0	0	0	0	0	0	0	0	0	0	0	0	0	0	0	0	0	0	0	0	0	0	0	0	0		
Y4	0	0	0	0	0	1	0	0	0	0	0	0	0	0	0	0	0	0	0	0	0	0	0	0	0	0	0	0	0	0	0	0	0	0	0		
Y5	0	0	0	0	0	0	1	0	1	0	0	0	0	0	0	0	0	0	0	0	0	0	0	0	0	0	0	0	0	0	0	0	0	0	0		
Y6	0	0	0	0	0	0	0	0	0	0	0	1	0	0	0	1	0	0	0	0	0	0	0	0	0	0	0	0	0	0	0	0	0	0	0	0	
Y7	0	0	0	0	0	0	0	1	0	0	0	0	0	0	0	0	0	0	0	0	0	0	0	0	0	0	0	0	0	0	0	0	0	0	0	0	
Y8	0	0	0	0	0	0	0	0	0	0	0	0	1	0	0	0	1	0	0	0	0	0	0	0	0	0	0	0	0	0	0	0	0	0	0	0	
Y9	0	0	0	0	0	0	0	0	0	1	0	0	0	0	0	0	0	0	0	0	0	0	0	0	0	0	0	0	0	0	0	0	0	0	0	0	
Y10	0	0	0	0	0	0	0	0	0	0	0	0	0	1	0	0	0	1	0	0	0	0	0	0	0	0	0	0	0	0	0	0	0	0	0	0	
Y11	0	0	0	0	0	0	0	0	0	0	0	2	3	3	0	0	0	0	0	0	0	0	0	0	0	0	0	0	0	0	0	0	0	0	0	0	
Y12	0	0	0	0	0	0	0	0	0	0	0	0	0	0	0	0	0	0	0	0	0	0	0	0	0	0	0	0	0	0	0	0	0	0	0	0	
Y13	0	0	0	0	0	0	0	0	0	0	0	0	0	0	0	0	0	0	0	0	0	0	0	0	0	0	0	0	0	0	0	0	0	0	0	0	
Y14	0	0	0	0	0	0	0	0	0	0	0	0	0	0	0	0	0	0	0	0	0	0	0	0	0	0	0	0	0	0	0	0	0	0	0	0	0
Y15	0	0	0	0	0	0	0	0	0	0	0	0	0	0	0	2	3	3	0	0	0	0	0	0	0	0	0	0	0	0	0	0	0	0	0	0	0
Y16	0	0	0	0	0	0	0	0	0	0	0	0	0	0	0	0	0	0	0	0	0	0	0	0	0	0	0	0	0	0	0	0	0	0	0	0	0
Y17	0	0	0	0	0	0	0	0	0	0	0	0	0	0	0	0	0	0	0	0	0	0	0	0	0	0	0	0	0	0	0	0	0	0	0	0	0
Y18	0	0	0	0	0	0	0	0	0	0	0	0	0	0	0	0	0	0	0	0	0	0	0	0	0	0	0	0	0	0	0	0	0	0	0	0	0
Y19	0	0	0	0	0	0	0	0	0	0	0	0	0	0	0	0	0	0	0	0	0	0	0	0	0	0	0	0	0	0	0	0	0	0	0	0	0
Y20	0	0	0	0	0	0	0	0	0	0	0	0	0	0	0	0	0	0	0	0	0	1	0	0	0	0	0	0	0	0	0	0	0	0	0	0	0
Y21	0	0	0	0	0	0	0	0	0	0	0	0	0	0	0	0	0	0	0	0	0	0	0	0	0	0	0	0	0	0	0	0	0	0	0	0	0
Y22	0	0	0	0	0	0	0	0	0	0	0	0	0	0	0	0	0	0	0	0	0	1	0	0	0	0	0	0	0	0	0	0	0	0	0	0	0
Y23	0	0	0	0	0	0	0	0	0	0	0	0	0	0	0	0	0	0	0	0	0	0	1	0	0	0	0	0	0	0	0	0	0	0	0	0	0
Y24	0	0	0	0	0	0	0	0	0	0	0	0	0	0	0	0	0	0	0	0	0	0	0	0	0	0	0	0	0	0	0	0	0	0	0	0	0
Y25	0	0	0	0	0	0	0	0	0	0	0	0	0	0	0	0	0	0	0	0	0	0	0	0	0	0	0	0	0	0	0	0	0	0	0	0	0
Y26	0	0	0	0	0	0	0	0	0	0	0	0	0	0	0	0	0	0	0	0	0	0	0	0	0	0	0	0	0	0	0	0	0	0	0	0	0

After applying the algorithm to determine the lumps at each level we had the following:

i. Level-1 lumping:

As shown in Figure 4.21, there are seven rectangles, each representing a concept, which is a lump where:

- F1 lump contains Y1 (CycD) and Y6 (CycD/Cdk4). CycD/Cdk4 is key element. Depending on the value of the variable AKEL, we can lump only one key element.
- F2 lump contains Y2 (CycE) and Y7 (CycE/Cdk2).
- F3 lump contains Y3 (CycA) and Y9 (CycA/Cdk2).
- F4 lump contains Y23 (Rb-PPP) and Y24 (Rb).
- F5 lump contains Y28 (Cdc25A) and Y29 (Cdc25A-P).
- F6 lump contains Y30 (Chk1) and Y31 (Chk1-P).
- F7 lump contains Y33 (B-Myb) and Y34 (B-Myb-P).

The number of concepts in the network Level-1 equals 28 (7 lumps and 21 nodes).

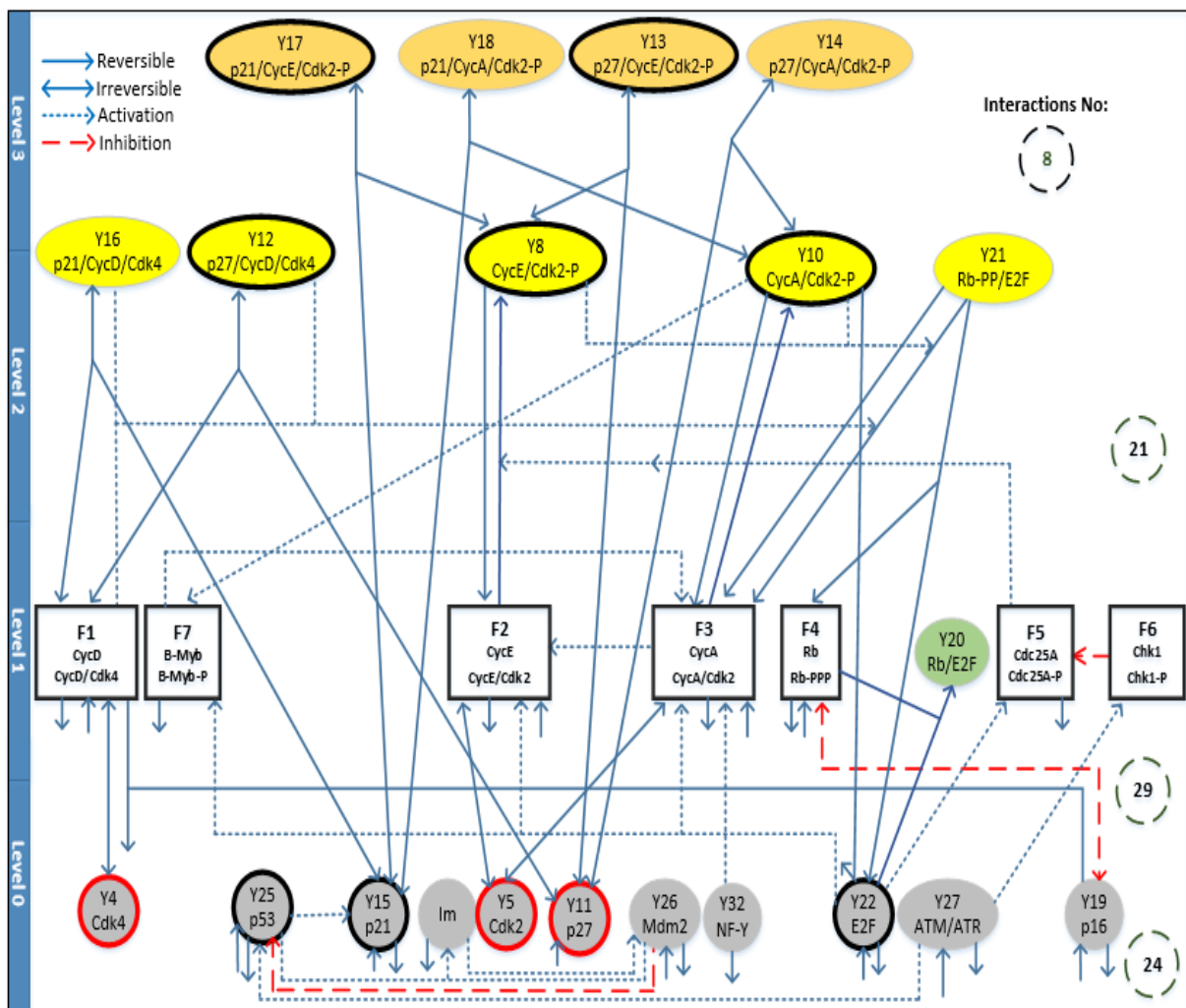


Figure 4.21 Network level-1 lumping

ii. **Level-2 lumping:**

As shown in Figure 4.22, there are seven rectangles, each representing a concept, which is a lump, where:

- F8 lump contains F1 lump and Y16 (p21/CycD/Cdk4).
- F2 lump contains Y2 (CycE) and Y7 (CycE/Cdk2).
- F3 lump contains Y3 (CycA) and Y9 (CycA/Cdk2).
- F9 lump contains F4 lump and Y21 (Rb-PP/E2F).
- F5 lump contains Y28 (Cdc25A) and Y29 (Cdc25A-P).
- F6 lump contains Y30 (Chk1) and Y31 (Chk1-P).
- F7 lump contains Y33 (B-Myb) and Y34 (B-Myb-P).

The number of concepts at network Level-2 equals 26 (7 lumps and 19 nodes).

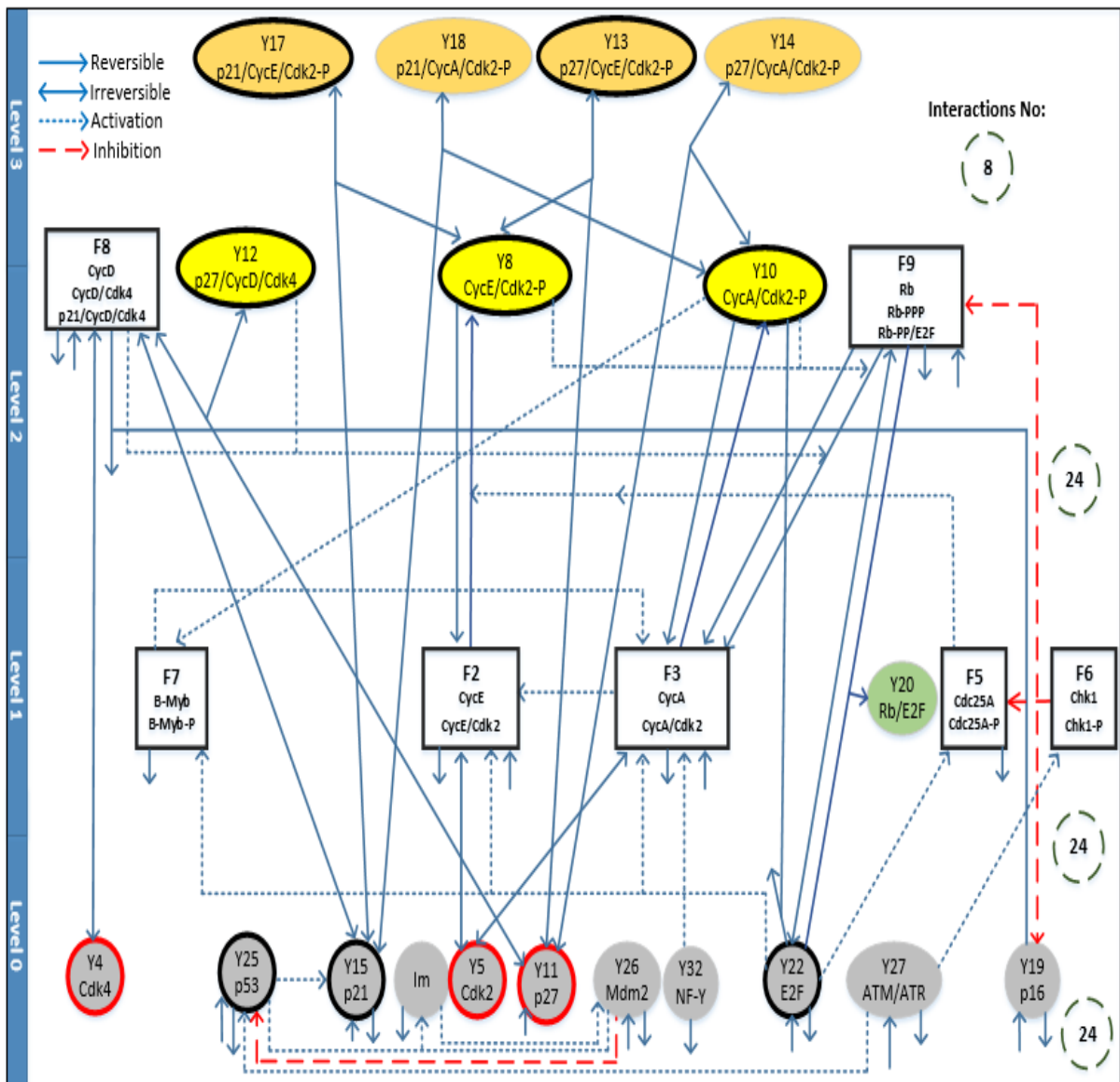


Figure 4.22 Network level-2 lumping

iii. Level-3 lumping:

As shown in Figure 4.23, there are seven rectangles, each representing a concept, which is a lump, where:

- F8 lump contains F1 lump and Y16 (p21/CycD/Cdk4).
- F2 lump contains Y2 (CycE) and Y7 (CycE/Cdk2).
- F10 lump contains F3 lump, Y14 (p27/CycA/Cdk2-P) and Y18 (p21/CycA/Cdk2-P).
- F9 lump contains F4 lump and Y21 (Rb-PP/E2F).
- F5 lump contains Y28 (Cdc25A) and Y29 (Cdc25A-P).
- F6 lump contains Y30 (Chk1) and Y31 (Chk1-P).
- F7 lump contains Y33 (B-Myb) and Y34 (B-Myb-P).

The number of concepts in the network Level-3 equals 24 (7 lumps and 17 nodes).

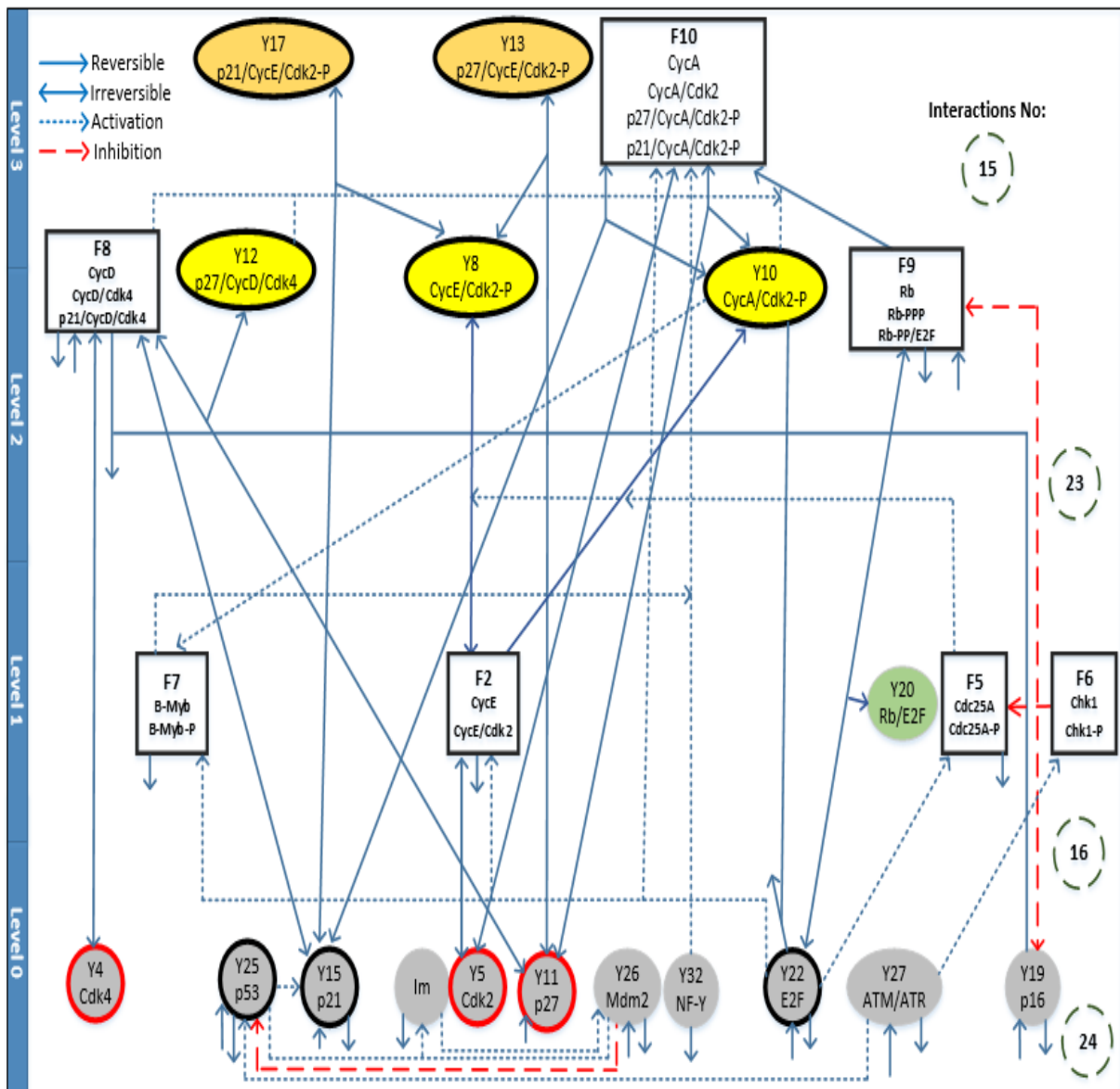


Figure 4.23 Network level-3 lumping

4.3.4.2 Rewrite the Equations

After applying the steps in Section 4.2.4.2 to optimise the ordinary differential equations (ODEs) to be suitable for the reduced model after lumping level-1, the attributes of the reduced system is determined.

Finding the concentration for each lump at $t=0$ is the first step in performing the rewrite of the equations by using Eq. 4.8, as shown in Table 4.5:

Table 4.5 The concentration for each lump at $t=0$, reduced model level-1

<i>Group node</i>	<i>Value</i>	<i>Initial value</i>
<i>F1</i>	= $Y1 + Y6$	$7.53E+00$
<i>F2</i>	= $Y2 + Y7$	$2.00E-03$
<i>F3</i>	= $Y3 + Y9$	$4.40E-04$
<i>F4</i>	= $Y23 + Y24$	$6.00E-02$
<i>F5</i>	= $Y28 + Y29$	$1.10E-03$
<i>F6</i>	= $Y30 + Y31$	$1.00E+00$
<i>F7</i>	= $Y33 + Y34$	0

In the second step we found the partial concentration for every species included in the lump at $t=0$ from Eq. 4.9, as shown in Table 4.6:

Table 4.6 Partial concentration of every species included in the lump at $t=0$, reduced model level-1

<i>Chemical species</i>	<i>Initial value</i>	<i>Chemical species</i>	<i>Initial value</i>	<i>Chemical species</i>	<i>Initial value</i>
<i>Y1p</i>	$3.98E-03$	<i>Y9p</i>	$9.09E-01$	<i>Y30p</i>	$9.90E-01$
<i>Y6p</i>	$9.96E-01$	<i>Y23p</i>	$1.67E-01$	<i>Y31p</i>	$1.00E-02$
<i>Y2p</i>	$5.00E-01$	<i>Y24p</i>	$8.33E-01$	<i>Y33p</i>	$0.00E+00$
<i>Y7p</i>	$5.00E-01$	<i>Y28p</i>	$9.09E-01$	<i>Y34p</i>	$0.00E+00$
<i>Y3p</i>	$9.09E-02$	<i>Y29p</i>	$9.09E-02$		

In third, fourth, fifth and sixth steps we show the steps to lump F1 in details and the same way process applies to the rest of the lumps.

The equation that calculates the rate change of concentration of F1 from Eq. 4.10 is as follows:

$$dF_1/dt = dY_1/dt \cup dY_6/dt$$

After replacing dY_1/dt and dY_6/dt , it becomes:

$$dF_1/dt = k_1 + k_4 Y_6 - (k_2 + k_3 Y_4) Y_1 + k_3 Y_1 Y_4 + k_{19} Y_{16} + k_{21} Y_{12} - (k_4 + k_{13} + k_{18} Y_{15} + k_{20} Y_{11} + k_{44} Y_{19}) Y_6$$

The equation after handling each term becomes:

$$dF_1/dt = B_1 + B_4 F_1 - (B_2 + B_3 Y_4) F_1 + B_3 F_1 Y_4 + B_{19} Y_{16} + B_{21} Y_{12} - (B_4 + B_{13} + B_{18} Y_{15} + B_{20} Y_{11} + B_{44} Y_{19}) F_1$$

Rewriting the equation by expanding the bracketed terms:

$$dF_1/dt = B_1 + B_4 F_1 - B_2 F_1 - B_3 Y_4 F_1 + B_3 F_1 Y_4 + B_{19} Y_{16} + B_{21} Y_{12} - B_4 F_1 - B_{13} F_1 - B_{18} Y_{15} F_1 - B_{20} Y_{11} F_1 - B_{44} Y_{19} F_1$$

After simplifying the lump equations by deleting or replacing the opposite terms (positive and negative):

$$dF_1/dt = B_1 + (B_3 dY_4) F_1 + B_{19} Y_{16} + B_{21} Y_{12} - (B_2 + B_{13} + B_{18} Y_{15} + B_{20} Y_{11} + B_{44} Y_{19}) F_1$$

For further simplification, we replace B_2 and B_{13} by one term B_2 , where $B_2 = B_2 + B_{13}$.

$$dF_1/dt = B_1 + (B_3 dY_4) F_1 + B_{19} Y_{16} + B_{21} Y_{12} - (B_2 + B_{18} Y_{15} + B_{20} Y_{11} + B_{44} Y_{19}) F_1$$

For initial conditions, lumps, partial elements, kinetic parameters and mass balance equations of ODE mathematical model of the DNA damage-signalling pathway and G1/S checkpoint in the reduced model level-1 see Appendix C.

For initial conditions, lumps, partial elements, kinetic parameters and mass balance equations of ODE mathematical model of the DNA damage-signalling pathway and G1/S checkpoint in the reduced model level-2 see Appendix D.

For initial conditions, lumps, partial elements, kinetic parameters and mass balance equations of ODE mathematical model of the DNA damage-signalling pathway and G1/S checkpoint in the reduced model level-3 see Appendix E.

This chapter included three sections. In Section 4.1, the base model was extracted from the Iwamoto model 2011. Then, in Section 4.2, we proposed a method to simplify biological networks based on hierarchical representation and lumping. In Section 4.3, we used the base model that presented in Section 4.1 (G1/S checkpoint pathway and DNA damage pathways model) as a complex system as a case study to apply our new reduction approach to clarify the steps involved.

Chapter 5

Results and Discussion

In this chapter, we validated the reduced model with the base model: firstly, by comparing the behaviour of the model elements, and secondly by comparing model results, and finding the root mean squared error (RMSE) and the root mean squared percentage error (RMSPE), to be sure that the reduced model was useful for a particular purpose and applicable to answer a specific set of questions. In this research, we used Microsoft Excel spreadsheets with Visual Basic for Applications (VBA) to simulate the base model, the reduced model (level-1), the reduced model (level-2) and the reduced model (level-3).

5.1 Element Behaviour

In biology, every biological entity in a model must have a biological description, which should be taken into consideration when comparing models. In other words, the meaning of the components of the model (substances, reactions, cell compartments, etc.) must be considered (Courtot et al., 2011).

In this section, we compare the behaviour of the elements in the base model and the reduced models (level-1), (level-2) and (level-3) in terms of the biological meaning of each element.

5.1.1 Comparison of the Reduced Model (level-1) with the Base Model

5.1.1.1 Reduced Model (level-1) Simulation without DNA Damage

Figure 5.1 illustrates the behaviour of $F1'$ lump ($CycD + CycD/Cdk4$) obtained from the reduced model (level-1) ($F1'$) superimposed on the original ODE solutions ($F1$). The results indicated that the reduced model (level-1) outcomes agreed with the ODE original solutions in representing the behaviour of $F1$ ($CycD + CycD/Cdk4$). This behavior is produced as follows in the early G1 phase the growth factors (GFs) propagate the proliferation signal that triggers synthesis of $CycD$, increasing its concentration. The $CycD$ produced binds to $CDK4$ to form the complex, $CycD/CDK4$, keeping it in an activated state. The $CycD/CDK4$ complex binds with free $p27$ to form the complex, $p27/CycD/CDK4$ (Obaya and Sedivy, 2002). These processes reduce the concentration of $F1$ ($CycD + CycD/Cdk4$) as in Figure 5.1 and, at the same time, increase the concentration of $p27/CycD/Cdk4$.

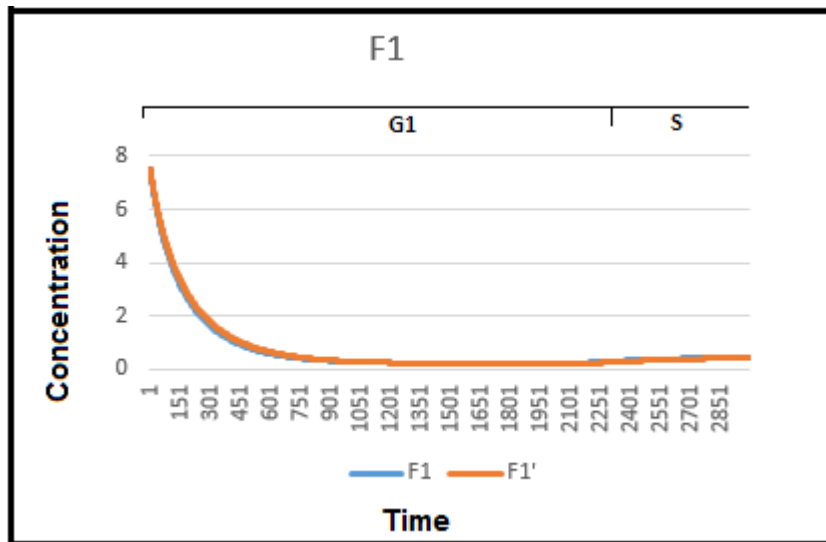


Figure 5.1 Comparison between the concentration history for F1(CycD + CycD/Cdk4) in the base model and F1' lump in the reduced model (level-1)

In the mid to late G1 phase the increase in the level of free E2F promotes the synthesis of CycE, which facilitates the association between CycE and CDK2 to form more of the complex, CycE/CDK2. This results in increased E2F activity and establishes a positive feedback loop between E2F and CycE further increasing CycE and CycE/Cdk2. This explains the behaviour of F2 (CycE + CycE/Cdk2) shown in Figure 5.2 indicating that F2 concentration increase from the mid G1 phase to reach a high level at the end of G1. This peak time of F2 was considered a boundary between the G1 and S phases. A perfect agreement between the two solutions is seen in Figure 5.2.

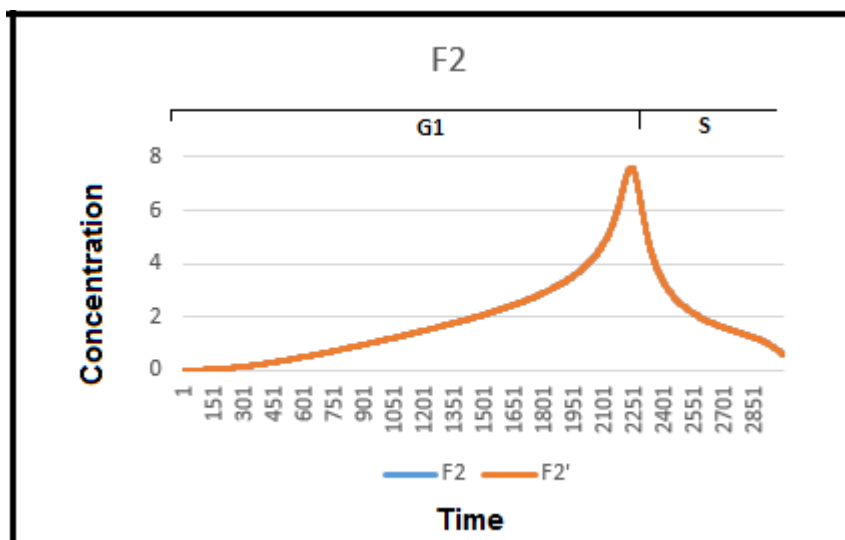


Figure 5.2 Comparison between the concentration history for F2(CycE + CycE/Cdk2) in the base model and F2' lump in the reduced model (level-1)

Figure 5.3 illustrates the behaviour of CycE/Cdk2-P obtained from the reduced model (level-1) (Y8') superimposed on the original ODE solution (Y8). The results indicate that the outcome of new model agreed with the original solutions in representing the behaviour of CycE/Cdk2-P.

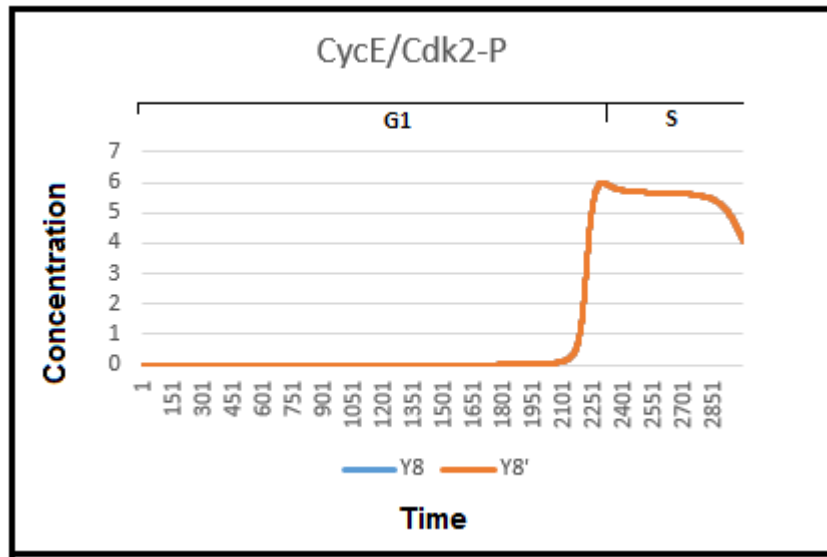


Figure 5.3 Comparison between the concentration history for Y8(CycE/Cdk2-P) in the base model and Y8'(CycE/Cdk2-P) in the reduced model (level-1)

As shown in Figure 5.4, the F3 lump (CycA + CycA/Cdk2) concentration stay at a low level in G1 and then rises beyond G1/S and into S phase. This concurs the logic that E2F subsequently promotes CycA expression at the G1/S transition with a significant increase in the S phase. In the S phase, the synthesized CycA binds to CDK2 to form the complex, CycA/CDK2. A close agreement between the two solutions is seen in Figure 5.4.

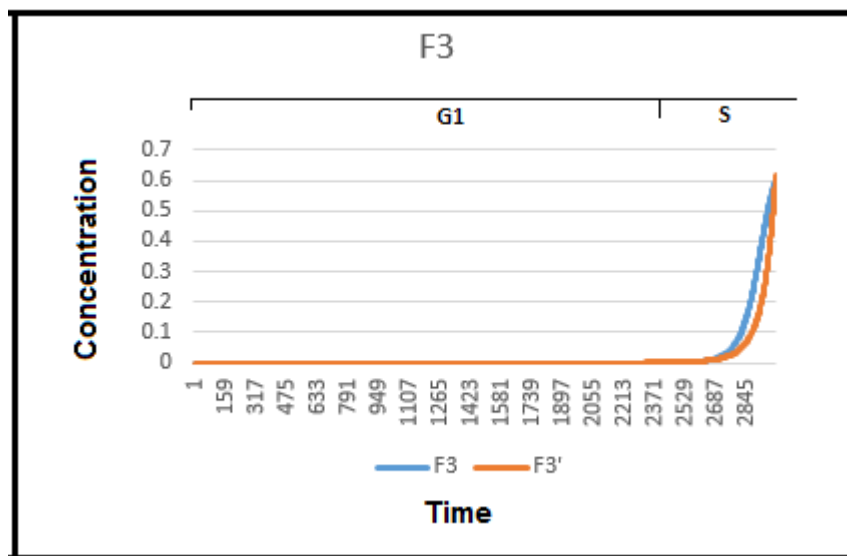


Figure 5.4 Comparison between the concentration history for F3(CycA + CycA/Cdk2) in the base model and F3' lump in the reduced model (level-1)

Figure 5.5 illustrates the behaviour of CycA/Cdk2-P obtained from the reduced model (level-1) superimposed on the original ODE solution (Y10). The results indicated that the outcome of the reduced model (level-1) agreed with the original solution in representing the behaviour of CycA/Cdk2-P.

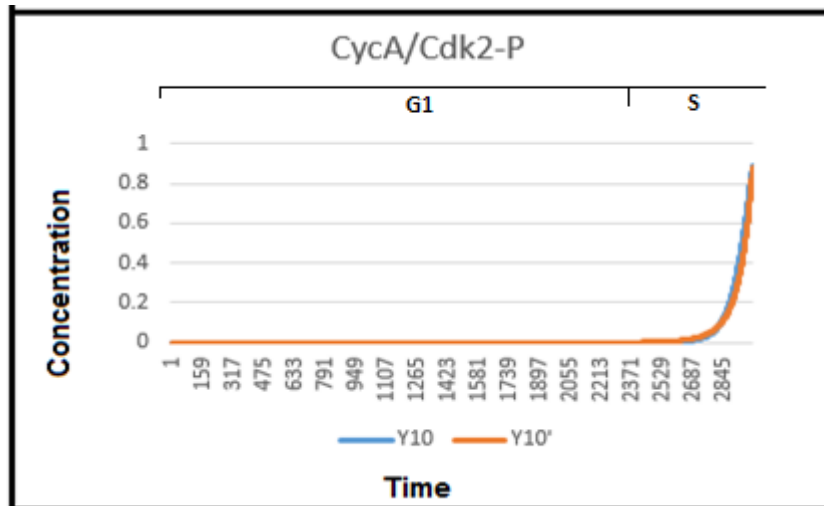


Figure 5.5 Comparison between the concentration history for Y10(CycA/Cdk2-P) in the base model and Y10'(CycA/Cdk2-P) in the reduced model level-1

As shown in Figure 5.6, the concentration of p27 is sustained at a high level in the early G1 phase (Donjerkovic and Scott, 2000). The CycD/CDK4 complex binds with free p27 to form the complex, p27/CycD/CDK4. This process causes a reduction in the concentration of p27 in the first quarter in G1. A significant degradation of p27 occurs at the end of G1, because the large amount of activated CycE/CDK2 can initiate p27 degradation by phosphorylating it at threonine when p27 was bound to CycE/CDK2 (Coqueret, 2003). A very close agreement between the two solutions is seen in Figure 5.6.

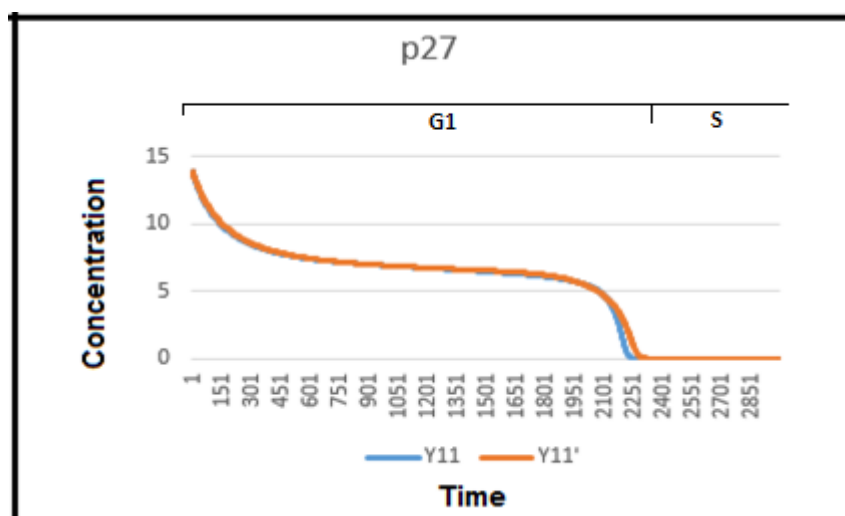


Figure 5.6 Comparison between the concentration history for Y11(p27) in the base model and Y11'(p27) in the reduced model (level-1)

As stated above, in early G1, CycD/CDK4 complex binds with free p27 to form the complex, p27/CycD/CDK4 that causes increase in p27/CycD/CDK4 concentration in the first quarter of G1. As shown in Figure 5.7 the results indicate that the outcome of the reduced model level-1 highly agrees with the original solution in representing the behaviour of p27/CycD/CDK4.

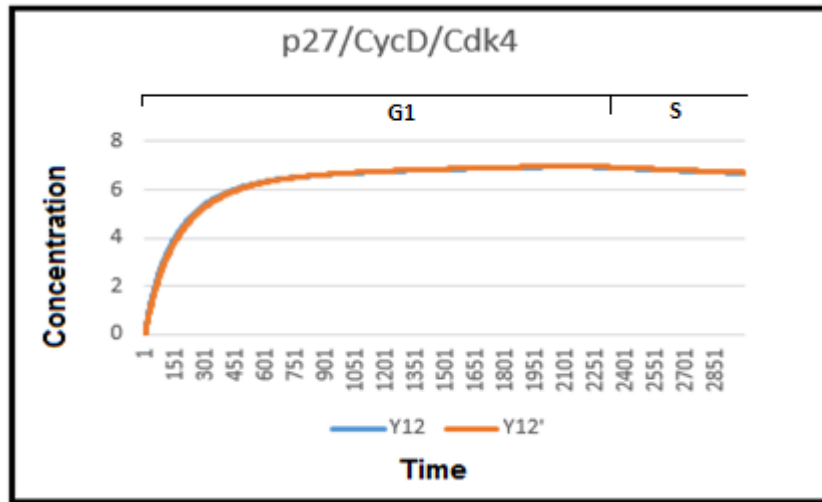


Figure 5.7 Comparison between the concentration history for Y12(p27/CycD/CDK4) in the base model and Y12'(p27/CycD/CDK4) in the reduced model (level-1)

The degradation of CycD occurs mid G1 phase and p16 inhibits the activation of CycD/Cdk4, which promotes the release of p27 bound to the complex CycD/CDK4. The free p27 is redistributed to new complexes, such as CycE/CDK2-P and CycA/CDK2-P, to form p27/CycE/CDK2-P and p27/CycA/CDK2-P, as shown in Figure 5.8 and 5.9. There was good agreement between the outcomes of the reduced model (level-1) and those of the base model.

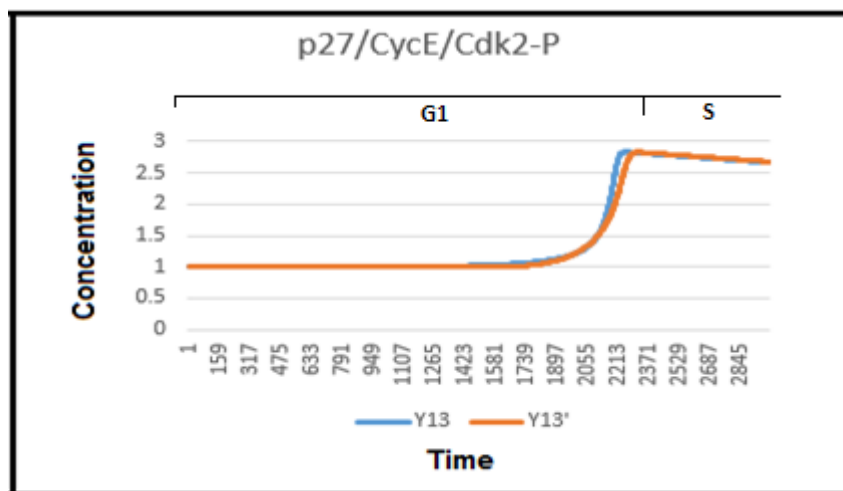


Figure 5.8 Comparison between the concentration history for Y13(p27/CycE/Cdk2-P) in the base model and Y13'(p27/CycE/Cdk2-P) in the reduced model (level-1)

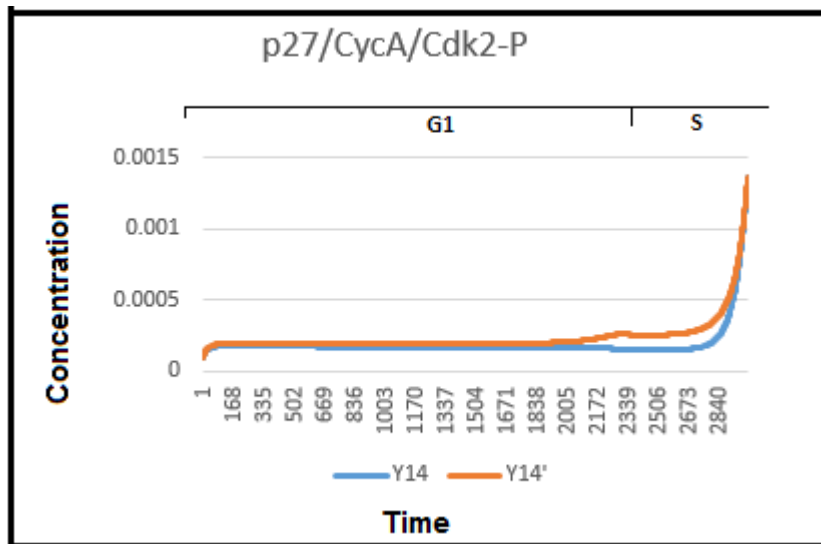


Figure 5.9 Comparison between the concentration history for Y14(p27/CycA/Cdk2-P) in the base model and Y14'(p27/CycA/Cdk2-P) in the reduced model (level-1)

p21 is up regulated when DNA damage occurs which inhibits the positive feedback loop between the Rb/E2F complex and both types of Cyc/Cdk complex (CycA/Cdk2-P and CycB/Cdk1-P) (Iwamoto et al., 2011). If no DNA damage occurs, a small amount of p21 is produced at the beginning of G1 phase, as shown in Figure 5.10. The p21 concentration stays at a low level during G1 phase. The quantity produced of p21 is bind with CycD/Cdk4 to form the complex protein p21/CycD/Cdk4, at beginning of the G1 phase. The concentration of p21/CycD/Cdk4 then starts to decrease because the disassociation rate ($5.00e-03$) is greater than the association rate ($5.00e-04$) of p21 with CycD/CDK4 as shown in Figure 5.11. There was a good agreement between the base model outcome and the reduced model (level-1) outcome for both p21 and p21/CycD/Cdk4 as shown in the two figures.

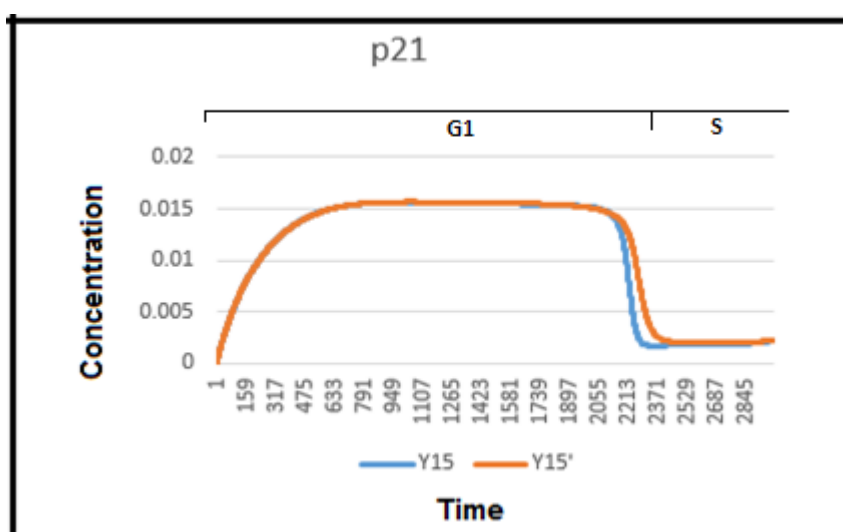


Figure 5.10 Comparison between the concentration history for Y15(p21) in the base model and Y15'(p21) in the reduced model (level-1)

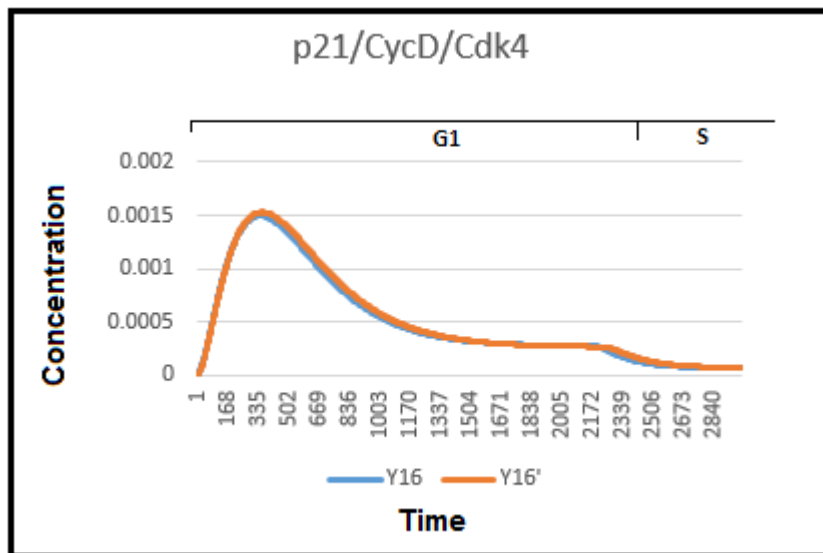


Figure 5.11 Comparison between the concentration history for Y16(p21/CycD/CDK4) in the base model and Y16'(p21/CycD/CDK4) in the reduced model (level-1)

p21/CycE/Cdk2-P and p21/CycA/Cdk2-P are shown in Figures 5.12 and 5.13, respectively. Without DNA damage, the concentrations all these species were maintained at a low level, and the inhibitory effect of p21 on these complexes can still be seen. The two figures indicate that the reduced model (level-1) outcomes agree with the base model solution in representing the behaviour of both p21/CycE/Cdk2-P and p21/CycA/Cdk2-P.

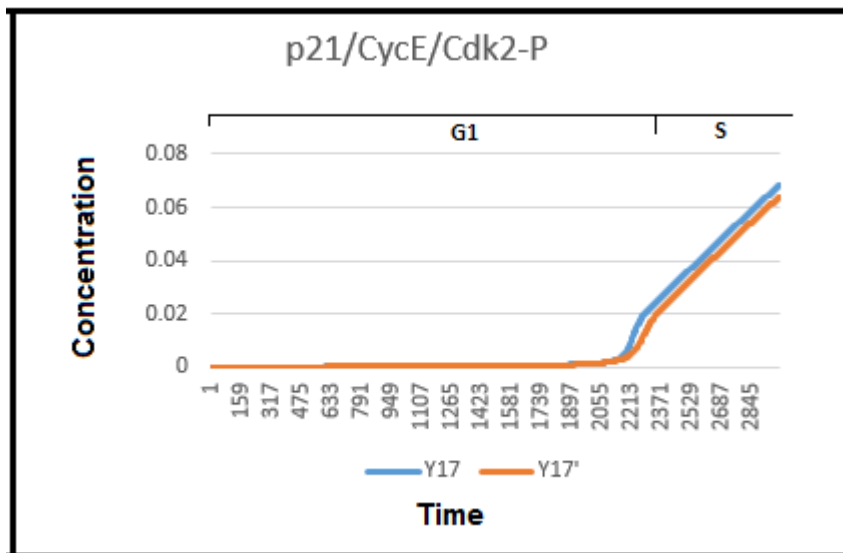


Figure 5.12 Comparison between the concentration history for Y17(p21/CycE/Cdk2-P) in the base model and Y17'(p21/CycE/Cdk2-P) in the reduced model (level-1)

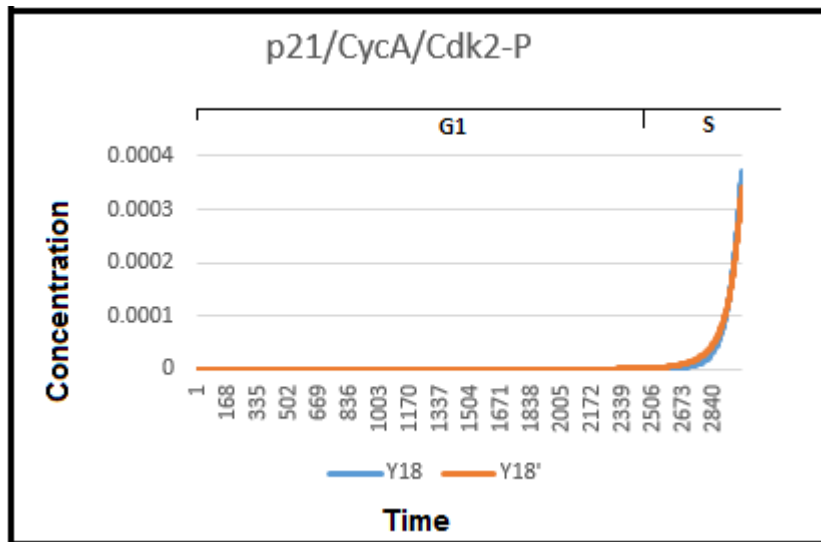


Figure 5.13 Comparison between the concentration history for Y18(p21/CycA/Cdk2-P) in the base model and Y18'(p21/CycA/Cdk2-P) in the reduced model (level-1)

p16 is considered to be one of three Cdk inhibitors that regulates G1/S progression (p16, p21, and p27). Both p21 and p27 represses CycE/Cdk2-P and CycA/Cdk2-P, while p16 inhibits the activation of CycD/Cdk4 (Parry et al., 1995; LaBaer et al., 1997). There was an inverse relationship between the level of increasing p16 and the concentration level of Rb, where the p16 level continues to rise steadily until Rb reaches its highest level late in the G1 phase. At this time, the amount of p16 increase becomes very small. As shown in Figure 5.14, there was a perfect match between the reduced model (level-1) outcome and the base model outcome.

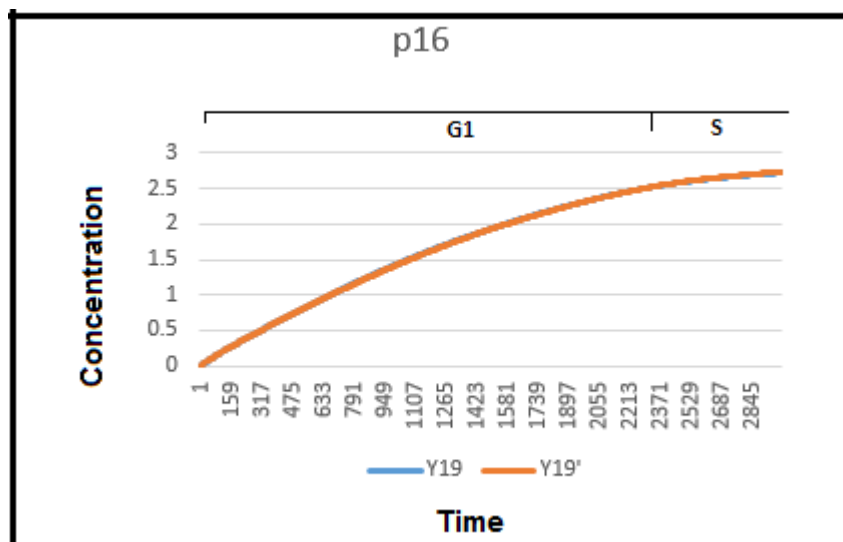


Figure 5.14 Comparison between the concentration history for Y19(p16) in the base model and Y19'(p16) in the reduced model (level-1)

In the early G1 phase the CycD/CDK4 complex initiate the phosphorylation of Rb bound to E2F to obtain the hypophosphorylated form (Rb-PP/E2F). This causes a decrease in the concentration of Rb/E2F and an increase in the concentration of Rb-PP/E2F, as shown in Figures 5.15 and 5.16, respectively. The results indicate that the reduced model (level-1) outcomes agree with the original solution in representing the behaviour of Rb/E2F and Rb-PP/E2F.

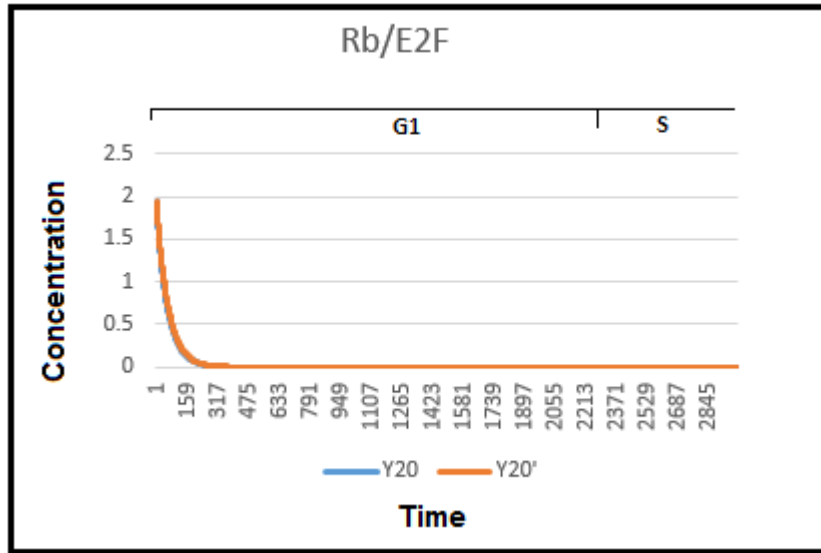


Figure 5.15 Comparison between the concentration history for Y20(Rb/E2F) in the base model and Y20'(Rb/E2F) in the reduced model (level-1)

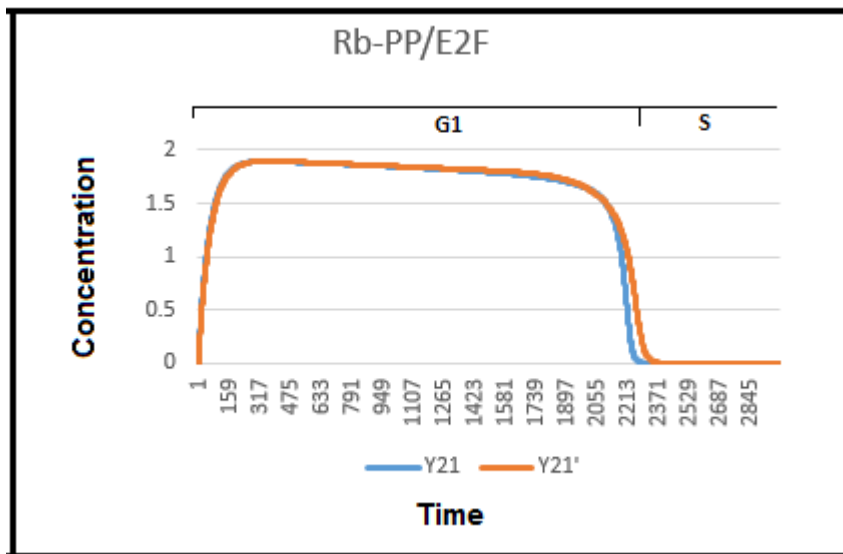


Figure 5.16 Comparison between the concentration history for Y21(Rb-PP/E2F) in the base model and Y21'(Rb-PP/E2F) in the reduced model level-1

In the mid to late G1 phase, the activated form of CycE/CDK2-P results in further hypophosphorylation of Rb-pp/E2F and, promotes the dissociation of E2F and Rb-PPP that releases E2F leading to increased E2F as shown in Figure 5.17 and increased Rb related compounds (lump F4 (Rb-PPP + Rb) shown in Figure 5.18. The increase in level of free E2F promotes synthesis of CycE, which facilitates the association between CycE and CDK2 to form more of the complex CycE/CDK2. This results in increase E2F activity and establishes a positive feedback loop between E2F and CycE. The outcomes of the reduced model (level-1) agree with the outcome of the base model.

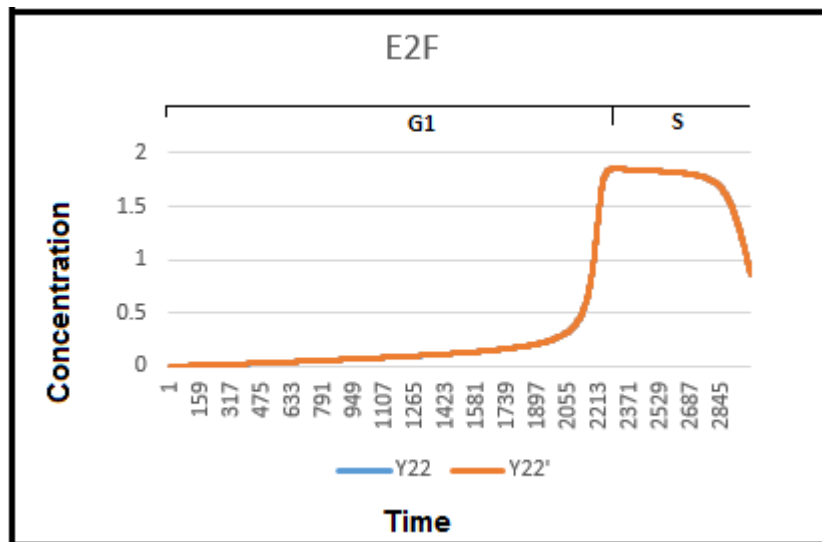


Figure 5.17 Comparison between the concentration history for Y22(E2F) in the base model and Y22'(E2F) in the reduced model (level-1)

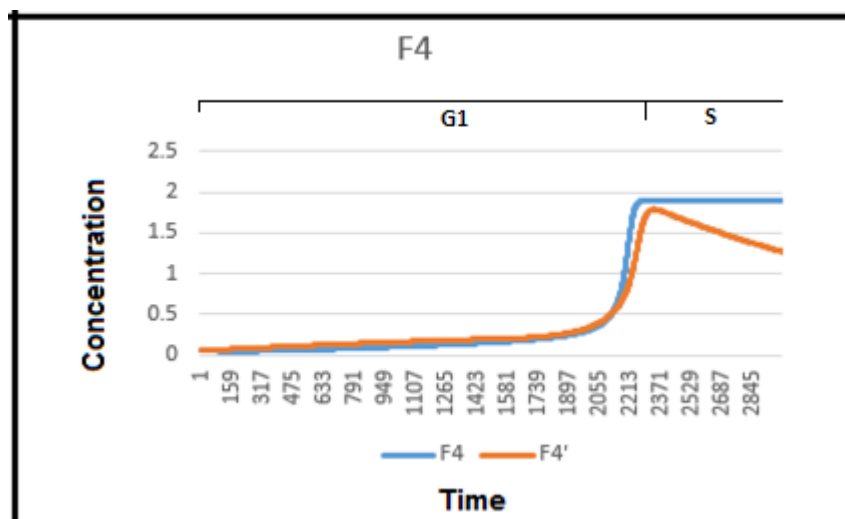


Figure 5.18 Comparison between the concentration history for F4(Rb-PPP + Rb) in the base model and F4' lump in the reduced model (level-1)

The behaviour of p21, p53, Mdm2 and ATM/ATR are shown in Figures 5.10, 5.19, 5.20 and 5.21, respectively. Without DNA damage, the concentrations of all these species were maintained at a low level and the results indicate that the outcome of the reduced model (level-1) agree with the original solution in representing the behaviour of these species.

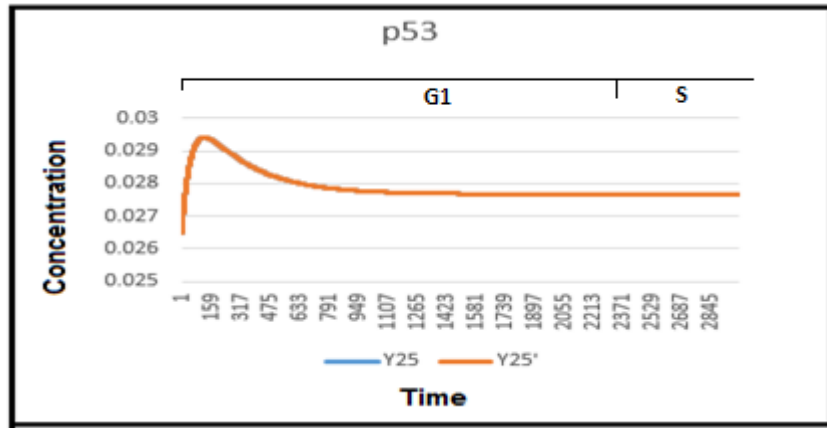


Figure 5.19 Comparison between the concentration history for Y25(p53) in the base model and Y25'(p53) in the reduced model (level-1)

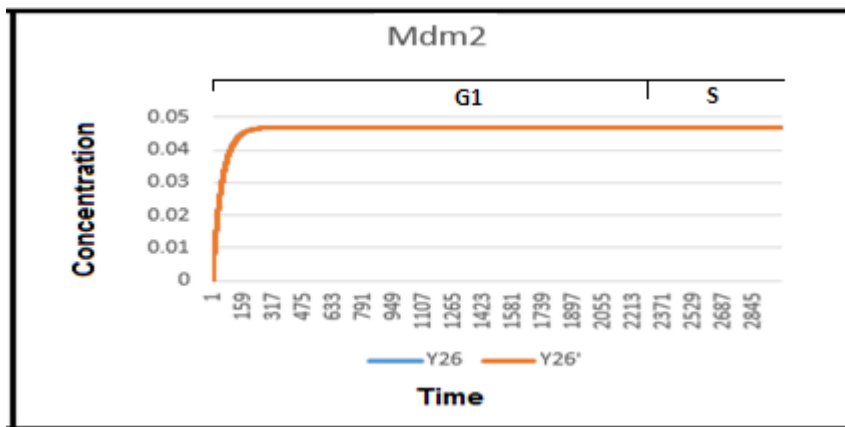


Figure 5.20 Comparison between the concentration history for Y26(Mdm2) in the base model and Y26'(Mdm2) in the reduced model (level-1)

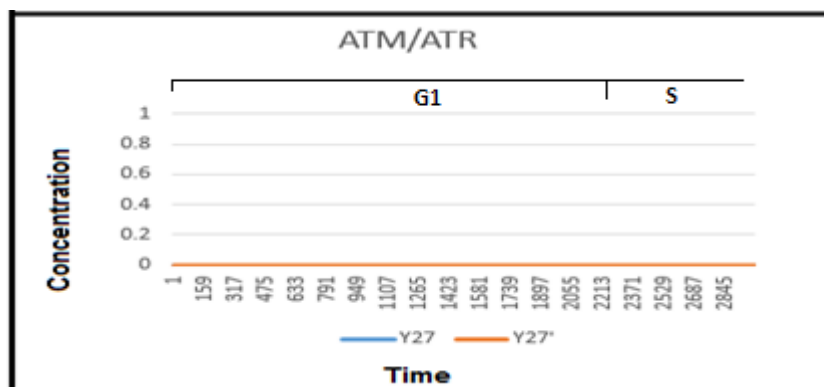


Figure 5.21 Comparison between the concentration history for Y27(ATM/ATR) in the base model and Y27'(ATM/ATR) in the reduced model (level-1)

Cdc25A is activated by E2F (Helin, 1998). Cdc25A dephosphorylates and activates CycE/Cdk2 and CycA/Cdk2 into the form CycE/Cdk2-P and CycA/Cdk2-P, respectively. The relations between Cdc25A and Cdc25A-P is the balancing feedback that stabilizes the concentration levels of the proteins. As shown in Figure 5.22 the outcome of the reduced model (level-1) agree with the base model outcome.

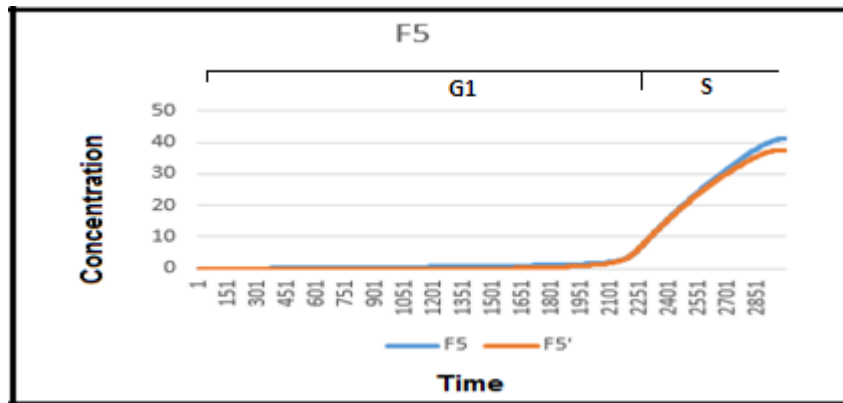


Figure 5.22 Comparison between the concentration history for F5(Cdc25A + Cdc25A-P) in the base model and F5' lump in the reduced model (level-1)

As shown in Figure 5.23, the concentration level of Chk1 and Chk1-P may not remain completely fixed, but it does stay within an acceptable range through phosphorylation and de-phosphorylation interactions (balancing feedback). The Chk1 protein is mainly restricted to the S and G2 phases (Lukas et al., 2001). The Chk1 becomes active when ATM/ATR is activated by DNA damage signal transduction at G1/S. Specifically, activated ATM phosphorylates and activates Chk1 (Gatei et al., 2003; Sørensen et al., 2003, Bartek and Lukas, 2003). Chk1-P promotes the transformation of Cdc25C-P to Cdc25CPs216-P, where Cdc25CPs216-P inhibits CycB/Cdk1-P, and G2 arrest is induced (Bartek and Lukas, 2003; Iwamoto et al., 2011). As shown in Figure 5.23, the outcome of the reduced model (level-1) agree with the outcome of the base model outcomes.

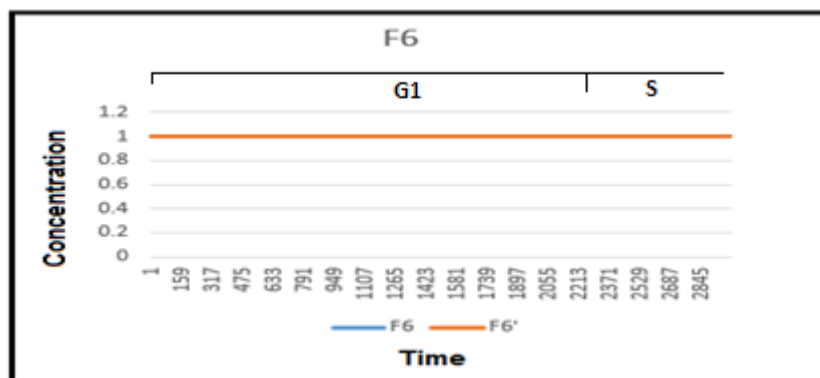


Figure 5.23 Comparison between the concentration history for F6(Chk1 + Chk1-P) in the base model and F6' lump in the reduced model (level-1)

As shown in Figure 5.24, the NF-Y concentration stays at a low level in G1 and becomes high in the late S phase. The following series of interactions explain why the concentration of NF-Y in phase S is high. NF-Y, B-Myb-P and E2F promote CycA expression at the G1/S transition with a significant increase in the S phase. In the S phase, the synthesized CycA also binds to CDK2 to form the complex, CycA/CDK2. From the late S phase to the G2 phase, Cdc25A dephosphorylates and activates CycA/Cdk2, which then forms CycA/Cdk2-P. CycA/Cdk2-P activates the transcription factor NF-Y, which induces the transcriptional activation of CycB (Chae et al., 2004). A perfect agreement between the base and the reduced model (level-1) is seen in the Figure 5.24.

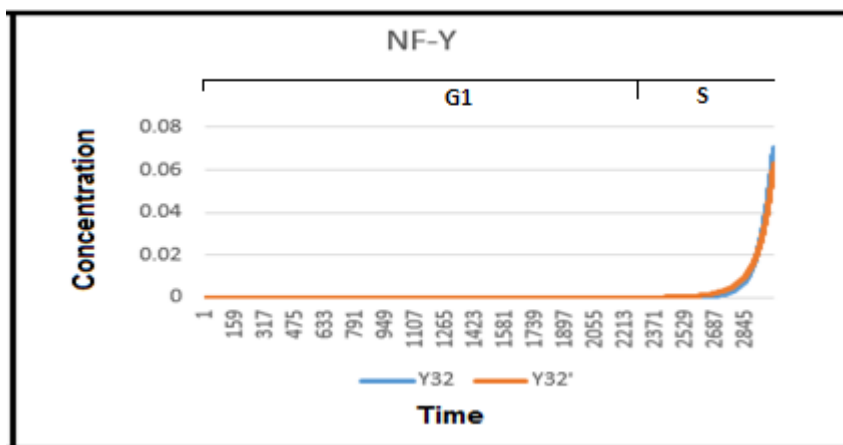


Figure 5.24 Comparison between the concentration history for Y32(NF-Y) in the base model and Y32'(NF-Y) in the reduced model (level-1)

Late in the G1 phase, the increase in level of free E2F promotes the synthesis of B-Myb. CycA/Cdk2-P promotes the phosphorylation of B-Myb to form B-Myb-P resulting in increased concentration of F7(B-Myb + B-Myb -P) in the late G1 phase as shown in Figure 5.25. The figure indicates that the outcome of the reduced model (level-1) agree with the outcome of the base model outcomes in representing the behaviour of these species.

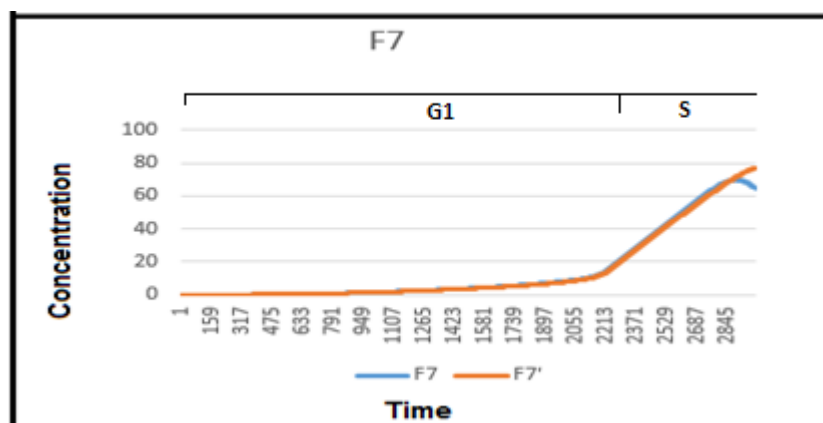


Figure 5.25 Comparison between the concentration history for F7(B-Myb + B-Myb-P) in the base model and F7' lump in the reduced model (level-1)

Intermediate specie (Im) is shown in Figure 5.26 without DNA damage, and the concentration of this species is maintained at a low level. As seen in Figure 5.26, there is a perfect agreement between the two solutions.

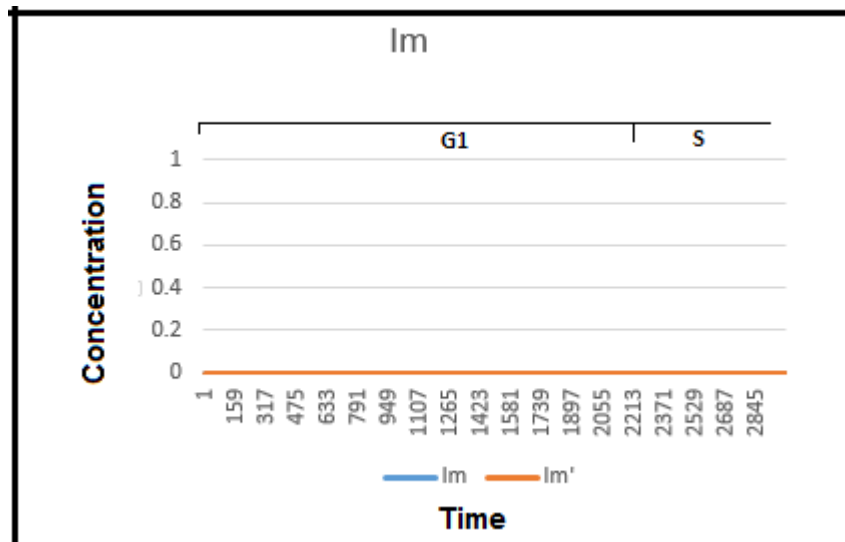


Figure 5.26 Comparison between the concentration history for Im in the base model and Im' in the reduced model (level-1)

5.1.1.2 Reduced Model (level-1) Simulation with DNA Damage

The reduced model (level-1) was run with four different levels of DNA damage (low damage = 0.002, medium damage = 0.004, high damage = 0.008, and excess damage = 0.016) to see how the reduced model (level-1) responded to DNA damage and produced cell cycle arrest. In the following results and discussion, we focused on the species that played a critical role in cell cycle arrest; that is, p53, p21, F2(CycE + CycE/Cdk2) and CycE/Cdk2-P.

When DNA is damaged, the DNA damage signal (DDS) activates p53. p53 promote the synthesis of p21 to act as a CDK inhibitor through binding to both CycE/CDK2-P and CycA/CDK2-P and delaying the activation of E2F by inhibiting the phosphorylation of Rb.

As shown in Figures 5.27 and 5.28, with low damage (DDS = 0.002) and medium damage (DDS = 0.004), the concentrations of both p53 and p21 increase, which mean G1 arrest. Also, when the reduced model (level-1) was run with high damage (DDS = 0.008) or excess damage (DDS = 0.016), p53 and p21 showed oscillations. This oscillation behaviour affected cell fate decision and the cell initiates apoptosis; this was in a good agreement with the experimental data (Lev Bar-Or et al., 2000; Lahav et al., 2004; Geva-Zatorsky et al., 2006) and the base model (Iwamoto et al., 2011).

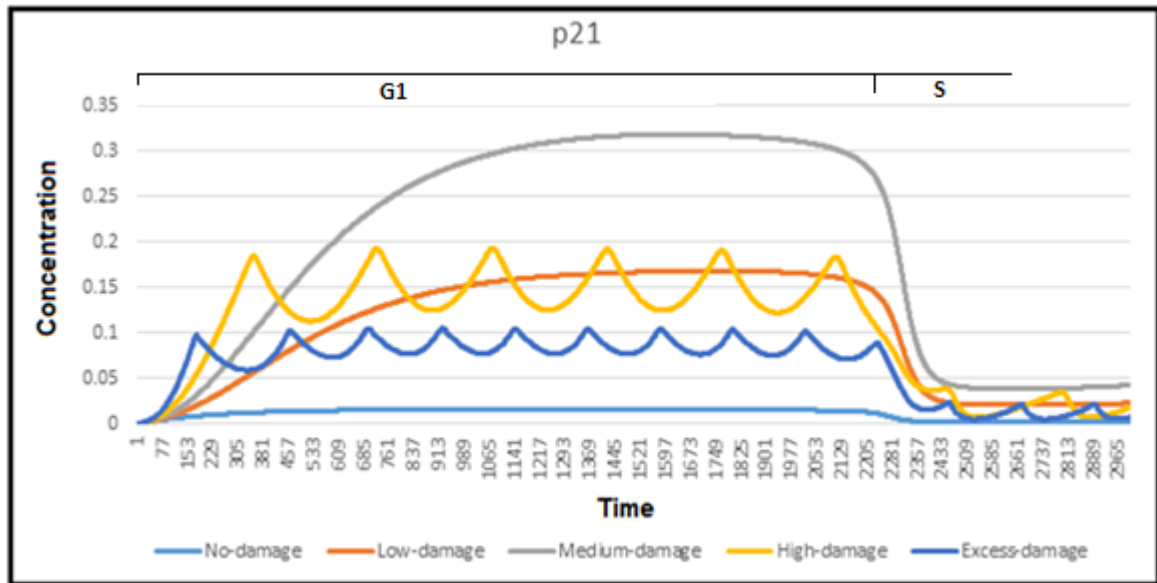


Figure 5.27 Time course of p21 resulting from the reduced model (level-1) run with different levels of DNA damage

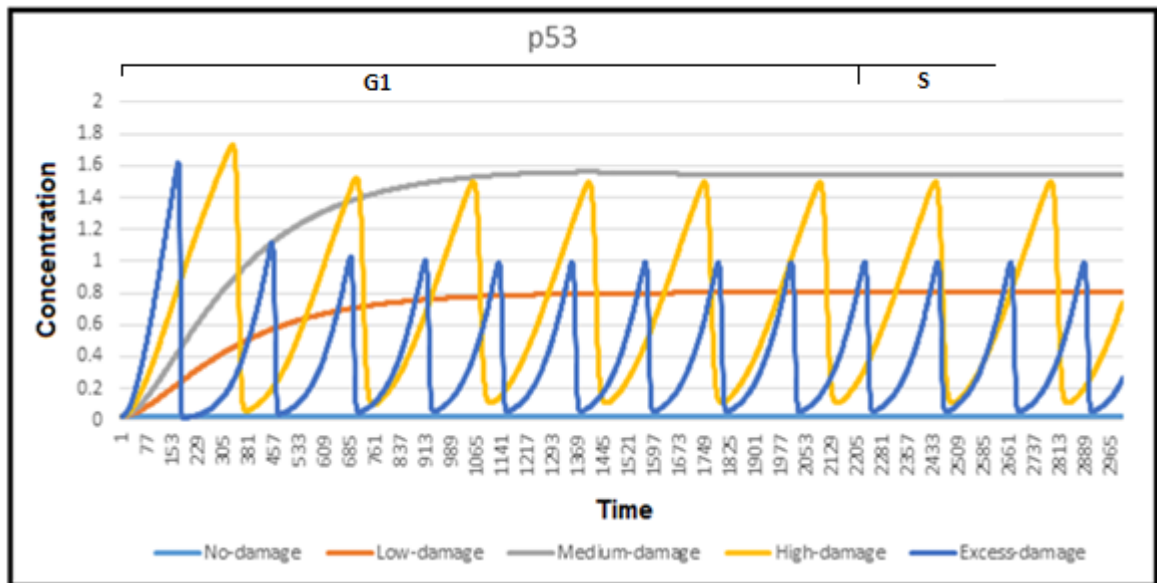


Figure 5.28 Time course of p53 resulting from the reduced model (level-1) run with different levels of DNA damage

The time courses of F2 (CycE + CycE/Cdk2) lump and CycE/Cdk2-P are shown in Figures 5.29 and 5.30, respectively. The G1/S transition was delayed for low damage or medium damage relative to the same without DNA damage, which means that it achieves G1 arrest. Also, in simulation runs with high damage or excess damage, the time to G1 arrest is short because the cell initiates apoptosis.

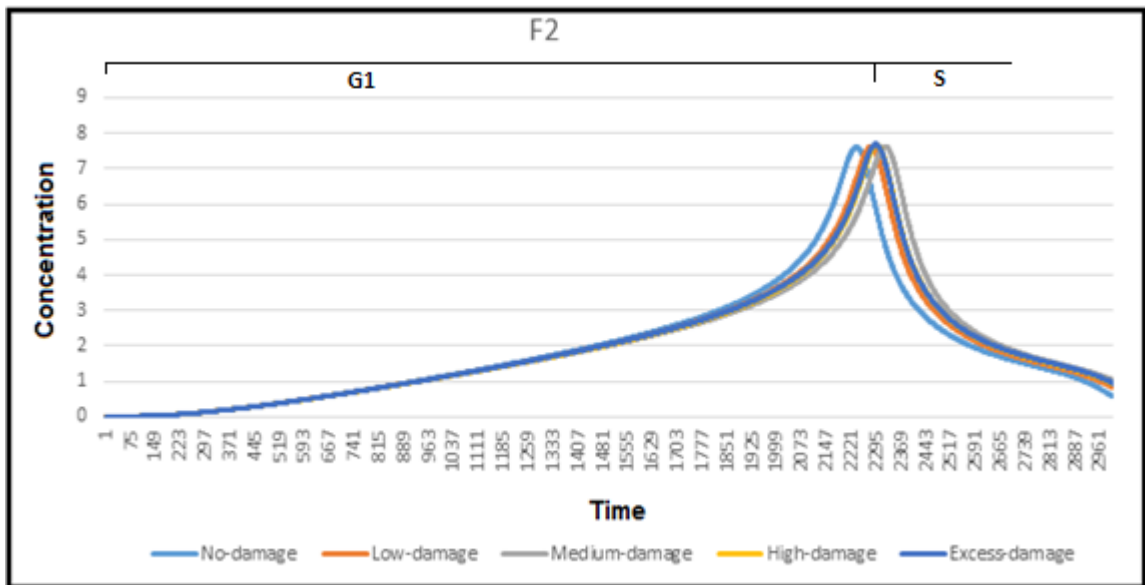


Figure 5.29 Time course of F2(CycE + CycE/Cdk2) lump resulting from the reduced model (level-1) runs with different levels of DNA damage

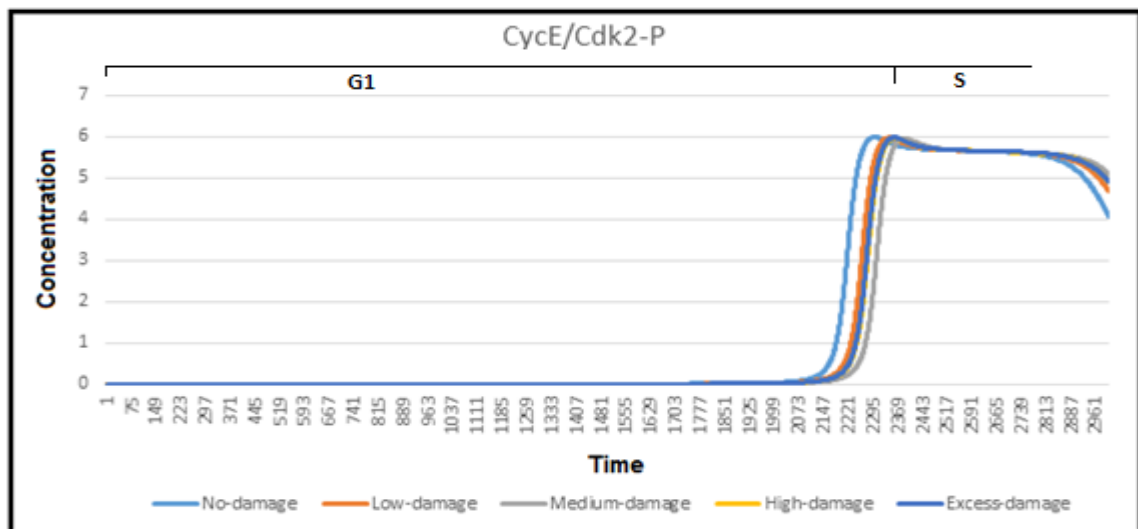


Figure 5.30 Time course of CycE/Cdk2-P resulting from the reduced model (level-1) runs with different levels of DNA damage

The results produced in this section indicate that the reduced model (level-1) simulation results of the G1/S checkpoint pathway with or without DNA-damage are similar to and consistent with the base model results (Iwamoto et al., 2011) and biological experiments. Therefore, the reduced model (level-1) can be used to evaluate the effects of DNA damage on G1 progression. To see all time courses of the elements of the reduced model (level-1) with and without DNA damage see Appendix F.

5.1.2 Comparison of the Reduced Model (level-2) with the Base Model

5.1.2.1 Reduced Model (level-2) Simulation without DNA Damage

As mentioned in Section 4.3.4.1 the reduced model (level-2) contains 26 concepts (seven lumps and 19 nodes), where F8 lump contains F1 lump and Y16 (p21/CycD/Cdk4), F2 lump contains Y2 (CycE) and Y7 (CycE/Cdk2), F3 lump contains Y3 (CycA) and Y9 (CycA/Cdk2), F9 lump contains F4 lump and Y21 (Rb-PP/E2F), F5 lump contains Y28 (Cdc25A) and Y29 (Cdc25A-P), F6 lump contains Y30 (Chk1) and Y31 (Chk1-P) and F7 lump contains Y33 (B-Myb) and Y34 (B-Myb-P).

In this section, we focus only on the time course of the new lumps and some elements. To see all time courses of the elements of the reduced model (level-2) with and without DNA damage see Appendix G.

Figure 5.31 illustrates the behaviour of the F8' lump (CycD, CycD/Cdk4 and p21/CycD/Cdk4) obtained from the reduced model (level-2) and F8 (CycD, CycD/Cdk4 and p21/CycD/Cdk4) obtained from the base model. From this figure, we note that there was no difference between the behaviour of F8 and the behaviour of F1 (Figure 5.1). The reason is that the highest concentration of the newly added species (p21/CycD/Cdk4) in the lump is no more than 0.0015 in the absence of DNA damage, as shown in Figure 5.11. This concentration was considered very small and negligible compared to the concentration of CycD and CycD/Cdk4. Figure 5.31 indicates that the outcome of the reduced model (level-2) agree with the outcome of the base model in representing the behaviour of these species.

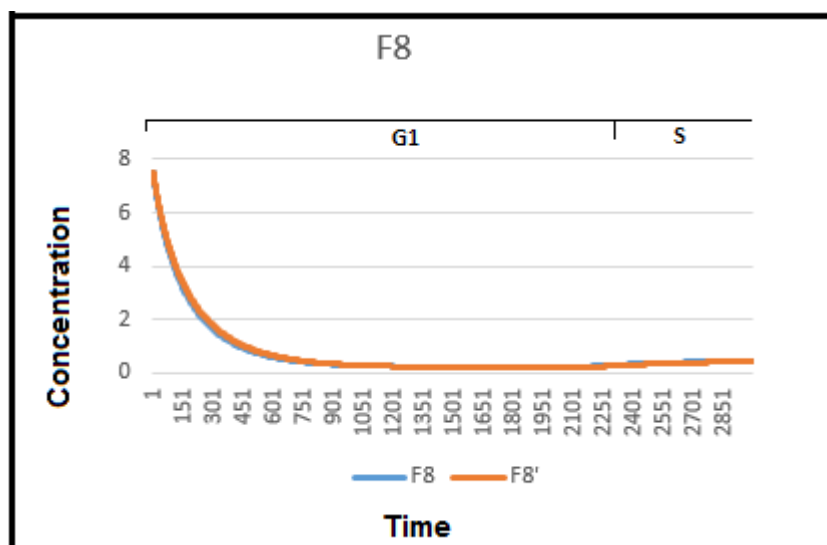


Figure 5.31 Comparison between the concentration history for F8(CycD + CycD/Cdk4 + p21/CycD/Cdk4) in the base model and F8' lump in the reduced model (level-2)

The other lump in the reduced model (level-1) that was changed F4, where Rb-PP/E2F was added to it and it became the F9 lump in the reduced model (level-2). Figure 5.32 illustrates the behaviour of the F9' lump (Rb-PPP + Rb + Rb-PP/E2F) obtained from the reduced model (level-2) and F9 (Rb-PPP + Rb + Rb-PP/E2F) obtained from the base model. From Figure 5.32, we note that there is a difference between the behaviour of F9 and the behaviour of F4 (Figure 5.18); where the concentration of the F9 lump increases at the beginning of G1 due to the high concentration of the Rb-PP/E2F element at the beginning of G1. The concentration of the F9 lump then remained relatively constant for the duration of G1/S. The Figure 5.32 indicates that the outcome of the reduced model (level-2) agree with the outcome of the base model in representing the behaviour of the F9 lump.

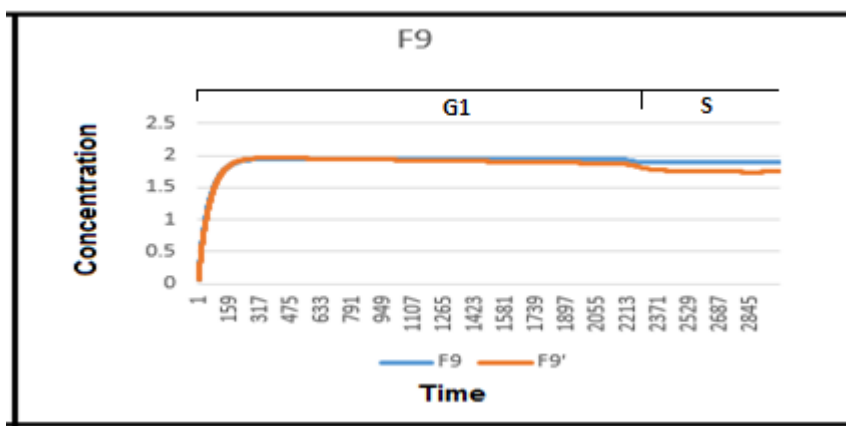


Figure 5.32 Comparison between the concentration history for F9(Rb-PPP + Rb + Rb-PP/E2F) in the base model and F9' lump in the reduced model (level-2)

The rest of the lumps did not receive any change at this level of the reduction. The following are some of concentration histories for the key species in G1/S obtained from the reduced model (level-2).

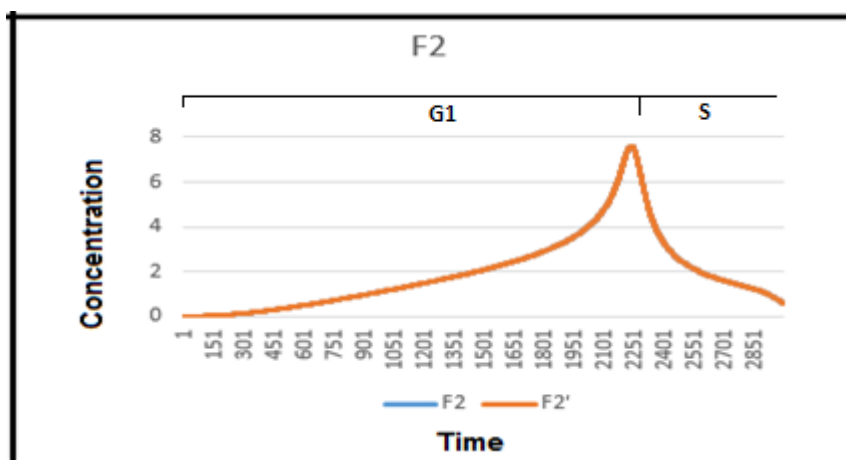


Figure 5.33 Comparison between the concentration history for F2(CycE + CycE/Cdk2) in the base model and F2' lump in the reduced model (level-2)

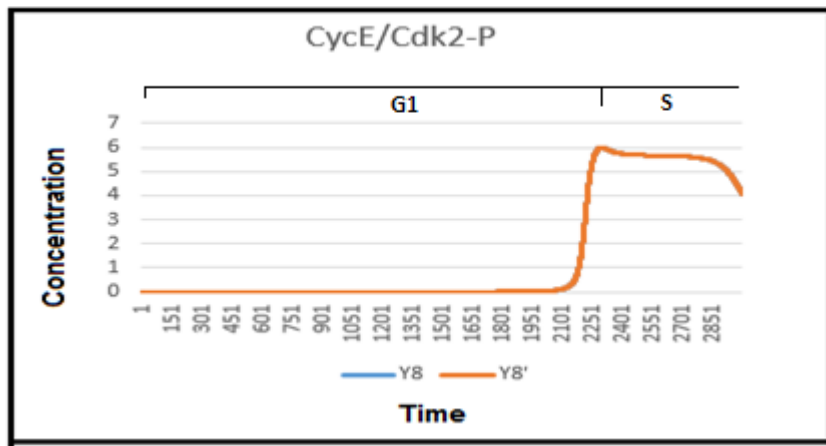


Figure 5.34 Comparison between the concentration history for Y8(CycE/Cdk2-P) in the base model and Y8'(CycE/Cdk2-P) in the reduced model (level-2)

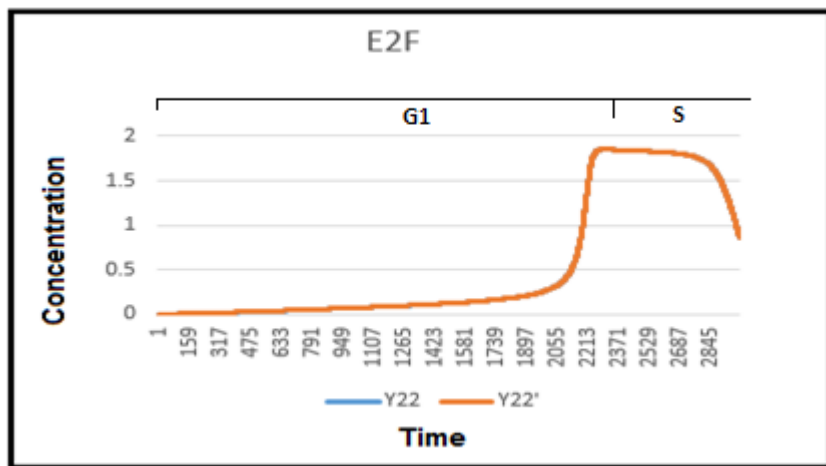


Figure 5.35 Comparison between the concentration history for Y22(E2F) in the base model and Y22'(E2F) in the reduced model (level-2)

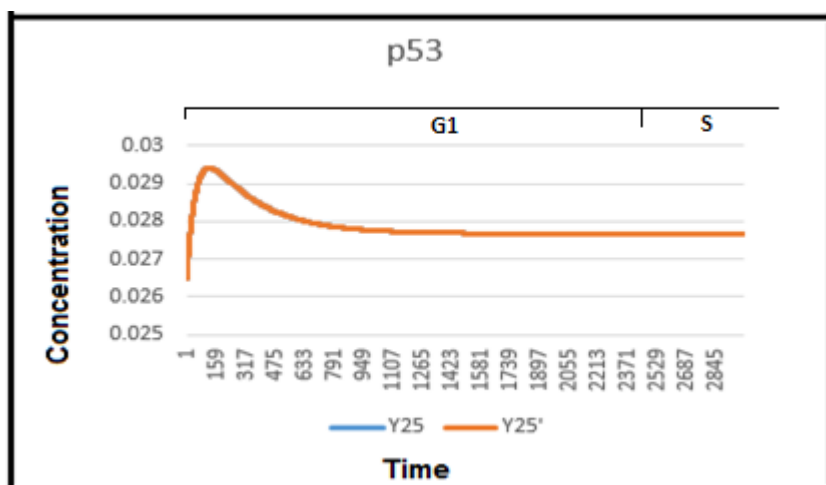


Figure 5.36 Comparison between the concentration history for Y25(p53) in the base model and Y25'(p53) in the reduced model (level-2)

Figures 5.33, 5.34, 5.35 and 5.36 show the concentration histories for the F2 lumps, CycE/Cdk2-P, E2F and p53, respectively. These figures indicate that the outcomes of the reduced model (level-2) agree with the outcomes of the base model in representing the behaviour of these species.

5.1.2.2 Reduced Model (level-2) Simulation with DNA Damage

As the reduced model (level-1) and the reduced model (level-2) runs with four different levels of DNA damage (low damage, medium damage, high damage and excess damage) to see how the reduced model (level-2) responded to DNA damage. Also, in Section 5.1.1.2, we focus on the species that played a critical role in cell cycle arrest, such as p53, p21, F2(CycE + CycE/Cdk2) and CycE/Cdk2-P.

As shown in Figures 5.37 and 5.38 with low damage and medium damage, the concentrations of both p53 and p21 increased, which resulted in the arrest G1. When high damage or excess damage occurred, p53 and p21 showed oscillations, which also meant cell apoptosis.

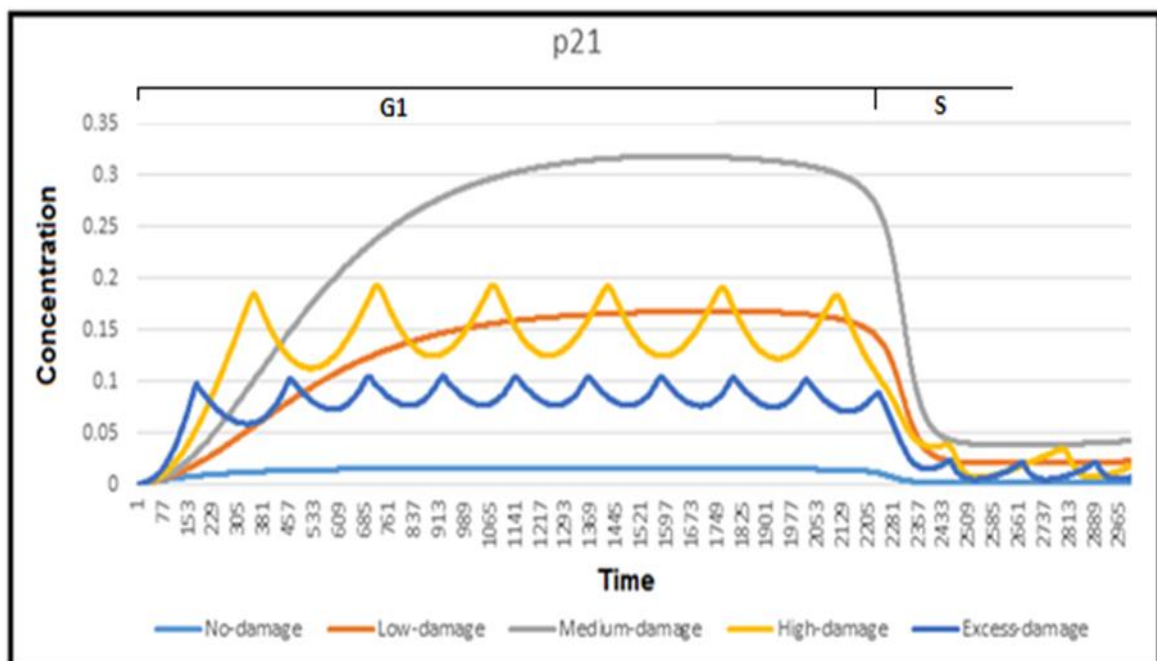


Figure 5.37 Time course of p21 resulting from the reduced model (level-2) runs with different levels of DNA damage

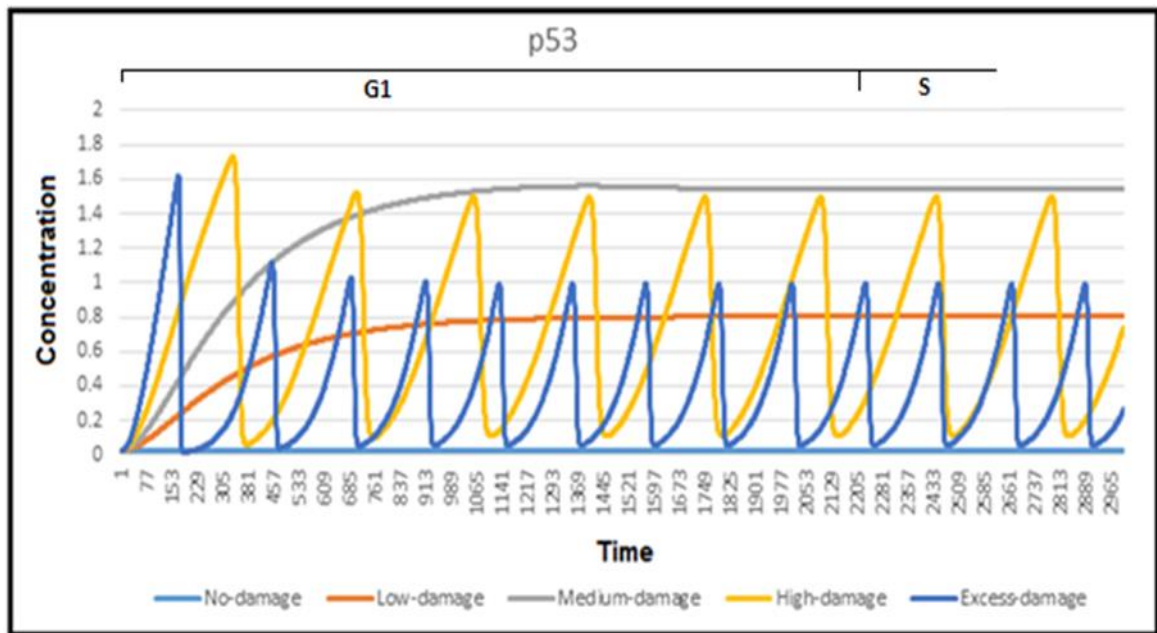


Figure 5.38 Time course of p53 resulting from the reduced model (level-2) runs with different levels of DNA damage

Figure 5.39 shows the time course of F2(CycE + CycE/Cdk2) and Figure 5.40 shows the time course of CycE/Cdk2-P. The G1/S boundary (the peak of F2) was delayed (G1 arrest) when there was low damage or medium damage relative to the G1/S boundary without DNA damage. With high damage or excess damage, the duration of the G1 arrest was shortened because the cell initiated apoptosis.

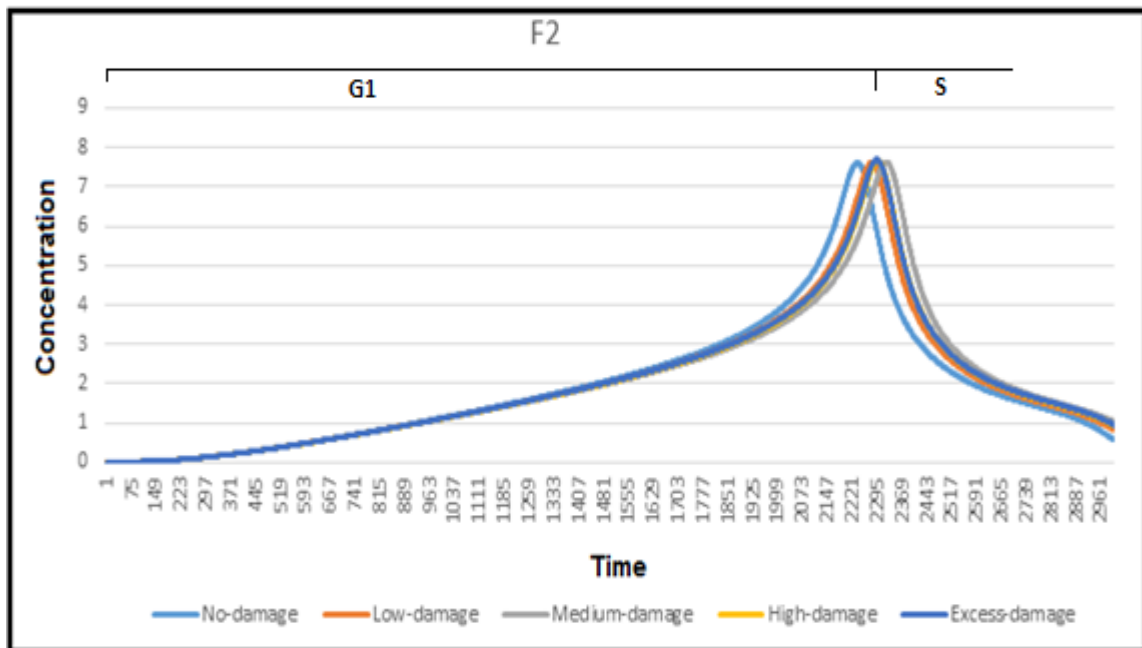


Figure 5.39 Time course of F2(CycE + CycE/Cdk2) lump resulting from the reduced model (level-2) runs with different levels of DNA damage

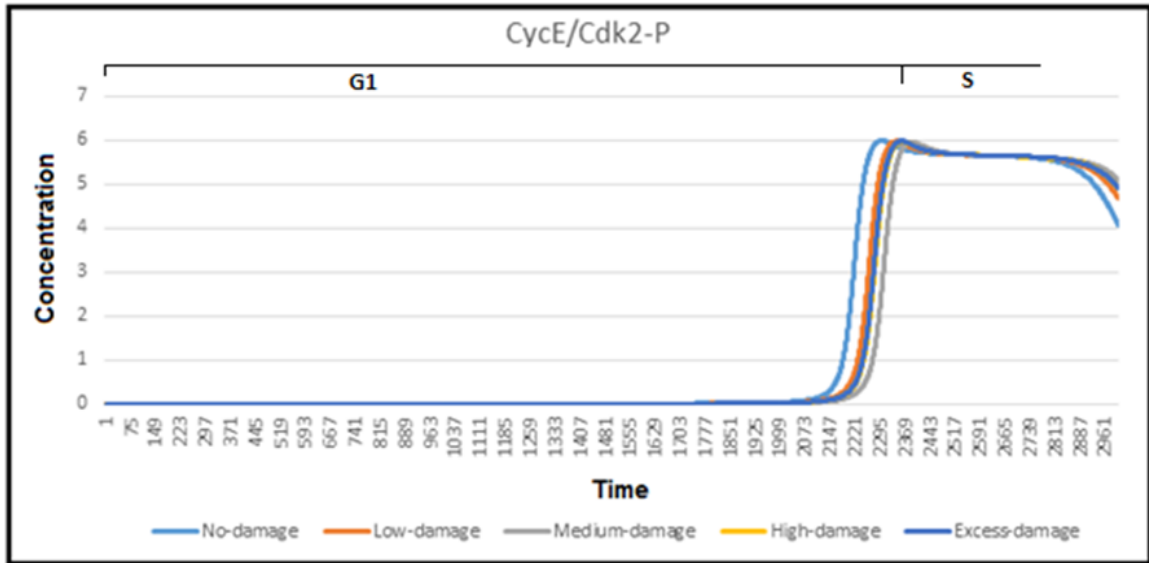


Figure 5.40 Time course of CycE/Cdk2-P resulting from the reduced model (level-2) runs with different levels of DNA damage

5.1.3 Comparison of the Reduced Model (level-3) with the Base Model

5.1.3.1 Reduced Model (level-3) Simulation without DNA Damage

As mentioned in Section 4.3.4.1, the reduced model (level-3) contained 24 concepts (seven lumps and 17 nodes) where F8 lump contained F1 lump and Y16 (p21/CycD/Cdk4), F2 lump contained Y2 (CycE) and Y7 (CycE/Cdk2), F10 lump contained F3 lump, Y14 (p27/CycA/Cdk2-P) and Y18 (p21/CycA/Cdk2-P), F9 lump contained F4 lump and Y21 (Rb-PP/E2F), F5 lump contained Y28 (Cdc25A) and Y29 (Cdc25A-P), F6 lump contained Y30 (Chk1) and Y31 (Chk1-P) and the F7 lump contained Y33 (B-Myb) and Y34 (B-Myb-P). Comparing to the reduced model (level-2) there is one new lump F10, and six lumps are existing and borrowed from the reduced model (level-2).

In this section, we focus only on the time course of the new lumps and some key elements. To see time courses for all the elements of the reduced model (level-3) with and without DNA damage see Appendix H.

One lump in the reduced model (level-2) that was changed F3(CycA and CycA/Cdk2) where p27/CycA/Cdk2-P and p21/CycA/Cdk2-P had been added to it and it became the F10 lump in the reduced model (level-3). Figure 5.41 illustrates the behaviour of the F10' lump obtained from the reduced model (level-3) and F10 obtained from the base model. From this figure, we note that there

is no difference between the behaviour of F10 and F3 see Figure 5.4. The reason is that the highest concentrations of the newly added species p27/CycA/Cdk2-P and p21/CycA/Cdk2-P in the lump was no more than 0.0015 and 0.0004, respectively, in the absence of DNA damage, as shown in Figures 5.9 and 5.13. These concentrations were considered to be very small and negligible compared to the concentration of CycA and CycA/Cdk2. Figure 5.41 indicates that the outcome of the reduced model (level-3) agreed with the outcome of the base model in representing the behaviour of these species.

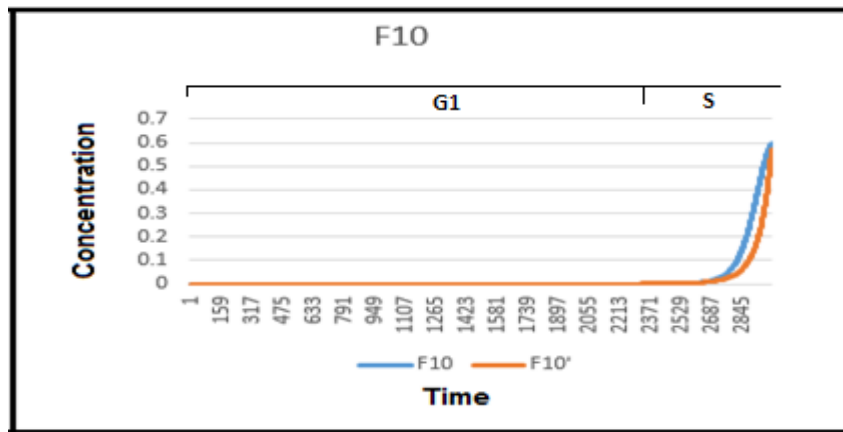


Figure 5.41 Comparison between the concentration history for F10(CycA + CycA/Cdk2 + p27/CycA/Cdk2-P + p21/CycA/Cdk2-P) in the base model and F10' lump in the reduced model (level-3)

The rest of the lumps did not receive any change at this level of reduction. The following are some of the concentration histories for the key species in G1/S from the reduced model (level-3).

As shown in Figure 5.42 a positive feedback loop between E2F and CycE is established in the mid G1 phase. This explains the behaviour of F2 (CycE and CycE/Cdk2) which; reaches a high concentration level at the end of G1. This peak time of F2 was considered to be the boundary between the G1 and S phases.

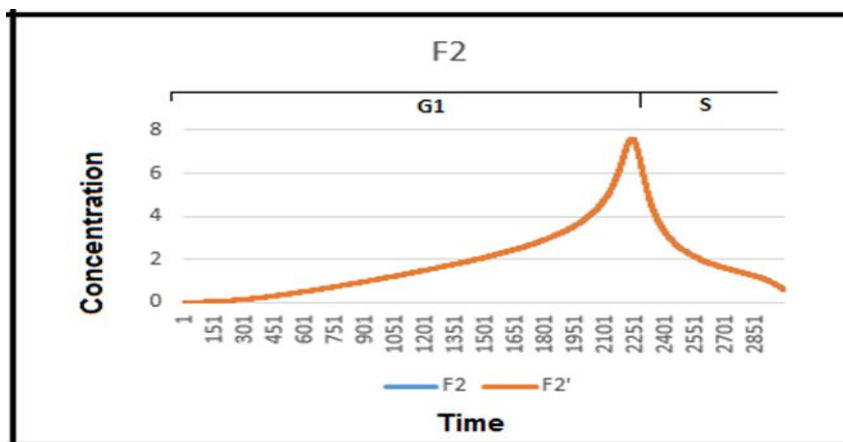


Figure 5.42 Comparison between the concentration history for F2(CycE + CycE/Cdk2) in the base model and F2' lump in the reduced model (level-3)

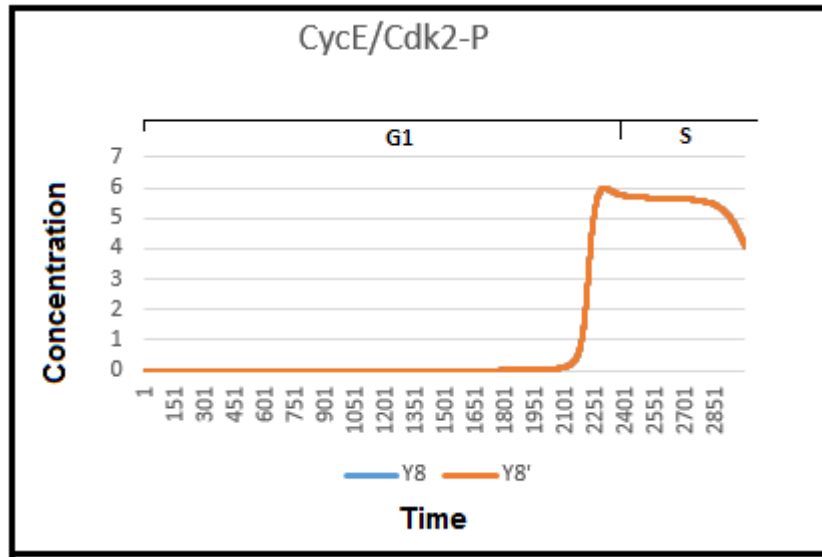


Figure 5.43 Comparison between the concentration history for Y8(CycE/Cdk2-P) in the base model and Y8'(CycE/Cdk2-P) in the reduced model (level-3)

In the mid to late G1 phase the activated form of CycE/CDK2-P results in further hypophosphorylation of Rb-pp/E2F, promoting the dissociation of E2F from Rb-PPP which releases E2F. The increase in the level of free E2F promotes the synthesis of CycE which facilitates the association between CycE and CDK2 to form more of complex CycE/CDK2. This results in increased E2F activity as a result of the establishment of a positive feedback loop between E2F and CycE. This explains the behaviour of E2F shown in Figure 5.44.

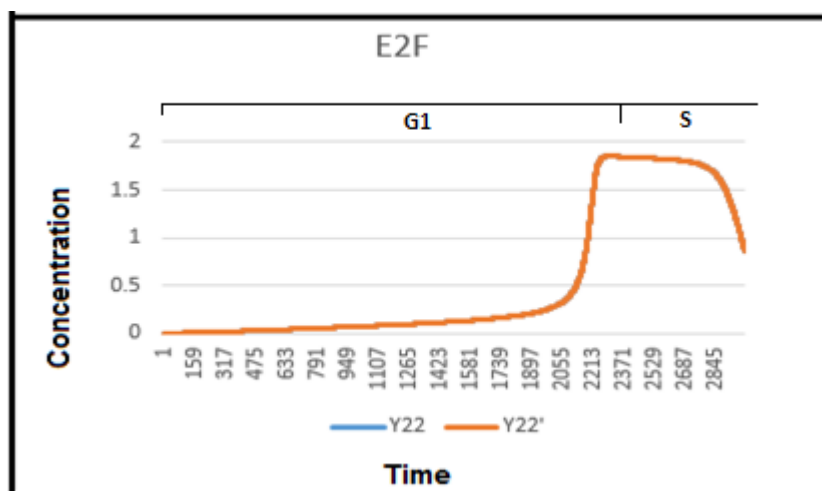


Figure 5.44 Comparison between the concentration history for Y22(E2F) in the base model and Y22'(E2F) in the reduced model (level-3)

If there was no DNA damage, a small amount of p21 was produced at the beginning of G1 phase as shown in Figure 5.45. The p21 concentration stayed in a low level in G1 phase.

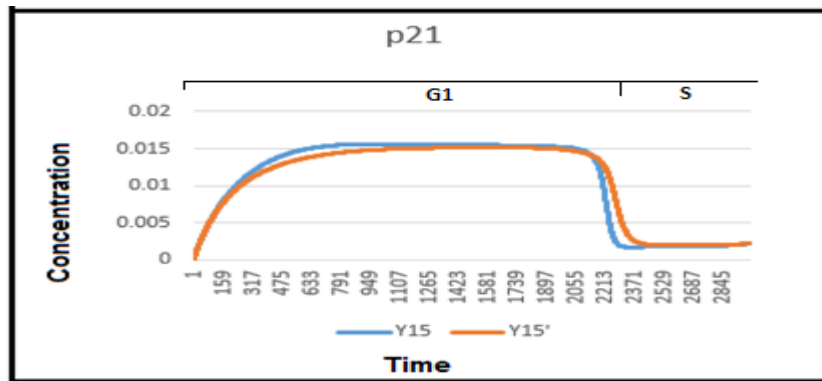


Figure 5.45 Comparison between the concentration history for Y15(p21) in the base model and Y15'(p21) in the reduced model (level-3)

Figures 5.42, 5.43, 5.44 and 5.45 show the concentration histories for F2 lump, CycE/Cdk2-P, E2F and p21, respectively. These figures indicate that the outcome of the reduced model (level-3) agreed with the outcome of the base model in representing the behaviour of these species.

5.1.3.2 Reduced Model (level-3) Simulation with DNA Damage

The reduced model (level-3) was run with four different levels of DNA damage (low damage, medium damage, high damage and excess damage) to see how the reduced model (level-3) responded to DNA damage.

As shown in Figure 5.46, the concentration of p21 increased with low damage and medium damage, and p21 showed oscillations as a result of high damage or excess damage.

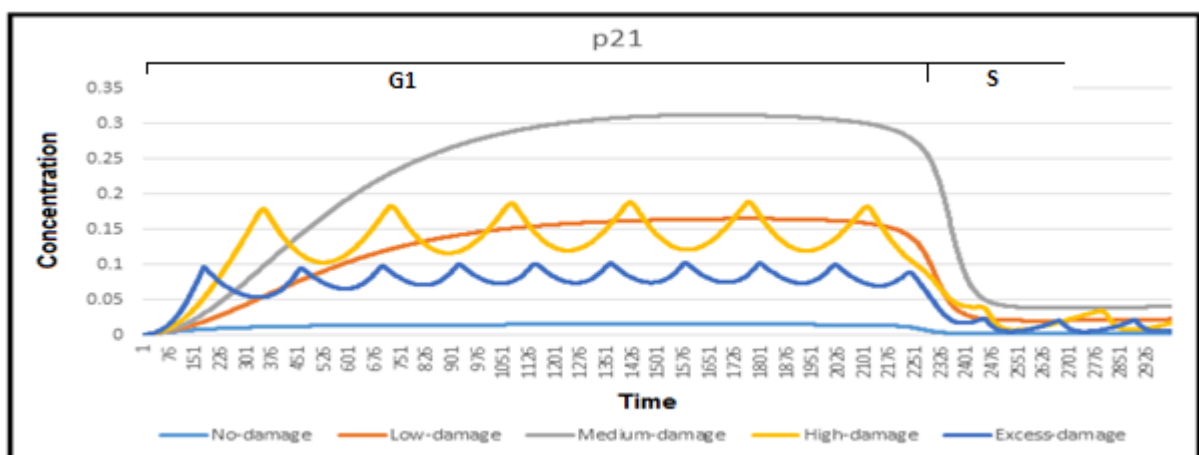


Figure 5.46 Time course of p21 resulting from the reduced model (level-3) runs with different levels of DNA damage

The same response to DNA damage was shown in the time course of p53 in Figure 5.47. The concentration of p53 increased with low damage and medium damage, and p53 showed oscillations as a result of high damage or excess damage.

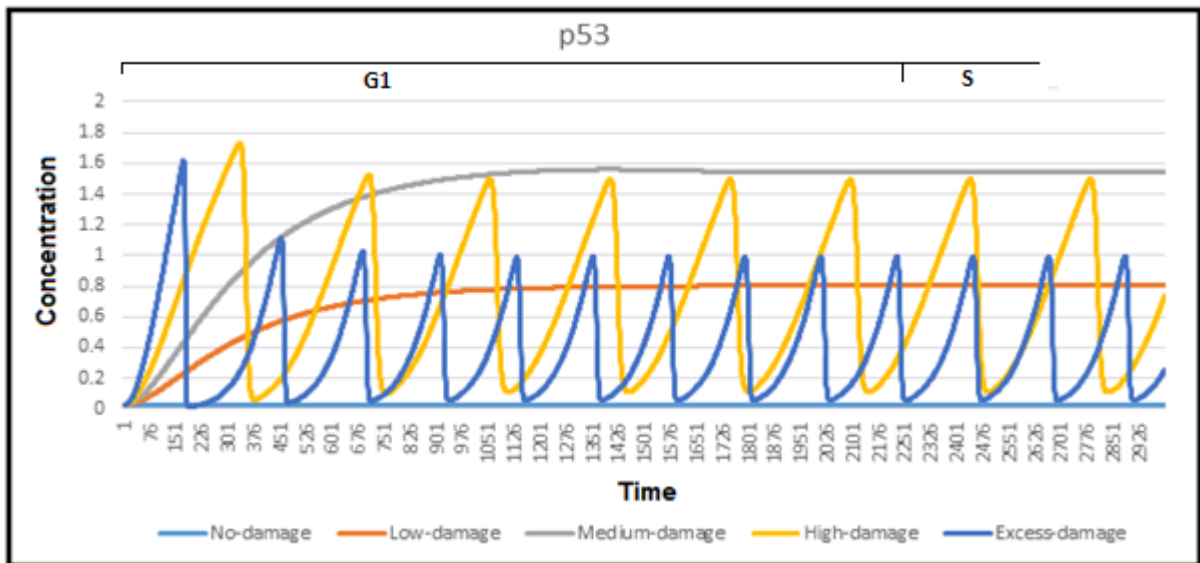


Figure 5.47 Time course of p53 resulting from the reduced model (level-3) runs with different levels of DNA damage

Figures 5.48 and 5.49 show the time course of F2 (CycE + CycE/Cdk2) and time course of CycE/Cdk2-P, respectively. As a result of low or medium damage, the G1/S arrest was delayed, and with high damage or excess damage, the duration of the G1 arrest has been shortened because the cell initiates apoptosis.

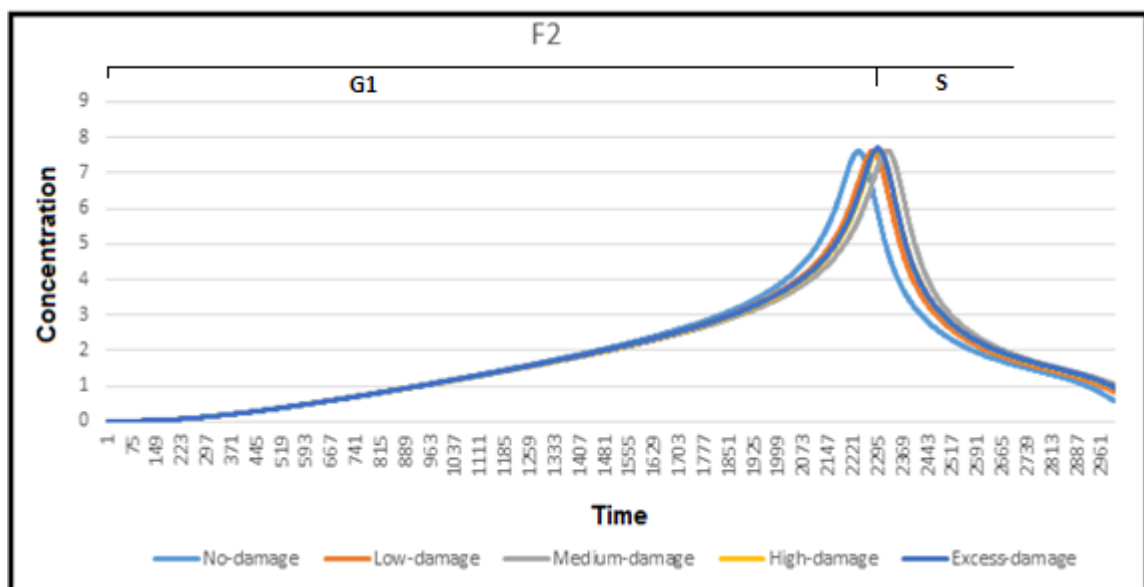


Figure 5.48 Time course of F2(CycE + CycE/Cdk2) lump resulting from the reduced model (level-3) runs with different levels of DNA damage

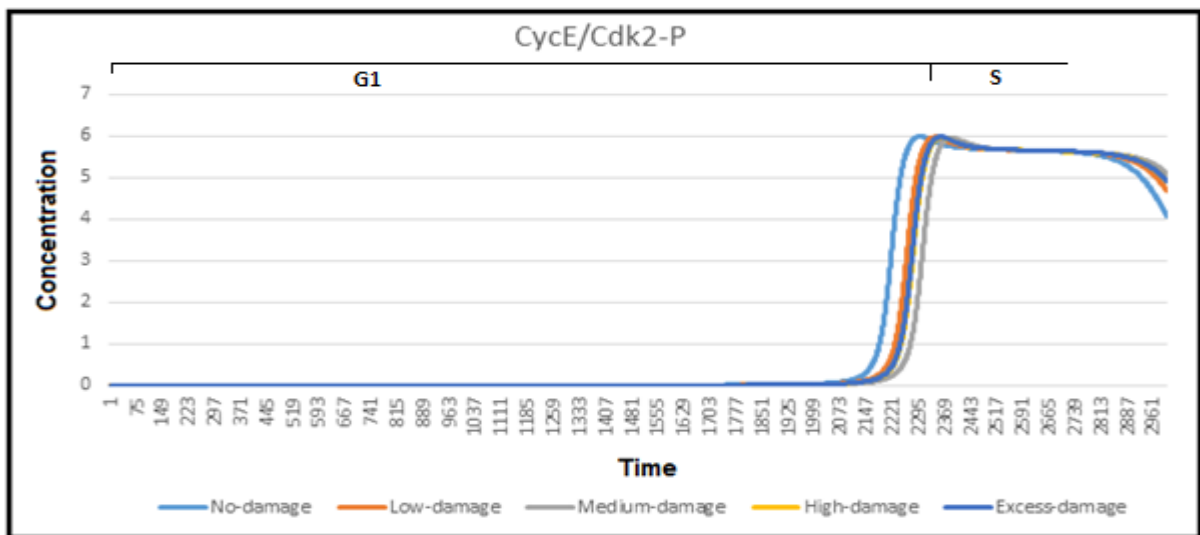


Figure 5.49 Time course of CycE/Cdk2-P resulting from the reduced model (level-3) runs with different levels of DNA damage

The reduced model (level-3) simulation results of the G1/S checkpoint pathway with or without DNA-damage were similar to and consistent with the results of the base model. that was consistent with biological experiments as reported by Iwamoto et al. (2011). Therefore, the reduced model (level-3) can be used to study G1 progression with and without DNA damage.

5.2 Evaluation of the Reduced Model using Root Mean Squared Error (RMSE) and the Root Mean Squared Percentage Error (RMSPE)

Both the root mean squared error (RMSE) and the root mean squared percentage error (RMSPE) were used to verify the model results in model evaluation. In this section, we used RMSE and RMSPE as measures of accuracy to compare forecasting errors of the reduced models (level-1), (level-2) and (level-3) against the base model without DNA damage. We also show concentration values for some species at different times from the base model, the reduced model (level-1), the reduced model (level-2) and the reduced model (level-3) for different levels of DNA damage.

Tables 5.1 to 5.3 present the values of RMSE and RMSPE for the reduced model (level-1), (level-2) and (level-3) with respect to the base model without DNA damage and with continuous outcomes. The tables show that for both RMSE and RMSPE values tended to increase with the increasing levels of lumping. Table 5.1 shows that the RMSPE between the base model and the reduced model (level-1) exceeded no more than 5% for any species. Furthermore, seven species (F2, Y19, Y25, Y26, Y27, F6 and Im), which represented 25% of the species of the reduced model (level-1), had 0% RMSPE. Moreover, Table 5.1 shows that the RMSE values did not have any value greater than 1.0 while the largest value

was 0.752273301 for lump F5 and the smallest value was 5.87313E-07 for lump F7. Table 5.1 demonstrated that the reduced model (level-1) results compare very well with the base model results indicating that it is a good model to simulate the G1/S checkpoint pathways integrated with DNA damage pathway.

Table 5.1 Reduced model (level-1) evaluation without DNA damage by using the root mean squared error (RMSE) and the root mean squared percentage error (RMSPE)

Node/Lump No.	Node/Lump name	RMSE	RMSPE
1	Y4	5.6770E-04	2%
2	Y5	5.7676E-04	1%
3	F1	6.2718E-02	2%
4	F2	5.7747E-05	0%
5	Y8	5.7201E-05	1%
6	F3	1.6871E-06	1%
7	Y10	3.2142E-03	3%
8	Y11	1.3396E-01	2%
9	Y12	4.9696E-02	2%
10	Y13	7.6647E-02	3%
11	Y14	6.2572E-05	3%
12	Y15	1.0544E-03	4%
13	Y16	2.4980E-05	4%
14	Y17	2.4425E-03	1%
15	Y18	3.9376E-06	1%
16	Y19	6.6400E-03	0%
17	Y20	2.2466E-04	3%
18	Y21	2.1374E-04	4%
19	Y22	5.7809E-05	2%
20	F4	5.3099E-02	5%
21	Y25	0.0000E+00	0%
22	Y26	3.0249E-02	0%
23	Y27	0.0000E+00	0%
24	F5	7.5227E-01	2%
25	F6	0.0000E+00	0%
26	Y32	1.0110E-04	2%
27	F7	5.8731E-07	4%
28	Im	0.0000E+00	0%

Table 5.2 shows that with regard to RMSPE between the base model and the reduced model (level-2), only one species (Y15) has 6% RMSPE and the rest of the species did not exceed 5% RMSPE. Furthermore, eight species (F2, Y19, F9, Y25, Y26, Y27, F6 and Im), which represent approximately 31%

of the species of the reduced model (level-2), had 0% RMSPE. We also noted that seven species (F3, Y10, Y15, Y17, Y18, F5 and Y32) had increased RMSPE values in the reduced model (level-2) compared with their RMSPE values in the reduced model (level-1) (but these increases are very minor ranging from 1 to 4%), while 14 species (Y4, Y5, F2, Y8, Y12, Y13, Y22, F9, Y25, Y26, Y27, F6, F7 and Im) have maintained their RMSPE value. Moreover, Table 5.2 shows that with regard to RMSE it has one value greater than 1.0 (equalling 1.558623053) for lump F7 and the RMSE value less than 1.0 for the rest of the species. The smallest RMSE value was 5.25861E-06 for Y18. Table 5.2 demonstrates that the reduced model (level-2) results compare well with the base model results and it is still a good model to simulate G1/S checkpoint pathways integrated with DNA damage pathway.

Table 5.2 Reduced model (level-2) evaluation without DNA damage by the using root mean squared error (RMSE) and the root mean squared percentage error (RMSPE)

Node/lump No.	Node/Lump name	RMSE	RMSPE
1	Y4	8.6830E-04	2%
2	Y5	1.1674E-03	1%
3	F8	6.2781E-02	5%
4	F2	6.8966E-05	0%
5	Y8	6.4016E-05	1%
6	F3	1.0708E-02	4%
7	Y10	2.0365E-02	4%
8	Y11	5.4230E-02	1%
9	Y12	4.8779E-02	2%
10	Y13	7.6622E-02	3%
11	Y14	7.2844E-06	1%
12	Y15	5.9816E-04	6%
13	Y17	1.5980E-03	5%
14	Y18	5.2586E-06	4%
15	Y19	6.6443E-03	0%
16	Y20	8.8235E-03	2%
17	Y22	1.1307E-04	2%
18	F9	4.2291E-02	0%
19	Y25	0.0000E+00	0%
20	Y26	0.0000E+00	0%
21	Y27	0.0000E+00	0%
22	F5	8.8215E-01	3%
23	F6	0.0000E+00	0%
24	Y32	1.3265E-03	3%
25	F7	1.5586E+00	4%
26	Im	0.0000E+00	0%

Table 5.3 shows that with regard to RMSPE between the base model and the reduced model (level-3), only one species (Y15) has 6% RMSPE and the rest of the species have no more than 5% RMSPE. Furthermore, seven species (F2, Y19, Y25, Y26, Y27, F6 and Im), which represents approximately 29% of the species of the reduced model (level-3), had 0% RMSPE. We also noted that two species (Y10 and F9) have increased RMSPE values in the reduced model (level-3) compared with their RMSPE values in the reduced model (level-2), while 21 species have maintained their RMSPE values. Table 5.3 shows that in terms of RMSE, there was one value greater than 1.0 for lump F7 and a RMSE value of less than 1.0 for the rest of the species. The largest value, 1.558623167, was for lump F7 and the smallest value was 5.72013E-05 for Y8. Table 5.3 demonstrates that the reduced model (level-3) compares well with the base model and thus it is still a good model to simulate the G1/S checkpoint pathways integrated with DNA damage pathway.

Table 5.3. Reduced model (level-3) evaluation without DNA damage by using the root mean squared error (RMSE) and the root mean squared percentage error (RMSPE) without DNA damage

Node/Lump No.	Node/Lump name	RMSE	RMSPE
1	Y4	8.6830E-04	2%
2	Y5	1.1674E-03	1%
3	F8	6.2781E-02	5%
4	F2	6.8966E-05	0%
5	Y8	5.7201E-05	1%
6	F10	1.3871E-02	3%
7	Y10	2.5056E-02	5%
8	Y11	5.4230E-02	1%
9	Y12	4.8779E-02	2%
10	Y13	7.6622E-02	3%
11	Y15	5.9816E-04	6%
12	Y17	1.5980E-03	5%
13	Y19	6.6443E-03	0%
14	Y20	8.8235E-03	2%
15	Y22	1.1307E-04	2%
16	F9	7.9026E-02	4%
17	Y25	0.0000E+00	0%
18	Y26	0.0000E+00	0%
19	Y27	0.0000E+00	0%
20	F5	8.8215E-01	3%
21	F6	0.0000E+00	0%
22	Y32	1.6247E-03	3%
23	F7	1.5586E+00	4%
24	Im	0.0000E+00	0%

The simulations with the base model, reduced model (level-1), reduced model (level-2) and reduced model (level-3) were run with four different levels of DNA damage to allow analysis of the differences in concentration of five species important in DNA damage response (CycE/Cdk2-P, p21, E2F, p21/CycE/Cdk2-P and p53) at t=1, t=500, t=1000, t=1500, t=2000 and t=2330. The results of these simulations are summarised in Tables 5.4 to 5.23. These show that the concentration of CycE/Cdk2-P, p21, E2F, p21/CycE/Cdk2-P and p53 for the base model and reduced model (level-1, 2 and 3); is not significantly different; all values agreed with values taken from experimental data.

Table 5.4 CycE/Cdk2-P values from the base model, the reduced model (level-1), the reduced model (level-2) and the reduced model (level-3) simulations with low DNA damage

Time	Base	L1	L2	L3
1	2.5746E-03	2.5463E-03	2.5483E-03	2.5483E-03
500	2.9894E-03	2.9566E-03	2.9589E-03	2.9578E-03
1000	3.6048E-03	3.5651E-03	3.5680E-03	3.5662E-03
1500	5.4841E-03	5.4238E-03	5.4281E-03	5.4207E-03
2000	2.6196E-02	2.5908E-02	2.5928E-02	2.5747E-02
2330	5.9561E+00	5.8906E+00	5.8953E+00	5.8907E+00

Table 5.5 CycE/Cdk2-P values from the base model, the reduced model (level-1), the reduced model (level-2) and the reduced model (level-3) simulations with medium DNA damage

Time	Base	L1	L2	L3
1	2.5746E-03	2.5463E-03	2.5483E-03	2.5483E-03
500	2.9600E-03	2.9275E-03	2.9298E-03	2.9288E-03
1000	3.5180E-03	3.4794E-03	3.4821E-03	3.4805E-03
1500	5.1865E-03	5.1295E-03	5.1336E-03	5.1272E-03
2000	2.0002E-02	1.9782E-02	1.9797E-02	1.9685E-02
2330	4.9744E+00	4.9197E+00	4.9237E+00	4.8746E+00

Table 5.6 CycE/Cdk2-P values from the base model, the reduced model (level-1), the reduced model (level-2) and the reduced model (level-3) simulations with high DNA damage

Time	Base	L1	L2	L3
1	2.5746E-03	2.5463E-03	2.5483E-03	2.5483E-03
500	2.9763E-03	2.9436E-03	2.9460E-03	2.9447E-03
1000	3.5889E-03	3.5495E-03	3.5523E-03	3.5508E-03
1500	5.3872E-03	5.3280E-03	5.3323E-03	5.3249E-03
2000	2.3462E-02	2.3204E-02	2.3223E-02	2.3074E-02
2330	5.7917E+00	5.7280E+00	5.7326E+00	5.7167E+00

Table 5.7 CycE/Cdk2-P values from the base model, the reduced model (level-1), the reduced model (level-2) and the reduced model (level-3) simulations with excess DNA damage

Time	Base	L1	L2	L3
1	2.5746E-03	2.5463E-03	2.5483E-03	2.5483E-03
500	2.9865E-03	2.9537E-03	2.9560E-03	2.9547E-03
1000	3.6239E-03	3.5841E-03	3.5870E-03	3.5851E-03
1500	5.4470E-03	5.3871E-03	5.3914E-03	5.3844E-03
2000	2.3713E-02	2.3452E-02	2.3471E-02	2.3321E-02
2330	5.8351E+00	5.7709E+00	5.7755E+00	5.7615E+00

Table 5.8 p21 values from the base model, the reduced model (level-1), the reduced model (level-2) and the reduced model (level-3) simulations with low DNA damage

Time	Base	L1	L2	L3
1	7.6500E-05	7.6500E-05	7.6500E-05	7.6500E-05
500	8.9925E-02	8.9784E-02	8.6148E-02	8.6148E-02
1000	1.5243E-01	1.5250E-01	1.4766E-01	1.4766E-01
1500	1.6661E-01	1.6698E-01	1.6347E-01	1.6347E-01
2000	1.6705E-01	1.6589E-01	1.6305E-01	1.6305E-01
2330	2.2156E-02	6.5078E-02	6.4116E-02	6.4116E-02

Table 5.9 p21 values from the base model, the reduced model (level-1), the reduced model (level-2) and the reduced model (level-3) simulations with medium DNA damage

Time	Base	L1	L2	L3
1	7.6500E-05	7.6500E-05	7.6500E-05	7.6500E-05
500	1.6563E-01	1.6538E-01	1.5927E-01	1.5927E-01
1000	2.8956E-01	2.8968E-01	2.8089E-01	2.8089E-01
1500	3.1724E-01	3.1788E-01	3.1136E-01	3.1136E-01
2000	3.1381E-01	3.1081E-01	3.0676E-01	3.0676E-01
2330	9.1402E-02	1.2503E-01	2.0345E-01	2.0345E-01

Table 5.10 p21 values from the base model, the reduced model (level-1), the reduced model (level-2) and the reduced model (level-3) simulations with high DNA damage

Time	Base	L1	L2	L3
1	7.6500E-05	7.6500E-05	7.6500E-05	7.6500E-05
500	1.1469E-01	1.1447E-01	1.0480E-01	1.0480E-01
1000	1.5406E-01	1.5421E-01	1.4692E-01	1.4692E-01
1500	1.4493E-01	1.4529E-01	1.4152E-01	1.4152E-01
2000	1.3463E-01	1.3353E-01	1.3111E-01	1.3111E-01
2330	2.4086E-02	5.1688E-02	6.3039E-02	6.3039E-02

Table 5.11 p21 values from the base model, the reduced model (level-1), the reduced model (level-2) and the reduced model (level-3) simulations with excess DNA damage

Time	Base	L1	L2	L3
1	7.6500E-05	7.6500E-05	7.6500E-05	7.6500E-05
500	8.9119E-02	8.8976E-02	8.1721E-02	8.1721E-02
1000	8.1550E-02	8.1630E-02	7.7017E-02	7.7017E-02
1500	7.7565E-02	7.7760E-02	7.5521E-02	7.5521E-02
2000	9.5152E-02	9.4439E-02	9.2962E-02	9.2962E-02
2330	9.1229E-03	2.6034E-02	3.1826E-02	3.1826E-02

Table 5.12 E2F values from the base model, the reduced model (level-1), the reduced model (level-2) and the reduced model (level-3) simulations with low DNA damage

Time	Base	L1	L2	L3
1	1.7713E-06	1.7713E-06	1.7713E-06	1.7713E-06
500	2.9045E-02	2.9016E-02	2.8978E-02	2.8977E-02
1000	6.8757E-02	6.8741E-02	6.8686E-02	6.8681E-02
1500	1.1917E-01	1.1913E-01	1.1914E-01	1.1914E-01
2000	2.3960E-01	2.3953E-01	2.3947E-01	2.3946E-01
2330	1.8517E+00	1.8516E+00	1.8515E+00	1.8515E+00

Table 5.13 E2F values from the base model, the reduced model (level-1), the reduced model (level-2) and the reduced model (level-3) simulations with medium DNA damage

Time	Base	L1	L2	L3
1	1.7713E-06	1.7713E-06	1.7713E-06	1.7713E-06
500	2.8926E-02	2.8896E-02	2.8858E-02	2.8858E-02
1000	6.7960E-02	6.7945E-02	6.7885E-02	6.7885E-02
1500	1.1652E-01	1.1648E-01	1.1649E-01	1.1649E-01
2000	2.2067E-01	2.2060E-01	2.2053E-01	2.2053E-01
2330	1.7734E+00	1.7733E+00	1.7732E+00	1.7732E+00

Table 5.14 E2F values from the base model, the reduced model (level-1), the reduced model (level-2) and the reduced model (level-3) simulations with high DNA damage

Time	Base	L1	L2	L3
1	1.7713E-06	1.7713E-06	1.7713E-06	1.7713E-06
500	2.8833E-02	2.8803E-02	2.8765E-02	2.8765E-02
1000	6.8386E-02	6.8370E-02	6.8310E-02	6.8310E-02
1500	1.1828E-01	1.1825E-01	1.1826E-01	1.1826E-01
2000	2.3195E-01	2.3188E-01	2.3181E-01	2.3181E-01
2330	1.8448E+00	1.8447E+00	1.8446E+00	1.8446E+00

Table 5.15 E2F values from the base model, the reduced model (level-1), the reduced model (level-2) and the reduced model (level-3) simulations with excess DNA damage

Time	Base	L1	L2	L3
1	1.7713E-06	1.7713E-06	1.7713E-06	1.7713E-06
500	2.8965E-02	2.8936E-02	2.8897E-02	2.8897E-02
1000	6.8826E-02	6.8810E-02	6.8750E-02	6.8750E-02
1500	1.1923E-01	1.1919E-01	1.1920E-01	1.1920E-01
2000	2.3396E-01	2.3389E-01	2.3382E-01	2.3382E-01
2330	1.8465E+00	1.8465E+00	1.8464E+00	1.8464E+00

Table 5.16 p21/CycE/Cdk2-P values from the base model, the reduced model (level-1), the reduced model (level-2) and the reduced model (level-3) simulations with low DNA damage

Time	Base	L1	L2	L3
1	1.4772E-09	1.4772E-09	1.4772E-09	1.4772E-09
500	3.8569E-04	3.8103E-04	3.6758E-04	3.6758E-04
1000	1.8683E-03	1.7959E-03	1.7294E-03	1.7294E-03
1500	4.2373E-03	3.5924E-03	3.4790E-03	3.4790E-03
2000	1.0443E-02	1.1162E-02	1.0897E-02	1.0897E-02
2330	2.1726E-01	1.5299E-01	1.5022E-01	1.5022E-01

Table 5.17 p21/CycE/Cdk2-P values from the base model, the reduced model (level-1), the reduced model (level-2) and the reduced model (level-3) simulations with medium DNA damage

Time	Base	L1	L2	L3
1	1.4772E-09	1.4772E-09	1.4772E-09	1.4772E-09
500	6.7528E-04	6.6722E-04	6.4620E-04	6.4620E-04
1000	3.4201E-03	3.2909E-03	3.1770E-03	3.1770E-03
1500	7.7653E-03	6.6431E-03	6.4397E-03	6.4397E-03
2000	1.7767E-02	2.0534E-02	1.8043E-02	1.8043E-02
2330	3.0070E-01	2.7969E-01	1.6720E-01	1.6720E-01

Table 5.18 p21/CycE/Cdk2-P values from the base model, the reduced model (level-1), the reduced model (level-2) and the reduced model (level-3) simulations with high DNA damage

Time	Base	L1	L2	L3
1	1.4772E-09	1.4772E-09	1.4772E-09	1.4772E-09
500	8.9197E-04	8.8100E-04	8.4613E-04	8.4613E-04
1000	2.4843E-03	2.4081E-03	2.2708E-03	2.2708E-03
1500	4.7001E-03	4.0974E-03	3.9029E-03	3.9029E-03
2000	9.4877E-03	1.0299E-02	9.6343E-03	9.6343E-03
2330	1.5400E-01	1.2090E-01	1.0075E-01	1.0075E-01

Table 5.19 p21/CycE/Cdk2-P values from the base model, the reduced model (level-1), the reduced model (level-2) and the reduced model (level-3) simulations with excess DNA damage

Time	Base	L1	L2	L3
1	1.4772E-09	1.4772E-09	1.4772E-09	1.4772E-09
500	5.7961E-04	5.7225E-04	5.3718E-04	5.3718E-04
1000	1.5473E-03	1.4991E-03	1.3951E-03	1.3951E-03
1500	2.7550E-03	2.4201E-03	2.2835E-03	2.2835E-03
2000	5.6904E-03	6.2466E-03	5.9638E-03	5.9638E-03
2330	9.9970E-02	7.7965E-02	6.7427E-02	6.7427E-02

Table 5.20 p53 values from the base model, the reduced model (level-1), the reduced model (level-2) and the reduced model (level-3) simulations with low DNA damage

Time	Base	L1	L2	L3
1	2.6574E-02	2.6574E-02	2.6574E-02	2.6574E-02
500	6.0887E-01	6.0887E-01	6.0887E-01	6.0887E-01
1000	7.7085E-01	7.7085E-01	7.7085E-01	7.7085E-01
1500	7.9809E-01	7.9809E-01	7.9809E-01	7.9809E-01
2000	8.0281E-01	8.0281E-01	8.0281E-01	8.0281E-01
2330	8.0361E-01	8.0361E-01	8.0361E-01	8.0361E-01

Table 5.21 p53 values from the base model, the reduced model (level-1), the reduced model (level-2) and the reduced model (level-3) simulations with medium DNA damage

Time	Base	L1	L2	L3
1	2.6574E-02	2.6574E-02	2.6574E-02	2.6574E-02
500	1.1901E+00	1.1901E+00	1.1901E+00	1.1901E+00
1000	1.5163E+00	1.5163E+00	1.5163E+00	1.5163E+00
1500	1.5574E+00	1.5574E+00	1.5574E+00	1.5574E+00
2000	1.5399E+00	1.5399E+00	1.5399E+00	1.5399E+00
2330	1.5426E+00	1.5426E+00	1.5426E+00	1.5426E+00

Table 5.22 p53 values from the base model, the reduced model (level-1), the reduced model (level-2) and the reduced model (level-3) simulations with high DNA damage

Time	Base	L1	L2	L3
1	2.6574E-02	2.6574E-02	2.6574E-02	2.6574E-02
500	3.8120E-01	3.8120E-01	3.8120E-01	3.8120E-01
1000	1.2190E+00	1.2190E+00	1.2190E+00	1.2190E+00
1500	2.0363E-01	2.0363E-01	2.0363E-01	2.0363E-01
2000	9.8040E-01	9.8040E-01	9.8040E-01	9.8040E-01
2330	8.8277E-01	8.8277E-01	8.8277E-01	8.8277E-01

Table 5.23 p53 values from the base model, the reduced model (level-1), the reduced model (level-2) and the reduced model (level-3) simulations with excess DNA damage

Time	Base	L1	L2	L3
1	2.6574E-02	2.6574E-02	2.6574E-02	2.6574E-02
500	6.3022E-02	6.3022E-02	6.3022E-02	6.3022E-02
1000	1.6623E-01	1.6623E-01	1.6623E-01	1.6623E-01
1500	4.4280E-01	4.4280E-01	4.4280E-01	4.4280E-01
2000	9.5634E-01	9.5634E-01	9.5634E-01	9.5634E-01
2330	2.1695E-01	2.1695E-01	2.1695E-01	2.1695E-01

5.3 Comparison of the Reduced Models (level-1), (level-2) and (level-3) with the Base Model from a Computational Viewpoint

In this section, we focus on comparing the complexity dimensions: level of details, simulation efficiency and simplification ratio to prove that the reduced models (level-1), (level-2) and (level-3) were simpler and more efficient to run the system and generate solutions than the ODE base model.

From a computational point of view, the reduced models (level-1), (level-2) and (level-3) were simpler in representing the G1/S checkpoint and DNA damage pathways than the ODE base model due to the reduced number of network nodes, number of interactions between nodes and number of system equations, as shown in Table 5.24.

Table 5.24 Simplification achieved by the reduced models (level1), (level-2) and (level-3), in comparison to the ODE base model

No.	Entities compared	Base model	Reduced model (L1)	Reduced model (L2)	Reduced model (L3)
1	No. of nodes	35	28	26	24
2	No. of interactions	88	82	80	78
3	No. of kinetic parameters	92	86	83	82
4	No. of equations	37	30	28	26

Table 5.25 shows the percentage reduction in the number of nodes in the reduced model (level-1), (level-2) and (level-3) compared to the base model, with up to 31% at the third level of reduction, the reduced model (level-3).

Table 5.25 Simplifying the percentages in the number of nodes of the reduced models (level1), (level-2) and (level-3) vs. the ODE base model

No.	Level No.	Lump nodes	Individual nodes	Total nodes	Percentage reduction
1	Base	0	35	35	0%
2	L1	7	21	28	20%
3	L2	7	19	26	26%
4	L3	7	17	24	31%

From a computational viewpoint, the reduced models (level-1), (level-2) and (level-3) were more efficient to run the system and generate solutions than the ODE base model as shown in Table 5.26; the efficiency is particularly pronounced for larger cell populations. The saving rates of the run times reached approximately 30%, 44% and 52% for the reduced models (level-1), (level-2) and (level-3), respectively.

Table 5.26 Efficiency the reduced model (level-1), (level-2) and (level-3) run time vs. the ODE base model run time

No.	Size of sample	Base model	Reduced model (L1)	Reduced model (L2)	Reduced model (L3)
1	10 cells	27 Sec.	19 Sec.	15 Sec.	13 Sec.
2	100 cells	4:30 Min.	3:10 Min.	2:30 Min.	2:10 Min.
3	1000 cells	45 Min.	31:40 Min.	25 Min.	21:40 Min.
4	100000 cells	75 Hr.	52:46:40 Hr.	41:40 Hr.	36:06:40 Hr.

Table 5.27 compares the level of complexity, level of details and run times between the base model and the three reduced models (level-1, 2 and 3) for the studied G1/S checkpoint and DNA damage pathways.

Table 5.27 General comparison between the base model and reduced models (level-1, 2 and 3)

Model	Complexity	Details	Run
The base	Very complex	Full of details	Slow
(Level-1)	Complex	High level of details	Normal
(Level-2)	Simple	Medium level of details	Fast
(Level-3)	Very simple	Low level of details	Very fast

Representation of the biological networks by lumping proteins together in containers (lumps) can make biological networks sharper and clearer for researchers as shown in Figure 5.50.

5.4 Summary of the Chapter

In this chapter, we validated the reduced models (level-1, 2 and 3) with the base model by using two types of comparison: firstly, by comparing the behaviour of the model elements. All simulation results of the reduced models (level-1, 2 and 3) of the G1/S checkpoint pathway with or without DNA-damage were similar to and consistent with the results of the base model, and that was consistent with biological experiments as reported by Iwamoto et al. (2011).

Secondly, by comparing model results, and finding the root mean squared error (RMSE) and the root mean squared percentage error (RMSPE). we used RMSE and RMSPE as measures of accuracy to compare forecasting errors of the reduced models (level-1, 2 and 3) against the base model without DNA damage. The comparison demonstrates that the reduced models (level-1, 2 and 3) compares well with the base model and thus it is still a good model to simulate the G1/S checkpoint pathways integrated with DNA damage pathway. Also, the simulations with the base model, reduced model (level-1, 2 and 3) were run with four different levels of DNA damage to allow analysis of the differences in concentration of five species important in DNA damage response (CycE/Cdk2-P, p21, E2F, p21/CycE/Cdk2-P and p53) at $t=1$, $t=500$, $t=1000$, $t=1500$, $t=2000$ and $t=2330$. The results of these simulations show that the concentration of CycE/Cdk2-P, p21, E2F, p21/CycE/Cdk2-P and p53 for the base model and the reduced model (level-1, 2 and 3); is not significantly different. Therefore, the reduced models (level-1, 2 and 3) can be used to study G1 progression with and without DNA damage.

Finally, we Compared the reduced models (level-1, 2 and 3) with the base model from a computational viewpoint. To prove that the reduced models were simpler and more efficient to run the system and generate solutions than the ODE base model. By compared the level of complexity, level of details and run times between the base model and the three reduced models for the studied G1/S checkpoint and DNA damage pathways. We proved the representation of the biological networks by lumping proteins together in containers (lumps) can make biological networks sharper and clearer for researchers and the three reduced models were simpler and more efficient to run the system and generate solutions than the ODE base model.

Chapter 6

Using Time Windows and Logical Representation to Reduce the G1/S Checkpoint Pathway with DNA Damage

The purpose of this chapter is to offer another method to aid in model reduction yielding the expected behaviour of the G1/S checkpoint with and without DNA damage. We, therefore, focus on simplifying the time dimension by dividing the G1/S checkpoint pathway into time windows (active time windows, and steady or frozen time windows). The active time windows were then represented by logical models. This was undertaken to aid the reduction process.

This chapter is organised as follows: after a brief Summary in Section 6.1 followed by Introduction and Background (Section 6.2), the approach to reduce the framework is described in the Research Methodology section (Section 6.3). The reduced approach is analysed in the Results and Discussion section (Section 6.4). The Conclusion (Section 6.5) is devoted to a further discussion on the efficiency of the reduction method and directions for future work.

6.1 Summary

Most knowledge about regulatory and signalling networks is of a qualitative nature, which allows these networks to be represented by logical models, where the state of a molecule is either 0 (inactive) or 1 (active). These models have many advantages, as simple models do not need specific values for kinetic parameters and are able to capture the essential behaviour of a network. However, they are not suitable to reproduce detailed time courses for the concentration of molecules.

Experiments nowadays yield more and more quantitative data, so many quantitative models have been built and most of these models are very complex. An obvious question, therefore, is how to reduce complex quantitative models, which can then be used to explain and predict the outcome of these experiments.

In this chapter, we present a way of reducing complex quantitative models into logical models, where the use of time windows allows reductions in time complexity, and a logical representation to remove the kinetic parameters from a system. The method is standardized and can readily be applied to other complex quantitative models. Moreover, we discuss and generalize the existing theoretical results about the relations between Boolean and continuous models. In a case study, a continuous ODE model was used to produce a reduced logical model that describes the G1/S checkpoint with and without DNA damage. We discuss how this model can explain and predict G1/S checkpoint behaviour with DNA

damage, including oscillations of some molecules and cell fate. This shows that the reduced is model is still useful for gaining biological insights and is easier to run and analyse.

The approach presented in this study greatly helps in simplifying complex quantitative models into simple models and will facilitate the interactions between modelling and experiments. Moreover, it will also help researchers who build the models to focus on understanding and representing system behaviour rather than focusing on determining the values of the kinetic parameters.

6.2 Introduction and Literature Review

The control of cell cycle progress is tightly regulated by complex proteins in regulatory networks to achieve the correct cell division (Behl & Ziegler, 2014). It has several checkpoints; for example, the G1/S and G2/M checkpoints (Saltman, 2005). Moreover, dysfunction in cell cycle can lead to changes in DNA, which means the development of diseases such as breast cancer (King et al., 2003; Azimi et al., 2017; Farr et al., 2017). A better understanding of protein regulatory networks will, therefore, not only advance our understanding of fundamental cell cycle regulation, such as the G1/S checkpoint, but also provide more understanding into disease processes; thus, increasing the efficiency in the treatment of diseases.

Biologists have used many ways to understand the mechanics of protein regulatory networks. One way is to construct models that simulate the mechanisms of the interactions between the proteins. Several types of models have been developed to represent cell cycle that involves protein to protein interactions. These types of models include: mathematical ordinary differential equations (ODE) (Aguda, 1999; Novak & Tyson, 2004; Tashima et al., 2007; Iwamoto et al., 2008; Ling et al., 2010; Iwamoto et al., 2011; Zhao et al., 2012), Boolean (Fauré et al., 2006), petri net (Kotani et al., 2002; Herajy et al., 2013), recurrent neural networks (Ling et al., 2013) and hybrid (Singhania et al., 2011).

ODE models are the most common type used for modelling biological networks. Over time the amount of data obtained from laboratory experiments increased, so these models became more complex; especially, if they contains hundreds or thousands of variables, they will be ineffective (Danos et al., 2007). Because of the complexity of these most widely used models they offer new opportunities for researchers to develop new methods to reduce biochemical reaction network models. Many approaches to model reduction have been proposed (Clarke, 1992; Maas & Pope, 1992; Lam & Goussis, 1994; Maas & Pope, 1994; Clarke et al., 1996; Gorban & Karlin, 2005; Feret et al., 2009; Gorban et al., 2010; Noel et al., 2011; Radulescu et al., 2012; Rao et al., 2013; Sondag et al., 2013; Rao et al., 2014; Radulescu et al., 2015).

For the purpose of the current study, a biological network model reduction is defined as any method designed to decompose/reproduce the original model into a smaller models that produces the same

behaviour as the original model. This is undertaken by reducing one or more dimensions of the complexity, of the biological network model (by reducing the number of species, reducing the number of reactions or reducing the model run time).

In this work, we focus on reducing complex ODE mathematical models resulting from modelling large regulatory and signalling networks and improving the reduction process by using time windows and simple logical models. As a case study, a continuous ODE model (Iwamoto et al., 2011) was reduced into a reduced logical model describing the G1/S checkpoint with and without DNA damage.

The regulatory and signalling networks have been represented by logical models since the time of Kauffman (1969), who was the pioneer in this field. A logical model is the simplest models that can be used to describe the dynamics of regulatory and signalling networks without the need of many parameters. A logical model contains a series of interconnected elements $Y_1 \dots Y_n$. Each element has only two possible states of activation, 1 (active) and 0 (inactive). The regulatory and signalling network is completely described by set of logical equations as shown in Eq. 6.1(a, b, c):

$$Y_i(t+1) = \begin{cases} (Y_1^a(t) \text{ OR } Y_2^a(t) \dots \text{ OR } Y_n^a(t)) \text{ AND NOT } (Y_1^i(t) \text{ OR } Y_2^i(t) \dots \text{ OR } Y_m^i(t)) & (6.1.a) \\ Y_1^a(t) \text{ OR } Y_2^a(t) \dots \text{ OR } Y_n^a(t) & (6.1.b) \\ \text{NOT } (Y_1^i(t) \text{ OR } Y_2^i(t) \dots \text{ OR } Y_m^i(t)) & (6.1.c) \end{cases}$$

where $Y_i \in \{0, 1\}$, $\{Y_n^a\}$ is the set of activators of Y_i , $\{Y_m^i\}$ is the set of inhibitors of Y_i . If Y_i has activators and inhibitors use Eq. 6.1.a, if Y_i has only activators use Eq. 6.1.b and if Y_i has only inhibitors use Eq. 6.1.c.

Building a logical model involves three steps: (i) find a regulatory graph for the system; (ii) define the logical parameters of the system; (iii) specify the logical equations (for updating). Figure 6.1 shows an example of building a logical model.

As seen in Figure 6.1, a logical model is represented by a Logic-based graph and every node in the logical model can be derived from the state of other nodes through a logical equation. change in the state of nodes from 'on' to 'off' or vice-versa through a sequence of changes in state is called a biological process. (Chen et al., 2016). The dynamics of a logical model are defined by synchronous (all nodes are updated at the same time) or asynchronous (each node is updated individually by sequential order) updating. The system dynamics are mainly determined by the choice of updating scheme (Aracena et al., 2009). Logical models have many advantages: it is easy to build, easy to compose and easy to simulate perturbations (Le Novère, 2015).

Several software tools exist that building and finding the dynamics of logical models, such as GINsim (Gonzalez et al., 2006), SQUAD (Di Cara et al., 2007), Boolean Net (Albert et al., 2008), Chem Chains (Helikar & Rogers, 2009), Odefy (Krumstiek et al., 2010), Bool Net (Müssel et al., 2010), Cell NOpt (Terfve et al., 2012), MaBoSS (Stolletal., 2012) and; Cell Collective (Helikar et al., 2013).

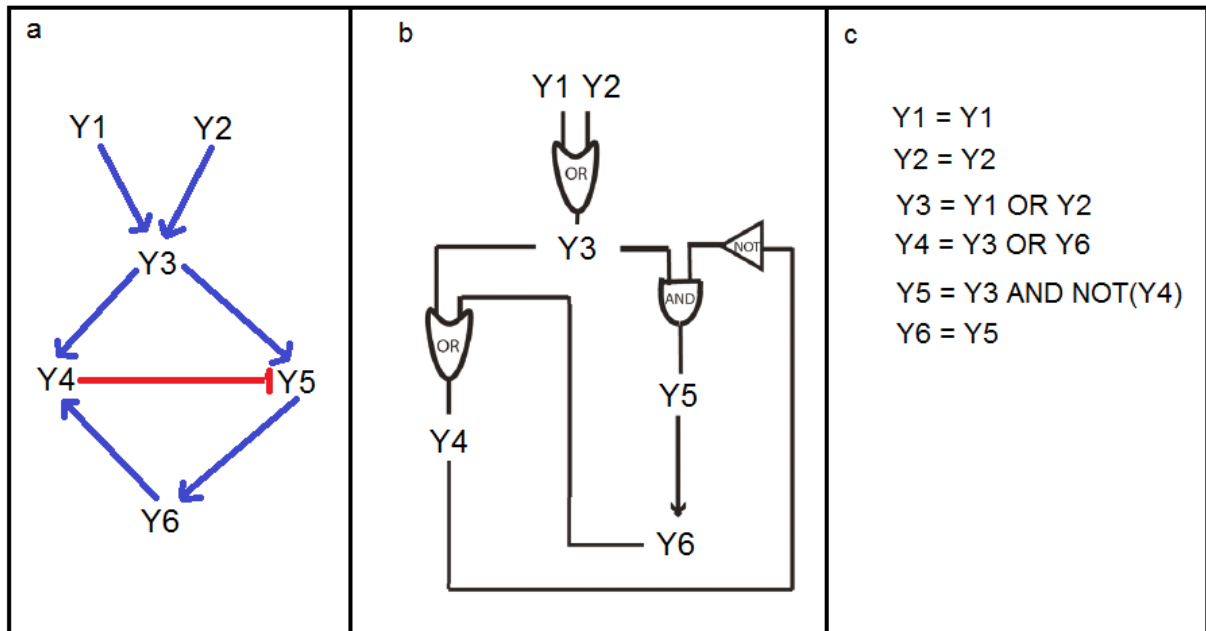


Figure 6.1 Interaction graph, logical model and logical equations of protein network examples (a) Interaction graph: The nodes (Y1, Y2 ... Y6) in the graph represent proteins, and the edges represent interactions. Blue arrows represent activations and red bar arrows inhibitions. (b) Logic-based representation of a logical model for the interaction graph given in (a). (c) Equations of a logical model for the interaction graph given in (a).

There are few logical models that have been applied to the mammalian cell cycle. To know more about these models, see (Huang & Ingber, 2000; Fauré et al., 2006; Sahin et al., 2009; Mombach et al., 2014, Tanaka et al., 2017). Moreover, many logical models have been built to model cell cycle of budding yeast (Li et al., 2004; Fauré et al., 2009; Irons, 2009; Todd & Helikar, 2012; Alcasabas et al., 2013; Rubinstein et al., 2013; Chasapi et al. 2015; Linke et al., 2017).

6.3 Research Methodology

Reducing a model of the biological network into a simple one using time windows and simple logical models involves the following tasks: (i) Understanding the protein interactions involved in the system; (ii) Dividing the dynamics of the system into time windows (active time windows, steady or frozen time windows); (iii) Determining the key elements in each active time windows; and (iv) Building a logical model for each active time window. Last task is divided into three sub-tasks: first, finding a regulatory graph for the system; secondly, defining the logical parameters of the system; and thirdly, specify the logical equations (for updating).

6.3.1 Understand the Protein Interactions Involved in the System

We used the base model presented in Section 4.1 (G1/S checkpoint pathway and DNA damage pathways model) as a complex system case study to apply our new reduction approach. Understanding protein interactions involves understanding system dynamics in the G1/S checkpoint pathway and the DNA damage pathway base model involving protein-protein interactions. This is considered the first step in the model reduction process.

The system and form of molecular interactions in the network were described in the section on the base model (Section 4.1). The base model, as shown in Figure 4.7, shows the reaction scheme of the proposed model, which integrated the G1/S model and the DNA damage signalling pathway. The model consists of 35 dependent variables, 88 interactions and 92 kinetic parameters (see Appendix B).

6.3.2 Divide the Dynamics of the System into Time Windows (Active Time Windows, Steady or Frozen Time Windows)

Biological processes can take place over a long timescale. For example, the G1/S network that generates a circadian rhythm, as shown in Figure 6.2, shows protein behaviour over three distinct time-windows. In time window A, some proteins undergo changes in concentration and in others, no change occurs. In time window B, there are no changes in most proteins. In time window C, some proteins have changes in concentration and, in others, no change occurs. To model a system that involves processes acting in different time-windows, primary time windows must be chosen (time window A and C). Other time-windows are then treated as being frozen in time (time window B).

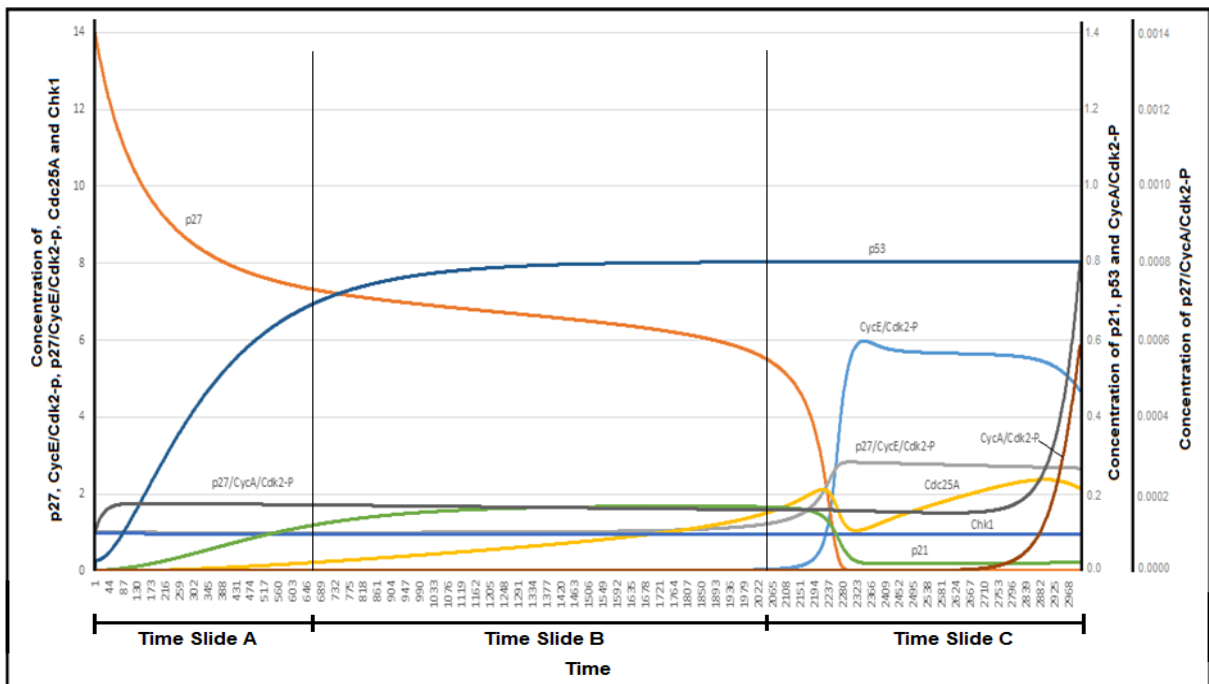


Figure 6.2 Behaviour of multiple time windows

These time window separations are made during model construction; they often motivate the decisions about what species and processes should be included in the model and what can be ignored. In other cases, existing models that incorporate separate time windows can be simplified. This model reduction process approximates the original model with a model of reduced complexity.

Model reduction by time window separation leads to similar results to an original model, where a differential equation describing a state variable is replaced by a new simple differential equation. The main idea in model reduction techniques by time windows is to treat a slow variable as a fixed parameter (constant value), rather than as a state variable. In the reduction method using time windows, the number of elements in the system depends on the time window and the number of elements changing with time.

6.3.3 Determine the Key Elements in Each Active Time Windows

After studying the G1/S checkpoint protein behaviour with and without DNA damage in multiple time slides, the key elements in each active time window are determined. Table 6.1 shows the G1/S checkpoint protein behaviour with and without DNA damage over multiple time windows:

Time window A contains 14 elements that play main roles in the time window A. These elements are CycD, Cdk4, CycD/Cdk4, p27, p27/CycD/Cdk4, p21, p21/CycD/Cdk4, p16, Rb/E2F, Rb-PP/E2F, Rb, p53, Mdm2 and ATM/ATR. Also, time window C contains 14 elements that play main roles in time window C. These elements are CycE, Cdk2, CycE/Cdk2, CycE/Cdk2-P, p27, p27/CycE/Cdk2-P, p21, p21/CycE/Cdk4-P, Rb-PP/E2F, E2F, Rb-PPP, p53, Mdm2 and ATM/ATR.

Table 6.1 G1/S checkpoint protein behaviour with and without DNA damage in multiple time windows

No	Molecular	A	B	C
1	<i>CycD</i>	Fast	Slow	Slow
2	<i>CycE</i>	Slow	Slow	Fast
3	<i>CycA</i>	Slow	Slow	Fast
4	<i>Cdk4</i>	Fast	Slow	Slow
5	<i>Cdk2</i>	Slow	Linear	Slow
6	<i>CycD/Cdk4</i>	Fast	Slow	Slow
7	<i>CycE/Cdk2</i>	Slow	Slow	Fast
8	<i>CycE/Cdk2-P</i>	Slow	Slow	Fast
9	<i>CycA/Cdk2</i>	Slow	Slow	Fast
10	<i>CycA/Cdk2-P</i>	Slow	Slow	Fast
11	<i>p27</i>	Fast	Slow	Fast
12	<i>p27/CycD/Cdk4</i>	Fast	Slow	Slow
13	<i>p27/CycE/Cdk2-P</i>	Slow	Slow	Fast
14	<i>p27/CycA/Cdk2-P</i>	Slow	Slow	Fast
15	<i>p21</i>	Fast	Slow	Fast
16	<i>p21/CycD/Cdk4</i>	Fast	Linear	Slow
17	<i>p21/CycE/Cdk2-P</i>	Slow	Slow	Fast
18	<i>p21/CycA/Cdk2-P</i>	Slow	Slow	Fast
19	<i>p16</i>	Linear	Linear	Linear
20	<i>Rb/E2F</i>	Fast	Slow	Slow
21	<i>Rb-PP/E2F</i>	Fast	Slow	Fast
22	<i>E2F</i>	Slow	Slow	Fast
23	<i>Rb-PPP</i>	Slow	Slow	Fast
24	<i>Rb</i>	Fast	Slow	Slow
25	<i>p53</i>	Fast	Slow	Slow
26	<i>Mdm2</i>	Fast	Slow	Slow
27	<i>ATM/ATR</i>	Fast	Slow	Slow
28	<i>Cdc25A</i>	Slow	Linear	Slow
29	<i>Cdc25A-P</i>	Slow	Slow	Slow
30	<i>Chk1</i>	Linear	Slow	Slow
31	<i>Chk1-P</i>	Slow	Slow	Slow
32	<i>NF-Y</i>	Slow	Slow	Slow
33	<i>B-Myb</i>	Linear	Linear	Slow
34	<i>B-Myb-P</i>	Slow	Slow	Slow
35	<i>Im</i>	Fast	Slow	Slow

6.3.4 Building Logical Model for each Active Time Window

We need to build two logical models, R1 and R2. R1 to represent the reduced model for time window A and R2 to represent the reduced model for time window C. The first step to construct any logical model is to find a regulatory graph for the system, which in our case depends on the ODE model. See Table I.1 in Appendix I, where it shows the ODEs of the reduced model (R1) after refinement, and see Table J.1 in Appendix J, where it shows the ODEs of the reduced model (R2) after refinement.

Figure 6.3 shows a regulatory graph for the reduced model (R1) and Figure 6.4 shows the regulatory graph for the reduced model (R2).

The second step is to convert a regulatory graph into a logic-based graph. Figure 6.5 shows the logical model with the underlying interaction graph given in Figure 6.3, while Figure 6.6 shows the logical model with underlying interaction graph given in Figure 6.4.

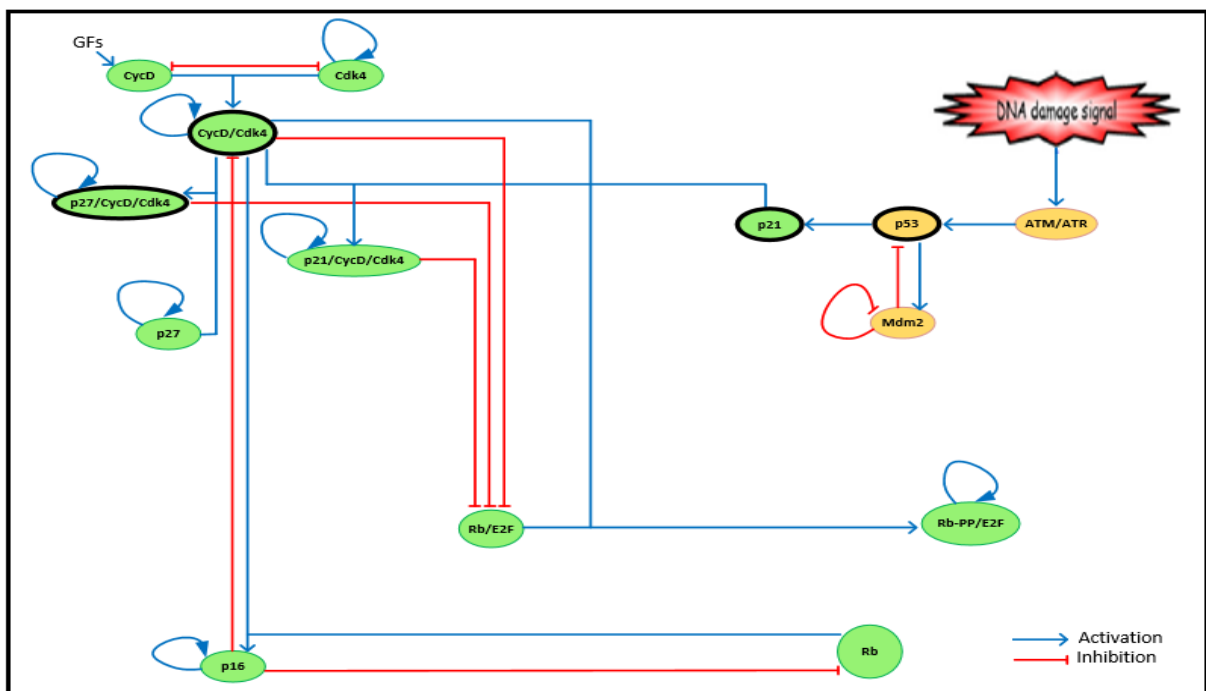


Figure 6.3 Regulatory graph for the reduced model (R1) for time window A

The last step is to specify the logical equations (for updating) and the initial values of the proteins. The reduced model (R1) represents 14 logical equations (see I.3 in Appendix I). Table I.2 shows the initial conditions of the reduced model (R1). Meanwhile, the reduced model (R2) represents 14 logical equations (see J.3 in Appendix J). Table J.2 shows the initial conditions of the reduced model (R2). Synchronous method is used to update the status of nodes.

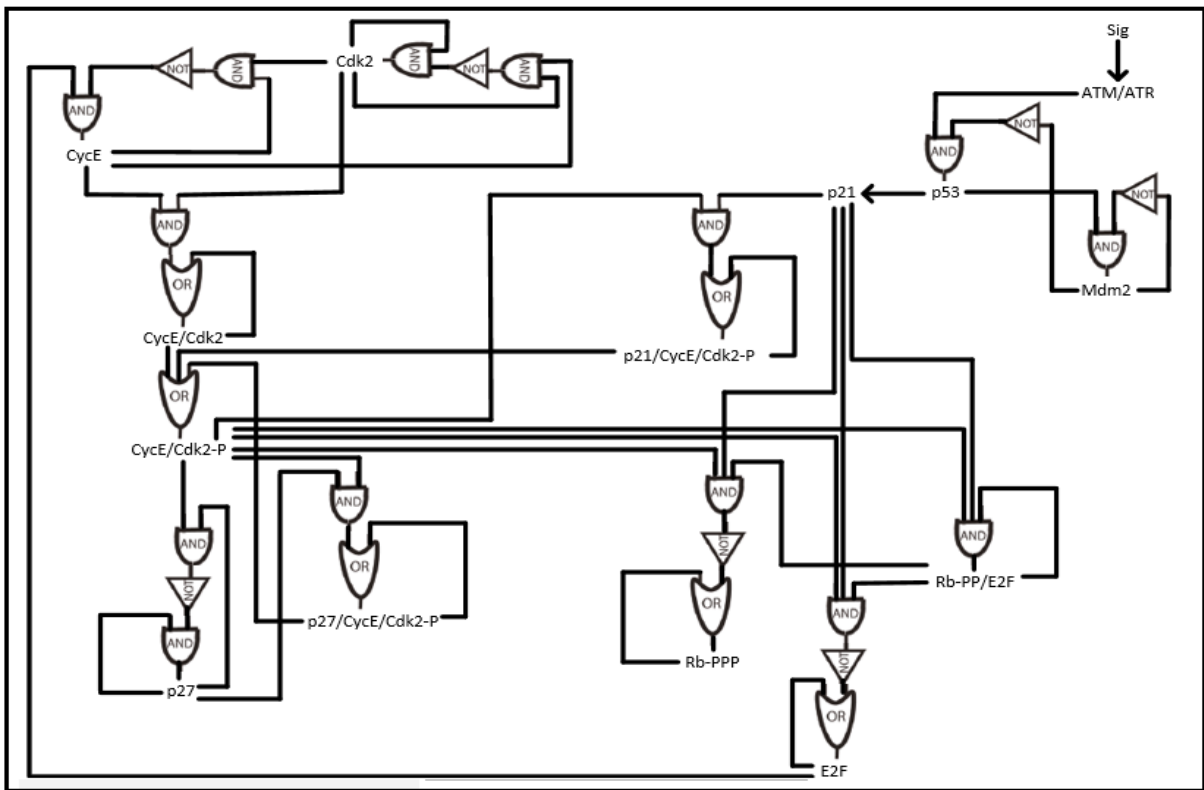


Figure 6.6 Logic-based graph for the reduced model (R2)

6.4 Results and Discussion

The simulation results of the reduced model (R1) and the reduced model (R2), with and without DNA damage, agreed with the biological knowledge from previous studies as described below. CycD and CycE play the main roles in mammalian G1-to-S transition. As shown in Figure 6.7, for the reduced model (R1) without DNA damage, the state of CycD becomes active in early G1/S. CycD binds to Cdk4 forming the binary complex, CycD/Cdk4. As shown (at time step 2), CycD/Cdk4 becomes active. Furthermore, the CycD/Cdk4 complex phosphorylates Rb bound to E2F, which becomes hypophosphorylated form, Rb-PP/E2F (Helin, 1998). We note that Rb/E2F becomes inactive (at time step 3), Rb-PP/E2F becomes active (at time step 4) and Rb becomes inactive (at time step 5). p53 and p21 stay inactive at all iterations in the simulation of the reduced model (R1) because there was no DNA damage.

Molecular	0	1	2	3	4	5	6	7	8	9	10
CycD	red	green	red	red	red	red	red	red	red	red	red
Cdk4	green	green	red	red	red	red	red	red	red	red	red
CycD/Cdk4	red	red	green	green	red	red	red	red	red	red	red
p27	green	green	green	green	green	green	green	green	green	green	green
p27/CycD/Cdk4	red	red	red	green	green	green	green	green	green	green	green
p21	red	red	red	red	red	red	red	red	red	red	red
p21/CycD/Cdk4	red	red	red	red	red	red	red	red	red	red	red
p16	red	red	red	green	green	green	green	green	green	green	green
Rb/E2F	green	green	green	red	red	red	red	red	red	red	red
Rb-PP/E2F	red	red	red	green	green	green	green	green	green	green	green
Rb	green	green	green	green	red	red	red	red	red	red	red
p53	red	red	red	red	red	red	red	red	red	red	red
Mdm2	red	red	red	red	red	red	red	red	red	red	red
ATM/ATR	red	red	red	red	red	red	red	red	red	red	red

Figure 6.7 Simulation results of the reduced model (R1) without DNA damage (green: active, red: inactive)

After damage occurred in DNA, the simulation results of the reduced model (R1) are shown in Figure 6.8. The DNA damage signal activates ATM/ATR (at time step 1). p53 is activated by ATM/ATR (at time step 2), which regulated transcription of the large number of genes required for different purposes, including damage recovery or cell death processes (Ciliberto et al., 2005; Harris & Levine, 2005; Geva-Zatorsky et al., 2006).

p53 activation leads to the activation of p21 (Yu et al., 1999). The role of p21 was to inhibit the activity of CDK to effect cell cycle arrest through inhibition or phosphorylation of Rb to keep E2F inactive (Campisi & Fabrizio, 2007). This explains the activation of p21/CycD/Cdk4 (at time step 4). Furthermore, as seen in Figure 6.8, there were oscillations in the behaviour of p53 and p21. This result agreed with the experimental results as described in the previous chapter.

Molecular	0	1	2	3	4	5	6	7	8	9	10
CycD	red	green	red	red	red	red	red	red	red	red	red
Cdk4	green	green	red	red	red	red	red	red	red	red	red
CycD/Cdk4	red	red	green	green	red	red	red	red	red	red	red
p27	green	green	green	green	green	green	green	green	green	green	green
p27/CycD/Cdk4	red	red	red	green	green	green	green	green	green	green	green
p21	red	red	red	red	green	red	green	red	green	red	green
p21/CycD/Cdk4	red	red	red	red	green	green	green	green	green	green	green
p16	red	red	red	green	green	green	green	green	green	green	green
Rb/E2F	green	green	green	red	red	red	red	red	red	red	red
Rb-PP/E2F	red	red	red	green	green	green	green	green	green	green	green
Rb	green	green	green	green	red	red	red	red	red	red	red
p53	red	red	green	red	green	red	green	red	green	red	green
Mdm2	red	red	red	green	red	green	red	green	red	green	red
ATM/ATR	red	green	green	green	green	green	green	green	green	green	green

Figure 6.8 Simulation results of the reduced model (R1) with DNA damage (green: active, red: inactive)

As shown in Figure 6.9, the simulation results of the reduced model (R2) without DNA damage are in mid G1. CycE/CDK2 activation is the main reason for further hyperphosphorylation of Rb-pp/E2F resulting in the dissociation of Rb-PPPP from E2F; thus, releasing E2F. As shown (at time step 1) in Figure 6.9, E2F and Rb-PPP become active. The increased concentration of E2F promotes the synthesis of CycE in the mid to late G1 phase (at time step 2). When CycE becomes active, this facilitates the binding between CycE and CDK2 to form more of CycE/CDK2 (at time step 3) so CycE/CDK2 becomes active. This results in further freeing of E2F; thus, establishing a positive feedback loop between E2F and CycE; increased concentrations of E2F and CycE move the cell from the G1/S checkpoint to the S phase (Satyanarayana & Kaldis, 2009). These results agree with the reported experimental results (Kohn, 1999; Hochegger et al., 2008).

Molecular	0	1	2	3	4
CycE	Red	Red	Green	Red	Green
Cdk2	Green	Green	Green	Red	Red
CycE/Cdk2	Red	Red	Red	Green	Green
CycE/Cdk2-P	Green	Red	Green	Green	Green
p27	Green	Red	Red	Red	Red
p27/CycE/Cdk2-P	Red	Green	Green	Green	Green
p21	Red	Red	Red	Red	Red
p21/CycE/Cdk2-P	Red	Red	Red	Red	Red
Rb-PP/E2F	Green	Red	Red	Red	Red
E2F	Red	Green	Green	Green	Green
Rb-PPP	Red	Green	Green	Green	Green
p53	Red	Red	Red	Red	Red
Mdm2	Red	Red	Red	Red	Red
ATM/ATR	Red	Red	Red	Red	Red

Figure 6.9 Simulation results of the reduced model (R2) without DNA damage (green: active, red: inactive)

As shown in Figure 6.10 for the simulation results of the reduced model (R2) with DNA damage, p21 active. The role of p21 to inhibit the activity of CDK to effect cell cycle arrest through inhibition of phosphorylation of Rb to keep E2F inactive (Campisi & Fabrizio, 2007). Protein p21 is bound to CycE/Cdk2-P forming the complex, p21/CycE/Cdk2-P. As shown (at time step 1), p21/CycE/Cdk2-P becomes active. This delays release of E2F from Rb-PP/E2F for one iteration more, which meant a delay in the synthesis of CycE. As shown in Figure 6.10, E2F becomes active (at time step 2) and CycE becomes active (at time step 3). This delay in activation represents cell cycle arrest. These results agree with experimental results (Lev Bar-Or et al., 2000; Batchelor et al., 2008).

Molecular	0	1	2	3	4
CycE	Red	Red	Red	Green	Red
Cdk2	Green	Green	Green	Green	Red
CycE/Cdk2	Red	Red	Red	Red	Green
CycE/Cdk2-P	Green	Red	Green	Green	Green
p27	Green	Red	Red	Red	Red
p27/CycE/Cdk2-P	Red	Green	Green	Green	Green
p21	Green	Red	Red	Green	Green
p21/CycE/Cdk2-P	Red	Green	Green	Green	Green
Rb-PP/E2F	Green	Green	Red	Red	Red
E2F	Red	Red	Green	Green	Green
Rb-PPP	Red	Red	Green	Green	Green
p53	Green	Red	Red	Green	Red
Mdm2	Green	Red	Red	Green	Red
ATM/ATR	Green	Green	Green	Green	Green

Figure 6.10 Simulation results of the reduced model (R2) with DNA damage (green: active, red: inactive)

6.5 Conclusions

There has been a great deal of interest in the reduction of complex ODE regulatory network models for many reasons: (i) Most of the models that have been built to understand regulatory networks were ODE mathematical models; (ii) Most of the ODE mathematical models were complex and needed kinetic information for molecules that was not easily gathered; (iii) Simplifying complex ODE mathematical models can lead to a better understanding and control of these systems.

We presented a way of reducing complex quantitative models into logical models where the use of time windows allowed the reduction of time complexity, and logical representation to get rid of the kinetic parameters in a system. The method is general and can be readily applied to complex quantitative models. Moreover, we discussed and generalized the existing theoretical results on the relations between Boolean and continuous models. As a case study, a continuous ODE model was changed into a reduced logical model to describe the G1/S checkpoint with and without DNA damage. We discussed how this model can explain and predict the G1/S checkpoint behaviour with DNA damage, including oscillations by some molecules and the fate of the cells. This showed the reduced model was still useful for obtaining biological insights and it was easier to run and to analyse.

The approach presented here greatly helped to simplify complex quantitative models into simple models and will facilitate the interactions between modelling and experiments. Moreover, it will help researchers and those who build these models to focus on understanding and representing system behaviour rather than focusing on determining values for the kinetic parameters.

Future work includes producing further reduction models yielding expected behaviour of whole cell cycle regulation with and without DNA damage. Moreover, the proposed reduced method could be improved by using time windows and multi-valued logical models (semi-quantitative models).

Chapter 7

Conclusions and Future Directions

The purpose of this research, and the preceding chapters, was to offer two methods to aid in reduction and approximation of complex ODE mathematical models. In particular, the ODE model of the G1/S checkpoint, with and without DNA damage, was offered as a motivating example of a complex system and two reduction methods were presented to aid in this reduction. This chapter includes four sections. Section 7.1 presents a general overview; and Section 7.2 presents the contributions made by the thesis. The future directions are presented in Section 7.3, and the overall conclusions are given in Section 7.4.

7.1 General Overview

This thesis addressed several issues related to complexity, model reduction and the control of complex systems. Two reduction methods were proposed in this thesis: the first approach was based on a hierarchical representation and lumping approach and the second approach used time windows and logical models. The issues studied in this thesis can be summarised as follows:

First, the thesis presented a review of issues and facts about complex systems, model reduction, complexity of biological networks and reduction methods used to reduce mathematical models of biological systems (Chapter 2).

Secondly, it provided a brief review of the biological background on the regulation of cell cycle and the details of the G1/S checkpoint and related models (Chapter 3).

Thirdly, we developed a new method to simplify biological networks using a hierarchical representation and lumping approach. It has been shown that the new method not only can simplify biological networks, but also can improve the speed of running the system and generate solutions easier than with the ODEs original model. The quality of representation of biological networks with ODEs generally deteriorates with increasing size of biological but the new reduced method over comes this difficulty, and therefore, when the size of the biological networks increases the complex ODE model can be replaced with the reduced model (Chapter 4).

Fourthly, we validated the reduced model output with base model through: comparing the behaviour of the elements of the model, the root mean squared error (RMSE) and the root mean squared percentage error (RMSPE); to be sure that the reduced model was useful for a particular purpose and applicable to answering a specific set of questions. Furthermore, the results showed that this new

reduce method was very effective; the reduced model generated faster solutions that were almost perfectly aligned with the behaviour of the complex biological network. In general, the reduced model achieved excellent agreement in results compared with original ODE model. This can lead to better understanding and help in the treatment of diseases, especially (cancer) (Chapter 5).

Fifthly, we offered another method to aid in the reduction yielding the expected behaviour of the G1/S checkpoint with and without DNA damage. We divided the G1/S checkpoint pathway into time windows (active time windows and steady or frozen time windows). The active time windows were then represented by logical models. The reduced model agreed with the original model results and biological evidence (Chapter 6).

Finally, we discussed the conclusions and outcomes from this research and proposed future research directions. The main conclusion was that relaxing the struggle with complexity of mathematical models was possible and the proposed reduction methods have the potential to make important impacts across many fields of biomedical and other research (Chapter 7).

7.2 Contributions

The contributions and outcomes from this thesis can be broken down as follows:

1. A review of complex systems and reduction methods that will open the minds of researchers to improve the existing reduction methods or to suggest new reduction methods.
2. A good summary of the regulation of cell cycle that will help researchers who do not have a strong biology background.
3. A new reduction method to simplify protein-protein interaction (PPI) networks based on a hierarchical representation and lumping approach that could be applied to different kinds of complex systems. The new reduction method provides possibility to zoom in and out several levels of complexity with good results. So, this make it unique compared to the existing ones.
4. A new reduction method to simplify complex ODE mathematical models of biological signalling networks, using time windows and logical models that could be applied to different kinds of complex systems. This new reduction method is the first method that combined Boolean models and time windows to reduce the complex biological models with good results. So, this makes it unique compared to the existing ones.
5. The two new reduction methods provided many advantages from two different perspectives (computational and biological):

- A. From a computational viewpoint:
 - i. The reduced model was more efficient in running the system and generating solutions than the ODE base model.
 - ii. The reduced model was easier to run and generate solutions than the ODE base model.
 - iii. The reduced model was easier to represent than the ODE base model through reducing the number of nodes in the network, thereby reducing the number of interactions between nodes and the number of system equations.

 - B. From biological viewpoint:
 - i. Better understanding of protein interactions.
 - ii. Easier understanding of system behaviour.
 - iii. Easier analysis of results.
 - iv. The reduction method allowed representation of biological networks in multiple levels of abstraction (zoom in, zoom out).
 - v. The reduction method allowed assembling different models of a biological system in one global view (a comprehensive biological network).
 - vi. Easier to apply perturbing functions in the reduced model than in the base model because the reduction method was based on a lumping approach, where every lump was a functional unit. Therefore, we can remove these lumps one by one and see what happens to the system behaviour.
 - vii. The reduced model enabled simulation of many scenarios for various emergent properties and behaviour.
6. A better understanding of intracellular signalling networks that can contribute to better treatment of diseases, especially (cancer).

7.3 Future Directions

The present work has, so far, helped in reducing complex ODE mathematical models resulting from modelling the G1/S checkpoint pathway with and without DNA damage, and made improvement in simulation and knowledge of a variety of possible scenarios using reduced models. Future work could continue to focus on these areas.

In future work, we intend to extend the method based on a hierarchical representation and lumping approach to more complex biological networks, such as the whole cell cycle with and without DNA damage. In addition to further development of the first reduction method, there are other lumping methods that could offer interesting results. For example, nested fuzzy cognitive maps (FCMs) can be used to obtain a hierarchical representation and, lumping as it follows similar in principles. the researcher believes that there must be a way to bring these methods together.

There are many open questions about the reduction of complex ODE mathematical models of biological systems that have been developed. How can we use the reduced models to build a comprehensive biological model? How can we balance the degree of simplification and accuracy of the results required in the reduction process, as well as other related research questions? These are all issues that should be considered in future development and could produce very interesting results.

Future extensions of the reduced method using time windows and logical models include reductions yielding the expected behaviour of the whole cell cycle regulation, with and without DNA damage. Moreover, the reduced method could be improved by using time windows and a multi-valued logical model (semi-quantitative models).

While this research offered two methods of reduction for complex ODE mathematical models, it should be obvious that there exists a great deal of room for future work (directly and indirectly) related to the current work.

7.4 Conclusions

There has been a great deal of interest in the reduction of complex ODE regulatory network models for many reasons: (i) Most of the models that have been built to understand regulatory networks were ODE mathematical models; (ii) Most of the ODE mathematical models were complex and needed kinetic information for molecules and that was not easily gathered; (iii) Simplifying the complex ODE mathematical models can lead to better understanding and control of these systems; and (iv) The known reduction methods often faced difficulties when applied to complex systems.

For the purpose of the current study, a biological network model reduction was defined as any method designed to reproduce the original model in a smaller model that produced the same behaviour as the original model, by reducing one or more dimensions in a biological network model.

In conclusion, behind each complex system there is a network that defines the interactions between the components. We will never understand complex systems unless we map and understand the networks behind them. Proposing simplified dynamic models for large and complex biological networks by using these new reduced techniques could allow building a comprehensive biological network. That would help researchers gain a greater understanding of the emerging properties of cellular activities. Hierarchical modelling is important when there is the need and possibility to zoom in and out several levels of complexity. Critical parameter identification is an important issue in systems biology. There are many reduction methods but a fully formal method that exploited the hierarchical orders for large volumes of variables was missing.

This thesis proposed and developed two ODE model reduction approaches to reduce the dimensions and complexity of highly-dimensional ODE models. The two approaches were then applied to an ODE model of G1/S checkpoint pathway integrated with DNA damage pathways.

The proposed approaches can help greatly simplify complex quantitative models into simple models that facilitate the interactions between the modelling and experiments. Moreover, they can help researchers and those who build the models to focus on understanding and representing system behaviour rather than focusing on determining the values of a large number of kinetic parameters. The advantage is greater in particular in application to molecular networks that have many well separated time windows. The reduced model has improved our understanding of the dynamics of the G1/S checkpoint pathway with and without DNA damage.

This work showed that relaxing the struggle with the complexity of mathematical models is possible and the proposed reduction methods have the potential to make an impact across many fields of biomedical and other research.

Appendix A

Initial conditions, kinetic parameters and mass balance equations of the ODE mathematical model for the DNA damage signalling pathway and whole cell cycle regulation

A.1 Initial conditions of the mathematical model (Iwamoto et al., 2011)

Table A.1 Initial conditions of the mathematical model

<i>Chemical species</i>	<i>Initial value</i>	<i>Chemical species</i>	<i>Initial value</i>	<i>Chemical species</i>	<i>Initial value</i>
Y_1	$3.00e-02$	Y_{19}	$1.00e-03$	Y_{37}	$1.00e-03$
Y_2	$1.00e-03$	Y_{20}	$1.95e+00$	Y_{38}	0
Y_3	$4.00e-05$	Y_{21}	$1.00e-03$	Y_{39}	0
Y_4	$5.00e+00$	Y_{22}	0	Y_{40}	0
Y_5	$1.50e+01$	Y_{23}	$1.00e-02$	Y_{41}	0
Y_6	$7.50e+00$	Y_{24}	$5.00e-02$	Y_{42}	$1.00e-06$
Y_7	$1.00e-03$	Y_{25}	$2.65e-02$	Y_{43}	$1.00e-06$
Y_8	$1.00e-03$	Y_{26}	$2.35e-04$	Y_{44}	$3.00e-02$
Y_9	$4.00e-04$	Y_{27}	0	Y_{45}	0
Y_{10}	$1.00e-04$	Y_{28}	$1.00e-03$	Y_{46}	$2.00e+00$
Y_{11}	$1.40e+01$	Y_{29}	$1.00e-04$	Y_{47}	$3.00e-02$
Y_{12}	$1.00e-03$	Y_{30}	$9.90e-01$	Y_{48}	$9.00e-01$
Y_{13}	$1.00e+00$	Y_{31}	$1.00e-02$	Y_{49}	$1.00e-01$
Y_{14}	$1.00e-04$	Y_{32}	0	Y_{50}	$1.00e-01$
Y_{15}	0	Y_{33}	0	Y_{51}	$9.00e-01$
Y_{16}	0	Y_{34}	$1.00e+01$	Y_{52}	0
Y_{17}	0	Y_{35}	$1.00e-04$	Y_{53}	0
Y_{18}	0	Y_{36}	$1.00e-04$	<i>Im</i>	0

Abbreviations are as follows: Y_1 : CycD, Y_2 : CycE, Y_3 : CycA, Y_4 : Cdk4, Y_5 : Cdk2, Y_6 : CycD/Cdk4, Y_7 : iCycE/Cdk2, Y_8 : aCycE/Cdk2, Y_9 : iCycA/Cdk2, Y_{10} : aCycA/Cdk2, Y_{11} : p27, Y_{12} : p27/CycD/Cdk4, Y_{13} : p27/CycE/Cdk2, Y_{14} : p27/CycA/Cdk2, Y_{15} : p21, Y_{16} : p21/CycD/Cdk4, Y_{17} : p21/CycE/Cdk2, Y_{18} : p21/CycA/Cdk2, Y_{19} : p16, Y_{20} : Rb/E2F, Y_{21} : Rb-PP/E2F, Y_{22} : E2F, Y_{23} : Rb-PPP, Y_{24} : Rb, Y_{25} : p53, Y_{26} : Mdm2, Y_{27} : ATM/ATR, Y_{28} : iCdc25A, Y_{29} : aCdc25A, Y_{30} : iChk1, Y_{31} : aChk1, Y_{32} : NF-Y, Y_{33} : CycB, Y_{34} : Cdk1, Y_{35} : iCycB/Cdk1cyto, Y_{36} : aCycB/Cdk1cyto, Y_{37} : Wee1, Y_{38} : Wee1p, Y_{39} : p21/CycB/Cdk1, Y_{40} : iB-Myb, Y_{41} : aB-Myb, Y_{42} : iCdc25C, Y_{43} : aCdc25C, Y_{44} : iCdc25Cps216, Y_{45} : aCdc25Cps216, Y_{46} : 14-3-3 σ , Y_{47} : 14-3-3 σ /iCdc25Cps216, Y_{48} : iAPC/Ccdc20, Y_{49} : aAPC/Ccdc20, Y_{50} : iAPC/Ccdh1, Y_{51} : aAPC/Ccdh1, Y_{52} : iCycB/Cdk1nuc, Y_{53} : aCycB/Cdk1nuc, *Im*: Intermediate, DDS: DNA damage signal

A.2 Kinetic parameters of the ODE mathematical model (Iwamoto et al., 2011)

Table A.2 Kinetic parameters of the ODE mathematical model

<i>Kinetic parameter</i>	<i>Value</i>	<i>Kinetic parameter</i>	<i>Value</i>	<i>Kinetic parameter</i>	<i>Value</i>	<i>Kinetic parameter</i>	<i>Value</i>
k_1	5.00e-04	k_{36}	1.50e-03	k_{71}	4.00e-03	k_{106}	5.00e-02
k_2	5.00e-04	k_{37}	5.00e-05	k_{72}	1.00e-08	k_{107}	2.00e-03
k_3	5.00e-03	k_{38}	1.00e-03	k_{73}	3.00e+00	k_{108}	1.00e-05
k_4	2.50e-03	k_{39}	5.00e-03	k_{74}	7.72e-01	k_{109}	1.00e-02
k_5	1.00e-01	k_{40}	2.00e-03	k_{75}	1.00e-05	k_{110}	1.00e+00
k_6	2.50e-03	k_{41}	5.00e-05	k_{76}	5.56e-02	k_{111}	1.00e-03
k_7	2.50e-03	k_{42}	1.00e-04	k_{77}	2.00e-02	k_{112}	1.00e-02
k_8	2.50e-05	k_{43}	5.00e-04	k_{78}	2.00e-01	k_{113}	1.00e-03
k_9	3.00e-04	k_{44}	5.00e-04	k_{79}	1.00e-02	k_{114}	1.00e-04
k_{10}	5.00e-04	k_{45}	5.00e-05	k_{80}	4.00e-02	k_{115}	1.00e-02
k_{11}	5.00e-04	k_{46}	2.50e-03	k_{81}	1.00e-03	k_{116}	1.00e+00
k_{12}	2.00e-04	k_{47}	2.50e-03	k_{82}	5.00e-02	k_{117}	1.00e+00
k_{13}	5.00e-04	k_{48}	2.50e-03	k_{83}	5.00e-03	k_{118}	1.00e-02
k_{14}	7.50e-03	k_{49}	4.00e-02	k_{84}	1.00e-03	k_{119}	1.00e+00
k_{15}	5.00e-03	k_{50}	2.50e-03	k_{85}	5.00e-03	k_{120}	1.00e+02
k_{16}	5.00e-03	k_{51}	5.00e-08	k_{86}	5.00e-04	k_{121}	1.00e+00
k_{17}	5.00e-02	k_{52}	5.00e-07	k_{87}	1.00e+00	k_{122}	5.00e-03
k_{18}	5.00e-04	k_{53}	5.00e-05	k_{88}	1.00e+00	k_{123}	1.00e-02
k_{19}	5.00e-03	k_{54}	1.00e-02	k_{89}	1.00e-03	k_{124}	1.00e-02
k_{20}	5.00e-04	k_{55}	5.00e-08	k_{90}	5.00e-04	k_{125}	5.00e-03
k_{21}	5.00e-05	k_{56}	5.00e-05	k_{91}	2.00e-02	k_{126}	5.00e-03
k_{22}	6.00e-03	k_{57}	5.00e-03	k_{92}	5.00e-03	k_{127}	5.00e-03
k_{23}	1.75e-03	k_{58}	5.00e-05	k_{93}	1.25e-03	k_{128}	1.00e-03
k_{24}	2.25e-02	k_{59}	5.00e-04	k_{94}	2.50e-04	k_{129}	3.00e-01
k_{25}	1.75e-04	k_{60}	1.00e-04	k_{95}	5.00e-02	k_{130}	3.00e-06
k_{26}	2.25e-02	k_{61}	7.00e-02	k_{96}	1.00e-04	k_{131}	1.00e-02
k_{27}	1.75e-04	k_{62}	1.00e-03	k_{97}	5.00e-03	k_{132}	5.00e-05
k_{28}	9.00e-04	k_{63}	9.40e-04	k_{98}	5.00e-03	k_{133}	5.00e-04
k_{29}	5.00e-05	k_{64}	2.00e-02	k_{99}	2.00e-04	k_{134}	1.00e-02
k_{30}	2.50e-03	k_{65}	9.50e+00	k_{100}	1.00e-01	k_{135}	5.00e-03
k_{31}	1.75e-04	k_{66}	1.00e+01	k_{101}	1.00e+00	k_{136}	5.00e-03
k_{32}	2.50e-03	k_{67}	5.00e-03	k_{102}	1.00e+00	k_{137}	3.00e-02
k_{33}	1.75e-04	k_{68}	5.00e-02	k_{103}	2.25e-02	DDS	*
k_{34}	5.00e-08	k_{69}	8.00e-04	k_{104}	1.75e-04		
k_{35}	5.00e-02	k_{70}	6.00e+00	k_{105}	5.00e-02		

* The values of DDS were as follows: 0 (no-damage), 0.002 (low-damage), 0.004 (medium-damage), 0.008 (high-damage), and 0.016 (excess-damage).

A.3 Mass balance equations of the ODE mathematical model (Iwamoto et al., 2011)

Table A.3 Mass balance equations of ODE mathematical model

dY_1/dt	$= k_1 + k_4Y_6 - (k_2 + k_3Y_4)Y_1$
dY_2/dt	$= k_5Y_{22} + k_8Y_7 - (k_6 + k_7Y_5)Y_2$
dY_3/dt	$= k_9Y_{41} + k_{130}Y_{22} + k_{12}Y_9 + k_{75}Y_{32} - (k_{10} + k_{11}Y_5 + k_{126}Y_{49} + k_{127}Y_{51})Y_3$
dY_4/dt	$= k_4Y_6 + k_{13}Y_6 - k_3Y_1Y_4$
dY_5/dt	$= k_8Y_7 + k_{12}Y_9 + k_{14}Y_{10}(Y_{49} + Y_{51}) + k_{15}Y_9(Y_{49} + Y_{51}) + k_{16}Y_7 + k_{17}Y_8Y_8 - (k_7Y_2 + k_{11}Y_3)Y_5$
dY_6/dt	$= k_3Y_1Y_4 + k_{19}Y_{16} + k_{21}Y_{12} - (k_4 + k_{13} + k_{18}Y_{15} + k_{20}Y_{11} + k_{44}Y_{19})Y_6$
dY_7/dt	$= k_7Y_2Y_5 + k_{23}Y_8 - (k_8 + k_{22}Y_{29} + k_{16})Y_7$
dY_8/dt	$= k_{22}Y_7Y_{29} + k_{25}Y_{13} + k_{27}Y_{17} - (k_{23} + k_{24}Y_{11} + k_{26}Y_{15} + k_{17}Y_8)Y_8$
dY_9/dt	$= k_{11}Y_3Y_5 + k_{29}Y_{10} - (k_{12} + k_{28}Y_{29} + k_{15}(Y_{49} + Y_{51}))Y_9$
dY_{10}/dt	$= k_{28}Y_9Y_{29} + k_{31}Y_{14} + k_{33}Y_{18} - (k_{29} + k_{30}Y_{11} + k_{32}Y_{15} + k_{14}(Y_{49} + Y_{51}))Y_{10}$
dY_{11}/dt	$= k_{34} + k_{21}Y_{12} + k_{25}Y_{13} + k_{31}Y_{14} - (k_{35}Y_8 + k_{36}Y_{10} + k_{20}Y_6 + k_{24}Y_8 + k_{30}Y_{10})Y_{11}$
dY_{12}/dt	$= k_{20}Y_6Y_{11} - k_{21}Y_{12}$
dY_{13}/dt	$= k_{24}Y_8Y_{11} - k_{25}Y_{13}$
dY_{14}/dt	$= k_{30}Y_{10}Y_{11} - k_{31}Y_{14}$
dY_{15}/dt	$= k_{37} + k_{38}Y_{25} + k_{19}Y_{16} + k_{27}Y_{17} + k_{33}Y_{18} + k_{104}Y_{39} - (k_{39} + k_{18}Y_6 + k_{26}Y_8 + k_{32}Y_{10} + k_{103}Y_{53})Y_{15}$
dY_{16}/dt	$= k_{18}Y_6Y_{15} - k_{19}Y_{16}$
dY_{17}/dt	$= k_{26}Y_8Y_{15} - k_{27}Y_{17}$
dY_{18}/dt	$= k_{32}Y_{10}Y_{15} - k_{33}Y_{18}$
dY_{19}/dt	$= k_{40} + k_{41}/(I + k_{42}Y_{24}) - (k_{43} + k_{44}Y_6)Y_{19}$
dY_{20}/dt	$= k_{45}Y_{22}Y_{24} - (k_{46}Y_6 + k_{47}Y_{12} + k_{48}Y_{16})Y_{20}$
dY_{21}/dt	$= k_{46}Y_6Y_{20} + k_{47}Y_{12}Y_{20} + k_{48}Y_{16}Y_{20} - (k_{49}Y_8 + k_{50}Y_{10})Y_{21}$
dY_{22}/dt	$= k_{49}Y_8Y_{21} + k_{50}Y_{10}Y_{21} + k_{51}Y_{22} + k_{52} - (k_{45}Y_{24} + k_{53} + k_{54}Y_{10})Y_{22}$
dY_{23}/dt	$= k_{49}Y_8Y_{21} + k_{50}Y_{10}Y_{21} - k_{55}Y_{23}$
dY_{24}/dt	$= k_{56} + k_{58}/(I + k_{59}Y_{19}) + k_{55}Y_{23} - (k_{57} + k_{45}Y_{22})Y_{24}$
dY_{25}/dt	$= k_{60} + k_{61}Y_{27} - (deg(t)Y_{26} + k_{62})Y_{25}$
dY_{26}/dt	$= k_{63} + (k_{66}Im^{50})/(k_{65}^{50} + Im^{50}) - k_{64}Y_{26}$
dY_{27}/dt	$= k_{78}sig(t) - k_{79}Y_{27}$
dY_{28}/dt	$= k_{80}Y_{22} + k_{85}Y_{29} - (k_{81}Y_{31} + k_{82}(Y_8 + Y_{10}) + k_{83})Y_{28}$
dY_{29}/dt	$= k_{82}(Y_8 + Y_{10})Y_{28} - (k_{84}Y_{31} + k_{85} + k_{86})Y_{29}$
dY_{30}/dt	$= k_{87}Y_{31} - k_{88}Y_{27}Y_{30}$
dY_{31}/dt	$= k_{88}Y_{27}Y_{30} - k_{87}Y_{31}$
dY_{32}/dt	$= k_{89}Y_{10} - k_{90}Y_{32}$
dY_{33}/dt	$= k_{91}Y_{32} + k_{94}Y_{35} - (k_{92} + k_{93}Y_{34} + k_{128}Y_{49} + k_{129}Y_{51})Y_{33}$
dY_{34}/dt	$= k_{94}Y_{35} + k_{97}Y_{35}(Y_{49} + Y_{51}) + k_{98}Y_{36}(Y_{49} + Y_{51}) - k_{93}Y_{33}Y_{34}$
dY_{35}/dt	$= k_{93}Y_{33}Y_{34} + k_{96}Y_{36} - (k_{94} + k_{95}(Y_{43} + Y_{45}) + k_{97}(Y_{49} + Y_{51}))Y_{35}$
dY_{36}/dt	$= k_{95}(Y_{43} + Y_{45})Y_{35} + k_{132}Y_{53} - (k_{96} + k_{98}(Y_{49} + Y_{51}) + k_{131}Y_{36})Y_{36}$
dY_{37}/dt	$= k_{99} + k_{101}Y_{38} - k_{100}Y_{53}Y_{37}$
dY_{38}/dt	$= k_{100}Y_{53}Y_{37} - (k_{101} + k_{102})Y_{38}$
dY_{39}/dt	$= k_{103}Y_{53}Y_{15} - k_{104}Y_{39}$
dY_{40}/dt	$= k_{105}Y_{22} - k_{106}Y_{10}Y_{40}$
dY_{41}/dt	$= k_{106}Y_{10}Y_{40} - k_{107}Y_{41}$
dY_{42}/dt	$= k_{108} + k_{109}Y_{43} - (k_{110}(Y_{36} + Y_{53}) + k_{111}Y_{31})Y_{42}$

dY_{43}/dt	$= k_{110}(Y_{36} + Y_{53})Y_{42} + k_{112}Y_{45} - (k_{109}Y_{43} + k_{113}Y_{31} + k_{114})Y_{43}$
dY_{44}/dt	$= k_{111}Y_{31}Y_{42} + k_{115}Y_{45} - (k_{116}(Y_{36} + Y_{53}) + k_{120}Y_{46})Y_{44}$
dY_{45}/dt	$= k_{113}Y_{31}Y_{43} + k_{116}(Y_{36} + Y_{53})Y_{44} - (k_{115} + k_{112})Y_{45}$
dY_{46}/dt	$= k_{117} + k_{118}Y_{25} - (k_{119} + k_{120}Y_{44})Y_{46}$
dY_{47}/dt	$= k_{120}Y_{44}Y_{46} - k_{121}Y_{47}$
dY_{48}/dt	$= k_{122}Y_{49}Y_{51} - k_{123}Y_{48}Y_{53}$
dY_{49}/dt	$= k_{123}Y_{48}Y_{53} - k_{122}Y_{49}Y_{51}$
dY_{50}/dt	$= k_{124}Y_{51}(Y_{53} + Y_{10}) - k_{125}Y_{50}$
dY_{51}/dt	$= k_{125}Y_{50} - k_{124}Y_{51}(Y_{53} + Y_{10})$
dY_{52}/dt	$= k_{133}Y_{53}Y_{37} - (k_{134}(Y_{43} + Y_{45}) + k_{136}(Y_{49} + Y_{51}))Y_{52}$
dY_{53}/dt	$= k_{131}Y_{36}Y_{36} + k_{134}(Y_{43} + Y_{45})Y_{52} + k_{104}Y_{39} - (k_{132} + k_{133}Y_{37} + k_{135}Y_{49} + k_{137}Y_{51} + k_{103}Y_{15})Y_{53}$
dIm/dt	$= k_{70}Y_{25}sig(t)/(1 + k_{71}Y_{25}Y_{26}) - k_{67}Im$
$sig(t)$	$= DDS \times exp(-k_{72} \times time)$
$deg(t)$	$= k_{76} - k_{74} \times (sig(t) - DDS \times exp(-k_{77} \times DDS \times time))$

Abbreviations are shown in Table A.1.

Appendix B

Initial conditions, kinetic parameters and mass balance equations of the ODE mathematical model for the DNA damage signalling pathway and G1/S checkpoint used as the basis for the current study

B.1 Initial conditions of the mathematical model used as the basis for the current study

Table B.1 Initial conditions of the mathematical model used as the basis for the current study

<i>Chemical species</i>	<i>Initial value</i>	<i>Chemical species</i>	<i>Initial value</i>	<i>Chemical species</i>	<i>Initial value</i>
<i>Y1</i>	<i>3.00e-02</i>	<i>Y13</i>	<i>1.00e+00</i>	<i>Y25</i>	<i>2.65e-02</i>
<i>Y2</i>	<i>1.00e-03</i>	<i>Y14</i>	<i>1.00e-04</i>	<i>Y26</i>	<i>2.35e-04</i>
<i>Y3</i>	<i>4.00e-05</i>	<i>Y15</i>	<i>0</i>	<i>Y27</i>	<i>0</i>
<i>Y4</i>	<i>5.00e+00</i>	<i>Y16</i>	<i>0</i>	<i>Y28</i>	<i>1.00e-03</i>
<i>Y5</i>	<i>1.50e+01</i>	<i>Y17</i>	<i>0</i>	<i>Y29</i>	<i>1.00e-04</i>
<i>Y6</i>	<i>7.50e+00</i>	<i>Y18</i>	<i>0</i>	<i>Y30</i>	<i>9.90e-01</i>
<i>Y7</i>	<i>1.00e-03</i>	<i>Y19</i>	<i>1.00e-03</i>	<i>Y31</i>	<i>1.00e-02</i>
<i>Y8</i>	<i>1.00e-03</i>	<i>Y20</i>	<i>1.95e+00</i>	<i>Y32</i>	<i>0</i>
<i>Y9</i>	<i>4.00e-04</i>	<i>Y21</i>	<i>1.00e-03</i>	<i>Y33</i>	<i>0</i>
<i>Y10</i>	<i>1.00e-04</i>	<i>Y22</i>	<i>0</i>	<i>Y34</i>	<i>0</i>
<i>Y11</i>	<i>1.40e+01</i>	<i>Y23</i>	<i>1.00e-02</i>	<i>Im</i>	<i>0</i>
<i>Y12</i>	<i>1.00e-03</i>	<i>Y24</i>	<i>5.00e-02</i>		

Abbreviations are as follows: Y1: CycD, Y2: CycE, Y3: CycA, Y4: Cdk4, Y5: Cdk2, Y6: CycD/Cdk4, Y7: CycE/Cdk2, Y8: CycE/Cdk2-P, Y9: CycA/Cdk2, Y10: CycA/Cdk2-P, Y11: p27, Y12: p27/CycD/Cdk4, Y13: p27/CycE/Cdk2-P, Y14: p27/CycA/Cdk2-P, Y15: p21, Y16: p21/CycD/Cdk4, Y17: p21/CycE/Cdk2-P, Y18: p21/CycA/Cdk2-P, Y19: p16, Y20: Rb/E2F, Y21: Rb-PP/E2F, Y22: E2F, Y23: Rb-PPP, Y24: Rb, Y25: p53, Y26: Mdm2, Y27: ATM/ATR, Y28: Cdc25A, Y29: Cdc25A-P, Y30: Chk1, Y31: Chk1-P, Y32: NF-Y, Y33: B-Myb, Y34: B-Myb-P, Im: Intermediate, DDS: DNA damage signal.

B.2 Kinetic parameters of the ODE mathematical model used as the basis for the current study

Table B.2 Kinetic parameters of the ODE mathematical model used as the basis for the current study

Kinetic parameter	Value	Kinetic parameter	Value	Kinetic parameter	Value	Kinetic parameter	Value
k_1	$5.00e-04$	k_{25}	$1.75e-04$	k_{49}	$4.00e-02$	k_{73}	$2.00e-03$
k_2	$5.00e-04$	k_{26}	$2.25e-02$	k_{50}	$2.50e-03$	k_{74}	$7.72e-01$
k_3	$5.00e-03$	k_{27}	$1.75e-04$	k_{51}	$5.00e-08$	k_{75}	$1.00e-05$
k_4	$2.50e-03$	k_{28}	$9.00e-04$	k_{52}	$5.00e-07$	k_{76}	$5.56e-02$
k_5	$1.00e-01$	k_{29}	$5.00e-05$	k_{53}	$5.00e-05$	k_{77}	$2.00e-02$
k_6	$2.50e-03$	k_{30}	$2.50e-03$	k_{54}	$1.00e-02$	k_{78}	$2.00e-01$
k_7	$2.50e-03$	k_{31}	$1.75e-04$	k_{55}	$5.00e-08$	k_{79}	$1.00e-02$
k_8	$2.50e-05$	k_{32}	$2.50e-03$	k_{56}	$5.00e-05$	k_{80}	$4.00e-02$
k_9	$3.00e-04$	k_{33}	$1.75e-04$	k_{57}	$5.00e-03$	k_{81}	$1.00e-03$
k_{10}	$5.00e-04$	k_{34}	$5.00e-08$	k_{58}	$5.00e-05$	k_{82}	$5.00e-02$
k_{11}	$5.00e-04$	k_{35}	$5.00e-02$	k_{59}	$5.00e-04$	k_{83}	$5.00e-03$
k_{12}	$2.00e-04$	k_{36}	$1.50e-03$	k_{60}	$1.00e-04$	k_{84}	$1.00e-03$
k_{13}	$5.00e-04$	k_{37}	$5.00e-05$	k_{61}	$7.00e-02$	k_{85}	$5.00e-03$
k_{14}	$7.50e-03$	k_{38}	$1.00e-03$	k_{62}	$1.00e-03$	k_{86}	$5.00e-04$
k_{15}	$5.00e-03$	k_{39}	$5.00e-03$	k_{63}	$9.40e-04$	k_{87}	$1.00e+00$
k_{16}	$5.00e-03$	k_{40}	$2.00e-03$	k_{64}	$2.00e-02$	k_{88}	$1.00e+00$
k_{17}	$5.00e-02$	k_{41}	$5.00e-05$	k_{65}	$9.50e+00$	k_{89}	$1.00e-03$
k_{18}	$5.00e-04$	k_{42}	$1.00e-04$	k_{66}	$1.00e+01$	k_{90}	$5.00e-04$
k_{19}	$5.00e-03$	k_{43}	$5.00e-04$	k_{67}	$5.00e-03$	k_{91}	$5.00e-03$
k_{20}	$5.00e-04$	k_{44}	$5.00e-04$	k_{68}	$5.00e-02$	k_{92}	$3.00e-06$
k_{21}	$5.00e-05$	k_{45}	$5.00e-05$	k_{69}	$5.00e-02$	DDS	*
k_{22}	$6.00e-03$	k_{46}	$2.50e-03$	k_{70}	$6.00e+00$		
k_{23}	$1.75e-03$	k_{47}	$2.50e-03$	k_{71}	$4.00e-03$		
k_{24}	$2.25e-02$	k_{48}	$2.50e-03$	k_{72}	$1.00e-08$		

* The values of DDS were as follows: 0 (no-damage), 0.002 (low-damage), 0.004 (medium-damage), 0.008 (high-damage), and 0.016 (excess-damage).

B.3 Biochemical meaning of the kinetic parameters of the G1/S base model

Table B.3 Biochemical meaning of the kinetic parameters of the G1/S base model

<i>Parameter</i>	<i>Biochemical Meaning</i>
<i>K1</i>	<i>Synthesis rate of CycD</i>
<i>K2</i>	<i>Degradation rate of CycD</i>
<i>K3</i>	<i>Association rate of CycD/CDK4</i>
<i>K4</i>	<i>Dissociation rate of CycD/CDK4</i>
<i>K5</i>	<i>Synthesis rate of CycE through E2F</i>
<i>K6</i>	<i>Degradation rate of CycE</i>
<i>K7</i>	<i>Association rate of CycE/CDK2</i>
<i>K8</i>	<i>Dissociation rate of CycE/CDK2</i>
<i>K9</i>	<i>Synthesis rate of CycA through B-Myb-P</i>
<i>K10</i>	<i>Degradation rate of CycA</i>
<i>K11</i>	<i>Association rate of CycA/CDK2</i>
<i>K12</i>	<i>Dissociation rate of CycA/CDK2</i>
<i>K13</i>	<i>Rate of CDK4 production through CycD/CDK4</i>
<i>K14</i>	<i>Rate of CDK2 production through CycA/CDK2-P</i>
<i>K15</i>	<i>Rate of CDK2 production through CycA/CDK2</i>
<i>K16</i>	<i>Rate of CDK2 production through CycE/CDK2</i>
<i>K17</i>	<i>Rate of CDK2 production through CycE/CDK2-P</i>
<i>K18</i>	<i>Association rate of p21/CycD/CDK4</i>
<i>K19</i>	<i>Disassociation rate of p21/CycD/CDK4</i>
<i>K20</i>	<i>Association rate of p27/CycD/CDK4</i>
<i>K21</i>	<i>Disassociation rate of p27/CycD/CDK4</i>
<i>K22</i>	<i>Phosphorylation rate of CycE/CDK2 to form CycE/CDK2-P</i>
<i>K23</i>	<i>De-phosphorylation rate of CycE/CDK2-P to form CycE/CDK2</i>
<i>K24</i>	<i>Association rate of p27/CycE/CDK2-P</i>
<i>K25</i>	<i>Disassociation rate of p27/CycE/CDK2-P</i>
<i>K26</i>	<i>Association rate of p21/CycE/CDK2-P</i>
<i>K27</i>	<i>Disassociation rate of p21/CycE/CDK2-P</i>
<i>K28</i>	<i>Phosphorylation rate of CycA/CDK2 to form CycA/CDK2-P</i>
<i>K29</i>	<i>De-phosphorylation rate of CycA/CDK2-P to form CycA/CDK2</i>
<i>K30</i>	<i>Association rate of p27/CycA/CDK2-P</i>
<i>K31</i>	<i>Disassociation rate of p27/CycA/CDK2-P</i>
<i>K32</i>	<i>Association rate of p21/CycA/CDK2-P</i>
<i>K33</i>	<i>Disassociation rate of p21/CycA/CDK2-P</i>
<i>K34</i>	<i>Synthesis rate of p27</i>
<i>K35</i>	<i>Association rate of p27/CycE/CDK2-P</i>
<i>K36</i>	<i>Association rate of p27/CycA/CDK2-P</i>
<i>K37</i>	<i>Synthesis rate of p21</i>
<i>K38</i>	<i>Rate of synthesis of p21 through p53</i>
<i>K39</i>	<i>Degradation rate of p21</i>
<i>K40</i>	<i>Synthesis rate of p16</i>
<i>K41</i>	<i>Constant as influx or precursor</i>
<i>K42</i>	<i>Rate of inhibition of synthesis p16 by Rb</i>
<i>K43</i>	<i>Degradation rate of p16</i>

K44	<i>Degradation rate of p16 by CycD/CDK4</i>
K45	<i>Association rate of Rb/E2F</i>
K46	<i>Phosphorylation rate of Rb/E2F to form Rb-PP/E2F through CycD/CDK4</i>
K47	<i>Phosphorylation rate of Rb/E2F to form Rb-PP/E2F through p27/CycD/CDK4</i>
K48	<i>Phosphorylation rate of Rb/E2F to form Rb-PP/E2F through p21/CycD/CDK4</i>
K49	<i>Rate of activation of E2F by CycE/CDK2-P</i>
K50	<i>Rate of activation of E2F by CycA/CDK2-P</i>
K51	<i>Rate of synthesis of E2F promoted by itself</i>
K52	<i>Synthesis rate of E2F</i>
K53	<i>Degradation rate of E2F</i>
K54	<i>Rate of E2F degradation by CycA/CDK2-P</i>
K55	<i>De-phosphorylation rate of Rb-PPP to Rb</i>
K56	<i>Synthesis rate of Rb</i>
K57	<i>Degradation rate of Rb</i>
K58	<i>Constant as influxes or precursor</i>
K59	<i>Rate of inhibition of synthesis Rb by p16</i>
K60	<i>Synthesis rate of p53</i>
K61	<i>Rate of synthesis of p53 through ATM/ATR</i>
K62	<i>Degradation rate of p53</i>
K63	<i>Synthesis rate of Mdm2</i>
K64	<i>Degradation rate of Mdm2</i>
K65	<i>Dissociation constant in the Hill function</i>
K66	<i>Rate of synthesis of Mdm2 through Im</i>
K67	<i>Degradation rate of Im</i>
K68	<i>Synthesis rate of B-Myb through E2F</i>
K69	<i>Phosphorylation rate of B-Myb to form B-Myb-P through CycA/Cdk2-P</i>
K70	<i>Rate of p53's sequence-specific DNA binding activity by DNA-damage signal</i>
K71	<i>Association rate of p53 and Mdm2</i>
K72	<i>Rate of DNA-damage repair</i>
K73	<i>Degradation rate of B-Myb-P</i>
K74	<i>Rate of inhibition of degradation of p53 and/or Mdm2 by DNA-damage signal</i>
K75	<i>Synthesis rate of CycA through NF-Y</i>
K76	<i>Strength rate of Mdm2's ability to promote p53 degradation</i>
K77	<i>Rate of inhibition of Mdm2-mediated p53 degradation under the initial damage signal</i>
K78	<i>Rate of synthesis of ATM/ATR through DNA-damage signal</i>
K79	<i>Degradation rate of ATM/ATR</i>
K80	<i>Rate of Cdc25A production through E2F</i>
K81	<i>Degradation rate of Cdc25A through Chk1-P</i>
K82	<i>Phosphorylation rate of Cdc25A to form Cdc25A-P through CycA/Cdk2-P and CycA/Cdk2-P</i>
K83	<i>Degradation rate of Cdc25A</i>
K84	<i>Degradation rate of Cdc25A-P through Chk1-P</i>
K85	<i>De-phosphorylation rate of Cdc25A-P to form Cdc25A through CycE/Cdk2 to be CycE/Cdk2-P</i>
K86	<i>De-phosphorylation rate of Cdc25A-P to form Cdc25A through CycA/Cdk2 to be CycA/Cdk2-P</i>
K87	<i>De-phosphorylation rate of Chk1-P to form Chk1</i>

<i>K88</i>	<i>Phosphorylation rate of Chk1 to form Chk1-P</i>
<i>K89</i>	<i>Synthesis rate of NF-Y through CycA/Cdk2-P</i>
<i>K90</i>	<i>Degradation rate of NF-Y</i>
<i>K91</i>	<i>Degradation rate of CycA</i>
<i>K92</i>	<i>Synthesis rate of CycA through E2F</i>

B.4 Mass balance equations of the ODE mathematical model used as the basis for the current study

Table B.4 Mass balance equations of the ODE mathematical model used as the basis for the current study

<i>CycD</i>	$dY_1/dt = k_1 + k_4Y_6 - (k_2 + k_3Y_4)Y_1$
<i>CycE</i>	$dY_2/dt = k_5Y_{22} + k_8Y_7 - (k_6 + k_7Y_5)Y_2$
<i>CycA</i>	$dY_3/dt = k_9Y_{34} + k_{92}Y_{22} + k_{12}Y_9 + k_{75}Y_{32} - (k_{10} + k_{11}Y_5 + k_{91})Y_3$
<i>Cdk4</i>	$dY_4/dt = k_4Y_6 + k_{13}Y_6 - k_3Y_1Y_4$
<i>Cdk2</i>	$dY_5/dt = k_8Y_7 + k_{12}Y_9 + k_{14}Y_{10} + k_{15}Y_9 + k_{16}Y_7 + k_{17}Y_8Y_8 - (k_7Y_2 + k_{11}Y_3)Y_5$
<i>CycD/Cdk4</i>	$dY_6/dt = k_3Y_1Y_4 + k_{19}Y_{16} + k_{21}Y_{12} - (k_4 + k_{13} + k_{18}Y_{15} + k_{20}Y_{11} + k_{44}Y_{19})Y_6$
<i>CycE/Cdk2</i>	$dY_7/dt = k_7Y_2Y_5 + k_{23}Y_8 - (k_8 + k_{22}Y_{29} + k_{16})Y_7$
<i>CycE/Cdk2-P</i>	$dY_8/dt = k_{22}Y_7Y_{29} + k_{25}Y_{13} + k_{27}Y_{17} - (k_{23} + k_{24}Y_{11} + k_{26}Y_{15} + k_{17}Y_8)Y_8$
<i>CycA/Cdk2</i>	$dY_9/dt = k_{11}Y_3Y_5 + k_{29}Y_{10} - (k_{12} + k_{28}Y_{29} + k_{15})Y_9$
<i>CycA/Cdk2-P</i>	$dY_{10}/dt = k_{28}Y_9Y_{29} + k_{31}Y_{14} + k_{33}Y_{18} - (k_{29} + k_{30}Y_{11} + k_{32}Y_{15} + k_{14})Y_{10}$
<i>p27</i>	$dY_{11}/dt = k_{34} + k_{21}Y_{12} + k_{25}Y_{13} + k_{31}Y_{14} - (k_{35}Y_8 + k_{36}Y_{10} + k_{20}Y_6 + k_{24}Y_8 + k_{30}Y_{10})Y_{11}$
<i>p27/CycD/Cdk4</i>	$dY_{12}/dt = k_{20}Y_6Y_{11} - k_{21}Y_{12}$
<i>p27/CycE/Cdk2-P</i>	$dY_{13}/dt = k_{24}Y_8Y_{11} - k_{25}Y_{13}$
<i>p27/CycA/Cdk2-P</i>	$dY_{14}/dt = k_{30}Y_{10}Y_{11} - k_{31}Y_{14}$
<i>p21</i>	$dY_{15}/dt = k_{37} + k_{38}Y_{25} + k_{19}Y_{16} + k_{27}Y_{17} + k_{33}Y_{18} - (k_{39} + k_{18}Y_6 + k_{26}Y_8 + k_{32}Y_{10})Y_{15}$
<i>p21/CycD/Cdk4</i>	$dY_{16}/dt = k_{18}Y_6Y_{15} - k_{19}Y_{16}$
<i>p21/CycE/Cdk2-P</i>	$dY_{17}/dt = k_{26}Y_8Y_{15} - k_{27}Y_{17}$
<i>p21/CycA/Cdk2-P</i>	$dY_{18}/dt = k_{32}Y_{10}Y_{15} - k_{33}Y_{18}$
<i>p16</i>	$dY_{19}/dt = k_{40} + k_{41}/(1 + k_{42}Y_{24}) - (k_{43} + k_{44}Y_6)Y_{19}$
<i>Rb/E2F</i>	$dY_{20}/dt = k_{45}Y_{22}Y_{24} - (k_{46}Y_6 + k_{47}Y_{12} + k_{48}Y_{16})Y_{20}$
<i>Rb-PP/E2F</i>	$dY_{21}/dt = k_{46}Y_6Y_{20} + k_{47}Y_{12}Y_{20} + k_{48}Y_{16}Y_{20} - (k_{49}Y_8 + k_{50}Y_{10})Y_{21}$
<i>E2F</i>	$dY_{22}/dt = k_{49}Y_8Y_{21} + k_{50}Y_{10}Y_{21} + k_{51}Y_{22} + k_{52} - (k_{45}Y_{24} + k_{53} + k_{54}Y_{10})Y_{22}$
<i>Rb-PPP</i>	$dY_{23}/dt = k_{49}Y_8Y_{21} + k_{50}Y_{10}Y_{21} - k_{55}Y_{23}$
<i>Rb</i>	$dY_{24}/dt = k_{56} + k_{58}/(1 + k_{59}Y_{19}) + k_{55}Y_{23} - (k_{57} + k_{45}Y_{22})Y_{24}$
<i>p53</i>	$dY_{25}/dt = k_{60} + k_{61}Y_{27} - (deg(t)Y_{26} + k_{62})Y_{25}$
<i>Mdm2</i>	$dY_{26}/dt = k_{63} + (k_{66}Im^{50})/(k_{65}^{50} + Im^{50}) - k_{64}Y_{26}$
<i>ATM/ATR</i>	$dY_{27}/dt = k_{78}sig(t) - k_{79}Y_{27}$
<i>Cdc25A</i>	$dY_{28}/dt = k_{80}Y_{22} + k_{85}Y_{29} - (k_{81}Y_{31} + k_{82}(Y_8 + Y_{10}) + k_{83})Y_{28}$
<i>Cdc25A-P</i>	$dY_{29}/dt = k_{82}(Y_8 + Y_{10})Y_{28} - (k_{84}Y_{31} + k_{85} + k_{86})Y_{29}$
<i>Chk1</i>	$dY_{30}/dt = k_{87}Y_{31} - k_{88}Y_{27}Y_{30}$
<i>Chk1-P</i>	$dY_{31}/dt = k_{88}Y_{27}Y_{30} - k_{87}Y_{31}$
<i>NF-Y</i>	$dY_{32}/dt = k_{89}Y_{10} - k_{90}Y_{32}$
<i>B-Myb</i>	$dY_{33}/dt = k_{68}Y_{22} - k_{69}Y_{10}Y_{33}$
<i>B-Myb-P</i>	$dY_{34}/dt = k_{69}Y_{10}Y_{33} - k_{73}Y_{34}$
<i>Im</i>	$dIm/dt = k_{70}Y_{25}sig(t)/(1 + k_{71}Y_{25}Y_{26}) - k_{67}Im$
<i>Sig</i>	$sig(t) = DDS \times \exp(-k_{72} \times time)$
<i>Deg</i>	$deg(t) = k_{76} - k_{74} \times (sig(t) - DDS \times \exp(-k_{77} \times DDS \times time))$

Abbreviations are shown in Table B.1.

Appendix C

Initial conditions, lump nodes, partial elements, kinetic parameters and mass balance equations of the reduced model (level-1)

C.1 Initial conditions of the reduced model (level-1)

Table C.1 Initial conditions of the reduced model (level-1)

<i>Chemical species</i>	<i>Initial value</i>	<i>Chemical species</i>	<i>Initial value</i>	<i>Chemical species</i>	<i>Initial value</i>
<i>F1</i>	$7.53E+00$	<i>Y14</i>	$1.00e-04$	<i>Y25</i>	$2.65e-02$
<i>F2</i>	$2.00E-03$	<i>Y15</i>	0	<i>Y26</i>	$2.35e-04$
<i>F3</i>	$4.40E-04$	<i>Y16</i>	0	<i>Y27</i>	0
<i>Y4</i>	$5.00e+00$	<i>Y17</i>	0	<i>F5</i>	$1.10E-03$
<i>Y5</i>	$1.50e+01$	<i>Y18</i>	0	<i>F6</i>	$1.00E+00$
<i>Y8</i>	$1.00e-03$	<i>Y19</i>	$1.00e-03$	<i>Y32</i>	0
<i>Y10</i>	$1.00e-04$	<i>Y20</i>	$1.95e+00$	<i>F7</i>	0
<i>Y11</i>	$1.40e+01$	<i>Y21</i>	$1.00e-03$	<i>Im</i>	0
<i>Y12</i>	$1.00e-03$	<i>Y22</i>	0		
<i>Y13</i>	$1.00e+00$	<i>F4</i>	$6.00E-02$		

Abbreviations are as follows: F1: (CycD, CycD/Cdk4), F2: (CycE, CycE/Cdk2), F3: (CycA, CycA/Cdk2), Y4: Cdk4, Y5: Cdk2, Y8: CycE/Cdk2-P, Y10: CycA/Cdk2-P, Y11: p27, Y12: p27/CycD/Cdk4, Y13: p27/CycE/Cdk2-P, Y14: p27/CycA/Cdk2-P, Y15: p21, Y16: p21/CycD/Cdk4, Y17: p21/CycE/Cdk2-P, Y18: p21/CycA/Cdk2-P, Y19: p16, Y20: Rb/E2F, Y21: Rb-PP/E2F, Y22: E2F, F4: (Rb-PPP, Rb), Y25: p53, Y26: Mdm2, Y27: ATM/ATR, F5: (Cdc25A, Cdc25A-P), F6: (Chk1, Chk1-P), Y32: NF-Y, F7: (B-Myb, B-Myb-P), Im: Intermediate, DDS: DNA damage signal.

C.2 Lump node composition of the reduced model (level-1)

Table C.2 Lump composition of the reduced model (level-1)

<i>Lump node</i>	<i>Value</i>
<i>F1</i>	$= Y1 + Y6$
<i>F2</i>	$= Y2 + Y7$
<i>F3</i>	$= Y3 + Y9$
<i>F4</i>	$= Y23 + Y24$
<i>F5</i>	$= Y28 + Y29$
<i>F6</i>	$= Y30 + Y31$
<i>F7</i>	$= Y33 + Y34$

C.3 Initial conditions of the reduced model (level-1) for partial elements

Table C.3 Initial conditions of the lumped nodes in the reduced model (level-1)

<i>Chemical species</i>	<i>Initial value</i>	<i>Chemical species</i>	<i>Initial value</i>	<i>Chemical species</i>	<i>Initial value</i>
Y_{1p}	3.98E-03	Y_{9p}	9.09E-01	Y_{30p}	9.90E-01
Y_{6p}	9.96E-01	Y_{23p}	1.67E-01	Y_{31p}	1.00E-02
Y_{2p}	5.00E-01	Y_{24p}	8.33E-01	Y_{33p}	0.00E+00
Y_{7p}	5.00E-01	Y_{28p}	9.09E-01	Y_{34p}	0.00E+00
Y_{3p}	9.09E-02	Y_{29p}	9.09E-02		

C.4 Kinetic parameters of the reduced model (level-1)

Table C.4 Kinetic parameters of the reduced model (level-1)

<i>Kinetic parameter</i>	<i>Value</i>	<i>Kinetic parameter</i>	<i>Value</i>	<i>Kinetic parameter</i>	<i>Value</i>	<i>Kinetic parameter</i>	<i>Value</i>
$B1$	4.59E-04	$B23$	1.75E-03	$B45$	1.22E-05	$B67$	5.00E-03
$B2$	4.29E-04	$B24$	2.25E-02	$B46$	2.14E-03	$B68$	5.00E-02
$B3$	7.11E-04	$B25$	1.75E-04	$B47$	2.50E-03	$B69$	5.00E-02
$B4$	2.14E-03	$B26$	2.25E-02	$B48$	2.50E-03	$B70$	6.00E+00
$B5$	1.00E-01	$B27$	1.75E-04	$B49$	4.00E-02	$B71$	4.00E-03
$B6$	4.38E-04	$B28$	5.63E-04	$B50$	2.50E-03	$B72$	1.00E-08
$B7$	4.38E-04	$B29$	5.00E-05	$B51$	5.00E-08	$B73$	1.00E-04
$B8$	2.06E-05	$B30$	2.50E-03	$B52$	5.00E-07	$B74$	7.72E-01
$B9$	5.00E-09	$B31$	1.75E-04	$B53$	5.00E-05	$B75$	1.00E-05
$B10$	1.71E-03	$B32$	2.50E-03	$B54$	1.00E-02	$B76$	5.56E-02
$B11$	1.42E-04	$B33$	1.75E-04	$B55$	5.00E-05	$B77$	2.00E-02
$B12$	1.38E-04	$B34$	5.00E-08	$B56$	3.00E-06	$B78$	2.00E-01
$B13$	2.70E-03	$B35$	5.00E-02	$B57$	6.00E-04	$B79$	1.00E-02
$B14$	7.50E-03	$B36$	1.50E-03	$B58$	5.00E-05	$B80$	4.00E-02
$B15$	3.45E-03	$B37$	5.00E-05	$B59$	5.00E-04	$B81$	1.00E-03*
$B16$	4.12E-03	$B38$	1.00E-03	$B60$	1.00E-04	$B82$	4.55E-02
$B17$	5.00E-02	$B39$	5.00E-03	$B61$	7.00E-02	$B83$	4.60E-03
$B18$	4.29E-04	$B40$	2.00E-03	$B62$	1.00E-03	$B84$	5.00E-04
$B19$	5.00E-03	$B41$	5.00E-05	$B63$	9.40E-04	$B85$	1.00E-03
$B20$	4.29E-04	$B42$	5.00E-10	$B64$	2.00E-02	$B86$	4.53E-05
$B21$	5.00E-05	$B43$	5.00E-04	$B65$	9.50E+00	DDS	**
$B22$	4.48E-04	$B44$	4.29E-04	$B66$	1.00E+01		

* If DDS <> 0 Then B81= 5.00E-05 else B81= 1.00E-03.

** The values of DDS were as follows: 0 (no-damage), 0.002 (low-damage), 0.004 (medium-damage), 0.008 (high-damage), and 0.016 (excess-damage).

C.5 Mass balance equations of the reduced model (level-1)

Table C.5 Mass balance equations of the reduced model (level-1)

<i>Cdk4</i>	$dY_4/dt = (B_4+B_2)F_1 - B_3F_1Y_4$
<i>Cdk2</i>	$dY_5/dt = (B_8+B_{16})F_2 + (B_{12}+B_{15})F_3 + B_{14}Y_{10} + B_{17}Y_8Y_8 - (B_7F_2 + B_{11}F_3)Y_5$
<i>F1</i>	$dF_1/dt = B_1 + (B_3dY_4)F_1 + B_{19}Y_{16} + B_{21}Y_{12} - (B_2 + B_{18}Y_{15} + B_{20}Y_{11} + B_{44}Y_{19})F_1$
<i>F2</i>	$dF_2/dt = B_5Y_{22} + B_7F_2dY_5 + B_{23}Y_8 - (B_6 + B_{22}F_5 + B_{16})F_2$
<i>aCycE/Cdk2</i>	$dY_8/dt = B_{22}F_2F_5 + B_{25}Y_{13} + B_{27}Y_{17} - (B_{23} + B_{24}Y_{11} + B_{26}Y_{15} + B_{17}Y_8)Y_8$
<i>F3</i>	$dF_3/dt = B_9F_7 + B_{56}Y_{22} + B_{11}F_3dY_5 + B_{75}Y_{32} + B_{29}Y_{10} - (B_{10} + B_{28}F_5 + B_{15})F_3$
<i>aCycA/Cdk2</i>	$dY_{10}/dt = B_{28}F_3F_5 + B_{31}Y_{14} + B_{33}Y_{18} - (B_{29} + B_{30}Y_{11} + B_{32}Y_{15} + B_{14})Y_{10}$
<i>p27</i>	$dY_{11}/dt = B_{34} + B_{21}Y_{12} + B_{25}Y_{13} + B_{31}Y_{14} - ((B_{35}+B_{24})Y_8 + (B_{36}+B_{30})Y_{10} + B_{20}F_1)Y_{11}$
<i>p27/CycD/Cdk4</i>	$dY_{12}/dt = B_{20}F_1Y_{11} - B_{21}Y_{12}$
<i>p27/CycE/Cdk2-P</i>	$dY_{13}/dt = B_{24}Y_8Y_{11} - B_{25}Y_{13}$
<i>p27/CycA/Cdk2-P</i>	$dY_{14}/dt = B_{30}Y_{10}Y_{11} - B_{31}Y_{14}$
<i>p21</i>	$dY_{15}/dt = B_{37} + B_{38}Y_{25} + B_{19}Y_{16} + B_{27}Y_{17} + B_{33}Y_{18} - (B_{39} + B_{18}F_1 + B_{26}Y_8 + B_{32}Y_{10})Y_{15}$
<i>p21/CycD/Cdk4</i>	$dY_{16}/dt = B_{18}F_1Y_{15} - B_{19}Y_{16}$
<i>p21/CycE/Cdk2-P</i>	$dY_{17}/dt = B_{26}Y_8Y_{15} - B_{27}Y_{17}$
<i>p21/CycA/Cdk2-P</i>	$dY_{18}/dt = B_{32}Y_{10}Y_{15} - B_{33}Y_{18}$
<i>p16</i>	$dY_{19}/dt = B_{40} + B_{41}/(1 + B_{42}F_4) - (B_{43} + B_{44}F_1)Y_{19}$
<i>Rb/E2F</i>	$dY_{20}/dt = B_{45}Y_{22}F_4 - (B_{46}F_1 + B_{47}Y_{12} + B_{48}Y_{16})Y_{20}$
<i>Rb-PP/E2F</i>	$dY_{21}/dt = B_{46}F_1Y_{20} + B_{47}Y_{12}Y_{20} + B_{48}Y_{16}Y_{20} - (B_{49}Y_8 + B_{50}Y_{10})Y_{21}$
<i>E2F</i>	$dY_{22}/dt = B_{49}Y_8Y_{21} + B_{50}Y_{10}Y_{21} + B_{51}Y_{22} + B_{52} - (B_{45}F_4 + B_{53} + B_{54}Y_{10})Y_{22}$
<i>F4</i>	$dF_4/dt = B_{55} + B_{49}Y_8Y_{21} + B_{50}Y_{10}Y_{21} + B_{58}/(1 + B_{59}Y_{19}) - (B_{57} + B_{45}Y_{22})F_4$
<i>p53</i>	$dY_{25}/dt = B_{60} + B_{61}Y_{27} - (deg(t)Y_{26} + B_{62})Y_{25}$
<i>Mdm2</i>	$dY_{26}/dt = B_{63} + (B_{66}Im^{50})/(B_{65}^{50} + Im^{50}) - B_{64}Y_{26}$
<i>ATM/ATR</i>	$dY_{27}/dt = B_{78}sig(t) - B_{79}Y_{27}$
<i>F5</i>	$dF_5/dt = B_{80}Y_{22} + B_{82}(Y_8 + Y_{10})dF_5 - B_{83} - (B_{81}F_6)F_5$
<i>F6</i>	$dF_6/dt = -B_{13}Y_{27}F_6$
<i>NF-Y</i>	$dY_{32}/dt = B_{85}Y_{10} - B_{84}Y_{32}$
<i>F7</i>	$dF_7/dt = B_{68}Y_{22} + B_{69}Y_{10}dF_7 - B_{73}F_7$
<i>Im</i>	$dIm/dt = B_{70}Y_{25}sig(t)/(1 + B_{71}Y_{25}Y_{26}) - B_{67}Im$
<i>Sig</i>	$sig(t) = DDS \times \exp(-B_{72} \times time)$
<i>Deg</i>	$deg(t) = B_{76} - B_{74} \times (sig(t) - DDS \times \exp(-B_{77} \times DDS \times time))$

Abbreviations are shown in Table C.1.

Appendix D

Initial conditions, lump nodes, partial elements, kinetic parameters and mass balance equations of the reduced model (level-2)

D.1 Initial conditions of the reduced model (level-2)

Table D.1 Initial conditions of the reduced model (level-2)

<i>Chemical species</i>	<i>Initial value</i>	<i>Chemical species</i>	<i>Initial value</i>	<i>Chemical species</i>	<i>Initial value</i>
<i>F8</i>	$7.53E+00$	<i>Y13</i>	$1.00e+00$	<i>Y25</i>	$2.65e-02$
<i>F2</i>	$2.00E-03$	<i>Y14</i>	$1.00e-04$	<i>Y26</i>	$2.35e-04$
<i>F3</i>	$4.40E-04$	<i>Y15</i>	0	<i>Y27</i>	0
<i>Y4</i>	$5.00e+00$	<i>Y17</i>	0	<i>F5</i>	$1.10E-03$
<i>Y5</i>	$1.50e+01$	<i>Y18</i>	0	<i>F6</i>	$1.00E+00$
<i>Y8</i>	$1.00e-03$	<i>Y19</i>	$1.00e-03$	<i>Y32</i>	0
<i>Y10</i>	$1.00e-04$	<i>Y20</i>	$1.95e+00$	<i>F7</i>	0
<i>Y11</i>	$1.40e+01$	<i>Y22</i>	0	<i>Im</i>	0
<i>Y12</i>	$1.00e-03$	<i>F9</i>	$6.10E-02$		

Abbreviations are as follows: F8: (CycD, CycD/Cdk4, p21/CycD/Cdk4), F2: (CycE, CycE/Cdk2), F3: (CycA, CycA/Cdk2), Y4: Cdk4, Y5: Cdk2, Y8: CycE/Cdk2-P, Y10: CycA/Cdk2-P, Y11: p27, Y12: p27/CycD/Cdk4, Y13: p27/CycE/Cdk2-P, Y14: p27/CycA/Cdk2-P, Y15: p21, Y17: p21/CycE/Cdk2-P, Y18: p21/CycA/Cdk2-P, Y19: p16, Y20: Rb/E2F, Y22: E2F, F9: (Rb-PP/E2F, Rb-PPP, Rb), Y25: p53, Y26: Mdm2, Y27: ATM/ATR, F5: (Cdc25A, Cdc25A-P), F6: (Chk1, Chk1-P), Y32: NF-Y, F7: (B-Myb, B-Myb-P), Im: Intermediate, DDS: DNA damage signal.

D.2 Lump node composition of the reduced model (level-2)

Table D.2 Lump node composition of the reduced model (level-2)

<i>Lump node</i>	<i>Value</i>
<i>F8</i>	$= Y1 + Y6 + Y16$
<i>F2</i>	$= Y2 + Y7$
<i>F3</i>	$= Y3 + Y9$
<i>F9</i>	$= Y21 + Y23 + Y24$
<i>F5</i>	$= Y28 + Y29$
<i>F6</i>	$= Y30 + Y31$
<i>F7</i>	$= Y33 + Y34$

D.3 Initial conditions of the reduced model (level-2) for partial elements

Table D.3. Initial conditions of the lumped nodes in the reduced model (level-2)

<i>Chemical species</i>	<i>Initial value</i>	<i>Chemical species</i>	<i>Initial value</i>	<i>Chemical species</i>	<i>Initial value</i>
Y_{1p}	3.98E-03	Y_{9p}	9.09E-01	Y_{30p}	9.90E-01
Y_{6p}	9.96E-01	Y_{21p}	1.64E-02	Y_{31p}	1.00E-02
Y_{16p}	0.00E+00	Y_{23p}	1.64E-01	Y_{33p}	0.00E+00
Y_{2p}	5.00E-01	Y_{24p}	8.20E-01	Y_{34p}	0.00E+00
Y_{7p}	5.00E-01	Y_{28p}	9.09E-01		
Y_{3p}	9.09E-02	Y_{29p}	9.09E-02		

D.4 Kinetic parameters of the reduced model (level-2)

Table D.4. Kinetic parameters of the reduced model (level-2)

<i>Kinetic parameter</i>	<i>Value</i>	<i>Kinetic parameter</i>	<i>Value</i>	<i>Kinetic parameter</i>	<i>Value</i>	<i>Kinetic parameter</i>	<i>Value</i>
C1	4.59E-04	C22	4.48E-04	C43	5.00E-04	C64	2.00E-02
C2	4.29E-04	C23	1.75E-03	C44	4.29E-04	C65	9.50E+00
C3	7.11E-04	C24	2.25E-02	C45	1.58E-06	C66	1.00E+01
C4	2.14E-03	C25	1.75E-04	C46	2.14E-03	C67	5.00E-03
C5	1.00E-01	C26	2.25E-02	C47	2.50E-03	C68	5.00E-02
C6	4.38E-04	C27	1.75E-04	C48	1.00E-03	C69	5.00E-02
C7	4.38E-04	C28	8.44E-04	C49	3.48E-02	C70	6.00E+00
C8	2.06E-05	C29	5.00E-05	C50	2.18E-03	C71	4.00E-03
C9	5.00E-09	C30	2.50E-03	C51	5.00E-08	C72	1.00E-08
C10	1.71E-03	C31	1.75E-04	C52	5.00E-07	C73	1.00E-04
C11	1.42E-04	C32	2.50E-03	C53	5.00E-05	C74	7.72E-01
C12	1.38E-04	C33	1.75E-04	C54	1.00E-02	C75	1.00E-05
C13	2.70E-03	C34	5.00E-08	C55	5.00E-05	C76	5.56E-02
C14	7.50E-03	C35	5.00E-02	C56	3.00E-06	C77	2.00E-02
C15	3.45E-03	C36	1.50E-03	C57	7.80E-05	C78	2.00E-01
C16	4.12E-03	C37	5.00E-05	C58	5.00E-05	C79	1.00E-02
C17	5.00E-02	C38	1.00E-03	C59	5.00E-04	C80	4.00E-02
C18	4.29E-04	C39	5.00E-03	C60	1.00E-04	C81	1.00E-03*
C19	5.00E-04	C40	2.00E-03	C61	7.00E-02	C82	4.55E-02
C20	4.29E-04	C41	5.00E-05	C62	1.00E-03	C83	4.60E-03
C21	5.00E-05	C42	6.47E-11	C63	9.40E-04	DDS	**

* If DDS <> 0 Then C81= 5.00E-05 else C81= 1.00E-03.

** The values of DDS were as follows: 0 (No-damage), 0.002 (Low-damage), 0.004 (Medium-damage), 0.008 (High-damage), and 0.016 (Excess-damage).

D.5 Mass balance equations of the reduced model (level-2)

Table D.5. Mass balance equations of the reduced model (level-2)

<i>Cdk4</i>	$dY_4/dt = (C_4 + C_2)F_8 - C_3F_8Y_4$
<i>Cdk2</i>	$dY_5/dt = (C_8 + C_{16})F_2 + (C_{12} + C_{15})F_3 + C_{14}Y_{10} + C_{17}Y_8Y_8 - (C_7F_2 + C_{11}F_3)Y_5$
<i>F8</i>	$dF_8/dt = C_1 + (C_3dY_4)F_8 + C_{21}Y_{12} - (C_2 + C_{18}dY_{15} + C_{20}Y_{11} + C_{44}Y_{19})F_8$
<i>F2</i>	$dF_2/dt = C_5Y_{22} + C_7F_2dY_5 + C_{23}Y_8 - (C_6 + C_{22}F_5 + C_{16})F_2$
<i>aCycE/Cdk2</i>	$dY_8/dt = C_{22}F_2F_5 + C_{25}Y_{13} + C_{27}Y_{17} - (C_{23} + C_{24}Y_{11} + C_{26}Y_{15} + C_{17}Y_8)Y_8$
<i>F3</i>	$dF_3/dt = C_9F_7 + C_{56}Y_{22} + C_{11}F_3dY_5 + C_{75}Y_{32} + C_{29}Y_{10} - (C_{10} + C_{28}F_5 + C_{15})F_3$
<i>aCycA/Cdk2</i>	$dY_{10}/dt = C_{28}F_3F_5 + C_{31}Y_{14} + C_{33}Y_{18} - (C_{29} + C_{30}Y_{11} + C_{32}Y_{15} + C_{14})Y_{10}$
<i>p27</i>	$dY_{11}/dt = C_{34} + C_{21}Y_{12} + C_{25}Y_{13} + C_{31}Y_{14} - ((C_{35} + C_{24})Y_8 + (C_{36} + C_{30})Y_{10} + C_{20}F_8)Y_{11}$
<i>p27/CycD/Cdk4</i>	$dY_{12}/dt = C_{20}F_8Y_{11} - C_{21}Y_{12}$
<i>p27/CycE/Cdk2-P</i>	$dY_{13}/dt = C_{24}Y_8Y_{11} - C_{25}Y_{13}$
<i>p27/CycA/Cdk2-P</i>	$dY_{14}/dt = C_{30}Y_{10}Y_{11} - C_{31}Y_{14}$
<i>p21</i>	$dY_{15}/dt = C_{37} + C_{38}Y_{25} + C_{27}Y_{17} + C_{33}Y_{18} - (C_{39} + C_{18}F_8 + C_{26}Y_8 + C_{32}Y_{10})Y_{15}$
<i>p21/CycE/Cdk2-P</i>	$dY_{17}/dt = C_{26}Y_8Y_{15} - C_{27}Y_{17}$
<i>p21/CycA/Cdk2-P</i>	$dY_{18}/dt = C_{32}Y_{10}Y_{15} - C_{33}Y_{18}$
<i>p16</i>	$dY_{19}/dt = C_{40} + C_{41}/(I + C_{42}F_9) - (C_{43} + C_{44}F_8)Y_{19}$
<i>Rb/E2F</i>	$dY_{20}/dt = C_{45}Y_{22}F_9 - (C_{46}F_8 + C_{47}Y_{12})Y_{20}$
<i>E2F</i>	$dY_{22}/dt = C_{49}Y_8F_9 + C_{50}Y_{10}F_9 + C_{51}Y_{22} + C_{52} - (C_{45}F_9 + C_{53} + C_{54}Y_{10})Y_{22}$
<i>F9</i>	$dF_9/dt = C_{55} + C_{46}F_8Y_{20} + C_{47}Y_{12}Y_{20} + C_{58}/(I + C_{59}Y_{19}) - (C_{57} + C_{45}Y_{22} + C_{49}dY_8 + C_{50}dY_{10})F_9$
<i>p53</i>	$dY_{25}/dt = C_{60} + C_{61}Y_{27} - (deg(t)Y_{26} + C_{62})Y_{25}$
<i>Mdm2</i>	$dY_{26}/dt = C_{63} + (C_{66}Im^{50})/(C_{65}^{50} + Im^{50}) - C_{64}Y_{26}$
<i>ATM/ATR</i>	$dY_{27}/dt = C_{78}sig(t) - C_{79}Y_{27}$
<i>F5</i>	$dF_5/dt = C_{80}Y_{22} + C_{82}(Y_8 + Y_{10})dF_5 - C_{83} - (C_{81}F_6)F_5$
<i>F6</i>	$dF_6/dt = -C_{13}Y_{27}F_6$
<i>NF-Y</i>	$dY_{32}/dt = C_{48}Y_{10} - C_{19}Y_{32}$
<i>F7</i>	$dF_7/dt = C_{68}Y_{22} + C_{69}Y_{10}dF_7 - C_{73}F_7$
<i>Im</i>	$dIm/dt = C_{70}Y_{25}sig(t)/(I + C_{71}Y_{25}Y_{26}) - C_{67}Im$
<i>Sig</i>	$sig(t) = DDS \times \exp(-C_{72} \times time)$
<i>Deg</i>	$deg(t) = C_{76} - C_{74} \times (sig(t) - DDS \times \exp(-C_{77} \times DDS \times time))$

Abbreviations are shown in Table D.1.

Appendix E

Initial conditions, lump nodes, partial elements, kinetic parameters and mass balance equations of the reduced model (level-3)

E.1 Initial conditions of the reduced model (level-3)

Table E.1 Initial conditions of the reduced model (level-3)

<i>Chemical species</i>	<i>Initial value</i>	<i>Chemical species</i>	<i>Initial value</i>	<i>Chemical species</i>	<i>Initial value</i>
<i>F8</i>	<i>7.53E+00</i>	<i>Y12</i>	<i>1.00e-03</i>	<i>Y25</i>	<i>2.65e-02</i>
<i>F2</i>	<i>2.00E-03</i>	<i>Y13</i>	<i>1.00e+00</i>	<i>Y26</i>	<i>2.35e-04</i>
<i>F10</i>	<i>5.40E-04</i>	<i>Y15</i>	<i>0</i>	<i>Y27</i>	<i>0</i>
<i>Y4</i>	<i>5.00e+00</i>	<i>Y17</i>	<i>0</i>	<i>F5</i>	<i>1.10E-03</i>
<i>Y5</i>	<i>1.50e+01</i>	<i>Y19</i>	<i>1.00e-03</i>	<i>F6</i>	<i>1.00E+00</i>
<i>Y8</i>	<i>1.00e-03</i>	<i>Y20</i>	<i>1.95e+00</i>	<i>Y32</i>	<i>0</i>
<i>Y10</i>	<i>1.00e-04</i>	<i>Y22</i>	<i>0</i>	<i>F7</i>	<i>0</i>
<i>Y11</i>	<i>1.40e+01</i>	<i>F9</i>	<i>6.10E-02</i>	<i>Im</i>	<i>0</i>

Abbreviations are as follows: F8: (CycD, CycD/Cdk4, p21/CycD/Cdk4), F2: (CycE, CycE/Cdk2), F10: (CycA, CycA/Cdk2, p27/CycA/Cdk2-P, p21/CycA/Cdk2-P), Y4: Cdk4, Y5: Cdk2, Y8: CycE/Cdk2-P, Y10: CycA/Cdk2-P, Y11: p27, Y12: p27/CycD/Cdk4, Y13: p27/CycE/Cdk2-P, Y15: p21, Y17: p21/CycE/Cdk2-P, Y19: p16, Y20: Rb/E2F, Y22: E2F, F9: (Rb-PP/E2F, Rb-PPP, Rb), Y25: p53, Y26: Mdm2, Y27: ATM/ATR, F5: (Cdc25A, Cdc25A-P), F6: (Chk1, Chk1-P), Y32: NF-Y, F7: (B-Myb, B-Myb-P), Im: Intermediate, DDS: DNA damage signal.

E.2 Lump node composition of the reduced model (level-3)

Table E.2 Lump node composition of the reduced model (level-3)

<i>Lump node</i>	<i>Value</i>
<i>F8</i>	$= Y1 + Y6 + Y16$
<i>F2</i>	$= Y2 + Y7$
<i>F10</i>	$= Y3 + Y9 + Y14 + Y18$
<i>F9</i>	$= Y21 + Y23 + Y24$
<i>F5</i>	$= Y28 + Y29$
<i>F6</i>	$= Y30 + Y31$
<i>F7</i>	$= Y33 + Y34$

E.3 Initial conditions of the lumped nodes in the reduced model (level-3)

Table E.3 Initial conditions of the lumped nodes in the reduced model (level-3)

<i>Chemical species</i>	<i>Initial value</i>	<i>Chemical species</i>	<i>Initial value</i>	<i>Chemical species</i>	<i>Initial value</i>
Y_{1p}	3.98E-03	Y_{9p}	7.41E-01	Y_{28p}	9.09E-01
Y_{6p}	9.96E-01	Y_{14p}	1.85E-01	Y_{29p}	9.09E-02
Y_{16p}	0.00E+00	Y_{18p}	0.00E+00	Y_{30p}	9.90E-01
Y_{2p}	5.00E-01	Y_{21p}	1.64E-02	Y_{31p}	1.00E-02
Y_{7p}	5.00E-01	Y_{23p}	1.64E-01	Y_{33p}	0.00E+00
Y_{3p}	7.41E-02	Y_{24p}	8.20E-01	Y_{34p}	0.00E+00

E.4 Kinetic parameters of the reduced model (level-3)

Table E.4 Kinetic parameters of the reduced model (level-3)

<i>Kinetic parameter</i>	<i>Value</i>	<i>Kinetic parameter</i>	<i>Value</i>	<i>Kinetic parameter</i>	<i>Value</i>	<i>Kinetic parameter</i>	<i>Value</i>
D1	4.59E-04	D22	4.48E-04	D43	5.00E-04	D64	2.00E-02
D2	4.29E-04	D23	1.75E-03	D44	4.29E-04	D65	9.50E+00
D3	7.11E-04	D24	2.25E-02	D45	1.58E-06	D66	1.00E+01
D4	2.14E-03	D25	1.75E-04	D46	2.14E-03	D67	5.00E-03
D5	1.00E-01	D26	2.25E-02	D47	2.50E-03	D68	5.00E-02
D6	4.38E-04	D27	1.75E-04	D48	1.00E-03	D69	5.00E-02
D7	4.38E-04	D28	5.63E-05	D49	3.48E-02	D70	6.00E+00
D8	2.06E-05	D29	5.00E-05	D50	2.18E-03	D71	4.00E-03
D9	5.00E-09	D30	2.50E-03	D51	5.00E-08	D72	1.00E-08
D10	1.71E-03	D31	2.00E-04	D52	5.00E-07	D73	1.00E-04
D11	1.42E-04	D32	2.50E-03	D53	5.00E-05	D74	7.72E-01
D12	1.38E-04	D33	4.60E-03	D54	1.00E-02	D75	1.00E-05
D13	2.70E-03	D34	5.00E-08	D55	5.00E-05	D76	5.56E-02
D14	7.50E-03	D35	5.00E-02	D56	3.00E-06	D77	2.00E-02
D15	3.45E-03	D36	1.50E-03	D57	7.80E-05	D78	2.00E-01
D16	4.12E-03	D37	5.00E-05	D58	5.00E-05	D79	1.00E-02
D17	5.00E-02	D38	1.00E-03	D59	5.00E-04	D80	4.00E-02
D18	4.29E-04	D39	5.00E-03	D60	1.00E-04	D81	1.00E-03
D19	5.00E-04	D40	2.00E-03	D61	7.00E-02	D82	4.55E-02
D20	4.29E-04	D41	5.00E-05	D62	1.00E-03	DDS	**
D21	5.00E-05	D42	6.47E-11	D63	9.40E-04		

* If DDS <> 0 Then D81= 5.00E-05 else D81= 1.00E-03.

** The values of DDS were as follows: 0 (no-damage), 0.002 (low-damage), 0.004 (medium-damage), 0.008 (high-damage), and 0.016 (excess-damage).

E.5 Mass balance equations of the reduced model (level-3)

Table E.5 Mass balance equations of the reduced model (level-3)

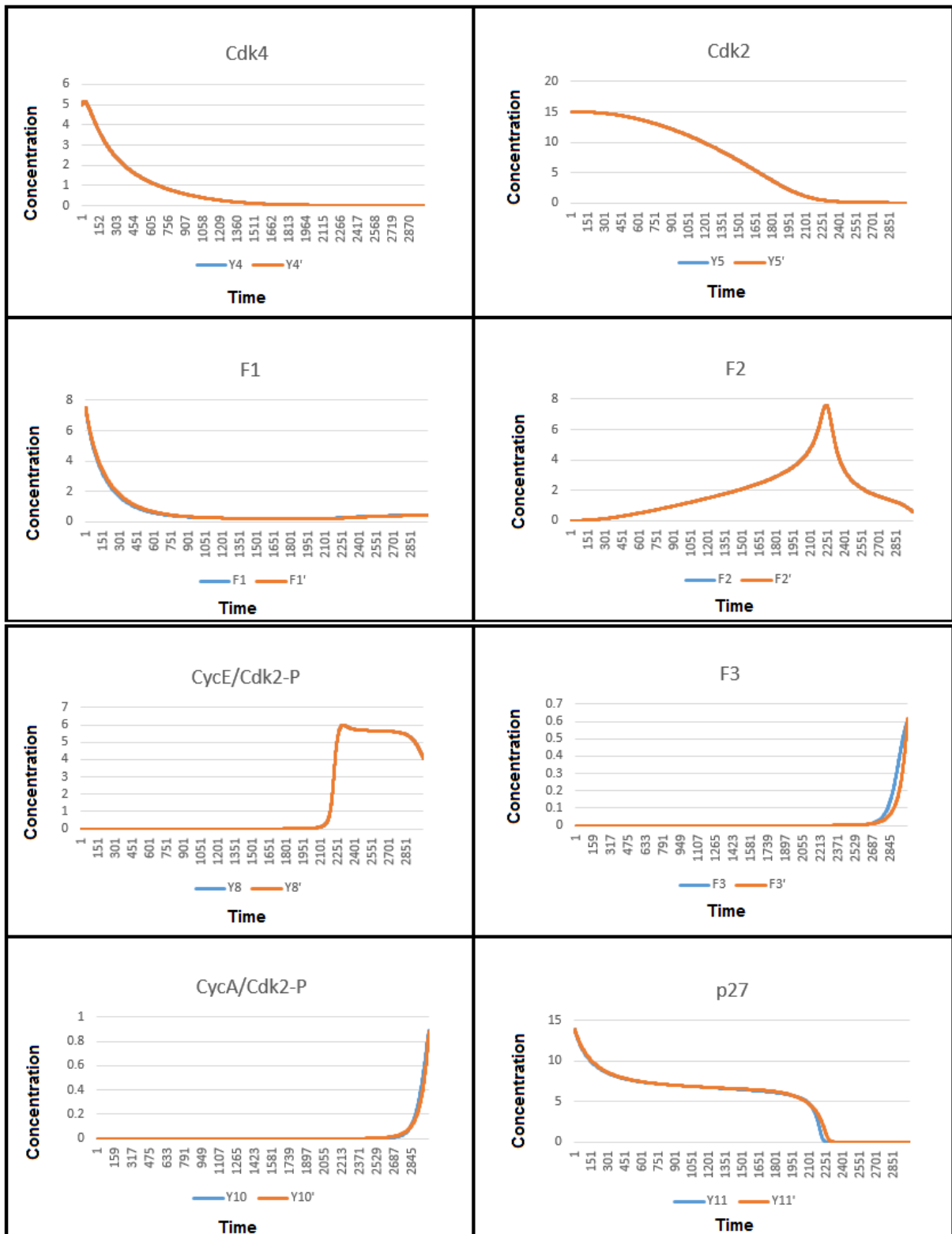
<i>Cdk4</i>	$dY_4/dt = (D_4+D_2)F_8 - D_3F_8Y_4$
<i>Cdk2</i>	$dY_5/dt = (D_8+D_{16})F_2 + (D_{12}+D_{15})F_{10} + D_{14}Y_{10} + D_{17}Y_8Y_8 - (D_7F_2 + D_{11}F_{10})Y_5$
<i>F8</i>	$dF_8/dt = D_1 + (D_3dY_4)F_8 + D_{21}Y_{12} - (D_2 + D_{18}dY_{15} + D_{20}Y_{11} + D_{44}Y_{19})F_8$
<i>F2</i>	$dF_2/dt = D_5Y_{22} + D_7F_2dY_5 + D_{23}Y_8 - (D_6 + D_{22}F_5 + D_{16})F_2$
<i>aCycE/Cdk2</i>	$dY_8/dt = D_{22}F_2F_5 + D_{25}Y_{13} + D_{27}Y_{17} - (D_{23} + D_{24}Y_{11} + D_{26}Y_{15} + D_{17}Y_8)Y_8$
<i>F10</i>	$dF_{10}/dt = D_9F_7 + D_{56}Y_{22} + D_{11}F_{10}dY_5 + D_{75}Y_{32} + D_{29}Y_{10} + D_{30}Y_{10}Y_{11} + D_{32}Y_{10}Y_{15} - (D_{10} + D_{28}F_5 + D_{15} + D_{31})F_{10}$
<i>aCycA/Cdk2</i>	$dY_{10}/dt = D_{28}F_{10}F_5 + D_{31}F_{10} - (D_{29} + D_{30}Y_{11} + D_{32}Y_{15} + D_{14})Y_{10}$
<i>p27</i>	$dY_{11}/dt = D_{34} + D_{21}Y_{12} + D_{25}Y_{13} + D_{31}F_{10} - ((D_{35}+D_{24})Y_8 + (D_{36}+D_{30})Y_{10} + D_{20}F_8)Y_{11}$
<i>p27/CycD/Cdk4</i>	$dY_{12}/dt = D_{20}F_8Y_{11} - D_{21}Y_{12}$
<i>p27/CycE/Cdk2-P</i>	$dY_{13}/dt = D_{24}Y_8Y_{11} - D_{25}Y_{13}$
<i>p21</i>	$dY_{15}/dt = D_{37} + D_{38}Y_{25} + D_{27}Y_{17} + D_{31}F_{10} - (D_{39} + D_{18}F_8 + D_{26}Y_8 + D_{32}Y_{10})Y_{15}$
<i>p21/CycE/Cdk2-P</i>	$dY_{17}/dt = D_{26}Y_8Y_{15} - D_{27}Y_{17}$
<i>p16</i>	$dY_{19}/dt = D_{40} + D_{41}/(1 + D_{42}F_9) - (D_{43} + D_{44}F_8)Y_{19}$
<i>Rb/E2F</i>	$dY_{20}/dt = D_{45}Y_{22}F_9 - (D_{46}F_8 + D_{47}Y_{12})Y_{20}$
<i>E2F</i>	$dY_{22}/dt = D_{49}Y_8F_9 + D_{50}Y_{10}F_9 + D_{51}Y_{22} + D_{52} - (D_{45}F_9 + D_{53} + D_{54}Y_{10})Y_{22}$
<i>F9</i>	$dF_9/dt = D_{55} + D_{46}F_8Y_{20} + D_{47}Y_{12}Y_{20} + D_{58}/(1 + D_{59}Y_{19}) - (D_{57} + D_{45}Y_{22} + D_{49}dY_8 + D_{50}dY_{10})F_9$
<i>p53</i>	$dY_{25}/dt = D_{60} + D_{61}Y_{27} - (deg(t)Y_{26} + D_{62})Y_{25}$
<i>Mdm2</i>	$dY_{26}/dt = D_{63} + (D_{66}Im^{50})/(D_{65}^{50} + Im^{50}) - D_{64}Y_{26}$
<i>ATM/ATR</i>	$dY_{27}/dt = D_{78}sig(t) - D_{79}Y_{27}$
<i>F5</i>	$dF_5/dt = D_{80}Y_{22} + D_{82}(Y_8 + Y_{10})dF_5 - D_{33} - (D_{81}F_6)F_5$
<i>F6</i>	$dF_6/dt = -D_{13}Y_{27}F_6$
<i>NF-Y</i>	$dY_{32}/dt = D_{48}Y_{10} - D_{19}Y_{32}$
<i>F7</i>	$dF_7/dt = D_{68}Y_{22} + D_{69}Y_{10}dF_7 - D_{73}F_7$
<i>Im</i>	$dIm/dt = D_{70}Y_{25}sig(t)/(1 + D_{71}Y_{25}Y_{26}) - D_{67}Im$
<i>Sig</i>	$sig(t) = DDS \times \exp(-D_{72} \times time)$
<i>Deg</i>	$deg(t) = D_{76} - D_{74} \times (sig(t) - DDS \times \exp(-D_{77} \times DDS \times time))$

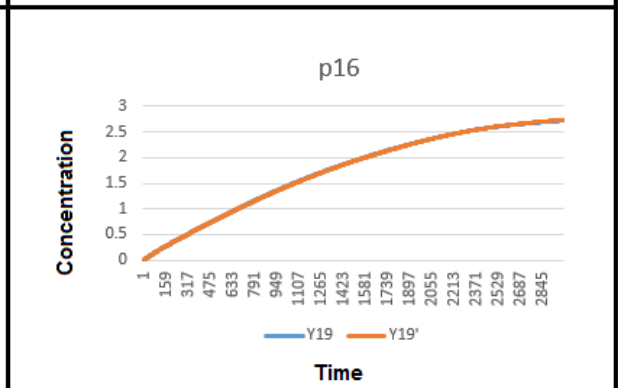
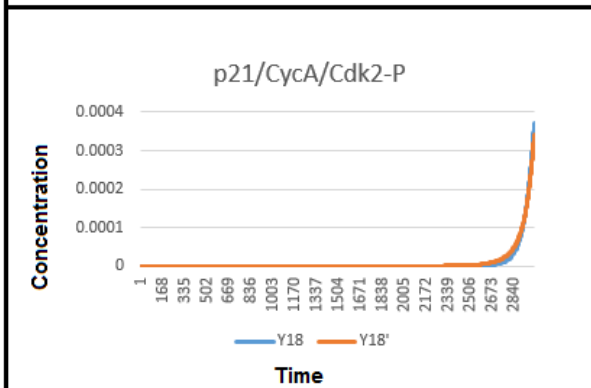
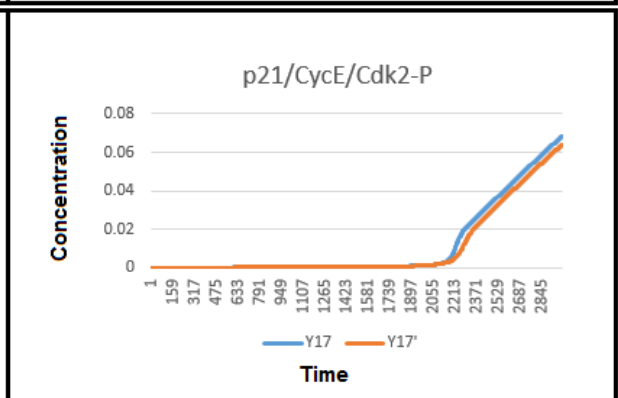
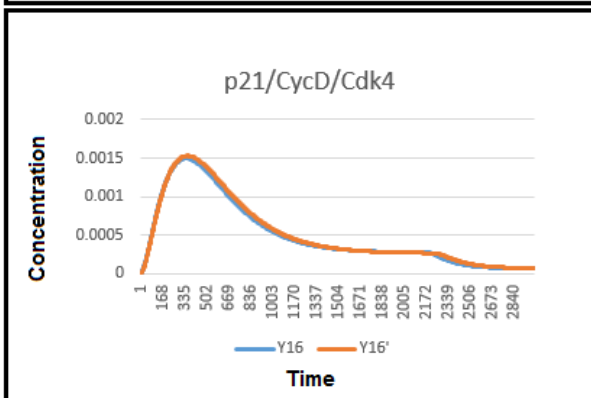
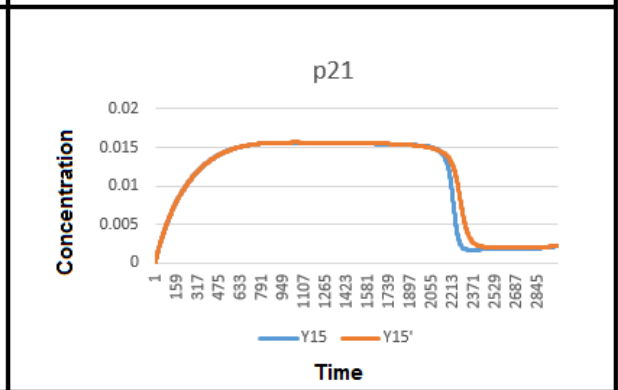
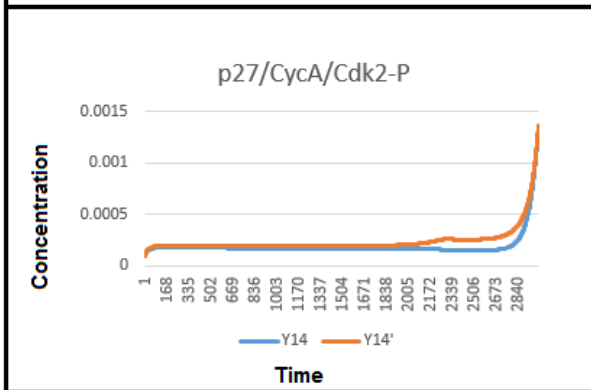
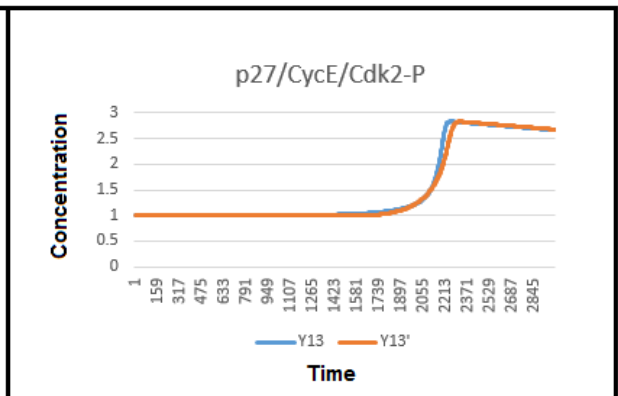
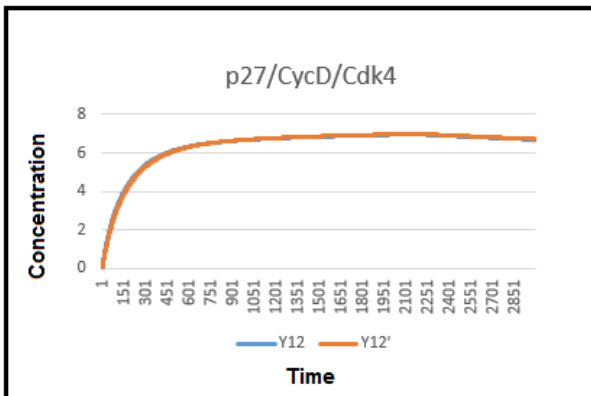
Abbreviations are shown in Table E.1.

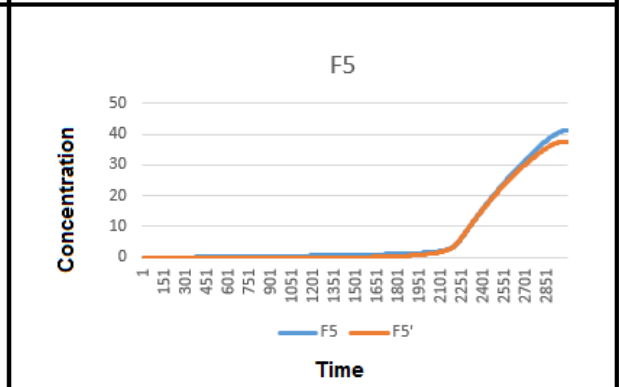
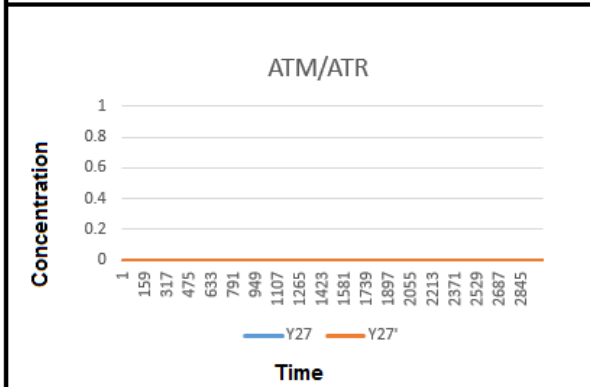
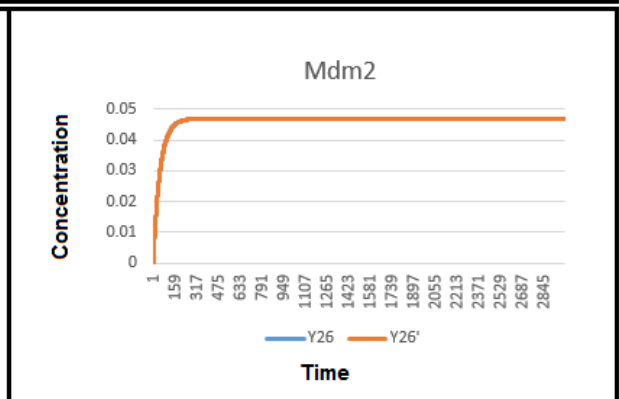
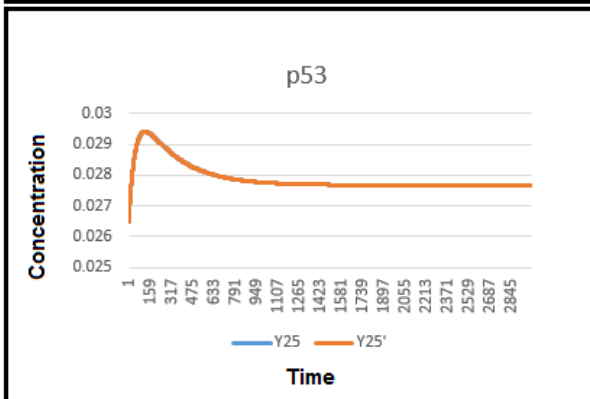
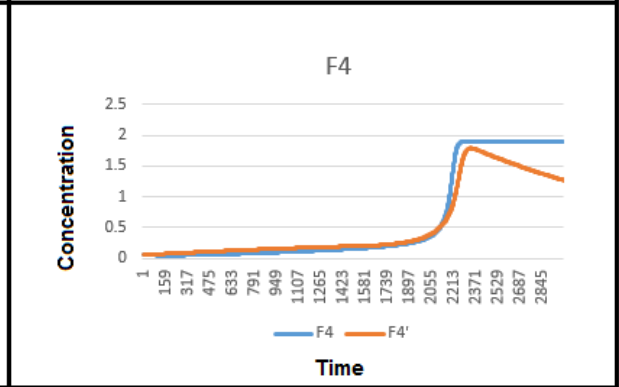
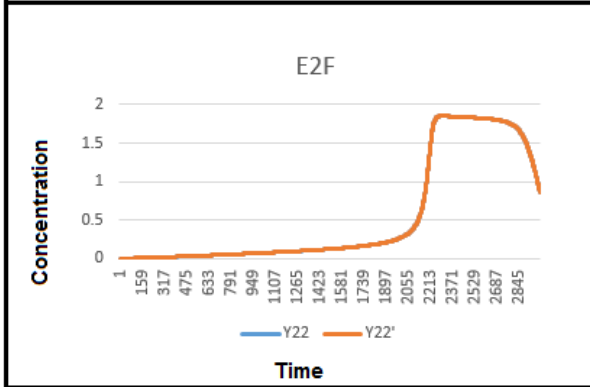
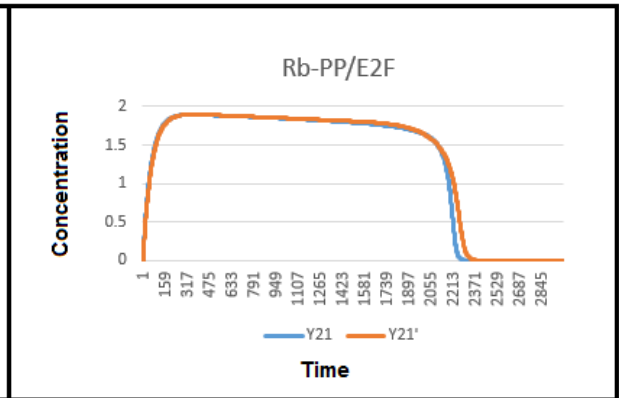
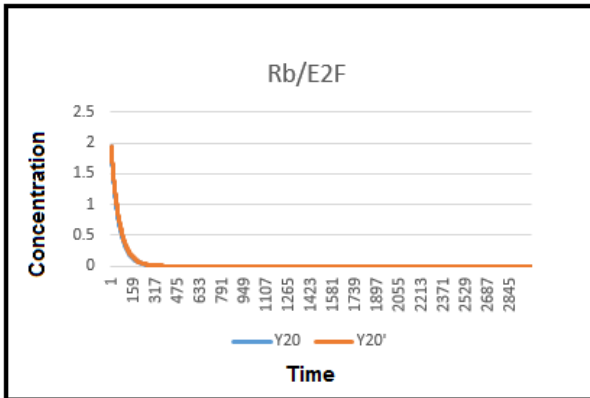
Appendix F

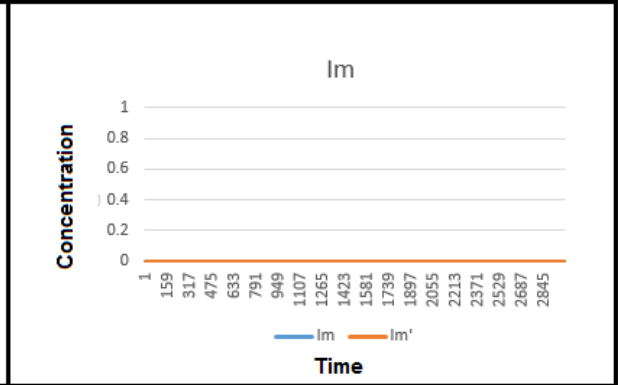
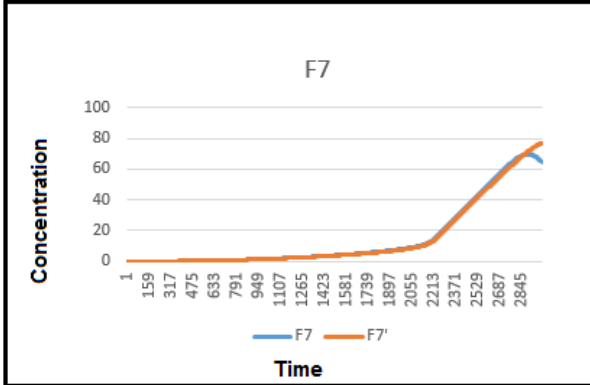
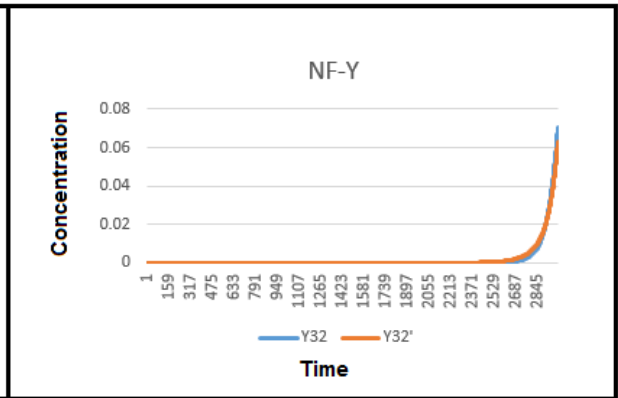
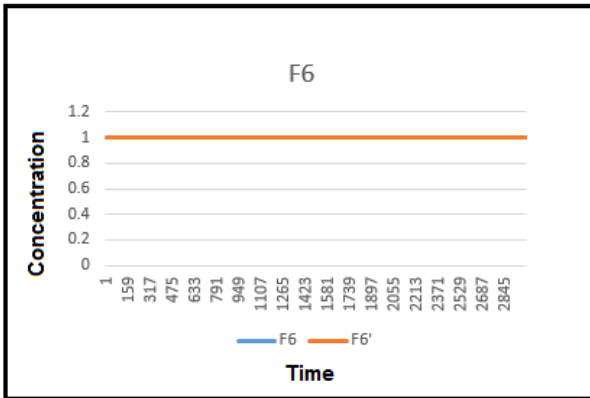
All time courses of the reduced model (level-1) elements

F.1 All time courses of the reduced model (level-1) elements without DNA damage vs the base model

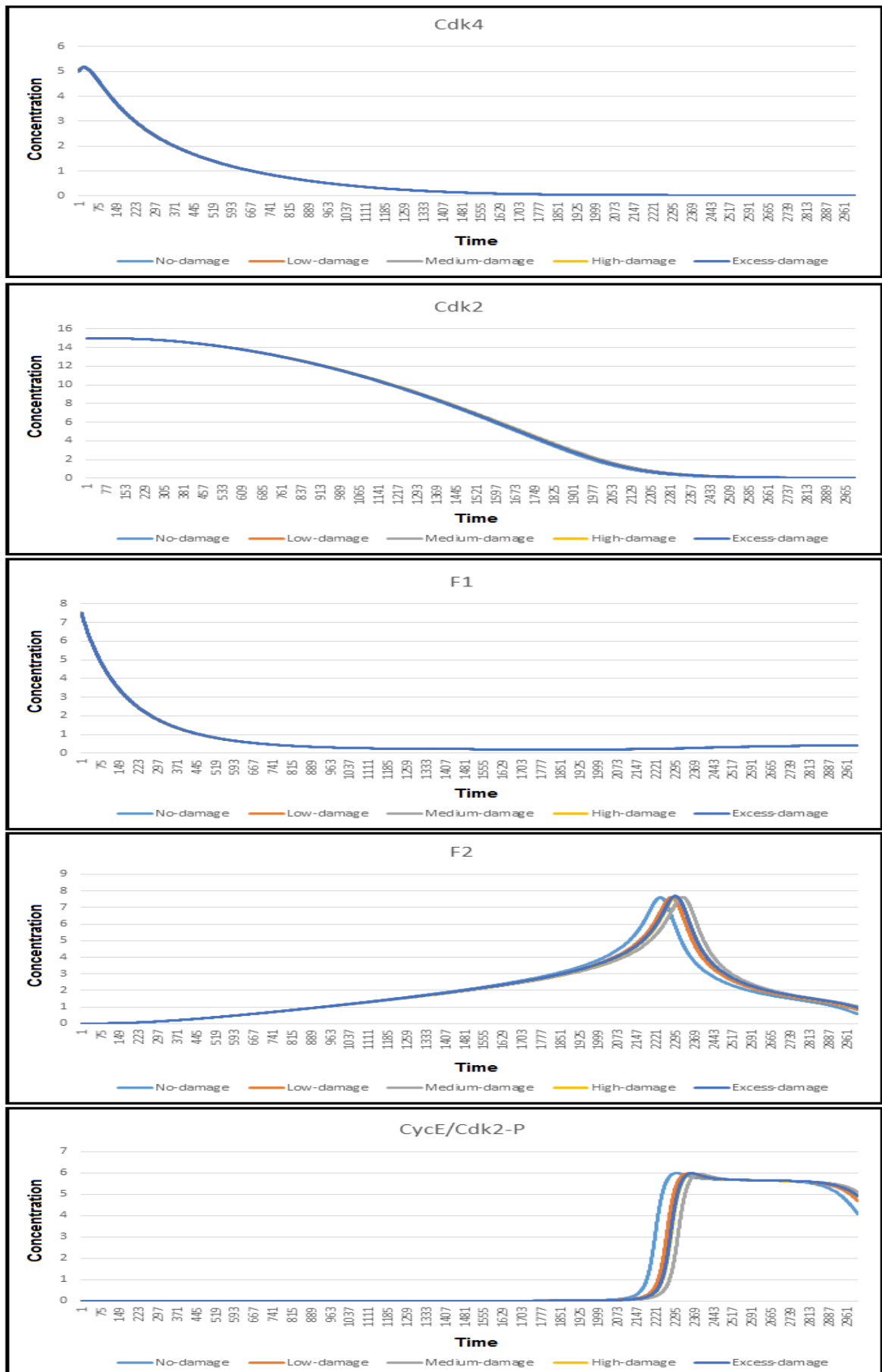


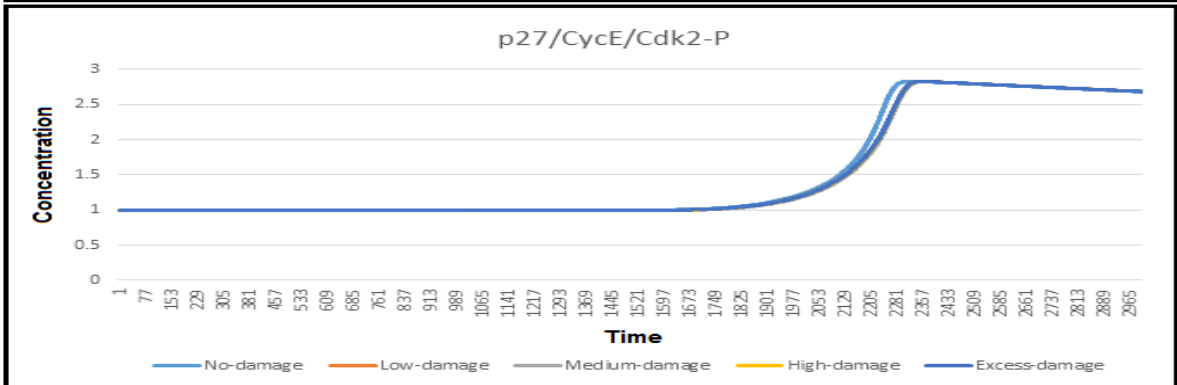
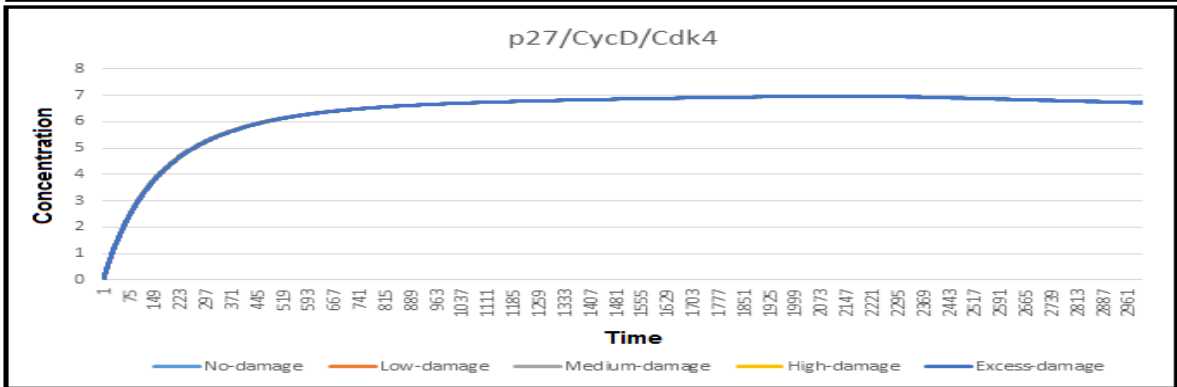
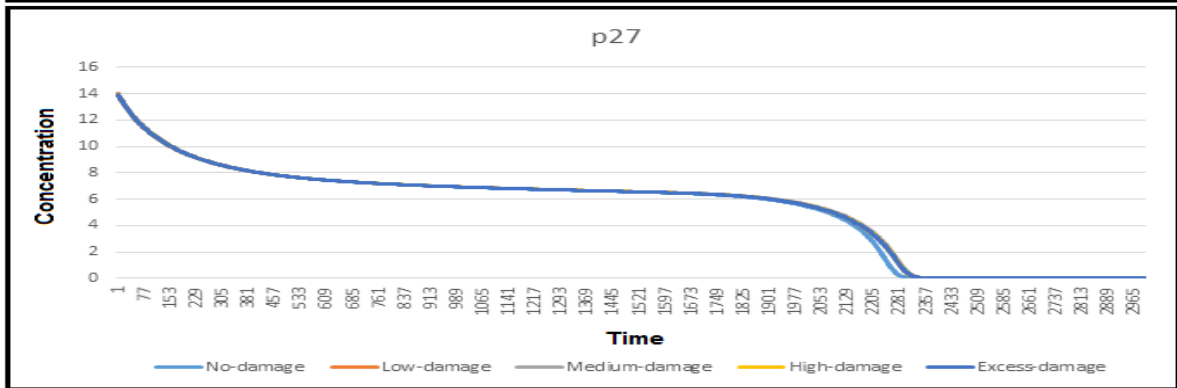
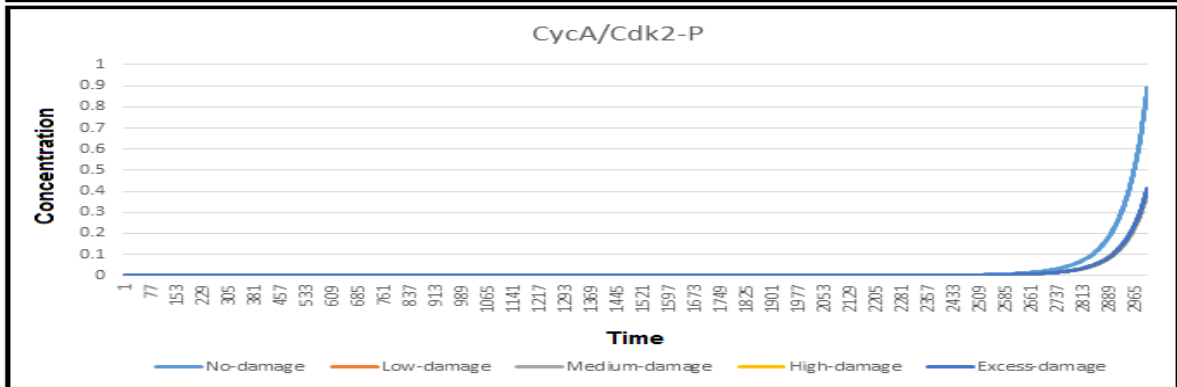
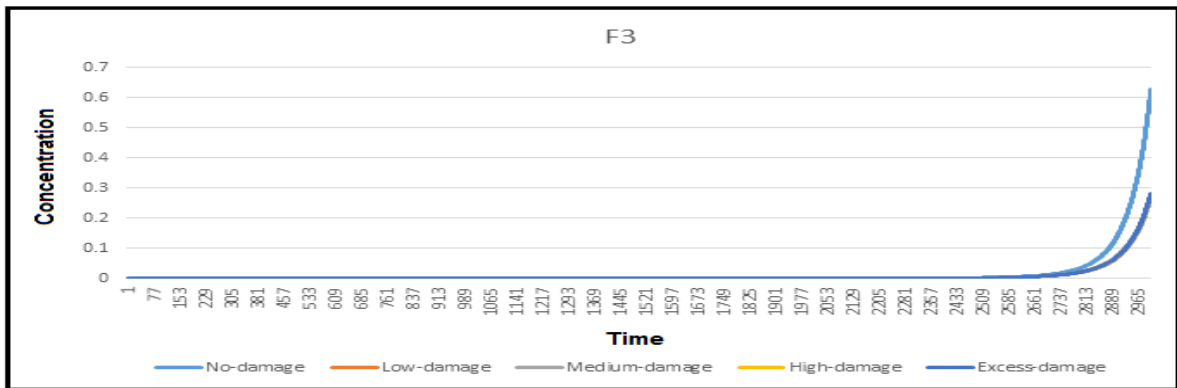


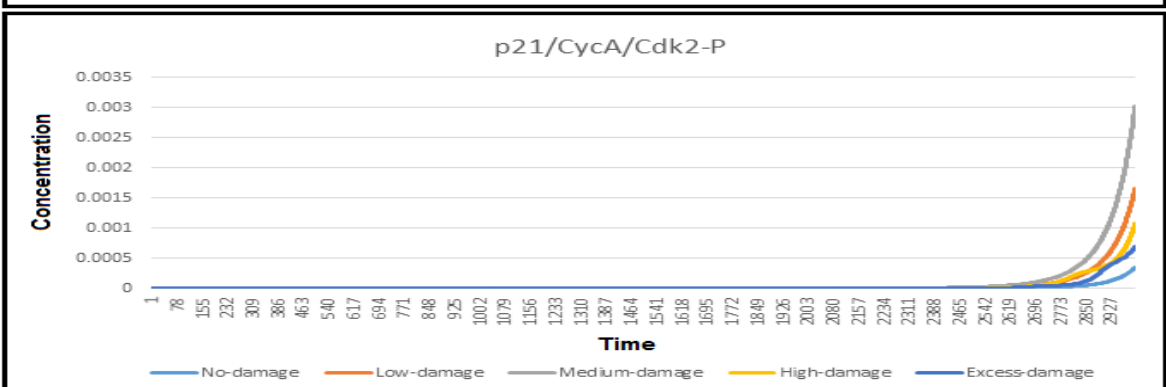
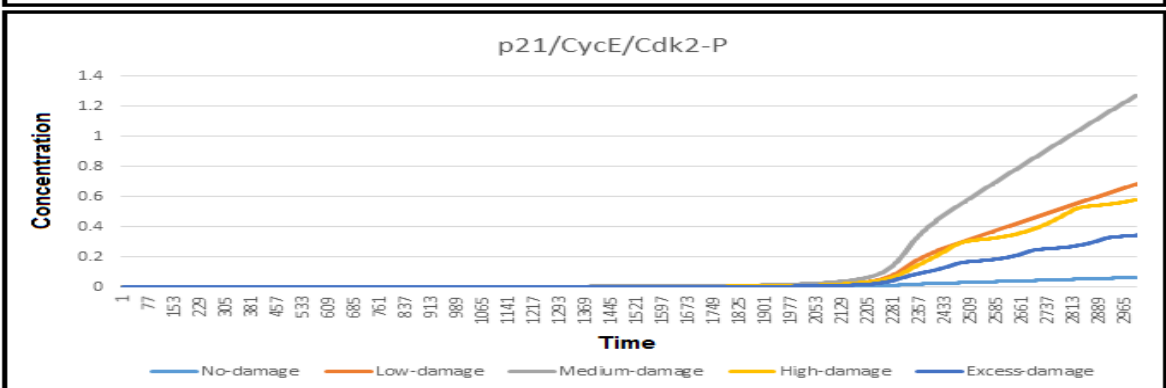
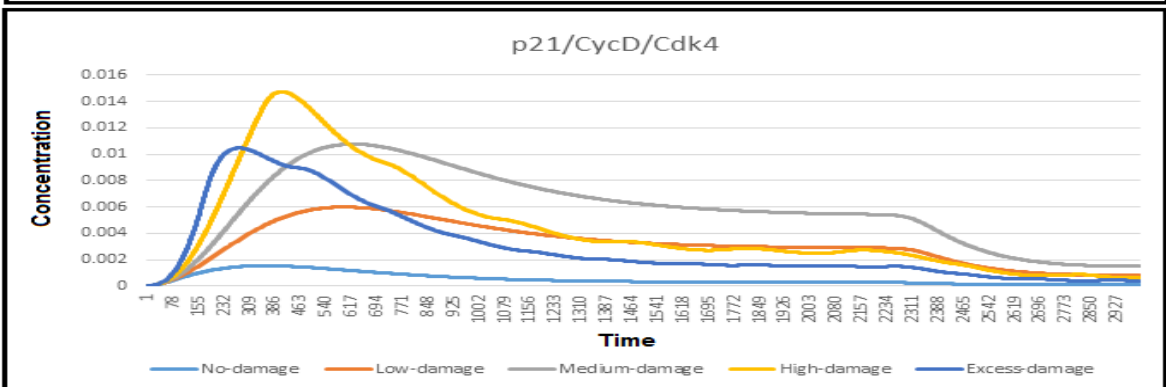
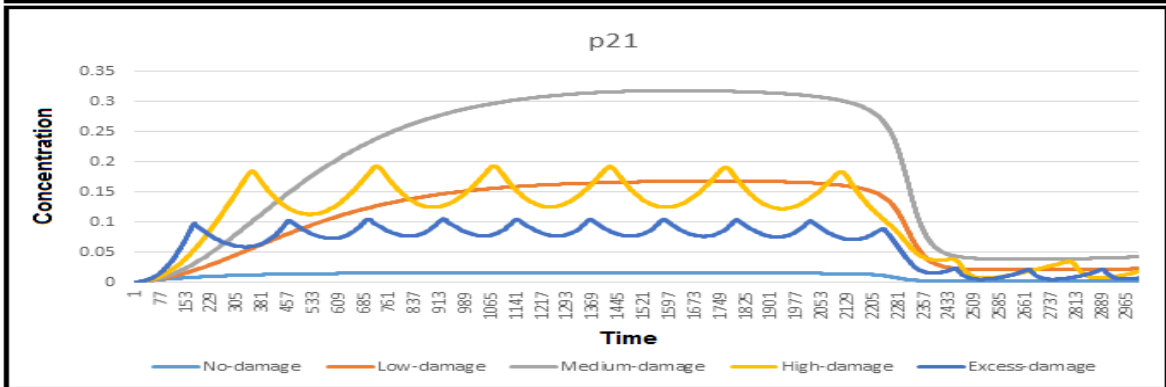
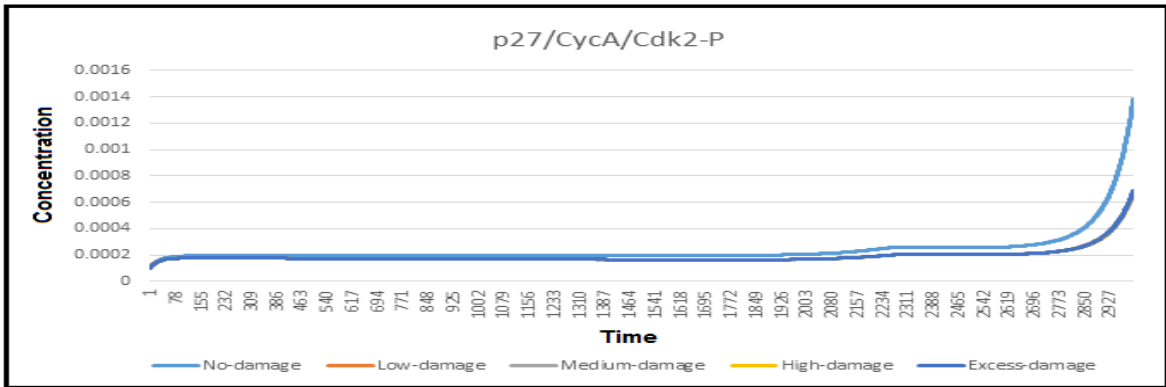


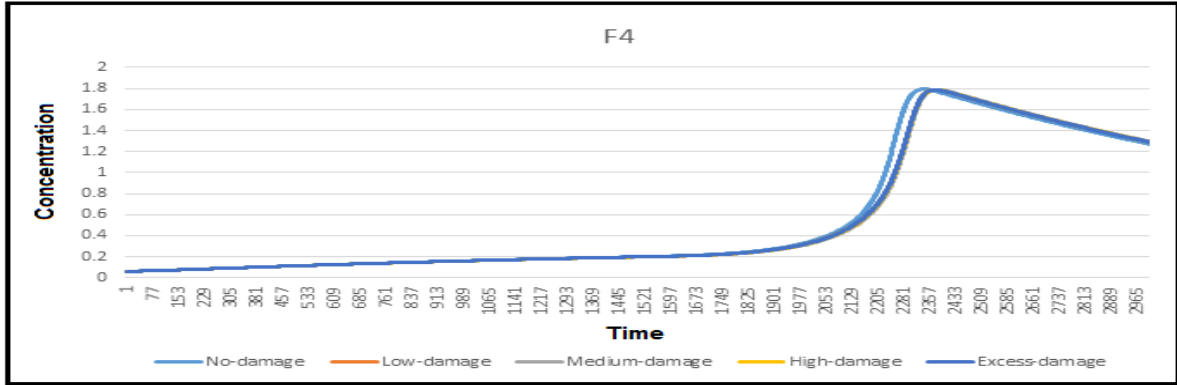
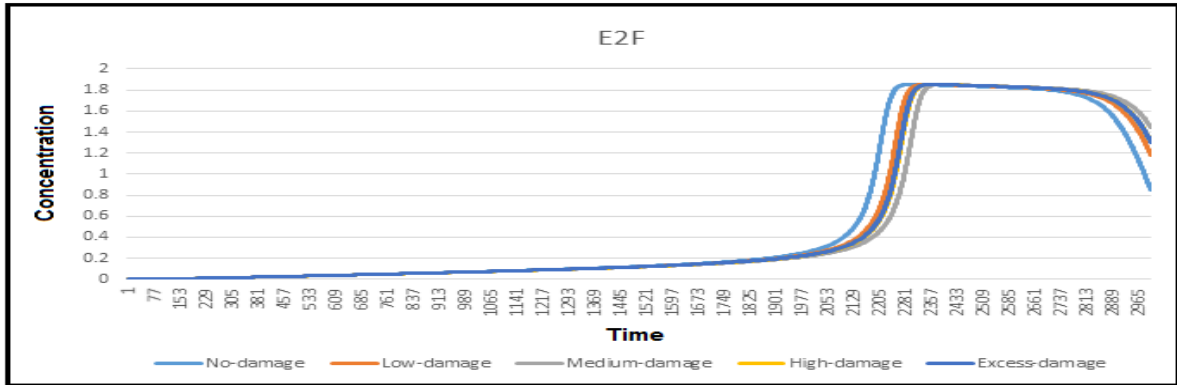
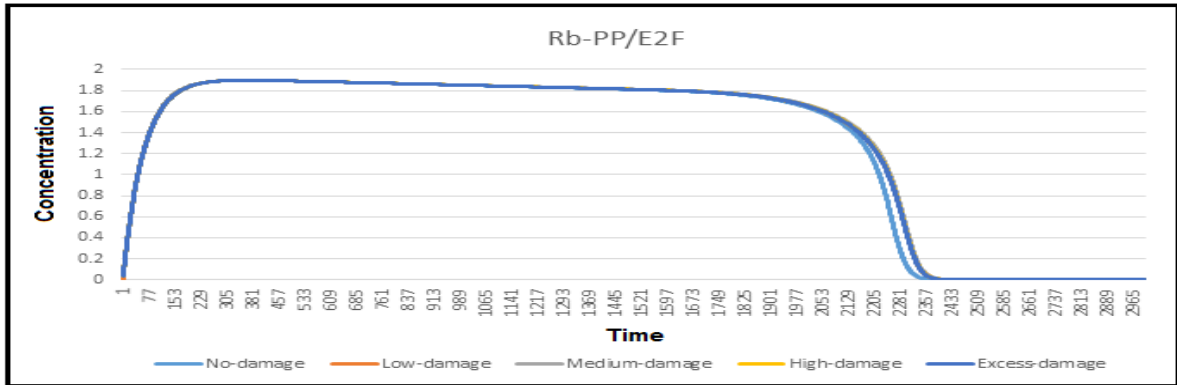
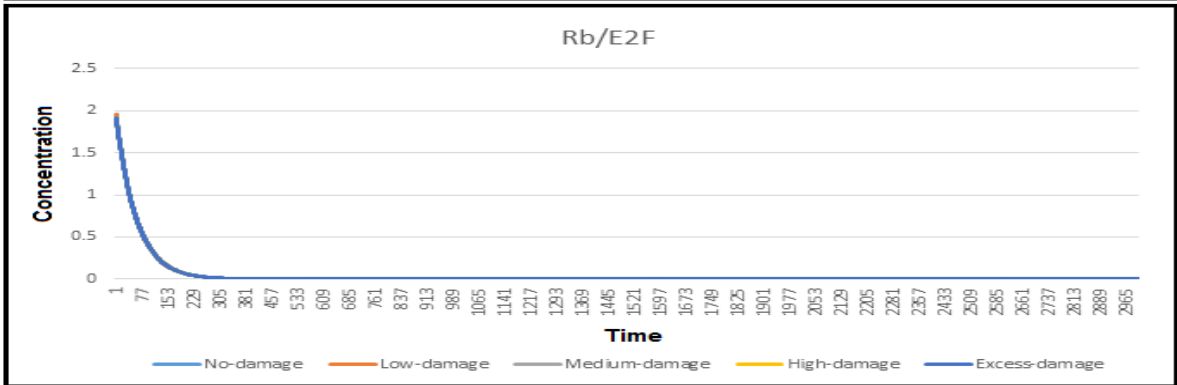
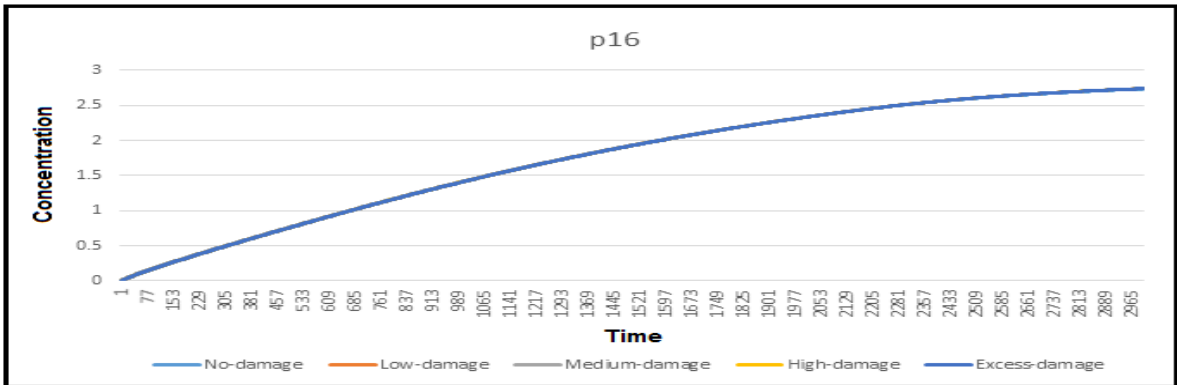


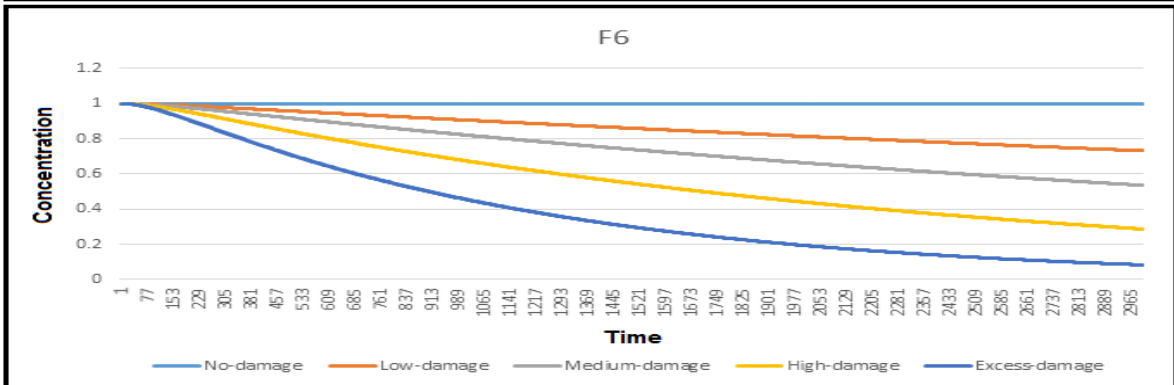
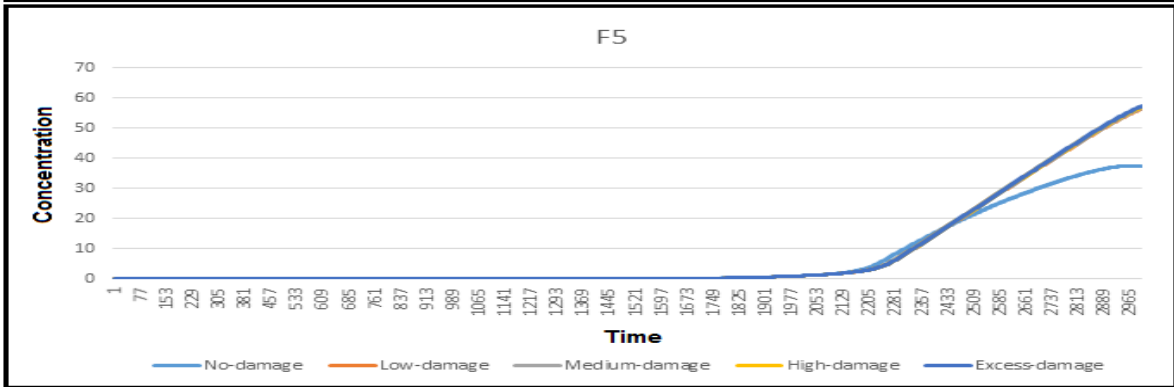
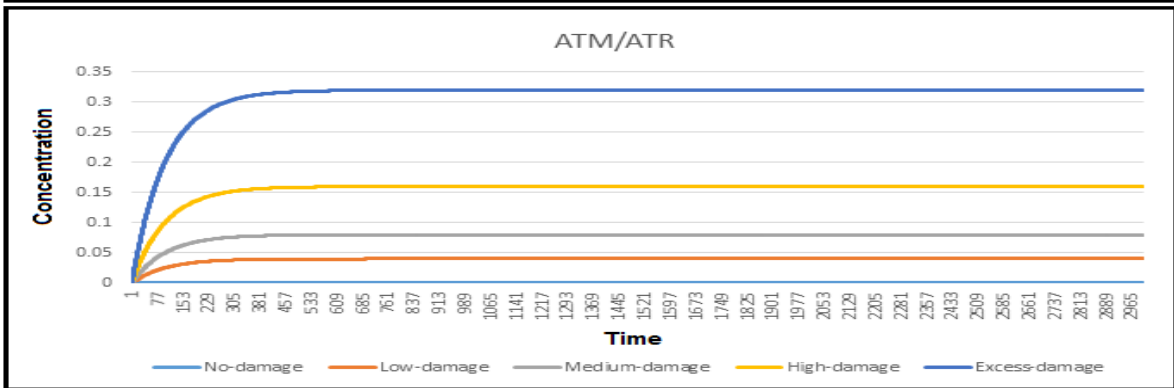
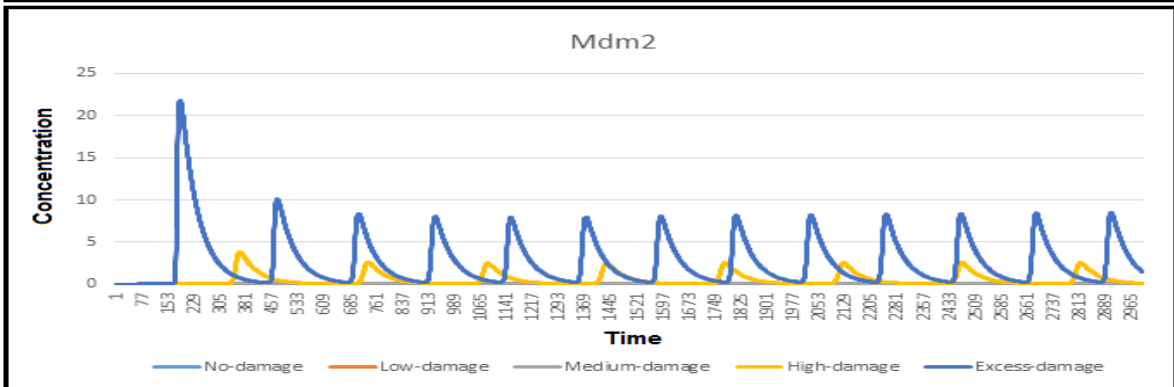
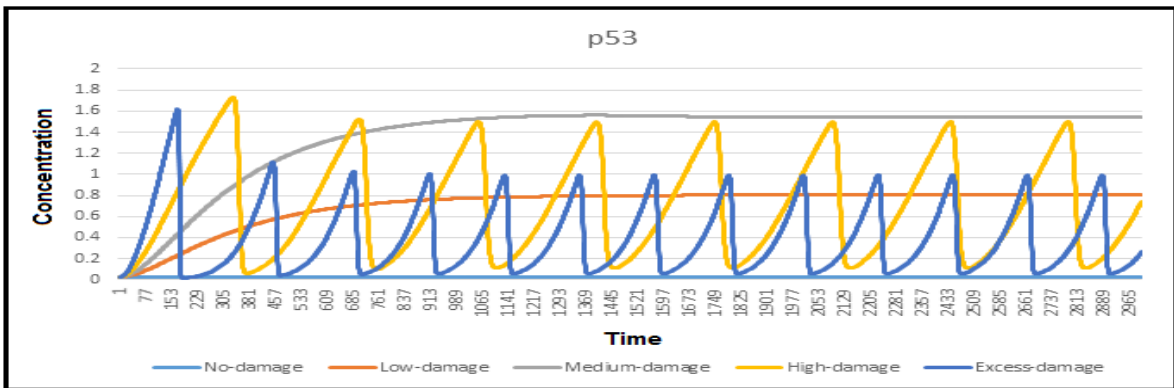
F.2 All time courses of the reduced model (level-1) elements with different levels of DNA damage

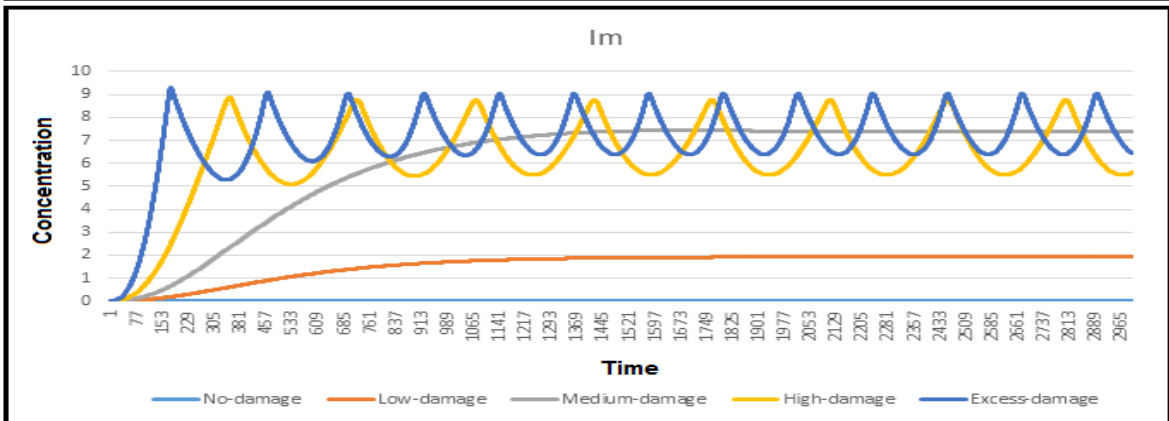
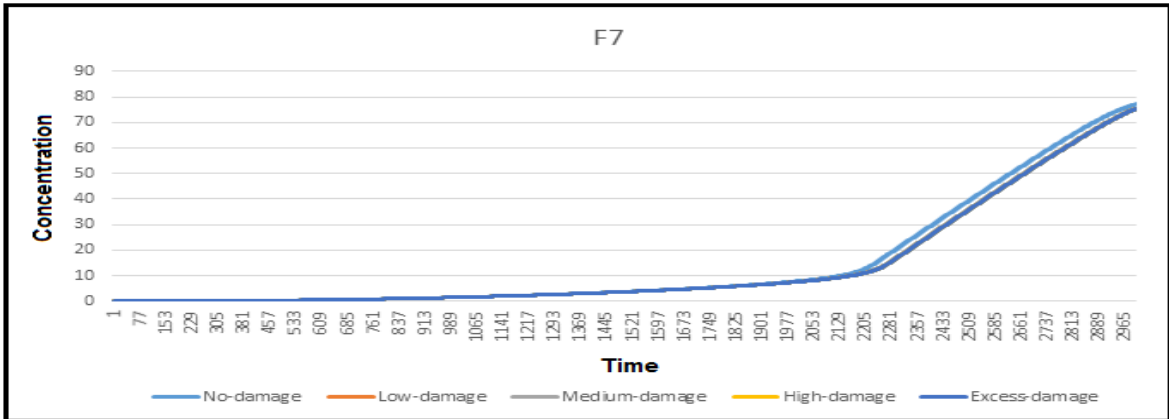
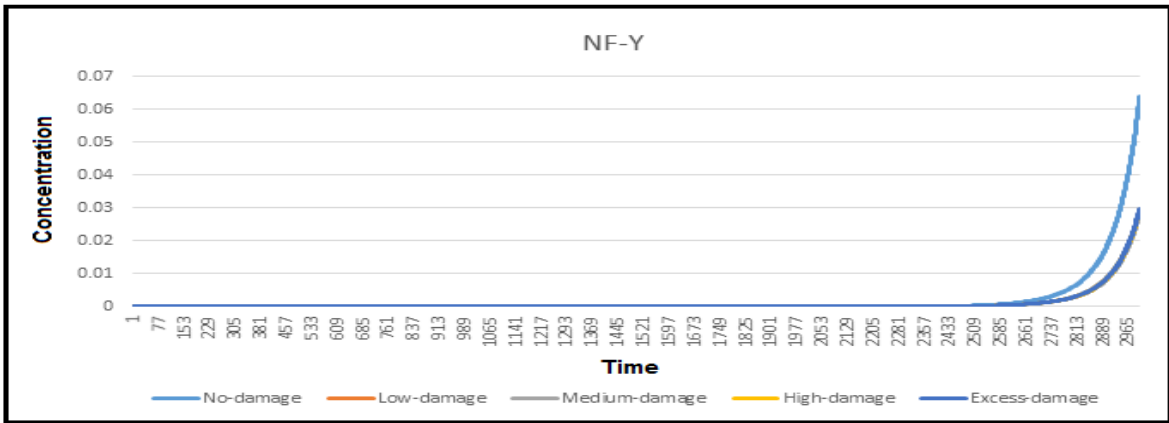








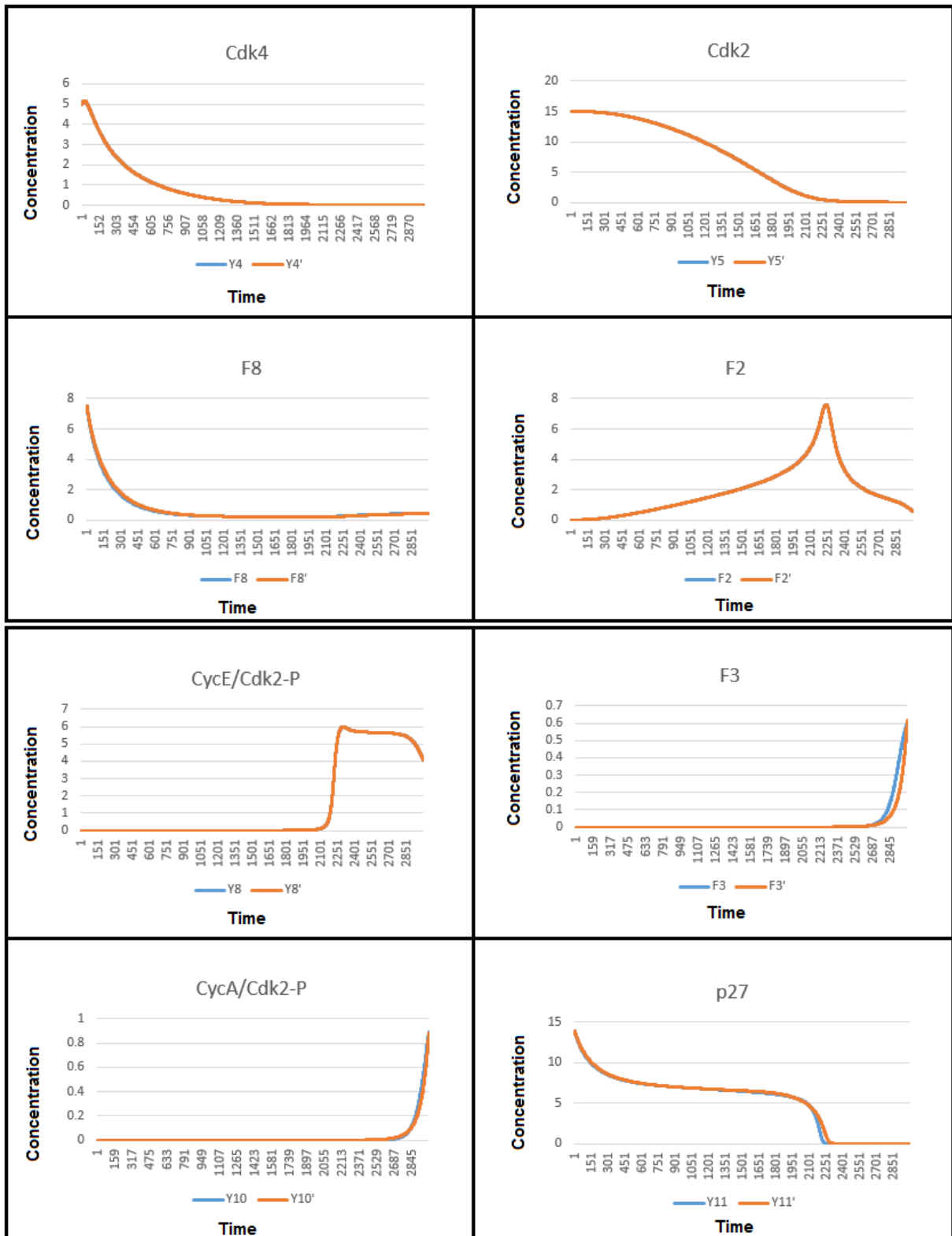


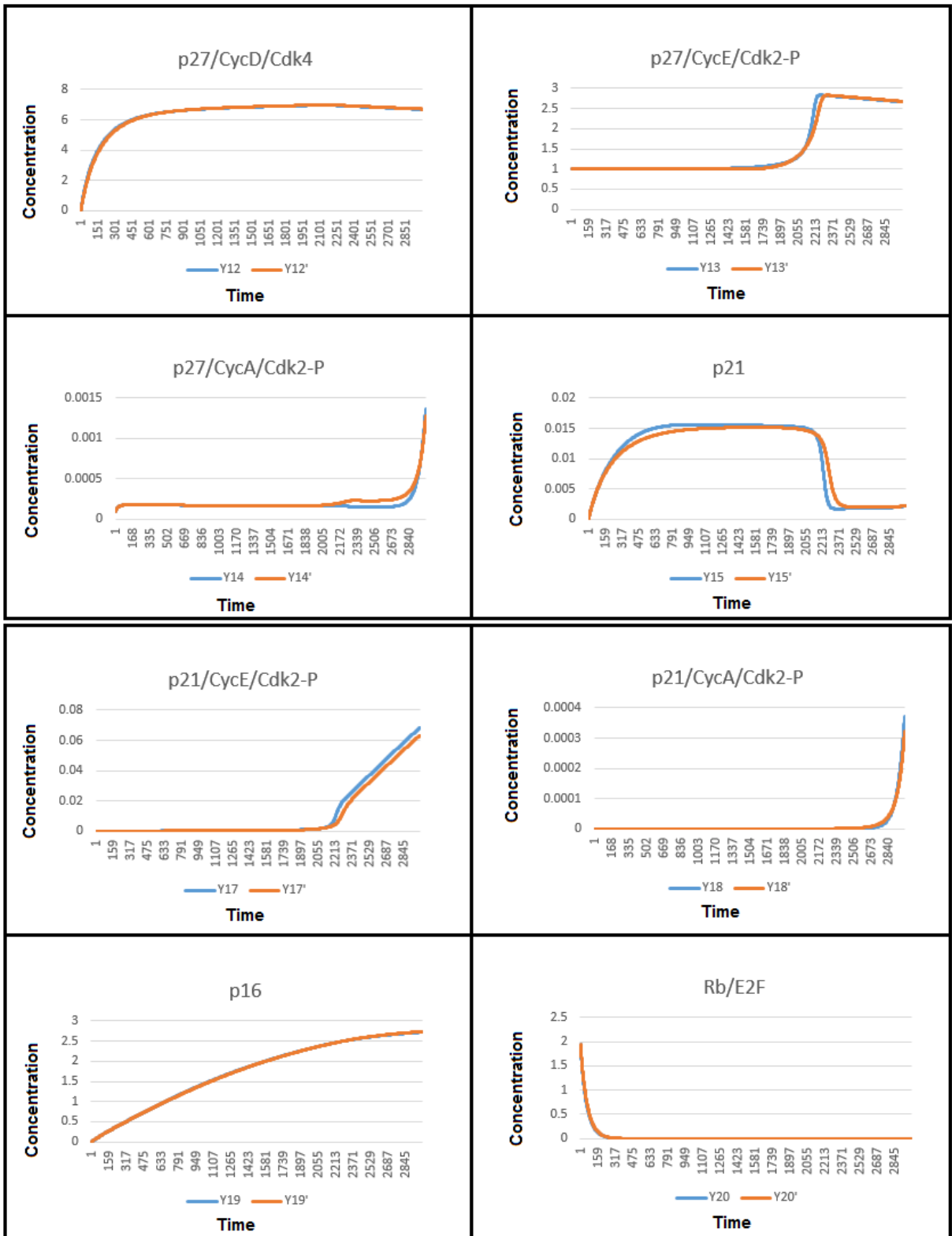


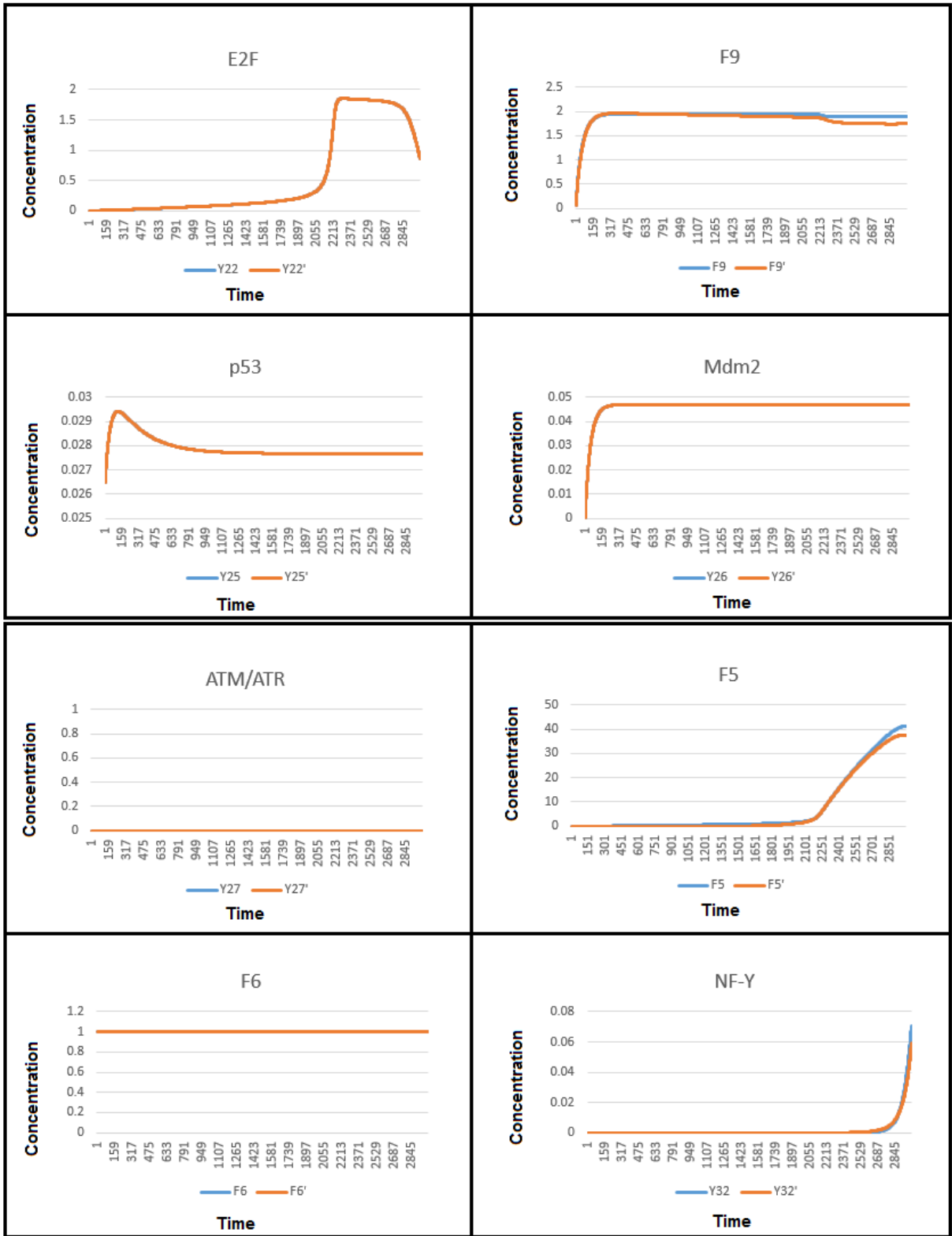
Appendix G

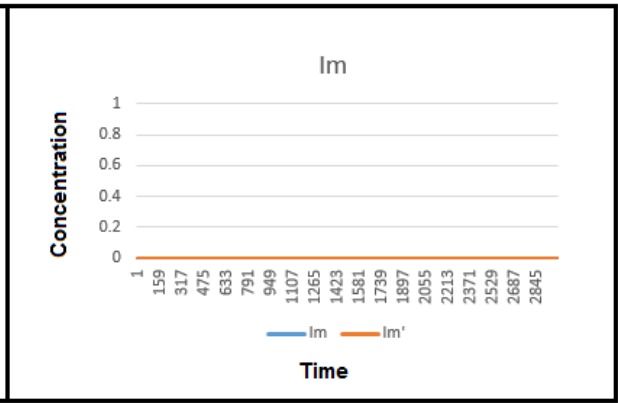
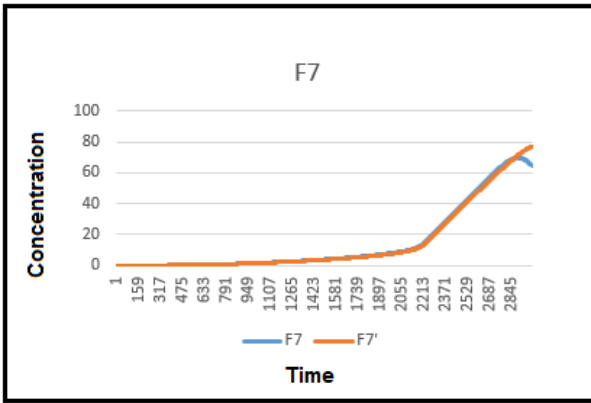
All time courses of the reduced model (level-2) elements

G.1 All time courses of the reduced model (level-2) elements without DNA damage vs the base model

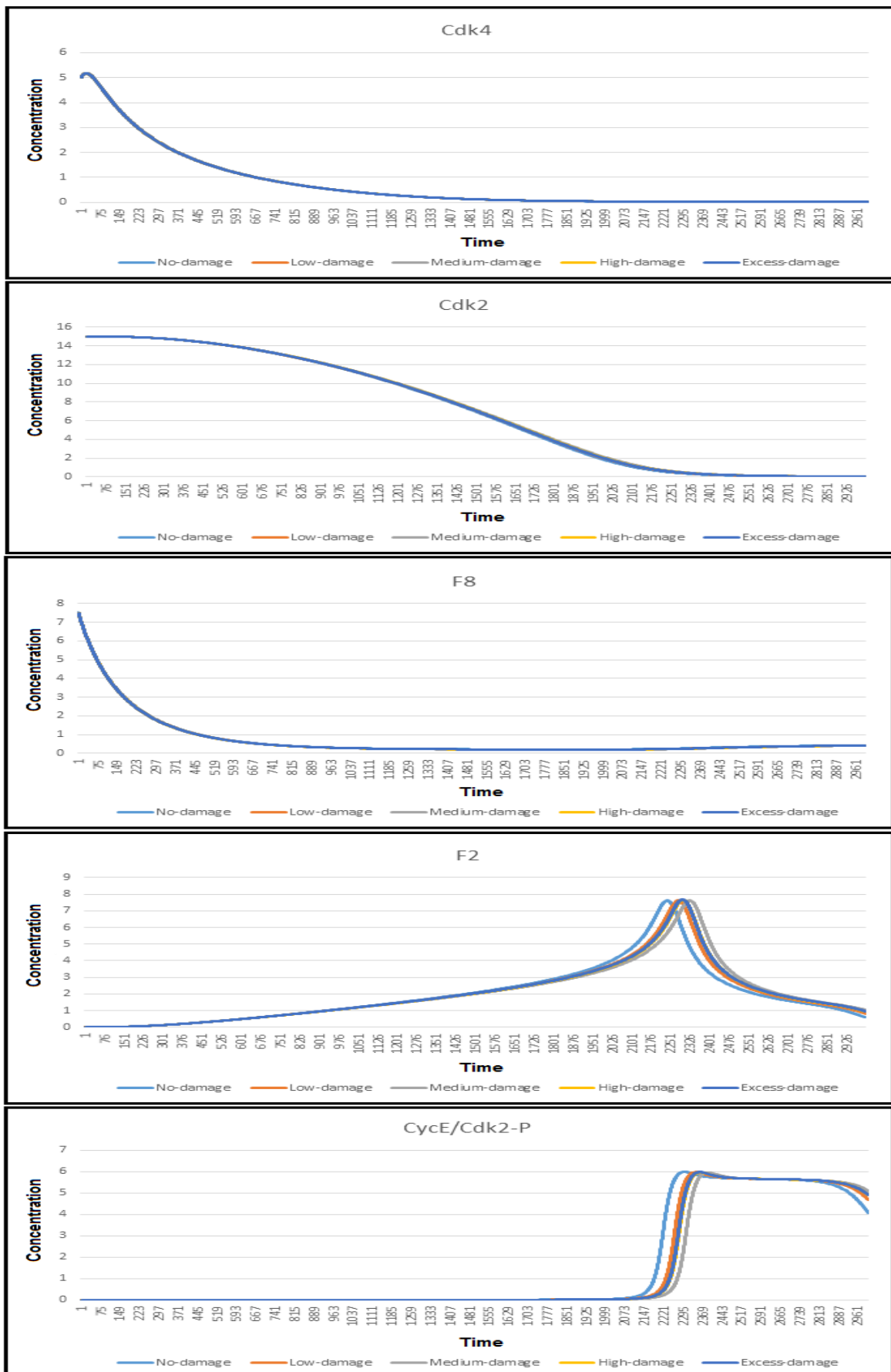


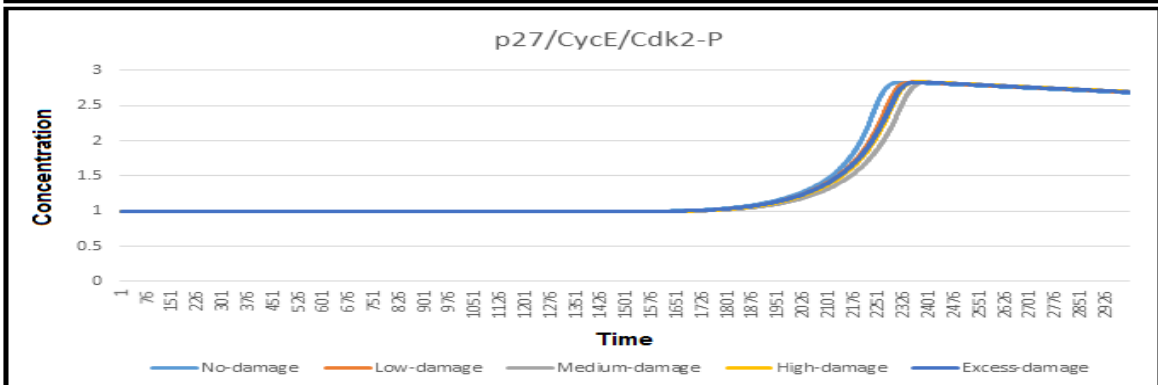
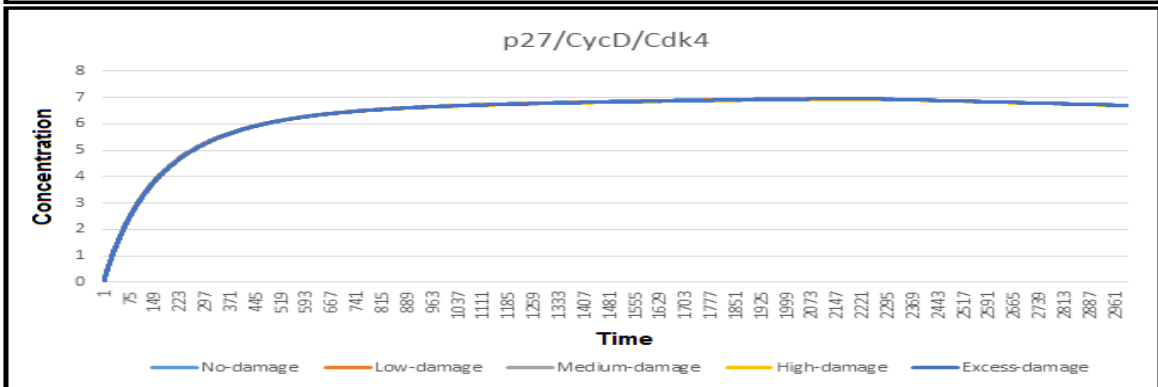
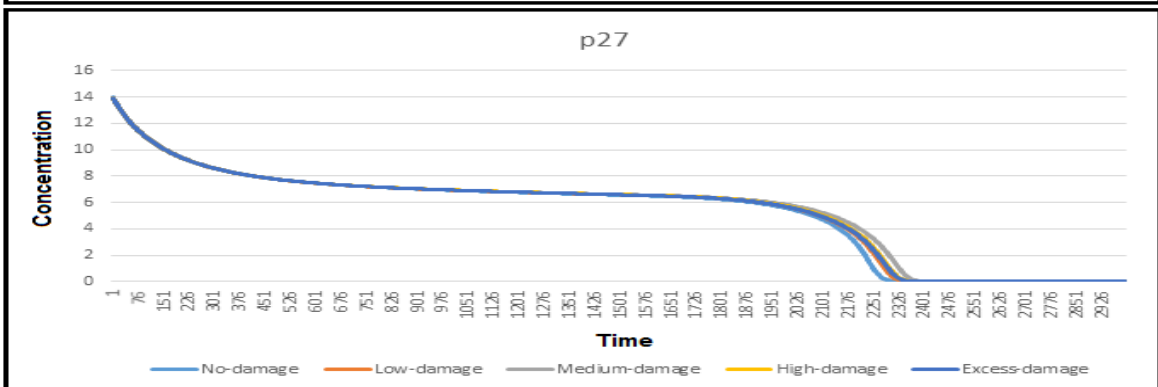
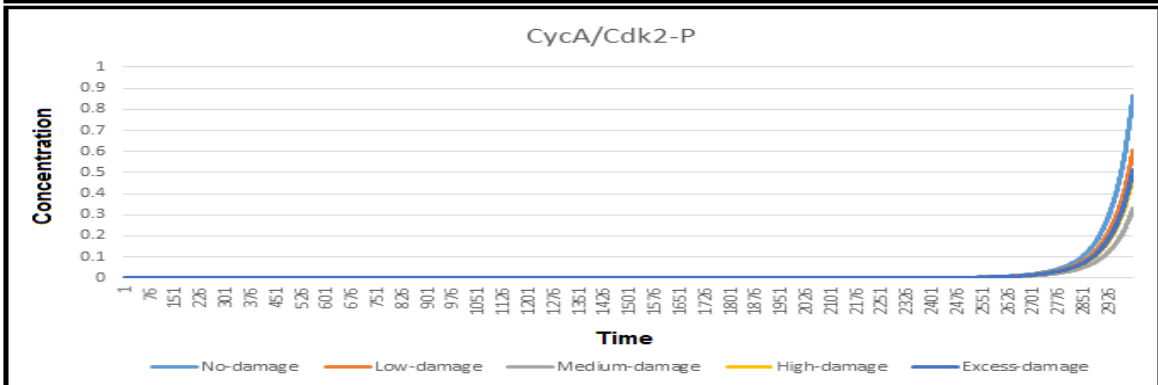
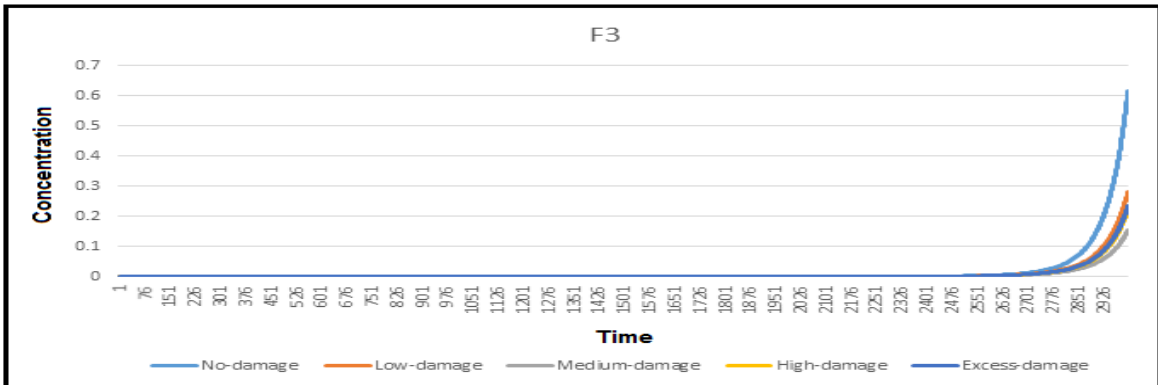


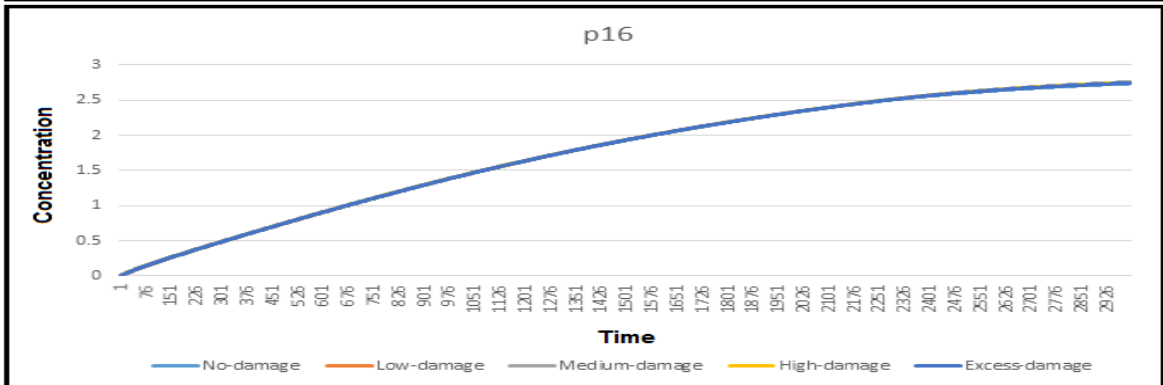
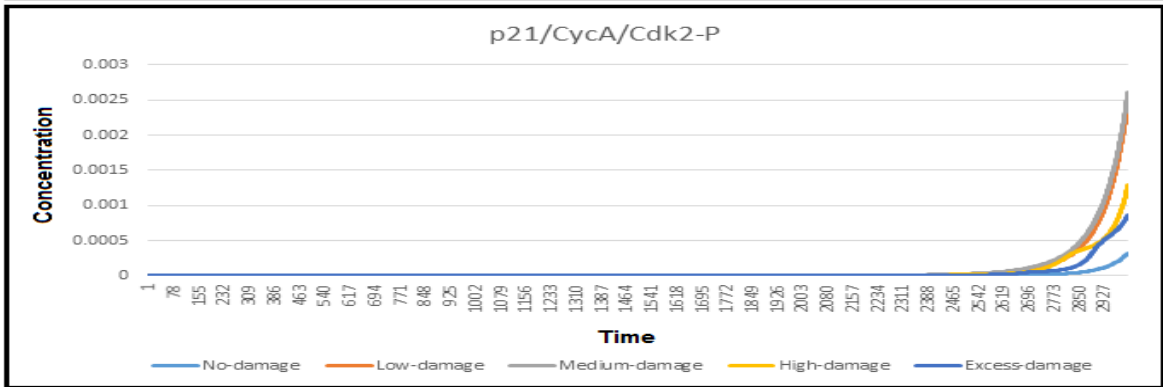
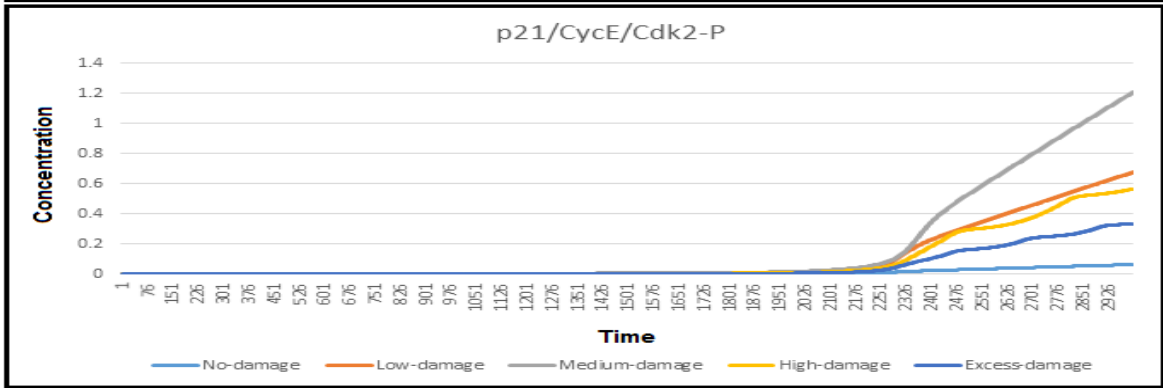
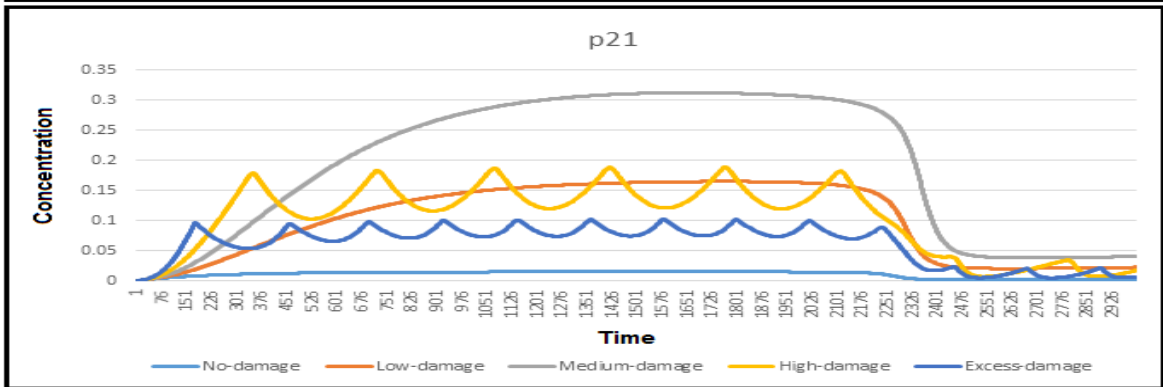
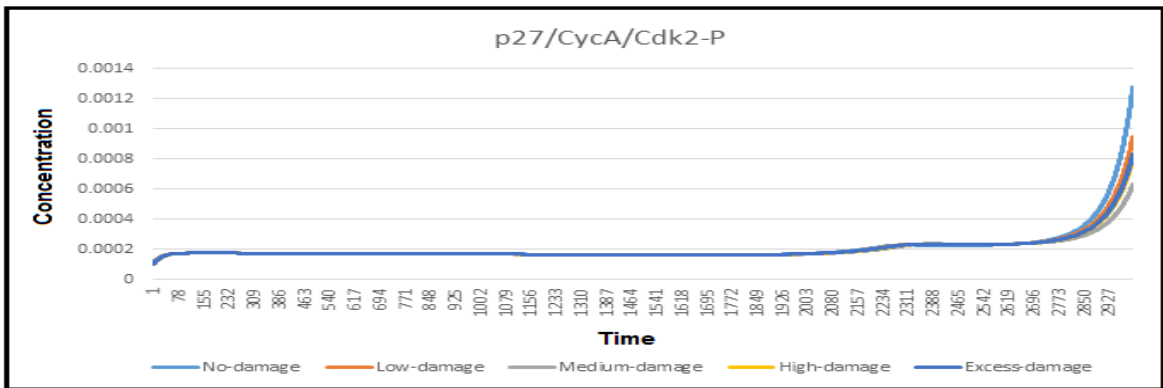


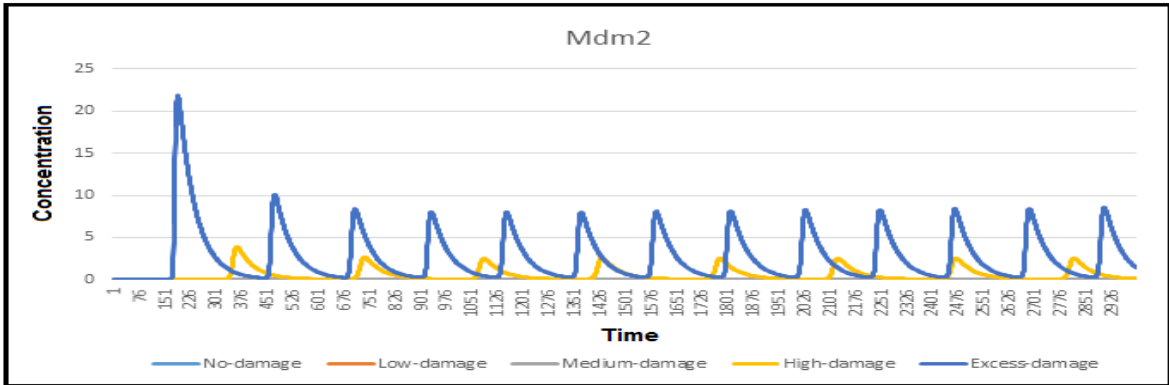
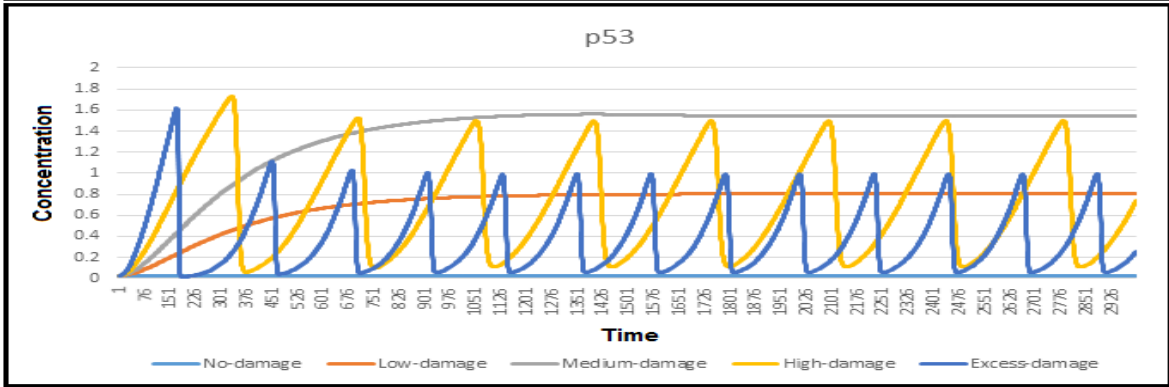
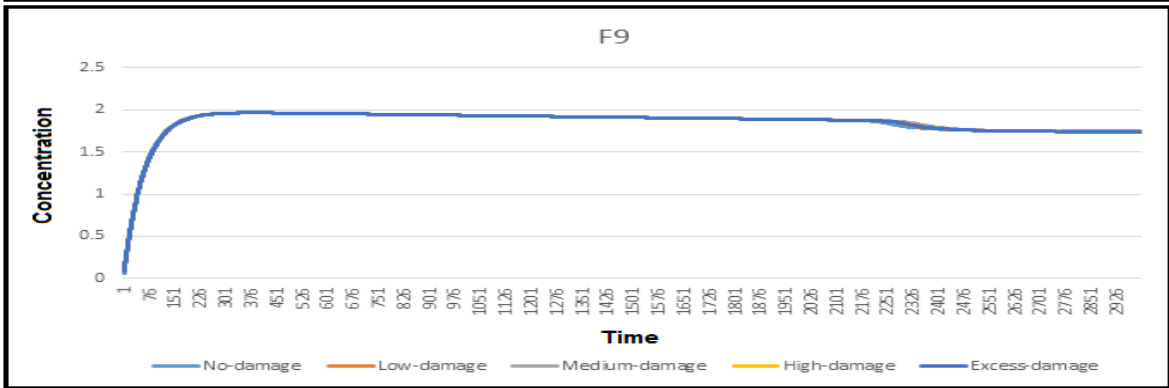
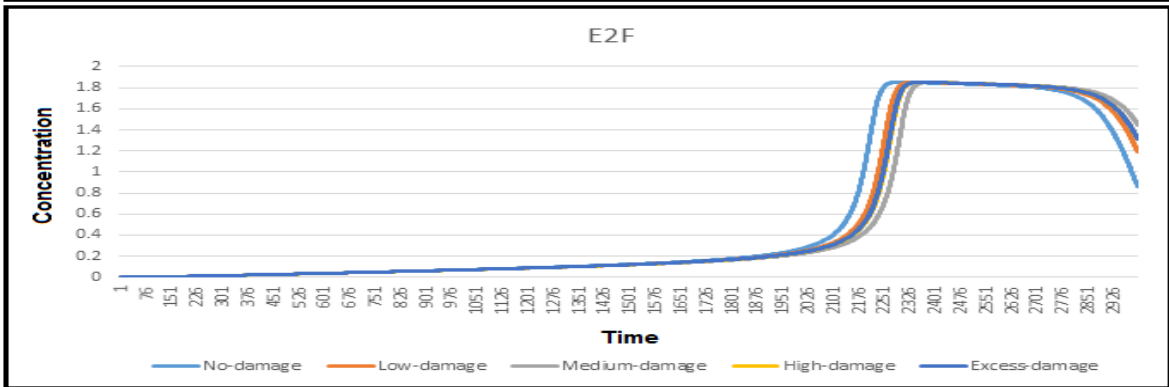
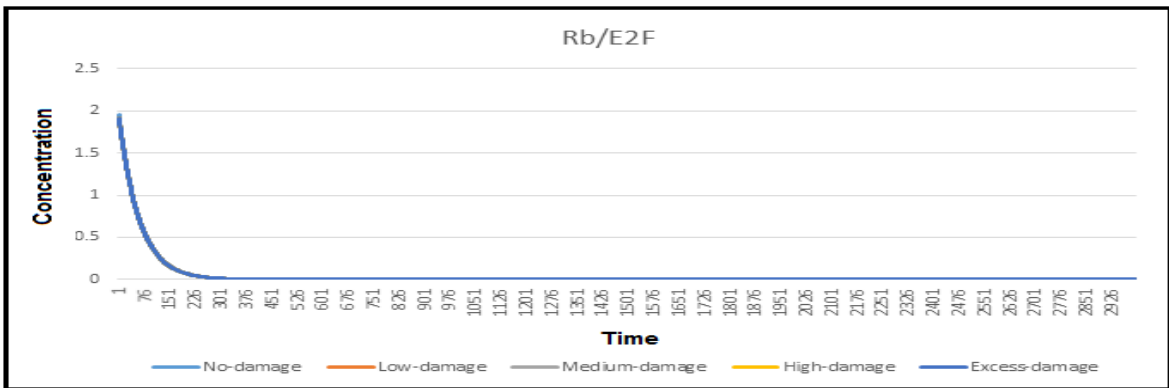


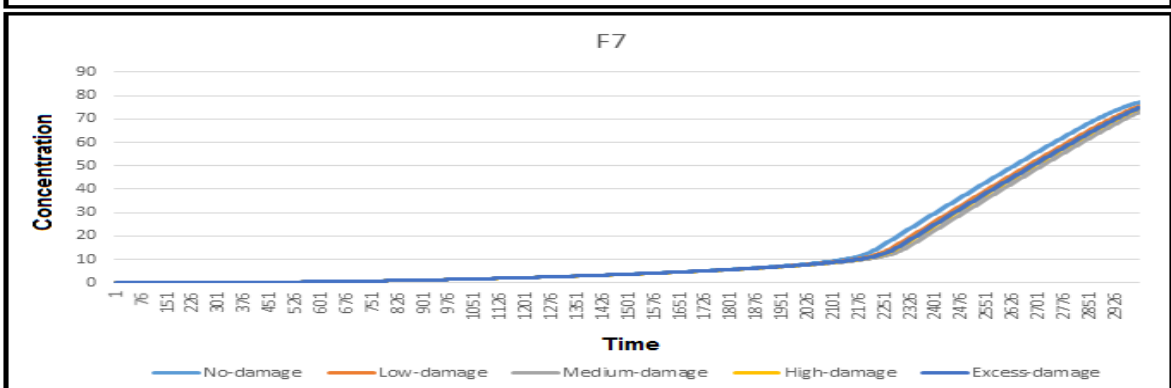
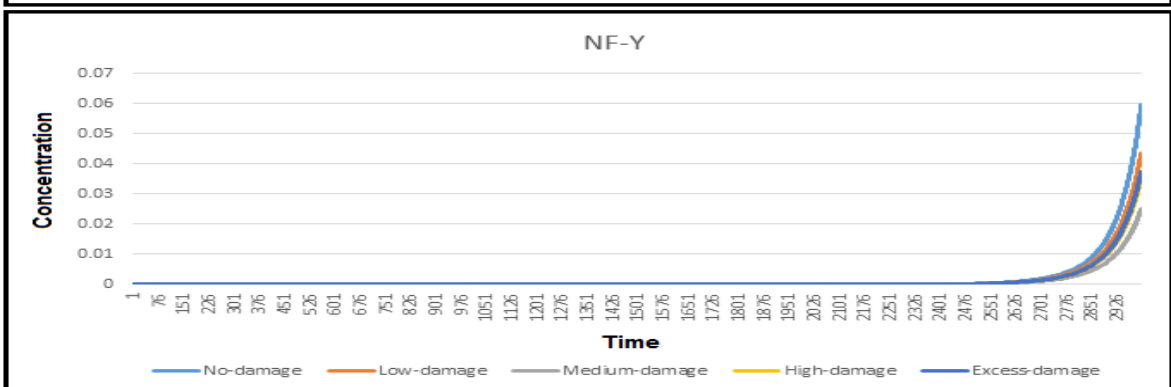
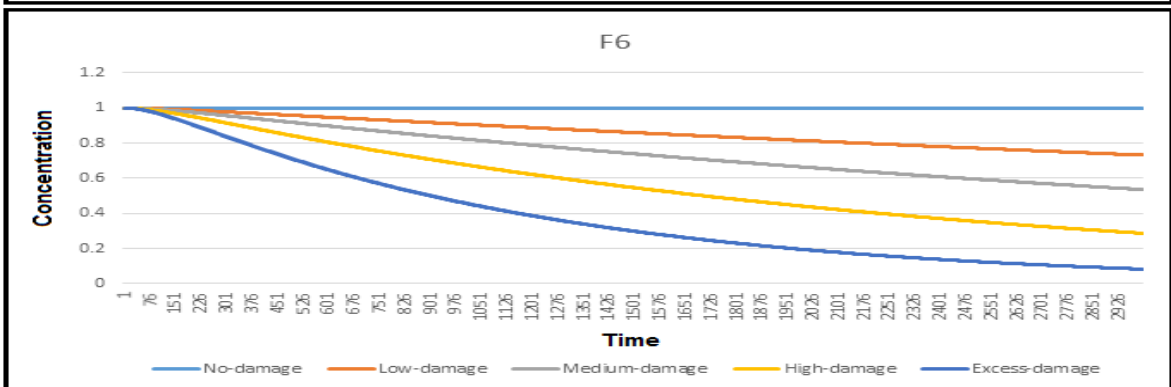
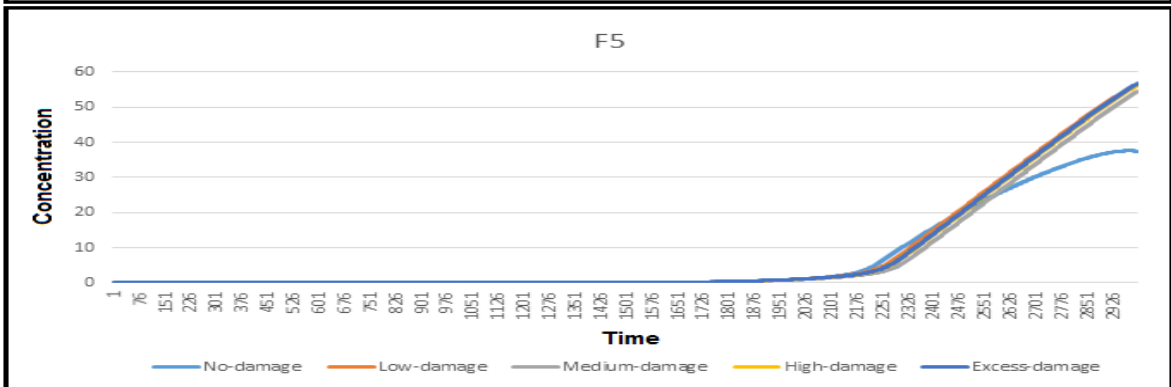
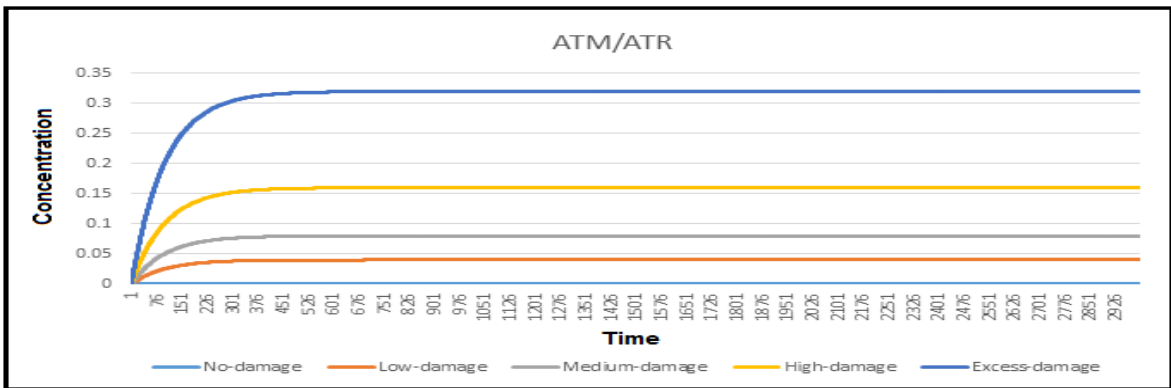
G.2 All time courses of the reduced model (level-2) elements with different levels of DNA damage

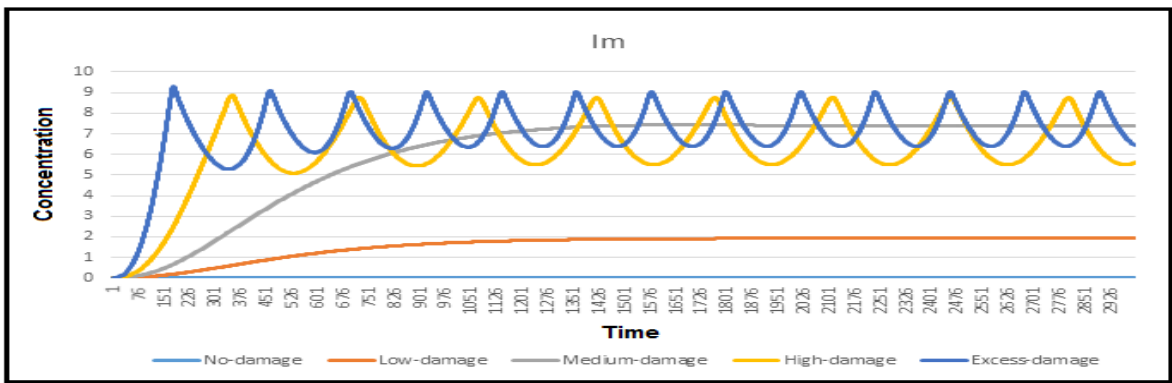








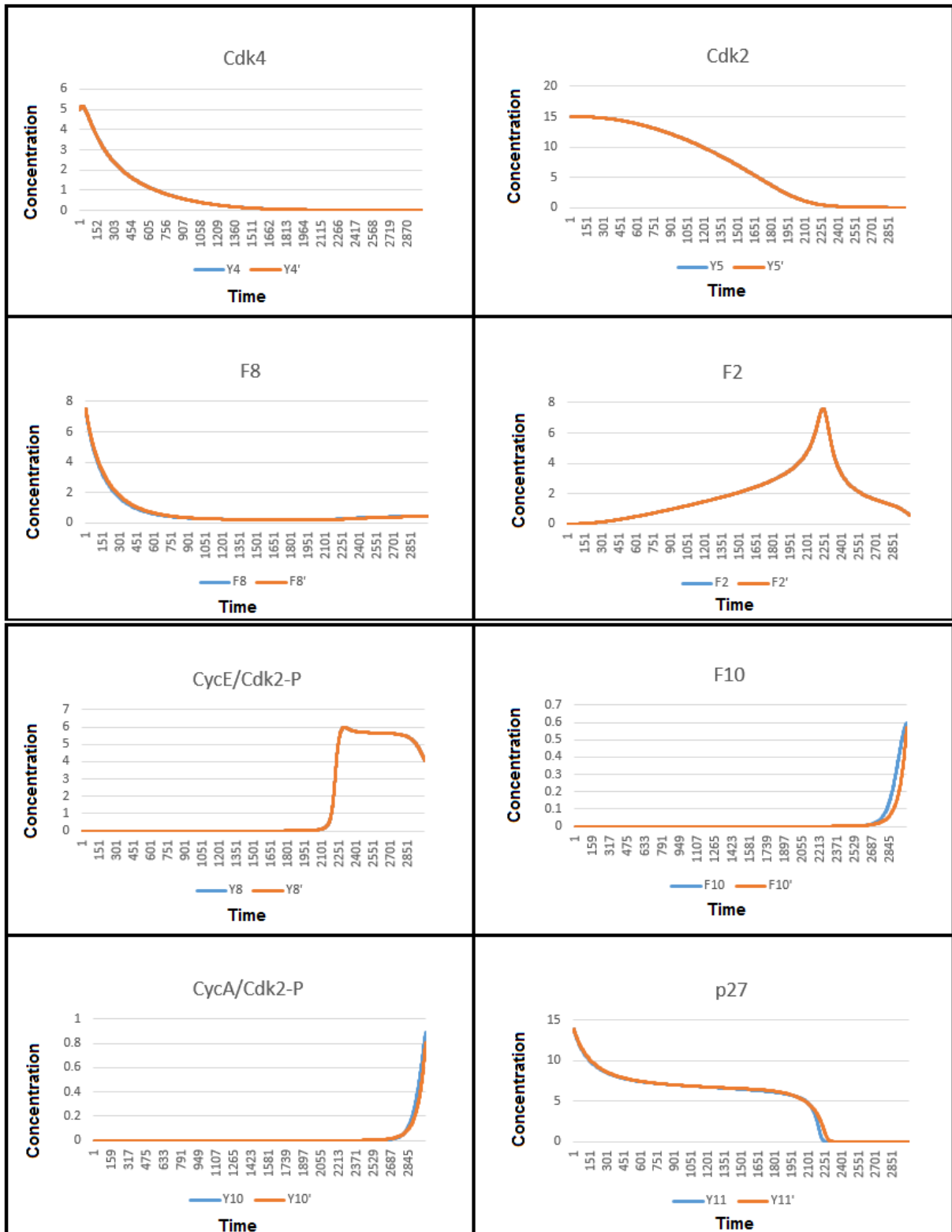


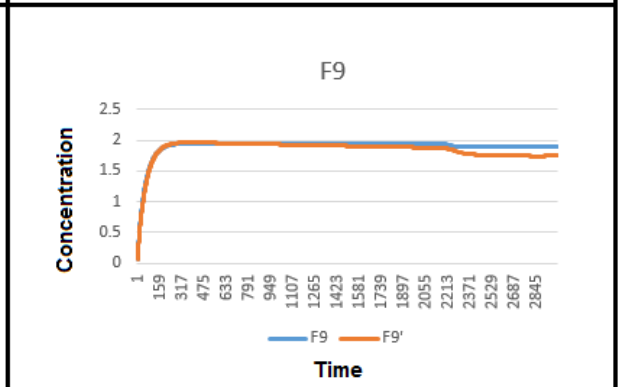
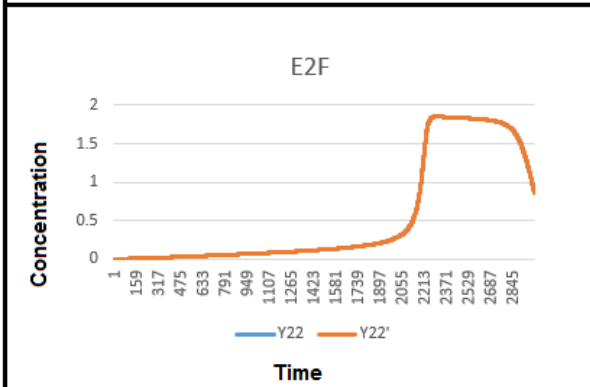
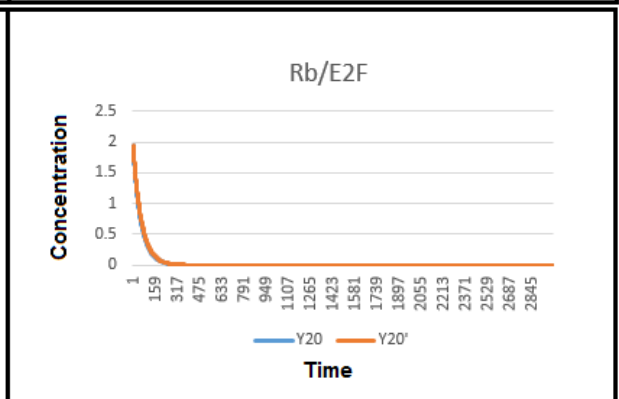
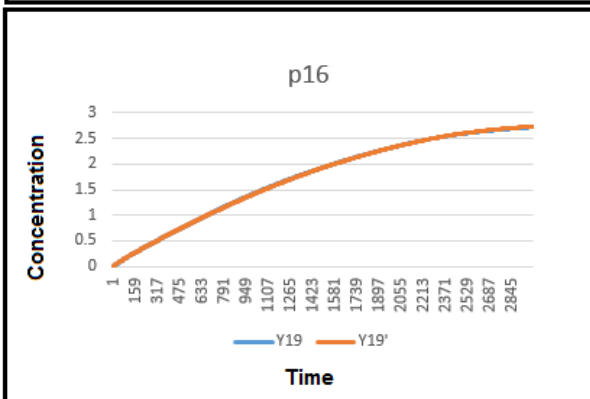
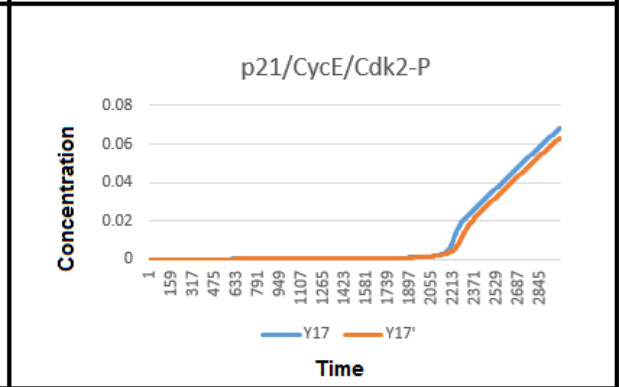
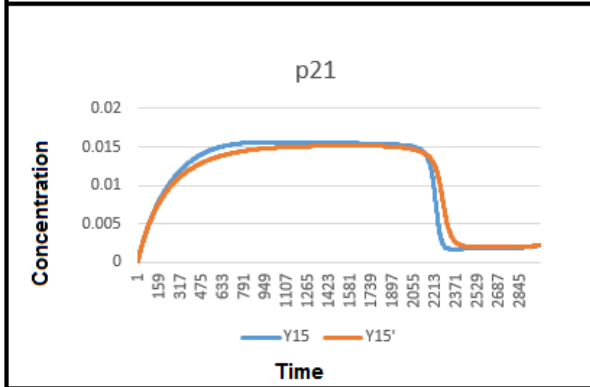
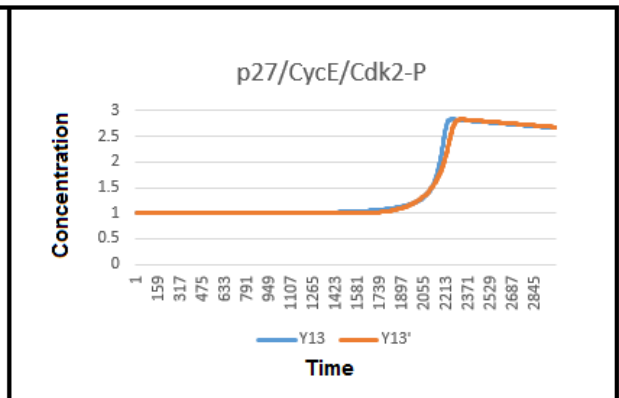
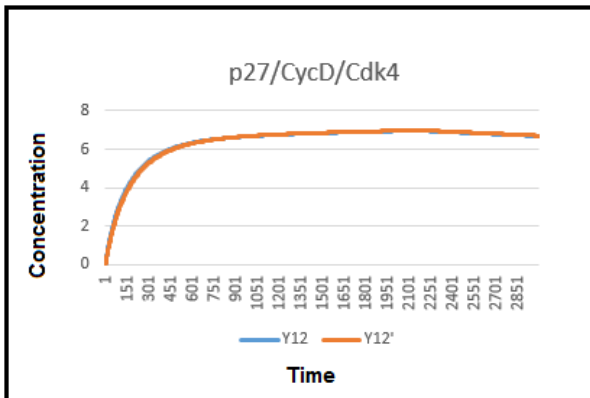


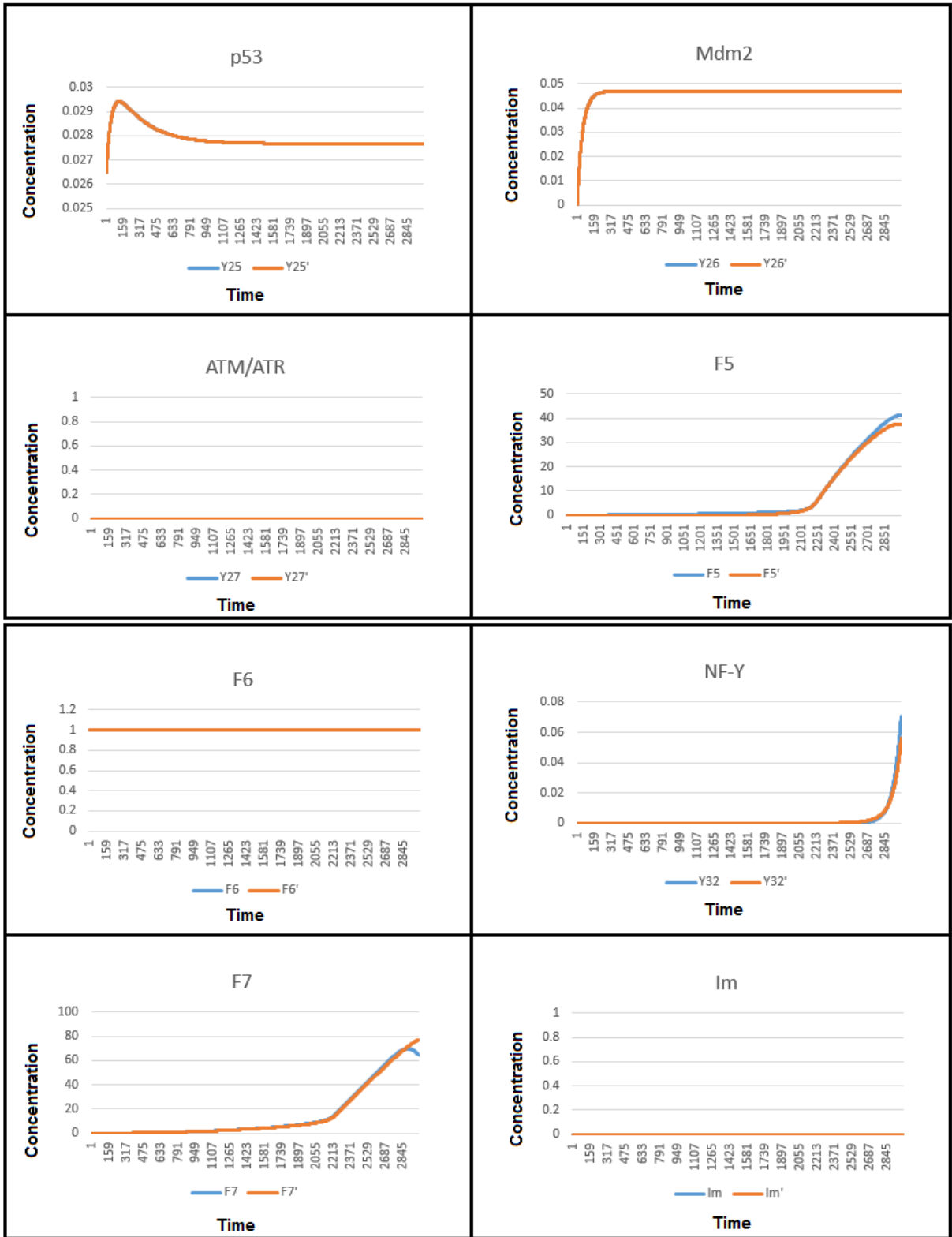
Appendix H

All time courses of the reduced model (level-3) elements

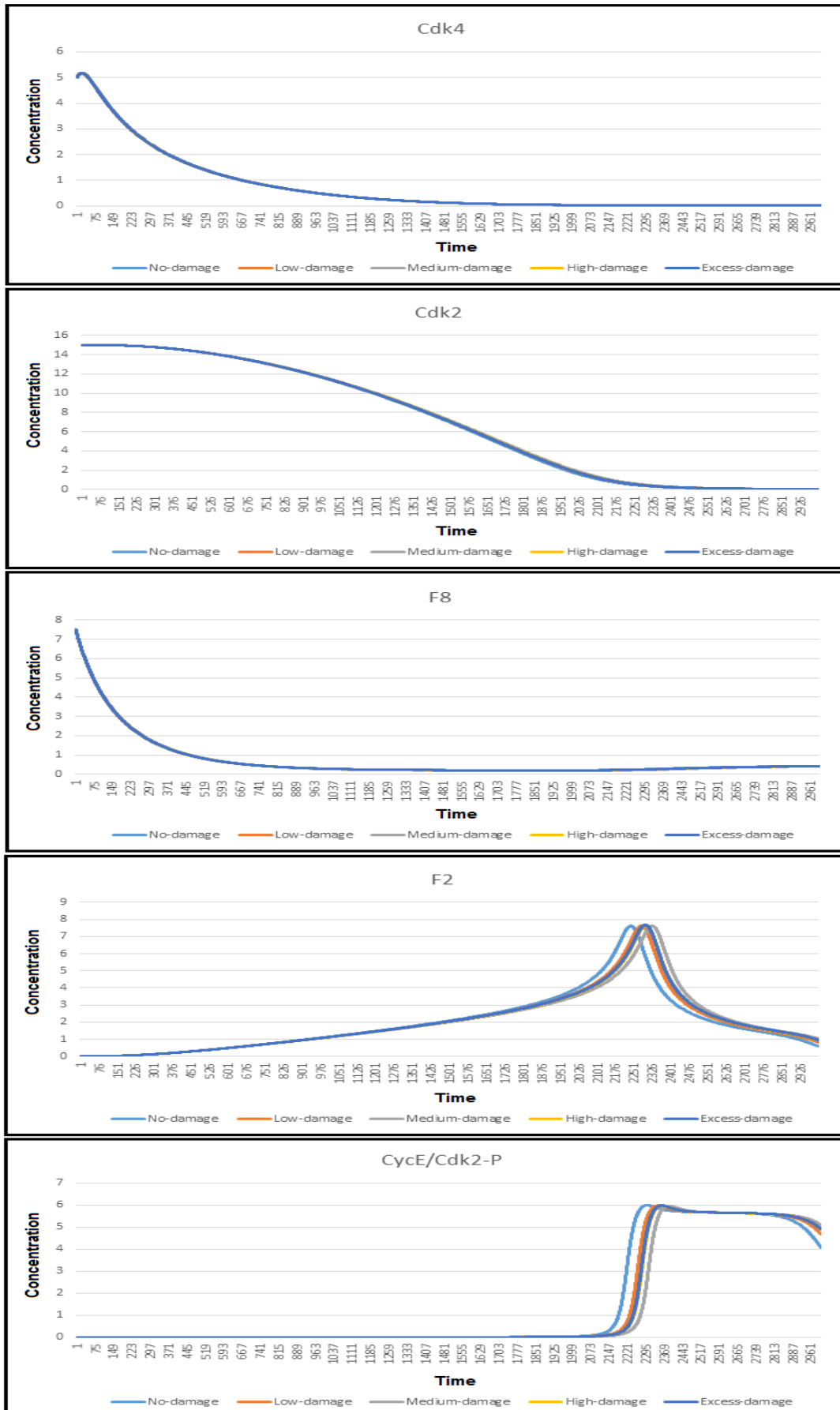
H.1 All time courses of the reduced model (level-3) elements without DNA damage vs the base model

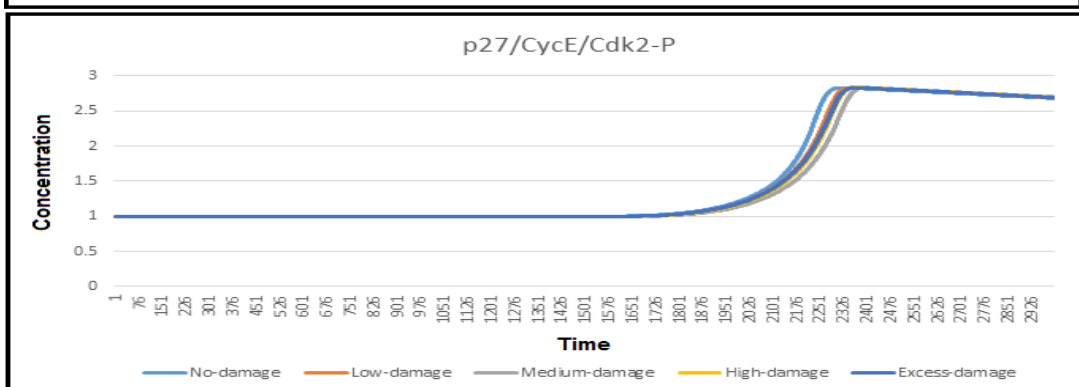
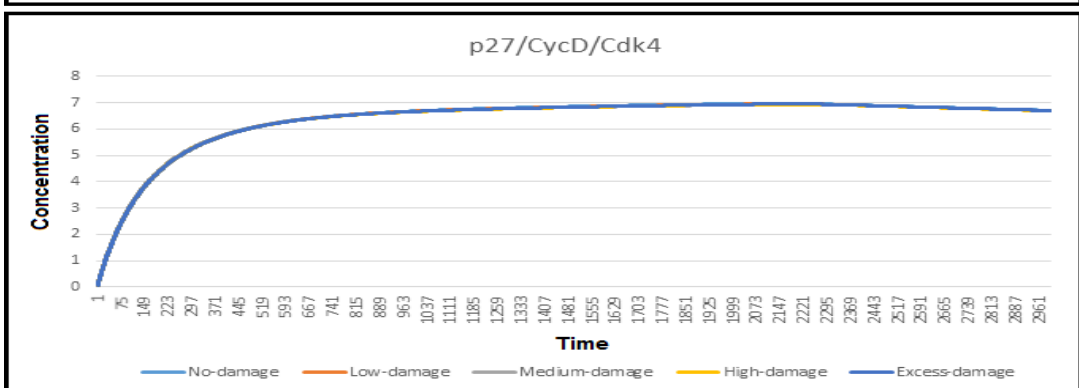
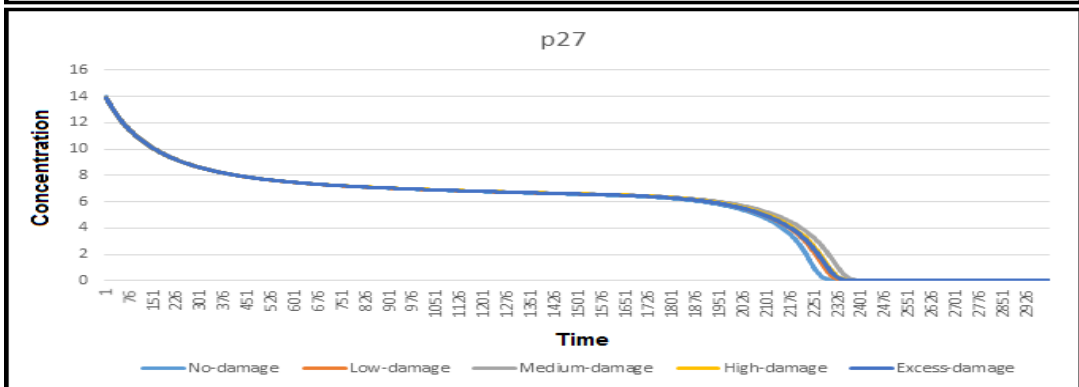
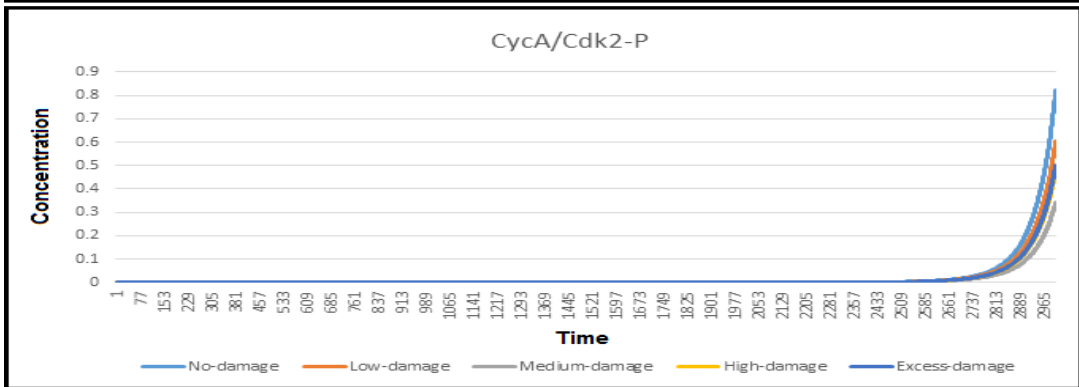
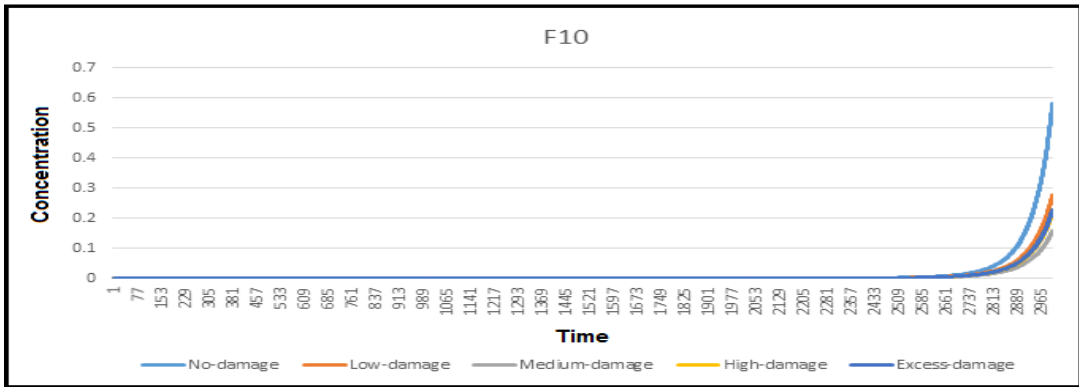


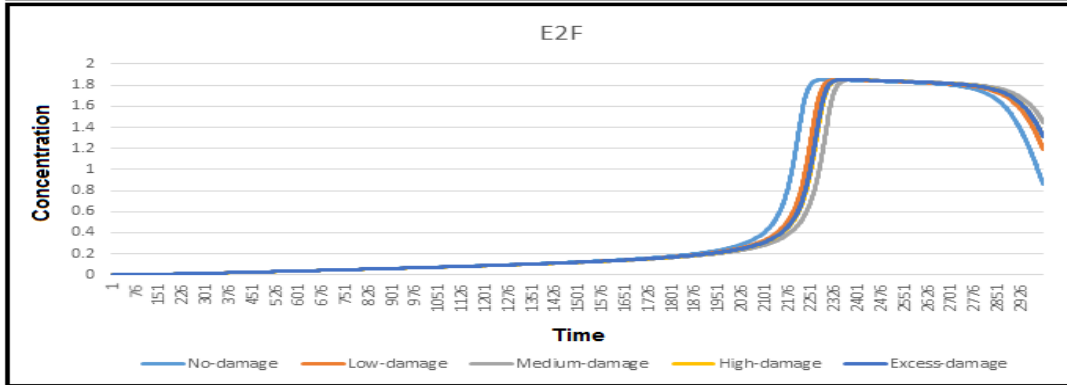
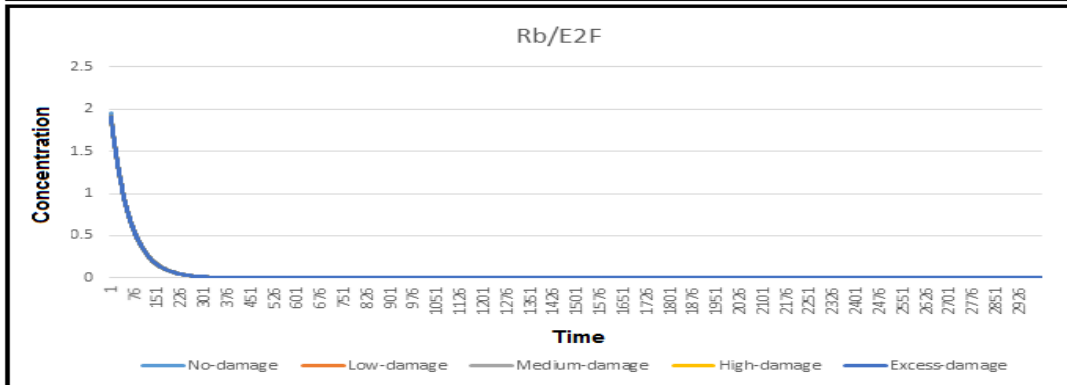
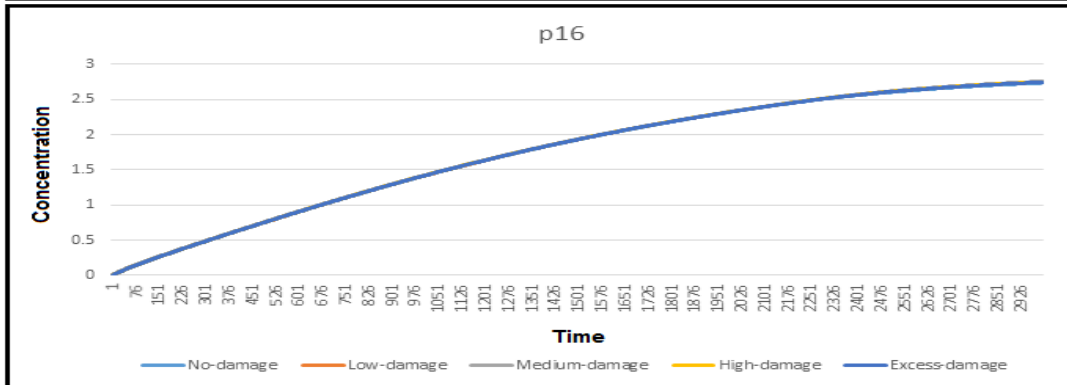
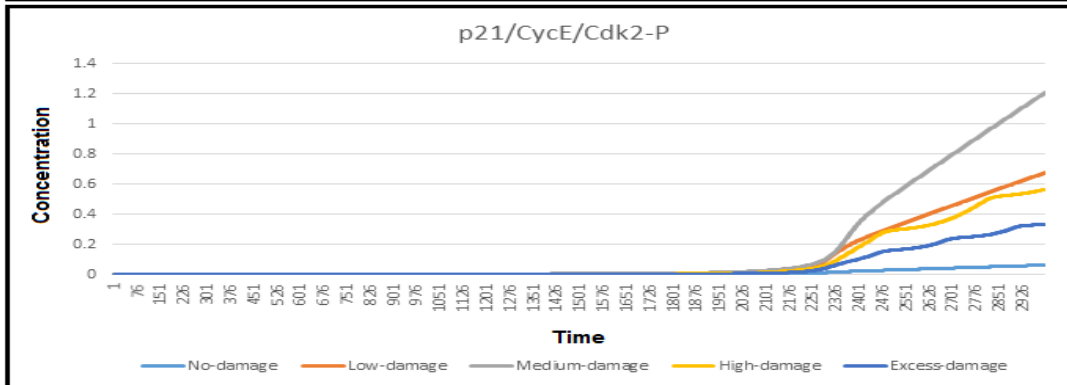
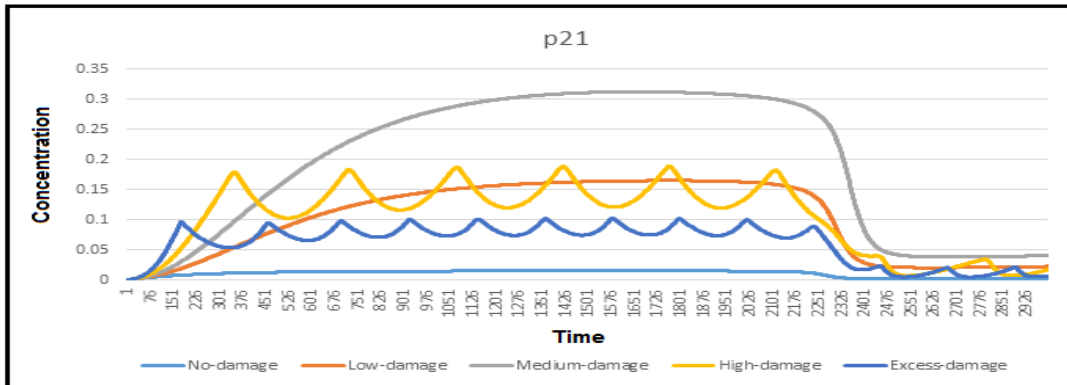


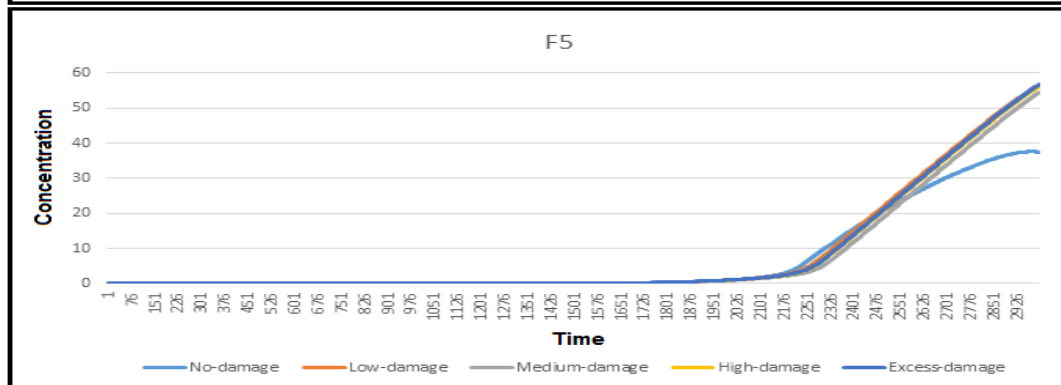
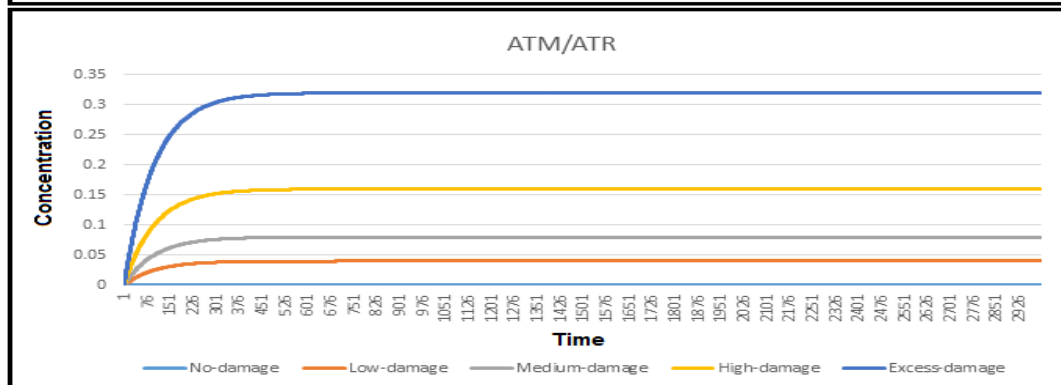
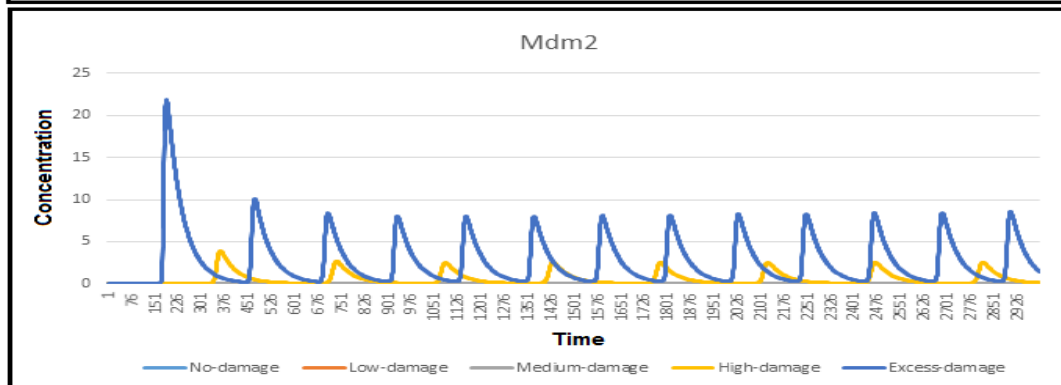
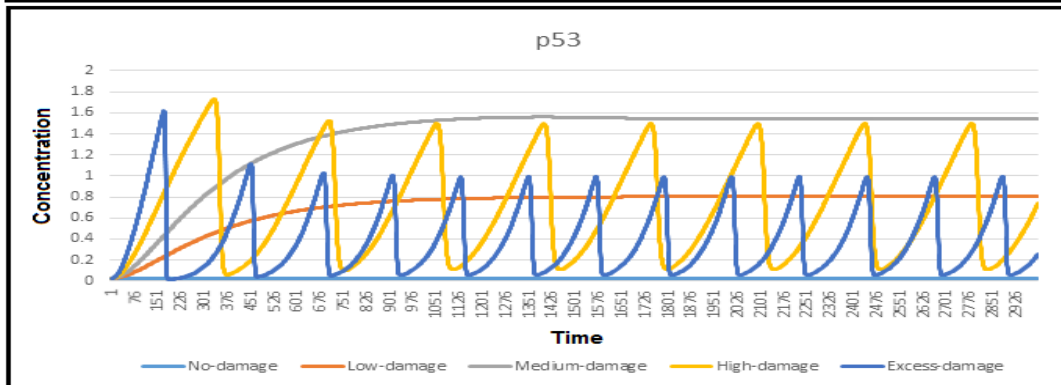
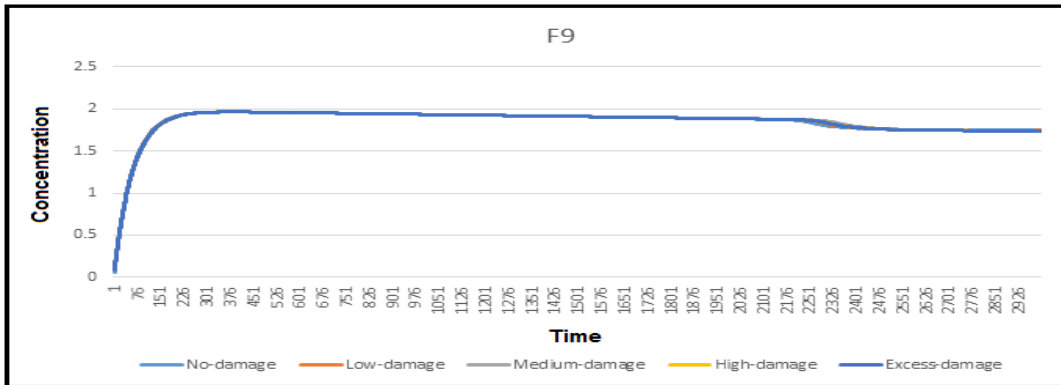


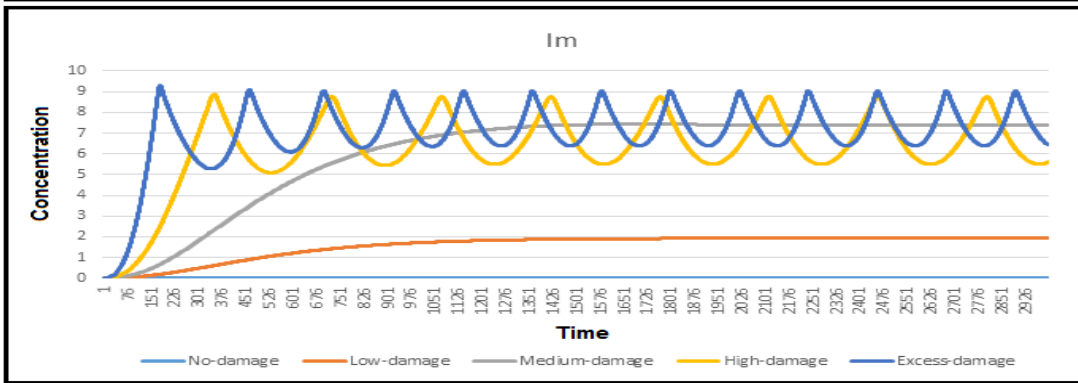
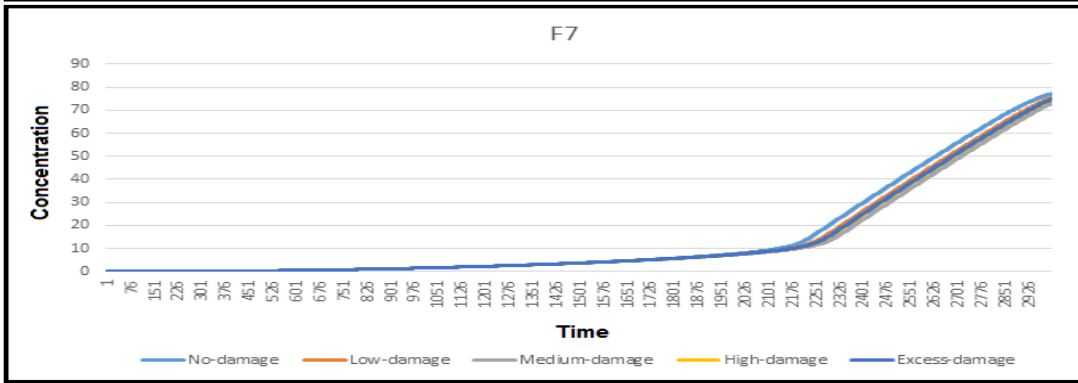
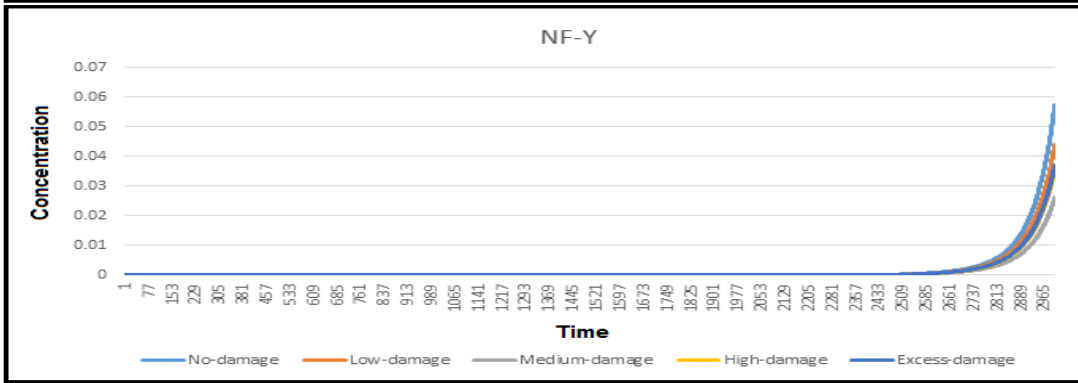
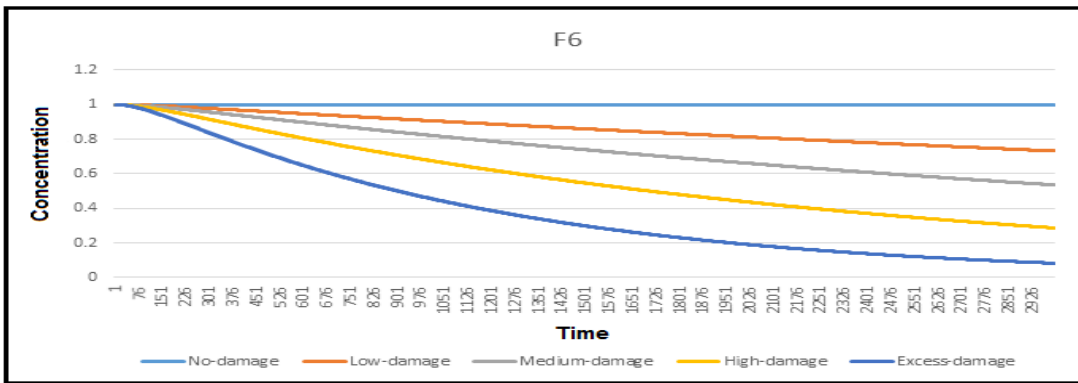
H.2 All time courses of the reduced model (level-3) elements with different levels of DNA damage











Appendix I

ODEs, initial conditions and logical equations of the reduced model (R1) (used for time slicing and logical modelling)

I.1 ODEs of the reduced model (R1)

Table I.1 ODEs of the reduced model (R1)

1	<i>CycD</i>	$dY_1/dt = k_1 + k_4Y_6 - (k_2 + k_3Y_4)Y_1$
2	<i>Cdk4</i>	$dY_4/dt = k_4Y_6 + k_{13}Y_6 - k_3Y_1Y_4$
3	<i>CycD/Cdk4</i>	$dY_6/dt = k_3Y_1Y_4 + k_{19}Y_{16} + k_{21}Y_{12} - (k_4 + k_{13} + k_{18}Y_{15} + k_{20}Y_{11} + k_{44}Y_{19})Y_6$
4	<i>p27</i>	$dY_{11}/dt = k_{34} + k_{21}Y_{12} - (k_{20}Y_6)Y_{11}$
5	<i>p27/CycD/Cdk4</i>	$dY_{12}/dt = k_{20}Y_6Y_{11} - k_{21}Y_{12}$
6	<i>p21</i>	$dY_{15}/dt = k_{37} + k_{38}Y_{25} + k_{19}Y_{16} - (k_{39} + k_{18}Y_6)Y_{15}$
7	<i>p21/CycD/Cdk4</i>	$dY_{16}/dt = k_{18}Y_6Y_{15} - k_{19}Y_{16}$
8	<i>p16</i>	$dY_{19}/dt = k_{40} + k_{41}/(1 + k_{42}Y_{24}) - (k_{43} + k_{44}Y_6)Y_{19}$
9	<i>Rb/E2F</i>	$dY_{20}/dt = - (k_{46}Y_6 + k_{47}Y_{12} + k_{48}Y_{16})Y_{20}$
10	<i>Rb-PP/E2F</i>	$dY_{21}/dt = k_{46}Y_6Y_{20} + k_{47}Y_{12}Y_{20} + k_{48}Y_{16}Y_{20}$
11	<i>Rb</i>	$dY_{24}/dt = k_{56} + k_{58}/(1 + k_{59}Y_{19}) - (k_{57})Y_{24}$
12	<i>p53</i>	$dY_{25}/dt = k_{60} + k_{61}Y_{27} - (deg(t)Y_{26} + k_{62})Y_{25}$
13	<i>Mdm2</i>	$dY_{26}/dt = k_{63} + (k_{66}Im^{50})/(k_{65}^{50} + Im^{50}) - k_{64}Y_{26}$
14	<i>ATM/ATR</i>	$dY_{27}/dt = k_{78}sig(t) - k_{79}Y_{27}$
15	<i>Im</i>	$dIm/dt = k_{70}Y_{25}sig(t)/(1 + k_{71}Y_{25}Y_{26}) - k_{67}Im$
16	<i>Sig</i>	$sig(t) = DDS \times exp(-k_{72} \times time)$
17	<i>Deg</i>	$deg(t) = k_{76} - k_{74} \times (sig(t) - DDS \times exp(-k_{77} \times DDS \times time))$

Abbreviations are as follows: Y1: CycD, Y4: Cdk4, Y6: CycD/Cdk4, Y11: p27, Y12: p27/CycD/Cdk4, Y15: p21, Y16: p21/CycD/Cdk4, Y19: p16, Y20: Rb/E2F, Y21: Rb-PP/E2F, Y24: Rb, Y25: p53, Y26: Mdm2, Y27: ATM/ATR, Im: Intermediate, DDS: DNA damage signal.

I.2 Initial conditions of the reduced model (R1)

Table I.2 Initial conditions of the reduced model (R1)

No	Chemical species	Initial value	No	Chemical species	Initial value
1	<i>CycD</i>	0	8	<i>p16</i>	0
2	<i>Cdk4</i>	1	9	<i>Rb/E2F</i>	1
3	<i>CycD/Cdk4</i>	0	10	<i>Rb-PP/E2F</i>	0
4	<i>p27</i>	1	11	<i>Rb</i>	1
5	<i>p27/CycD/Cdk4</i>	0	12	<i>p53</i>	0
6	<i>p21</i>	0	13	<i>Mdm2</i>	0
7	<i>p21/CycD/Cdk4</i>	0	14	<i>ATM/ATR</i>	0

I.3 Logical equations of the reduced model (R1)

Table I.3 Logical equations of the reduced model (R1)

1	<i>CycD</i>	= <i>GFs</i> And Not (<i>CycD</i> And <i>Cdk4</i>)
2	<i>Cdk4</i>	= <i>Cdk4</i> And Not (<i>CycD</i> And <i>Cdk4</i>)
3	<i>CycD/Cdk4</i>	= (<i>CycD/Cdk4</i> Or (<i>CycD</i> And <i>Cdk4</i>)) And Not <i>p16</i>
4	<i>p27</i>	= <i>p27</i>
5	<i>p27/CycD/Cdk4</i>	= (<i>p27</i> And <i>CycD/Cdk4</i>) Or <i>p27/CycD/Cdk4</i>
6	<i>p21</i>	= <i>p53</i>
7	<i>p21/CycD/Cdk4</i>	= (<i>p21</i> And <i>CycD/Cdk4</i>) Or <i>p21/CycD/Cdk4</i>
8	<i>p16</i>	= <i>p16</i> Or (<i>Rb</i> And <i>CycD/Cdk4</i>)
9	<i>Rb/E2F</i>	= Not (<i>CycD/Cdk4</i> Or <i>p27/CycD/Cdk4</i> Or <i>p21/CycD/Cdk4</i>)
10	<i>Rb-PP/E2F</i>	= <i>Rb-PP/E2F</i> Or (<i>CycD/Cdk4</i> And <i>Rb/E2F</i>)
11	<i>Rb</i>	= Not <i>p16</i>
12	<i>p53</i>	= <i>ATM/ATR</i> And Not <i>Mdm2</i>
13	<i>Mdm2</i>	= <i>p53</i> And Not <i>Mdm2</i>
14	<i>ATM/ATR</i>	= <i>Sig</i>

*** *GFs*: Growth factors equals 1 at t=1, *Sig*: DNA damage signal (0 or 1).

Appendix J

ODEs, initial conditions and logical equations of the reduced model (R2) (used for time slicing and logical modelling)

J.1 ODEs of the reduced model (R2)

Table J.1 ODEs of the reduced model (R2)

1	<i>CycE</i>	$dY_2/dt = k_5Y_{22} + k_8Y_7 - (k_6 + k_7Y_5)Y_2$
2	<i>Cdk2</i>	$dY_5/dt = k_8Y_7 + k_{16}Y_7 + k_{17}Y_8Y_8 - (k_7Y_2)Y_5$
3	<i>CycE/Cdk2</i>	$dY_7/dt = k_7Y_2Y_5 + k_{23}Y_8 - (k_8 + k_{16})Y_7$
4	<i>CycE/Cdk2-P</i>	$dY_8/dt = k_{25}Y_{13} + k_{27}Y_{17} - (k_{23} + k_{24}Y_{11} + k_{26}Y_{15} + k_{17}Y_8)Y_8$
5	<i>p27</i>	$dY_{11}/dt = k_{34} + k_{25}Y_{13} - (k_{35}Y_8 + k_{24}Y_8)Y_{11}$
6	<i>p27/CycE/Cdk2-P</i>	$dY_{13}/dt = k_{24}Y_8Y_{11} - k_{25}Y_{13}$
7	<i>p21</i>	$dY_{15}/dt = k_{37} + k_{38}Y_{25} + k_{27}Y_{17} - (k_{39} + k_{26}Y_8)Y_{15}$
8	<i>p21/CycE/Cdk2-P</i>	$dY_{17}/dt = k_{26}Y_8Y_{15} - k_{27}Y_{17}$
9	<i>Rb-PP/E2F</i>	$dY_{21}/dt = - (k_{49}Y_8)Y_{21}$
10	<i>E2F</i>	$dY_{22}/dt = k_{49}Y_8Y_{21} + k_{51}Y_{22} + k_{52} - (k_{45}Y_{24} + k_{53})Y_{22}$
11	<i>Rb-PPP</i>	$dY_{23}/dt = k_{49}Y_8Y_{21} - k_{55}Y_{23}$
12	<i>p53</i>	$dY_{25}/dt = k_{60} + k_{61}Y_{27} - (deg(t)Y_{26} + k_{62})Y_{25}$
13	<i>Mdm2</i>	$dY_{26}/dt = k_{63} + (k_{66}Im^{50})/(k_{65}^{50} + Im^{50}) - k_{64}Y_{26}$
14	<i>ATM/ATR</i>	$dY_{27}/dt = k_{78}sig(t) - k_{79}Y_{27}$
15	<i>Im</i>	$dIm/dt = k_{70}Y_{25}sig(t)/(1 + k_{71}Y_{25}Y_{26}) - k_{67}Im$
16	<i>Sig</i>	$sig(t) = DDS \times exp(-k_{72} \times time)$
17	<i>Deg</i>	$deg(t) = k_{76} - k_{74} \times (sig(t) - DDS \times exp(-k_{77} \times DDS \times time))$

Abbreviations are as follows: Y2: CycE, Y5: Cdk2, Y7: CycE/Cdk2, Y8: CycE/Cdk2-P, Y11: p27, Y13: p27/CycE/Cdk2-P, Y15: p21, Y17: p21/CycE/Cdk2-P, Y21: Rb-PP/E2F, Y22: E2F, Y23: Rb-PPP, Y25: p53, Y26: Mdm2, Y27: ATM/ATR, Im: Intermediate, DDS: DNA damage signal.

J.2 Initial conditions of the reduced model (R2)

Table J.2 Initial conditions of the reduced model (R2)

No	Chemical species	Initial value	No	Chemical species	Initial value
1	<i>CycE</i>	0	8	<i>p21/CycE/Cdk2-P</i>	0
2	<i>Cdk2</i>	1	9	<i>Rb-PP/E2F</i>	1
3	<i>CycE/Cdk2</i>	0	10	<i>E2F</i>	0
4	<i>CycE/Cdk2-P</i>	1	11	<i>Rb-PPP</i>	0
5	<i>p27</i>	1	12	<i>p53</i>	0
6	<i>p27/CycE/Cdk2-P</i>	0	13	<i>Mdm2</i>	0
7	<i>p21</i>	0	14	<i>ATM/ATR</i>	0

*** Initial values of P53, p21, Mdm2 and ATM/ATR are 1 if there is DNA damage.

J.3 Logical equations of the reduced model (R2)

Table J.3 Logical equations of the reduced model (R2)

1	<i>CycE</i>	= <i>E2F</i> And Not (<i>CycE</i> And <i>Cdk2</i>)
2	<i>Cdk2</i>	= <i>Cdk2</i> And Not (<i>CycE</i> And <i>Cdk2</i>)
3	<i>CycE/Cdk2</i>	= <i>CycE/Cdk2</i> Or (<i>CycE</i> And <i>Cdk2</i>)
4	<i>CycE/Cdk2-P</i>	= (<i>p21/CycE/Cdk2-P</i> Or <i>p27/CycE/Cdk2-P</i> Or <i>CycE/Cdk2</i>)
5	<i>p27</i>	= <i>p27</i> And Not (<i>p27</i> And <i>CycE/Cdk2-P</i>)
6	<i>p27/CycE/Cdk2-P</i>	= <i>p27/CycE/Cdk2-P</i> Or (<i>p27</i> And <i>CycE/Cdk2-P</i>)
7	<i>p21</i>	= <i>p53</i>
8	<i>p21/CycE/Cdk2-P</i>	= <i>p21/CycE/Cdk2-P</i> Or (<i>p21</i> And <i>CycE/Cdk2-P</i>)
9	<i>Rb-PP/E2F</i>	= <i>Rb-PP/E2F</i> And <i>CycE/Cdk2-P</i> And <i>p21</i>
10	<i>E2F</i>	= <i>E2F</i> Or Not (<i>Rb-PP/E2F</i> And <i>CycE/Cdk2-P</i> And <i>p21</i>)
11	<i>Rb-PPP</i>	= <i>Rb-PPP</i> Or Not (<i>Rb-PP/E2F</i> And <i>CycE/Cdk2-P</i> And <i>p21</i>)
12	<i>p53</i>	= <i>ATM/ATR</i> And Not <i>Mdm2</i>
13	<i>Mdm2</i>	= <i>p53</i> And Not <i>Mdm2</i>
14	<i>ATM/ATR</i>	= <i>Sig</i>

*** Sig: DNA damage signal (0 or 1).

References

- Abelson, H., Allen, D., Coore, D., Hanson, C., Homsy, G., Knight Jr, T. F., . . . Weiss, R. (2000). Amorphous computing. *Communications of the ACM*, 43(5), 74-82.
- Aguda, B. D. (1999). A quantitative analysis of the kinetics of the G2 DNA damage checkpoint system. *Proceedings of the National Academy of Sciences*, 96(20), 11352-11357.
- Aguda, B., & Tang, Y. (1999). The kinetic origins of the restriction point in the mammalian cell cycle. *Cell Proliferation*, 32(5), 321-335.
- Albert, I., Thakar, J., Li, S., Zhang, R., & Albert, R. (2008). Boolean network simulations for life scientists. *Source code for biology and medicine*, 3(1), 16.
- Alberts, B., Bray, D., Hopkin, K., Johnson, A., Lewis, J., Raff, M., . . . Walter, P. (2013). *Essential cell biology*: Garland Science.
- Alberts, B., Johnson, A., Lewis, J., Raff, M., Roberts, K., & Walter, P. (2010). *Molecular Biology of the Cell*. New York: Garland Science; 2008. Classic textbook now in its 5th Edition.
- Alcasabas, A. A., de Clare, M., Pir, P., & Oliver, S. G. (2013). Control analysis of the eukaryotic cell cycle using gene copy-number series in yeast tetraploids. *BMC genomics*, 14(1), 744.
- Alfieri, R., Bartocci, E., Merelli, E., & Milanesi, L. (2011). Modeling the cell cycle: From deterministic models to hybrid systems. *Biosystems*, 105(1), 34-40.
- Alves, R., Antunes, F., & Salvador, A. (2006). Tools for kinetic modeling of biochemical networks. *Nature Biotechnology*, 24(6), 667-672.
- Anderson, J., Chang, Y. C., & Papachristodoulou, A. (2011). Model decomposition and reduction tools for large-scale networks in systems biology. *Automatica*, 47(6), 1165-1174.
- Antoulas, A. C. (2005). *Approximation of Large-Scale Dynamical Systems*. SIAM, Philadelphia, Pa, USA.
- Aracena, J., Goles, E., Moreira, A., & Salinas, L. (2009). On the robustness of update schedules in Boolean networks. *Biosystems*, 97(1), 1-8.
- Aubin, J. P. (2010). Macroscopic traffic models: shifting from densities to “celerities”. *Applied Mathematics and Computation*, 217(3), 963-971.
- Azimi, I., Milevskiy, M. J., Kaemmerer, E., Turner, D., Yapa, K. T., Brown, M. A., ... & Monteith, G. R. (2017). TRPC1 is a differential regulator of hypoxia-mediated events and Akt signaling in PTEN-deficient breast cancer cells. *J Cell Sci*, jcs-196659.
- Barillot, E., Calzone, L., Hupe, P., Vert, J. P., & Zinovyev, A. (2012). *Computational systems biology of cancer*. CRC Press.
- Bar-Yam, Y. (2002). General features of complex systems. *Encyclopedia of Life Support Systems (EOLSS)*, UNESCO, EOLSS Publishers, Oxford, UK.
- Bartek, J., Lukas, J., (2003). Chk1 and Chk2 kinases in checkpoint control and cancer. *Cancer Cell* 3 (5), 421–429.
- Behl, C., & Ziegler, C. (2014). *Cell Aging: Molecular Mechanisms and Implications for Disease*: Springer Berlin.
- Bertrand P., Saintigny Y., & Lopez BS. (2004). p53's double life: transactivation-independent repression of homologous recombination. *Trends Genet* 20:235–243.

- Birouche, A., Mourllion, B., & Basset., M., (2012). Model order-reduction for discretetime switched linear systems. *International Journal of Systems Science*, 43(9):1753–1763.
- Bodenstein, M. (1913). Eine theorie der photochemischen reaktionsgeschwindigkeiten. *Zeitschrift für physikalische Chemie*, 85(1), 329-397.
- Botchkarev, A. (2015). Assessing Excel VBA Suitability for Monte Carlo Simulation. arXiv preprint arXiv:1503.08376.
- Bouman, R. (2007). *Microbiology with diseases by taxonomy*: Pearson Benjamin cummings, San Fransisco, Page 56, 88.
- Boyd, R. K. (1978). Some common oversimplifications in teaching chemical kinetics. *J. Chem. Educ*, 55(2), 84.
- Bunge, M. A., & Popper, K. R. (1964). *The Critical Approach to Science and Philosophy*. Edited by Mario Bunge in Honour of Karl R. Popper.
- Calladine, C. R., & Drew, H. (1997). *Understanding DNA: the molecule and how it works*: Academic press.
- Campisi, J., Fabrizio, d.A.d.F., (2007). Cellular senescence: when bad things happen to good cells. *Nat. Rev. Mol. Cell Biol.* 8 (9), 729–740.
- Cantwell, B. (2002). *Introduction to Symmetry Analysis Paperback with CD-ROM (Vol. 29)*. Cambridge University Press.
- Castiglione, F., Pappalardo, F., Bianca, C., Russo, G., & Motta, S. (2014). Modeling biology spanning different scales: an open challenge. *BioMed Research International*.
- Cetin, N. I., Bashirov, R., & Tüzmen, S. (2013). Petri net based modelling and simulation of p16-Cdk4/6-Rb pathway. *Proceedings of CEUR Workshop*, Vol. 988 (pp. 30-44).
- Chae, H.D., Yun, J., Bang, Y.J., Shin, D.Y., (2004). Cdk2-dependent phosphorylation of the NF-Y transcription factor is essential for the expression of the cell cycle-regulatory genes and cell cycle G1/S and G2/M transitions. *Oncogene* 23, 4084–4088.
- Chasapi, A., Wachowicz, P., Niknejad, A., Collin, P., Krapp, A., Cano, E., ... & Xenarios, I. (2015). An extended, Boolean model of the Septation Initiation Network in *S. pombe* provides insights into its regulation. *PloS One*, 10(8), e0134214.
- Chen, H., Wang, G., Simha, R., Du, C., & Zeng, C. (2016). Boolean models of biological processes explain cascade-like behaviour. *Scientific reports*, 7.
- Christiansen, J. A. (1953). The elucidation of reaction mechanisms by the method of intermediates in quasi-stationary concentrations. *Advances in Catalysis*, 5, 311-353.
- Chytas, P., Glykas, M., & Valiris, G. (2011). A proactive balanced scorecard. *International Journal of Information Management*, 31(5), 460-468.
- Ciliberto, A., Novak, B., Tyson, J., (2005). Steady states and oscillations in the p53/Mdm2 network. *Cell Cycle* 4 (3), 488–493.
- Clarke, B. L. (1992). General method for simplifying chemical networks while preserving overall stoichiometry in reduced mechanisms. *The Journal of Chemical Physics*, 97(6), 4066-4071.
- Coqueret, O., (2003). New roles for p21 and p27 cell-cycle inhibitors: a function for each cell compartment? *Trends Cell Biol.* 13 (2), 65–70.

- Courtot, M., Juty, N., Knüpfner, C., Waltemath, D., Zhukova, A., Dräger, A., ... & Hoops, S. (2011). Controlled vocabularies and semantics in systems biology. *Molecular Systems Biology*, 7(1), 543.
- Crick, F. (1970). Central dogma of molecular biology. *Nature*, 227(5258), 561-563.
- Crudu, A., Debussche, A., & Radulescu, O. (2009). Hybrid stochastic simplifications for multiscale gene networks. *BMC Systems Biology*, 3(1), 1.
- Danos, V., Feret, J., Fontana, W., Harmer, R., & Krivine, J. (2007). Rule-based modelling of cellular signalling. In *International Conference on Concurrency Theory* (pp. 17-41). Springer Berlin Heidelberg.
- Desai U. B. and Pal. D. (1984). A transformation approach to stochastic model reduction. *IEEE Transactions on Automatic Control*, 29(2):1097–1100.
- Di Cara, A., Garg, A., De Micheli, G., Xenarios, I., & Mendoza, L. (2007). Dynamic simulation of regulatory networks using SQUAD. *BMC Bioinformatics*, 8(1), 462.
- Dokoumetzidis, A., & Aarons, L. (2009). Proper lumping in systems biology models. *IET Systems Biology*, 3(1), 40-51.
- Donjerkovic, D., & Scott, D. W. (2000). Regulation of the G1 phase of the mammalian cell cycle. *Cell research*, 10(1), 1.
- Doolittle, W. F. (2000). Uprooting the tree of life. *Scientific American*, 282(2), 90.
- Dsilva, C. J., Talmon, R., Gear, C. W., Coifman, R. R., & Kevrekidis, I. G. (2015). Data-driven reduction for multiscale stochastic dynamical systems. *arXiv preprint arXiv:1501.05195*.
- Dulic, V., Kaufmann, W.K., Wilson, S.J., Tisty, T.D., Lees, E., Harper, J.W., Elledge, S.J., Reed, S.I., (1994). p53 - dependent inhibition of cyclin-dependent kinase activities in human fibroblasts during radiation-induced G1 arrest. *Cell* 76 (6), 1013–1023.
- Endy, D., & Brent, R. (2001). Modelling cellular behaviour. *Nature*, 409(6818), 391-395.
- Enns, D. (1984). Model reduction with balanced realizations: An error bound and a frequency weighted generalization. In *Proceedings of the 23rd IEEE conference on Decision and Control*, volume 23, pages 127–132.
- Ermentrout, B. (2002). *Simulating, Analyzing, and Animating Dynamical Systems: A Guide to XPPAUT for Researchers and Students*. Soc. for Industrial and Applied Math, Philadelphia.
- Farr, K. J., Gallaway, P. J., & Hongu, N. (2017). *Breast Cancer Prevention: Exercise and Healthy Diet*. The University of Arizona Cooperative Extension.
- Fauré, A., Naldi, A., Chaouiya, C., & Thieffry, D. (2006). Dynamical analysis of a generic Boolean model for the control of the mammalian cell cycle. *Bioinformatics*, 22(14), e124-e131.
- Fauré, A., Naldi, A., Lopez, F., Chaouiya, C., Ciliberto, A., & Thieffry, D. (2009). Modular logical modelling of the budding yeast cell cycle. *Molecular BioSystems*, 5(12), 1787-1796.
- Feldman P. & Freund. R. W. (1995). Efficient linear circuit analysis by Pade approximation via a Lanczos method. *IEEE Transactions on Computer-aided Design*, 14:639–649.
- Fenichel, N. (1979). Geometric singular perturbation theory for ordinary differential equations. *Journal of Differential Equations*, 31(1), 53-98.
- Feret, J., Danos, V., Krivine, J., Harmer, R., & Fontana, W. (2009). Internal coarse-graining of molecular systems. *Proceedings of the National Academy of Sciences*, 106(16), 6453-6458.

- Fuxreiter, M. (2012). Fuzziness: linking regulation to protein dynamics. *Molecular BioSystems*, 8(1), 168-177.
- Gallagher, P. M., Athayde, A. L., & Ivory, C. F. (1986). The combined flux technique for diffusion reaction problems in partial equilibrium: Application to the facilitated transport of carbon dioxide in aqueous bicarbonate solutions. *Chemical Engineering Science*, 41(3), 567-578.
- Gallagher, R., Appenzeller, T., & Normile, D. (1999). Beyond reductionism. *Science*, 284(5411), 79.
- Gao, H., Lam, J & Wang, C. (2006). Model simplification for switched hybrid systems. *Systems and Control Letters*, 55(12):1015–1021.
- Gatei, M., Sloper, K., Sørensen, C.S., Syljuåsen, R., Falck, J., Hobson, J., Zhou, B.-B., Bartek, J., and Khanna, K.K. (2003). ATM and DBS1 dependent phosphorylation of CHK1 on S317 in response to IR. *J. Biol. Chem.* 278, 14806–14811. Published online February 14, 2003. 10.1074/jbc.M210862200.
- Gatz SA., & Wiesmüller L. (2006). p53 in recombination and repair. *Cell Death Differ* 13:1003–1006.
- Gay, S., Soliman, S., & Fages, F. (2010). A graphical method for reducing and relating models in systems biology. *Bioinformatics*, 26(18), i575-i581.
- Genyuan, L. (1984). A lumping analysis in mono-or/and bimolecular reaction systems. *Chemical Engineering Science*, 39(7-8), 1261-1270.
- Gest, H. (2004). The discovery of microorganisms by Robert Hooke and Antoni Van Leeuwenhoek, fellows of the Royal Society. *Notes and records of the Royal Society of London*, 58(2), 187-201.
- Geva-Zatorsky, N., Rosenfeld, N., Itzkovitz, S., Milo, R., Sigal, A., Dekel, E., Yarnitzky, T., Liron, Y., Polak, P., Lahav, G., Alon, U., (2006). Oscillations and variability in the p53 system. *Mol. Syst. Biol.*, 2.
- Goldenfeld, N., & Kadanoff, L. P. (1999). Simple lessons from complexity. *Science*, 284(5411), 87-89.
- Gonzalez, A. G., Naldi, A., Sanchez, L., Thieffry, D., & Chaouiya, C. (2006). GINsim: a software suite for the qualitative modelling, simulation and analysis of regulatory networks. *Biosystems*, 84(2), 91-100.
- Gorban, A. N., & Karlin, I. V. (2003). Method of invariant manifold for chemical kinetics. *Chemical Engineering Science*, 58(21), 4751-4768.
- Gorban, A. N., Karlin, I. V., & Zinovyev, A. Y. (2004A). Constructive methods of invariant manifolds for kinetic problems. *Physics Reports*, 396(4), 197-403.
- Gorban, A. N., Karlin, I. V., & Zinovyev, A. Y. (2004B). Invariant grids for reaction kinetics. *Physica A: Statistical Mechanics and its Applications*, 333, 106-154.
- Gorban, A., Karlin, I., & Zinovyev, A. (2004C). Invariant grids: Method of complexity reduction in reaction networks. *Complexus*, 2(3-4), 110-127.
- Gorban, A., & Karlin, I. (2005). Invariant manifolds for physical and chemical kinetics. *Lecture Notes in Physics*, 660, 1-489.
- Gorban, A. N., & Radulescu, O. (2008). Dynamic and static limitation in multiscale reaction networks, revisited. *Advances in Chemical Engineering*, 34, 103-173.
- Gorban, A. N. (2009). Multigrid Integrators on Multiscale Reaction Networks. Keynote talk given at Algorithms for Approximation VI.
- Gorban, A. N., Radulescu, O., & Zinovyev, A. Y. (2010). Asymptotology of chemical reaction networks. *Chemical Engineering Science*, 65(7), 2310-2324.
- Gorban, A. N., & Yablonsky, G. S. (2013). Grasping complexity. arXiv preprint arXiv:1303.3855.

- Grimme, E. J. (1997). Krylov Projection Methods for Model Reduction. PhD thesis, ECE Dept., U. of Illinois, Urbana-Champaign.
- Guo, Y., Wu, W., Zhang, B., & Sun, H. (2015). A distributed state estimation method for power systems incorporating linear and nonlinear models. *International Journal of Electrical Power & Energy Systems*, 64, 608-616.
- Haberichter, T., Mädge, B., Christopher, R. A., Yoshioka, N., Dhiman, A., Miller, R., . . . Dowdy, S. F. (2007). A systems biology dynamical model of mammalian G1 cell cycle progression. *Molecular Systems Biology*, 3(1) pp. 149-166.
- Hanahan, D., & Weinberg, R. A. (2011). Hallmarks of cancer: the next generation. *cell*, 144(5), 646-674.
- Harary, F., Norman, R. Z., & Cartwright, D. (1965). *Structural Models: An Introduction to the Theory of Directed Graphs* New York: John Wiley & Sons.
- Harris, S.L., Levine, A.J., (2005). The p53 pathway: positive and negative feedback loops. *Oncogene* 24, 2899–2908.
- Hartwell, L. H., & Weinert, T. A. (1989). Checkpoints: controls that ensure the order of cell cycle events. *Science* 246: 629–634.
- Hase, T., Tanaka, H., Suzuki, Y., Nakagawa, S., & Kitano, H. (2009). Structure of protein interaction networks and their implications on drug design. *PLoS Comput Biol*, 5(10), e1000550.
- Hasty, J., McMillen, D., Isaacs, F., & Collins, J. J. (2001). Computational studies of gene regulatory networks: in numero molecular biology. *Nature Reviews Genetics*, 2(4), 268-279.
- Hatzimanikatis, V., Lee, K., & Bailey, J. (1999). A mathematical description of regulation of the G1-S transition of the mammalian cell cycle. *Biotechnology and Bioengineering*, 65(6), 631-637.
- Hatzimanikatis, V., Lee, K. H., Renner, W. A., & Bailey, J. E. (1995). A mathematical model for the G1/S transition of the mammalian cell cycle. *Biotechnology Letters*, 17(7), 669-674.
- Helffferich, F. G. (1989). Systematic approach to elucidation of multistep reaction networks. *The Journal of Physical Chemistry*, 93(18), 6676-6681.
- Helikar, T., & Rogers, J. A. (2009). ChemChains: a platform for simulation and analysis of biochemical networks aimed to laboratory scientists. *BMC Systems Biology*, 3(1), 58.
- Helikar, T., Kowal, B., & Rogers, J. A. (2013). A cell simulator platform: the cell collective. *Clin. Pharmacol. Ther.* 93, 393–395. doi:10.1038/clpt.2013.41.
- Helin, K., (1998). Regulation of cell proliferation by the E2F transcription factors. *Curr. Opin. Genet.* 8, 28–35.
- Herajy, M., Schwarick, M., & Heiner, M. (2013). Hybrid Petri Nets for Modelling the Eukaryotic Cell Cycle Transactions on Petri Nets and Other Models of Concurrency VIII pp. 123-141: Springer.
- Hlavacek, W. S. (2009). How to deal with large models?. *Molecular Systems Biology*, 5(1), 240. Ho, M. W. (2004). Death of the central dogma. *Science in Society*, 24(4).
- Huang, H., Fairweather, M., Tomlin, A. S., Griffiths, J. F., & Brad, R. B. (2005). A dynamic approach to the dimension reduction of chemical kinetic schemes. *Computer Aided Chemical Engineering*, 20, 229-234.
- Huang, S., & Ingber, D. E. (2000). Shape-dependent control of cell growth, differentiation, and apoptosis: switching between attractors in cell regulatory networks. *Experimental Cell Research*, 261(1), 91-103.

- Hurty, W. C. (1965). Dynamic analysis of structural systems using component modes. *AIAA journal*, 3(4), 678-685.
- Ideker T, Galitski T, Hood L (2001). A new approach to decoding life: systems biology. *Annual review of Genomics and Human Genetics* 2: 343-372.
- Ideker, T., Winslow, L. R., & Lauffenburger, D. A. (2006). Bioengineering and systems biology. *Annals of Biomedical Engineering*, 34(7), 1226-1233.
- Imura, J. (2012). Clustered model reduction of large-scale complex networks. In proceeding of the 20th International Symposium on Mathematical Theory of Networked and Systems, Melbourne, Australia.
- Irons, D. J. (2009). Logical analysis of the budding yeast cell cycle. *Journal of Theoretical Biology*, 257(4), 543-559.
- Isambert, H., & Stein, R. R. (2009). On the need for widespread horizontal gene transfers under genome size constraint. *Biology Direct*, 4(1), 1.
- Ishizaki, T., Kashima, K., Imura, J. & Aihara, K. (2012). Model reduction of multiinput dynamical networks based on clusterwise controllability. In Proc. of American Control Conference, pages 2301–2306.
- Ishizaki, T., Kashima, K., Imura, J. I., & Aihara, K. (2014). Model reduction and clusterization of large-scale bidirectional networks. *IEEE Transactions on Automatic Control*, 59(1), 48-63.
- Iwamoto, K., Hamada, H., Eguchi, Y., & Okamoto, M. (2011). Mathematical modeling of cell cycle regulation in response to DNA damage: exploring mechanisms of cell-fate determination. *Biosystems*, 103(3), 384-391.
- Iwamoto, K., Tashima, Y., Hamada, H., Eguchi, Y., & Okamoto, M. (2006). Mathematical Modeling of G1/S Phase in the Cell Cycle with Involving the p53/Mdm2 Network.
- Iwamoto, K., Tashima, Y., Hamada, H., Eguchi, Y., & Okamoto, M. (2008). Mathematical modeling and sensitivity analysis of G1/S phase in the cell cycle including the DNA-damage signal transduction pathway. *Biosystems*, 94(1), 109-117.
- Jacobs, J.J., de Lange, T., (2004). Significant role for p16(INK4a) in p53-independent telomere-directed senescence. *Curr. Biol.* 14, 2302–2308.
- Jaimoukha I. M. & Kasenally E. M. (1997). Implicitly restarted Krylov subspace methods for stable partial realizations. *SIAM Journal on Matrix Analysis and Applications*, 18:633–652.
- Johnson, S. (2001). *The connected lives of ants, brains, cities and software*: Penguin.
- Johnston, H. S. (1966). *Gas phase reaction rate theory*. Ronald Press Co.
- Jones, C. (1995). Geometric singular perturbation theory. *Dynamical Systems*, 44-118.
- Judson, O. P. (1994). The rise of the individual-based model in ecology. *Trends in Ecology & Evolution*, 9(1), 9-14.
- Karadeniz, H., Soyhan, H. S., & Sorusbay, C. (2012). Reduction of large kinetic mechanisms with a new approach to the necessity analysis method. *Combustion and Flame*, 159(4), 1467-1480.
- Kauffman, S. A. (1969). Metabolic stability and epigenesis in randomly constructed genetic nets. *Journal of Theoretical Biology*, 22(3), 437-467.
- Kauffman, S. A. (1976). Articulation of parts explanation in biology and the rational search for them. In *Topics in the Philosophy of Biology* (pp. 245-263). Springer Netherlands.

- Kholodenko, B. N. (2006). Cell-signalling dynamics in time and space. *Nature Reviews Molecular Cell Biology*, 7(3), 165-176.
- Kim, P. S., Levy, D., & Lee, P. P. (2009). Modeling and simulation of the immune system as a self-regulating network. *Methods in Enzymology*, 467, 79-109.
- King, M. C., Marks, J. H., & Mandell, J. B. (2003). Breast and ovarian cancer risks due to inherited mutations in BRCA1 and BRCA2. *Science*, 302(5645), 643-646.
- Kitano, H. (2002). Computational systems biology. *Nature*, 420(6912), 206-210.
- Kitano, H. (2004). Biological robustness. *Nature Reviews Genetics*, 5(11), 826-837.
- Koch, C., & Laurent, G. (1999). Complexity and the nervous system. *Science*, 284(5411), 96-98.
- Kohn, K. W. (1998). Functional capabilities of molecular network components controlling the mammalian G1/S cell cycle phase transition. *Oncogene*, 16(8).
- Kohn, K. W. (1999). Molecular interaction map of the mammalian cell cycle control and DNA repair systems. *Molecular Biology of the Cell*, 10(8), 2703-2734.
- Koonin, E. V. (2009). The Origin at 150: is a new evolutionary synthesis in sight?. *Trends in Genetics*, 25(11), 473-475.
- Koonin, E. V., & Wolf, Y. I. (2009). Is evolution Darwinian or/and Lamarckian?. *Biology Direct*, 4(1), 42.
- Kooshkbaghi, M., Frouzakis, C. E., Boulouchos, K., & Karlin, I. V. (2014). Entropy production analysis for mechanism reduction. *Combustion and Flame*, 161(6), 1507-1515.
- Kotani, S., Yoshioka, T., & Konagaya, A. (2002). A Computational Model of Mammalian Cell Cycle Using Petri Nets. *Genome Informatics Series*, 459-460.
- Kourdis, P. D., Palasantza, A. G., & Goussis, D. A. (2013). Algorithmic asymptotic analysis of the NF- κ B signaling system. *Computers & Mathematics with Applications*, 65(10), 1516-1534.
- Krauskopf, B., Osinga, H. M., Doedel, E. J., Henderson, M. E., Guckenheimer, J., Vladimirov, A., Dellnitz, M., & Junge, O. (2005). A survey of methods for computing (un) stable manifolds of vector fields. *International Journal of Bifurcation and Chaos*, 15(03), 763-791.
- Krumsiek, J., Pölsterl, S., Wittmann, D. M., & Theis, F. J. (2010). Odefy—from discrete to continuous models. *BMC bioinformatics*, 11(1), 233.
- Kruskal, M. (1963). Asymptotology, *Proceedings of Conference on Mathematical Models on Physical Sciences Englewood Cliffs, NJ: Prentice–Hall*, 17–48.
- Kruskal, M. D., & Drobot, S. (1963). *Mathematical models in physical sciences*. S. Drobot Ed., pp. 17–48.
- Kutumova, E., Zinovyev, A., Sharipov, R., & Kolpakov, F. (2013). Model composition through model reduction: a combined model of CD95 and NF- κ B signaling pathways. *BMC Systems Biology*, 7(1), 1.
- LaBaer, I., Garrett, M.D., Stevenson, L.F., Slingerland, J.M., Sandhu, C., Chou, H.S., Fattaey, A., Harlow, E. (1997). New functional activities for the p21 family of CDK inhibitors. *Genes Dev.* 11 (7), 847–862.
- Lahav, G., Rosenfeld, N., Sigal, A., Geva-Zatorsky, N., Levine, A.J. (2004). Dynamics of the p53-Mdm2 feedback loop in individual cells. *Nat. Genet.* 36, 147–150.
- Lam, S. H., & Goussis, D. A. (1994). The CSP method for simplifying kinetics. *International Journal of Chemical Kinetics*, 26(4), 461-486.

- Le Novere, N. (2015). Quantitative and logic modelling of gene and molecular networks. *Nature Reviews. Genetics*, 16(3), 146.
- Lee, C. H., & Othmer, H. G. (2010). A multi-time-scale analysis of chemical reaction networks: I. Deterministic systems. *Journal of Mathematical Biology*, 60(3), 387-450.
- Lee, K. J., McCormick, W. D., Ouyang, Q., & Swinney, H. L. (1993). Pattern formation by interacting chemical fronts. *Science-New York then Washington-*, 261, 192-192.
- Lee, T. J., Tan, C. M., Tu, D., & You, L. C. (2007). Modelling cellular networks. *Bioinformatics: An Engineering Case-based Approach*, 151-172.
- Lev Bar-Or, R., Maya, R., Lee, A.S., Uri, A., Arnold, J.L., Moshe, O., (2000). Generation of oscillations by the p53-Mdm2 feedback loop: a theoretical and experimental study. *Proc. Natl. Acad. Sci. U.S.A.* 97, 11250–11255.
- Li, F., Long, T., Lu, Y., Ouyang, Q., & Tang, C. (2004). The yeast cell-cycle network is robustly designed. *Proceedings of the National Academy of Sciences of the United States of America*, 101(14), 4781-4786.
- Li, G., & Ho, V. (1998). p53-dependent DNA repair and apoptosis respond differently to high-and low-dose ultraviolet radiation. *British Journal of Dermatology*, 139(1), 3-10.
- Li, G., & Rabitz, H. (1989). A general analysis of exact lumping in chemical kinetics. *Chemical Engineering Science*, 44(6), 1413-1430.
- Li, G., & Rabitz, H. (1990). A general analysis of approximate lumping in chemical kinetics. *Chemical Engineering Science*, 45(4), 977-1002.
- Li, G., & Rabitz, H. (1991). A general lumping analysis of a reaction system coupled with diffusion. *Chemical Engineering Science*, 46(8), 2041-2053.
- Li, G., Rabitz, H., & Tóth, J. (1994). A general analysis of exact nonlinear lumping in chemical kinetics. *Chemical Engineering Science*, 49(3), 343-361.
- Li, M., Wang, I. X., Li, Y., Bruzel, A., Richards, A. L., Toung, J. M., & Cheung, V. G. (2011). Widespread RNA and DNA sequence differences in the human transcriptome. *Science*, 333(6038), 53-58.
- Lin, C. A. & Chiu, T. Y. (1992). Model reduction via frequency weighted balanced realization. *Control Theory and Advanced Technology*, 8:341–351.
- Ling, H., Kulasiri, D., & Samarasinghe, S. (2010). Robustness of G1/S checkpoint pathways in cell cycle regulation based on probability of DNA-damaged cells passing as healthy cells. *Biosystems*, 101(3), 213-221.
- Ling, H., Samarasinghe, S., & Kulasiri, D. (2013a). Computational experiments reveal the efficacy of targeting CDK2 and CKIs for significantly lowering cellular senescence bar for potential cancer treatment. *Biosystems*, 111(2), 71-82.
- Ling, H., Samarasinghe, S., & Kulasiri, D. (2013b). Novel recurrent neural network for modelling biological networks: Oscillatory p53 interaction dynamics. *Biosystems*, 114(3), 191-205.
- Linke, C., Chasapi, A., González-Novo, A., Al Sawad, I., Tognetti, S., Klipp, E., ... & Barberis, M. (2017). A Clb/Cdk1-mediated regulation of Fkh2 synchronizes CLB expression in the budding yeast cell cycle. *npj Systems Biology and Applications*, 3, 1.
- Litvinov, G. L., & Maslov, V. P. (1996). Idempotent mathematics: a correspondence principle and its applications to computing. *Russian Mathematical Surveys*, 51(6), 1210-1211.
- Lu, T., Ju, Y., & Law, C. K. (2001). Complex CSP for chemistry reduction and analysis. *Combustion and Flame*, 126(1), 1445-1455.

- Lukas, C., Bartkova, J., Latella, L., Falck, J., Mailand, N., Schroeder, T., Sehested, M., Lukas, J., and Bartek, J. (2001). DNA damage-activated kinase Chk2 is independent of proliferation or differentiation yet correlates with tissue biology. *Cancer Res.* 61, 4990–4993.
- Lundberg, A.S., Weinberg, R.A., (1998). Functional inactivation of the retinoblastoma protein requires sequential modification by at least two distinct cyclin-cdk complexes. *Mol. Cell. Biol.* 18, 753–761.
- Maas, U., & Pope, S. B. (1992). Simplifying chemical kinetics: intrinsic low-dimensional manifolds in composition space. *Combustion and Flame*, 88(3), 239-264.
- Maas, U., & Pope, S. B. (1994). Laminar flame calculations using simplified chemical kinetics based on intrinsic low-dimensional manifolds. In *Symposium (International) on Combustion (Vol. 25, No. 1, pp. 1349-1356)*. Elsevier.
- Matheson, I., Walls, D. F., & Gardiner, C. W. (1975). Stochastic models of firstorder nonequilibrium phase transitions in chemical reactions. *Journal of Statistical Physics*, 12(1), 21-34.
- Matthews, M. L., & Williams, C. M. (2012). Region of attraction estimation of biological continuous Boolean models. In *2012 IEEE International Conference on Systems, Man, and Cybernetics (SMC)* (pp. 1700-1705). IEEE.
- Maurya, M. R., Bornheimer, S. J., Venkatasubramanian, V., & Subramaniam, S. (2009). Mixed-integer nonlinear optimisation approach to coarse-graining biochemical networks. *IET Systems Biology*, 3(1), 24-39.
- Mayes, J. (2012). *Reduction and Approximation in Large and Infinite Potential-Driven Flow Networks* (Doctoral dissertation, University of Notre Dame).
- McNeil, K. J., & Walls, D. F. (1974). Nonequilibrium phase transitions in chemical reactions. *Journal of Statistical Physics*, 10(6), 439-448.
- Michaelis, L., & Menten, M. L. (1913). Die kinetik der invertinwirkung. *Biochem. z.* 49(333-369), 352.
- Miller, J. H., & Page, S. E. (2007). *Complex Adaptive Systems: An introduction to computational models of social life*, pp. 288-301.
- Momand, J., Wu, H.-H., & Dasgupta, G. (2000). MDM2—master regulator of the p53 tumor suppressor protein. *Gene*, 242(1), 15-29.
- Mombach, J. C., Bugs, C. A., & Chaouiya, C. (2014). Modelling the onset of senescence at the G1/S cell cycle checkpoint. *BMC Genomics*, 15(7), S7.
- Monshizadeh, N. (2013). *Model reduction and control of complex systems* (Doctoral dissertation, PhD thesis, University of Groningen).
- Moore, B. C. (1981). Principle component analysis in linear system: controllability, observability and model reduction. *IEEE Transactions on Automatic Control*, AC-26.
- Mullis, C. T. & Roberts, R. A. (1976). Synthesis of minimum roundoff noise fixed point digital filters. *IEEE Transactions on Circuits and Systems*, CAS-23:551–562.
- Murdoch, J. R. (1981). What is the rate-limiting step of a multistep reaction?. *J. Chem. Educ*, 58(1), 32.
- Müssel, C., Hopfensitz, M., & Kestler, H. A. (2010). BoolNet—an R package for generation, reconstruction and analysis of Boolean networks. *Bioinformatics*, 26(10), 1378-1380.
- Nagy, T., & Turányi, T. (2009). Reduction of very large reaction mechanisms using methods based on simulation error minimization. *Combustion and Flame*, 156(2), 417-428.

- Nägele, T., Henkel, S., Hörmiller, I., Sauter, T., Sawodny, O., Ederer, M., & Heyer, A. G. (2010). Mathematical modeling of the central carbohydrate metabolism in Arabidopsis reveals a substantial regulatory influence of vacuolar invertase on whole plant carbon metabolism. *Plant Physiology*, 153(1), 260-272.
- Neves, S. R., & Iyengar, R. (2002). Modeling of signaling networks. *Bioessays*, 24(12), 1110-1117.
- Nigg, E. A. (1995). Cyclin-dependent protein kinases: key regulators of the eukaryotic cell cycle. *Bioessays*, 17(6), 471-480.
- Nitzan, A., Ortoleva, P., Deutch, J., & Ross, J. (1974). Fluctuations and transitions at chemical instabilities: The analogy to phase transitions. *The Journal of Chemical Physics*, 61(3), 1056-1074.
- Noel, V., Grigoriev, D., Vakulenko, S., & Radulescu, O. (2012). Hybrid models of the cell cycle molecular machinery.
- Noel, V., Grigoriev, D., Vakulenko, S., & Radulescu, O. (2012). Tropical geometries and dynamics of biochemical networks application to hybrid cell cycle models. *Electronic Notes in Theoretical Computer Science*, 284, 75-91.
- Noel, V., Vakulenko, S., & Radulescu, O. (2010). Piecewise smooth hybrid systems as models for networks in molecular biology. In *Proceedings of JOBIM*.
- Noel, V., Vakulenko, S., & Radulescu, O. (2011). Algorithm for identification of piecewise smooth hybrid systems: application to eukaryotic cell cycle regulation. In *International Workshop on Algorithms in Bioinformatics* (pp. 225-236). Springer Berlin Heidelberg.
- Novak B., Sible J.C., & Tyson, J.J. (2002). Checkpoints in the cell cycle. In: *Encyclopedia of life sciences*. Macmillan Publishers Ltd., Nature Publishing Group.
- Novak, B., & Tyson, J. J. (2004). A model for restriction point control of the mammalian cell cycle. *Journal of Theoretical Biology*, 230(4), 563-579.
- Nowell, P. C., & Hungerford, D. A. (1960). Chromosome studies on normal and leukemic human leukocytes. *Journal of the National Cancer Institute*, 25(1), 85-109.
- Obaya, A.J., Sedivy, J.M., (2002). Regulation of cyclin-Cdk activity in mammalian cells. *Cell. Mol. Life Sci.* 59, 126–142.
- Ober, R. (1991). Balanced parametrization of classes of linear systems. *SIAM Journal of Control and Optimization*, 29(6):1251–1287.
- Obeyesekere, M., Knudsen, E., Wang, J., & Zimmerman, S. (1997). A mathematical model of the regulation of the G1 phase of Rb^{+/+} and Rb^{-/-} mouse embryonic fibroblasts and an osteosarcoma cell line. *Cell Proliferation*, 30(3-4), 171-194.
- Obeyesekere, M. N., Zimmerman, S. O., Tecarro, E. S., & Auchmuty, G. (1999). A model of cell cycle behaviour dominated by kinetics of a pathway stimulated by growth factors. *Bulletin of Mathematical Biology*, 61(5), 917-934.
- Ohtsubo, M., Theodoras, A.M., Schumacher, J., Roberts, J.M., Pagano, M., (1995). Human cyclin E, a nuclear protein essential for the G1-to-S phase transition. *Mol. Cell. Biol.* 15, 2612–2624.
- Opdenacker P. C. and Jonckheere. E. A. (1988). A contraction mapping preserving balanced reduction scheme and its infinity norm error bounds. *IEEE Transactions on Circuits and Systems*, CAS-35:184–189.
- Pachter, L., & Sturmfels, B. (2004). Tropical geometry of statistical models. *Proceedings of the National Academy of Sciences of the United States of America*, 101(46), 16132-16137.

- Palmer, C., & Chung, P. W. H. (1998). Eliminating ambiguities in qualitative causal feedback Proceedings of Computers & Chemical Engineering, 22, S843-S846.
- Palsson, B. (2006). Properties of Reconstructed Networks. Cambridge: Systems Biology.
- Parry, D., Bates, S., Mann, D.J., Peters, G., (1995). Lack of cyclin D-Cdk complexes in Rb-negative cells correlates with high levels of p16INK4/MTS1 tumour suppressor gene product. EMBO J. 14 (3), 503–511.
- Pawson, T., & Nash, P. (2000). Protein–protein interactions define specificity in signal transduction. Genes & Development, 14(9), 1027-1047.
- Pernebo, L. & Silverman, L.M. (1982). Model reduction via balanced state space representation. IEEE Transactions on Automatic Control, AC-27:382–387.
- Petzold, L., & Zhu, W. (1999). Model reduction for chemical kinetics: An optimization approach. American Institute of Chemical Engineers. AIChE Journal, 45(4), 869.
- Popovici, C. (2010). Aspects of DNA cryptography. Annals of the University of Craiova-Mathematics and Computer Science Series, 37(3), 147-151.
- Pramanik, J., Keasling, J. (1997). Stoichiometric model of Escherichia coli metabolism: Incorporation of growth-rate dependent biomass composition and mechanistic energy requirements. Biotechnology and Bioengineering 56: 398-421.
- Prigogine, I., & Stengers, I. (1997). The end of certainty. Simon and Schuster.
- Prescott, T. P., & Papachristodoulou, A. (2014). Layered decomposition for the model order reduction of timescale separated biochemical reaction networks. Journal of Theoretical Biology, 356, 113-122.
- Price ND, Reed JL, Palsson BØ (2004). Genome-scale models of microbial cells: evaluating the consequences of constraints. Nature Reviews Microbiology 2: 886-897.
- Purushotham, A. D., & Sullivan, R. (2009). Darwin, medicine and cancer. Annals of Oncology, mdp537.
- Qu, Z., Weiss, J. N., & MacLellan, W. R. (2003). Regulation of the mammalian cell cycle: a model of the G1-to-S transition. American Journal of Physiology-Cell Physiology, 284(2), C349-C364.
- Radulescu, O., Gorban, A. N., Vakulenko, S., & Zinovyev, A. (2006). Hierarchies and modules in complex biological systems. Proceedings of ECCS'06.
- Radulescu, O., Gorban, A. N., Zinovyev, A., & Lilienbaum, A. (2008). Robust simplifications of multiscale biochemical networks. BMC Systems Biology, 2(1), 86.
- Radulescu, O., Gorban, A. N., Zinovyev, A., & Noel, V. (2012). Reduction of dynamical biochemical reaction networks in computational biology. arXiv preprint arXiv:1205.2851.
- Radulescu, O., Vakulenko, S., & Grigoriev, D. (2015). Model reduction of biochemical reactions networks by tropical analysis methods. Mathematical Modelling of Natural Phenomena, 10(3), 124-138.
- Rao, C. V., & Arkin, A. P. (2001). Control Motifs for Intracellular Regulatory Networks*. Annual Review of Biomedical Engineering, 3(1), 391-419.
- Rao, S., van der Schaft, A., & Jayawardhana, B. (2013). A graph-theoretical approach for the analysis and model reduction of complex-balanced chemical reaction networks. Journal of Mathematical Chemistry, 51(9), 2401-2422.
- Rao, S., Van der Schaft, A., Van Eunen, K., Bakker, B. M., & Jayawardhana, B. (2014). A model reduction method for biochemical reaction networks. BMC Systems Biology, 8(1), 52-69.

- Richards, F. (1959). A flexible growth function for empirical use. *Journal of Experimental Botany*, 10(2), 290-301.
- Rind, D. (1999). Complexity and climate. *Science*, 284(5411), 105-107.
- Rodin, V., Querrec, G., Ballet, P., Bataille, F., Desmeulles, G., Abgrall, J. F., (2009). Multi-Agents System to model cell signalling by using Fuzzy Cognitive Maps. Application to computer simulation of Multiple Myeloma, Proc. Ninth IEEE International Conference on Bioinformatics and Bioengineering, pp. 236-241.
- Roesky, P. W., Doumbouya, S. I., & Schneider, F. W. (1993). Chaos induced by delayed feedback. *The Journal of Physical Chemistry*, 97(2), 398-402.
- Rojas, J. M. (2002). Why polyhedra matter in non-linear equation solving. arXiv preprint math/0212309.
- Rossetti, M. D. (2015). Simulation modelling and Arena. Book. John Wiley & Sons.
- Roussel, M. R., & Fraser, S. J. (1991). On the geometry of transient relaxation. *The Journal of Chemical Physics*, 94(11), 7106-7113.
- Rubinstein, A., Hazan, O., Chor, B., Pinter, R. Y., & Kassir, Y. (2013). The effective application of a discrete transition model to explore cell-cycle regulation in yeast. *BMC Research Notes*, 6(1), 311.
- Sagan, L. (1967). On the origin of mitosing cells. *Journal of Theoretical Biology*, 14(3), 225-226.
- Sahin, Ö., Fröhlich, H., Löbke, C., Korf, U., Burmester, S., Majety, M., . . . Thieffry, D. (2009). Modeling ERBB receptorregulated G1/S transition to find novel targets for de novo trastuzumab resistance. *BMC Systems Biology*, 3(1), 1.
- Saltsman, K. (2005). Cellular Reproduction: Multiplication by Division. Inside the Cell. National Institute of General Medical Sciences. NIH Publication.
- Samarasinghe, S., 2006. Neural Networks for Applied Sciences and Engineering: from Fundamentals to Complex Pattern Recognition. Auerbach, Boca Raton, FL.
- Samarasinghe, S. & Ling, H. (2017). A system of recurrent neural networks for modularising, parameterising and dynamic analysis of cell signalling networks. *BioSystems* 153 6–25.
- Satyanarayana, A., Kaldis, P., (2009). Mammalian cell-cycle regulation: several Cdks, numerous cyclins and diverse compensatory mechanisms. *Oncogene* 28 (33), 2925–2939.
- Sauer, U., Heinemann, M., & Zamboni, N. (2007). Getting closer to the whole picture. *Science (Washington)* 316: 550-551.
- Schank, J. C. (2001). Beyond reductionism: Refocusing on the individual with individual-based modeling. *Complexity*, 6(3), 33-40.
- Schneider, K. R., & Wilhelm, T. (2000). Model reduction by extended quasi-steady-state approximation. *Journal of Mathematical Biology*, 40(5), 443-450.
- Schnell, S., & Maini, P. K. (2002). Enzyme kinetics far from the standard quasi-steady-state and equilibrium approximations. *Mathematical and Computer Modelling*, 35(1-2), 137-144.
- Schon, T., Gustafsson, F., & Nordlund, P. J. (2005). Marginalized particle filters for mixed linear/nonlinear state-space models. *IEEE Transactions on Signal Processing*, 53(7), 2279-2289.
- Segel, L. A., & Slemrod, M. (1989). The quasi-steady-state assumption: a case study in perturbation. *SIAM Review*, 31(3), 446-477.

- Semenoff, N. (1939). On the kinetics of complex reactions. *The Journal of Chemical Physics*, 7(8), 683-699.
- Sengupta, A. (2010). Gravitational collapse, negative world and complex holism. *Nonlinear Analysis: Real World Applications*, 11(5), 4378-4403.
- Sengupta, A. (2011). *Adventures Beyond Reductionism: The Wondrous Manifesto of Holism*. arXiv preprint arXiv:1109.3889.
- Shaker, H. & Wisniewski, R. (2011). Generalized gramian framework for model/controller order reduction of switched systems. *International Journal of Systems Science*, 42(8):1277–1291.
- Shapiro, J. A. (2009). Revisiting the central dogma in the 21st century. *Annals of the New York Academy of Sciences*, 1178(1), 6-28.
- Sherr, C.J., Roberts, J.M., (2004). Living with or without cyclins and cyclin-dependent kinases. *Genes Dev.* 18, 2699–2711.
- Singhania, R., Sramkoski, R. M., Jacobberger, J. W., & Tyson, J. J. (2011). A hybrid model of mammalian cell cycle regulation. *PLoS Computational Biology*, 7(2), pp. 1061-1077.
- Sobieszczanski-Sobieski, J. (1990). Sensitivity of complex, internally coupled systems. *AIAA journal*, 28(1), 153-160.
- Sonday, B., Singer, A., & Kevrekidis, I. G. (2013). Noisy dynamic simulations in the presence of symmetry: data alignment and model reduction. *Computers & Mathematics with Applications*, 65(10), 1535-1557.
- Sørensen, C.S., Syljuåsen, R.G., Falck, J., Schroeder, T., Rønnstrand, L., Zhou, B.-B., Bartek, J., and Lukas, J. (2003). Chk1 regulates the S-phase checkpoint by coupling the physiological turnover and ionizing radiation-induced accelerated proteolysis of Cdc25A. *Cancer Cell* 3, 247–258.
- Sorensen, D.C. (1992). Implicit application of polynomial fillters in a k-step arnoldi method. *SIAM Journal on Matrix Analysis and Applications*, 13(1):357–385.
- Stein, G.H., Drullinger, L.F., Soulard, A., Dulic, V., (1999). Differential roles for cyclin-dependent kinase inhibitors p21 and p16 in the mechanisms of senescence and differentiation in human fibroblasts. *Mol. Cell. Biol.* 19, 2109–2117.
- Stelling, J. (2004). Mathematical models in microbial systems biology. *Current Opinion in Microbiology*, 7(5), 513-518.
- Stewart, J. P. (1964). *Concurring opinion in Jacobellis v. Ohio*, 378.
- Stoll, G., Surdez, D., Tirode, F., Laud, K., Barillot, E., Zinovyev, A., & Delattre, O. (2013). Systems biology of Ewing sarcoma: a network model of EWS-FLI1 effect on proliferation and apoptosis. *Nucleic Acids Research*, 41(19), 8853-8871.
- Stoll, G., Viara, E., Barillot, E., & Calzone, L. (2012). Continuous time Boolean modelling for biological signaling: application of Gillespie algorithm. *BMC Syst. Biol.* 6: 116. doi: 10.1186/1752-0509-6-116.
- Sturmfels, B. (2002). *Solving Systems of Polynomial Equations* (American Mathematical Society, Providence, RI).
- Sugii, M., Wingender, E., & Matsuno, H., (2013). Petri Net Modelling of Oscillatory Processes in the Activation of Cell Cycle Proteins. *Proceedings of International Technical Conference on Circuits/Systems, Computers and Communications (ITC-CSCC 2013)*, Yeosu, Korea.
- Sun, X., & Medvedovic, M. (2016). Model reduction and parameter estimation of non-linear dynamical biochemical reaction networks. *IET Systems Biology*, 10(1), 10-16.

- Taleb, N. N. (2007). *The black swan: The impact of the highly improbable*. Random house.
- Tanaka, H., Fauré, A., & Matsuno, H. (2017). Boolean modelling of mammalian cell cycle and cancer pathways. *The 2017 International Conference on Artificial Life and Robotics (ICAROB 2017)*, Seagaia Convention Center, Miyazaki, Japan, (pp. 507-510).
- Tashima, Y., Hamada, H., Okamoto, M., & Hanai, T. (2008). Prediction of key factors controlling G1/S phase in the mammalian cell cycle using system analysis. *Journal of Bioscience and Bioengineering*, 106(4), 368-374.
- Tashima, Y., Hanai, T., Hamada, H., & Okamoto, M. (2003). Kinetics behaviour of G1-to-S cell cycle phase transition model. *Genome Informatics Series*, pp. 607-608.
- Tashima, Y., Hanai, T., Hamada, H., & Okamoto, M. (2004). Simulation for detailed mathematical model of G1-to-S cell cycle phase transition. *Genome Informatics*, 9. 607-608.
- Tashima, Y., Hanai, T., Hamada, H., Eguchi, Y., & Okamoto, M. (2007). Mathematical modelling of G2/M phase in the cell cycle with involving the p53/Mdm2 oscillation system. In *World Congress on Medical Physics and Biomedical Engineering 2006* (pp. 197-200). Springer Berlin Heidelberg.
- Terfve, C., Cokelaer, T., Henriques, D., MacNamara, A., Goncalves, E., Morris, M. K., ... & Saez-Rodriguez, J. (2012). CellNOptR: a flexible toolkit to train protein signaling networks to data using multiple logic formalisms. *BMC Systems Biology*, 6(1), 133.
- Tikhonov, A. N. (1952). Systems of differential equations containing small parameters in the derivatives. *Matematicheskii sbornik*, 73(3), 575-586.
- Tjio, J.-H., & Puck, T. T. (1958). Genetics of somatic mammalian cells: II. Chromosomal constitution of cells in tissue culture. *The Journal of Experimental Medicine*, 108(2), 259.
- Todd, R. G., & Helikar, T. (2012). Ergodic sets as cell phenotype of budding yeast cell cycle. *PloS One*, 7(10), e45780.
- Tokino T., & Nakamura Y. (2000) The role of p53-target genes in human cancer. *Crit Rev Oncol Hematol* 33(1):1–6
- Tompa, P., & Fuxreiter, M. (2008). Fuzzy complexes: polymorphism and structural disorder in protein–protein interactions. *Trends in Biochemical Sciences*, 33(1), 2-8.
- Tyler, A. L., Asselbergs, F. W., Williams, S. M., & Moore, J. H. (2009). Shadows of complexity: what biological networks reveal about epistasis and pleiotropy. *Bioessays*, 31(2), 220-227.
- Vasil, I. K. (2008). A history of plant biotechnology: from the cell theory of Schleiden and Schwann to biotech crops. *Plant Cell Reports*, 27(9), 1423-1440.
- Vasiliev, V. M., Volpert, A. I., & Hudiaev, S. I. (1973). On the method of quasi-stationary concentrations for chemical kinetics equations. *J. Computation. math. Mathematical Phys*, (3), 687-697.
- Vogelstein, B., Lane, D. & Levine, AJ. (2000). Surfing the p53 network. *Nature* 408(6810):307–310.
- Volpert, A. I., & Khudyaev, S. I. (1985). *Analysis in classes of discontinuous functions and equations of mathematical physics*, Nijoff. Dordrecht, The Netherlands.
- Vousden KH, Lu X (2002) Live or let die: the cell's response to p53. *Nat Rev Cancer* 2(8):594–604.
- Wagner, A. (2005). *Robustness and evolvability in living systems*. Princeton Studies in Complexity. Princeton University Press. Princeton NJ, USA.
- Waltemath, D., Henkel, R., Hoehndorf, R., Kacprowski, T., Knuepfer, C., & Liebermeister, W. (2016). Notions of similarity for computational biology models. *bioRxiv*, 044818.

- Wang, G., Sreeram, V. and Liu, W. Q. (1999). A new frequency weighted balanced truncation method and an error bound. *IEEE Transactions on Automatic Control*, 44:1734–1737.
- Wei, J., & Kuo, J. C. (1969). Lumping analysis in monomolecular reaction systems. Analysis of the exactly lumpable system. *Industrial & Engineering Chemistry Fundamentals*, 8(1), 114-123.
- Weng, G., Bhalla, U. S., & Iyengar, R. (1999). Complexity in biological signaling systems. *Science*, 284(5411), 92-96.
- West, S., Bridge, L. J., White, M. R., Paszek, P., & Biktashev, V. N. (2015). A method of ‘speed coefficients’ for biochemical model reduction applied to the NF- κ B system. *Journal of Mathematical Biology*, 70(3), 591-620.
- Weston, A. D., & Hood, L. (2004). Systems biology, proteomics, and the future of health care: toward predictive, preventative, and personalized medicine. *Journal of Proteome Research*, 3(2), 179-196.
- White, J. G., Southgate, E., Thomson, J. N., & Brenner, S. (1986). The structure of the nervous system of the nematode *Caenorhabditis elegans*. *Philos Trans R Soc Lond B Biol Sci*, 314(1165), 1-340.
- Wille, J. J., Pittelkow, M. R., Shipley, G. D., & Scott, R. E. (1984). Integrated control of growth and differentiation of normal human prokeratinocytes cultured in serum-free medium: Clonal analyses, growth kinetics, and cell cycle studies. *Journal of Cellular Physiology*, 121(1), 31-44.
- Wimsatt, W. C. (1980). Reductionistic research strategies and their biases in the units of selection controversy. In *Scientific discovery: Case studies* (pp. 213-259). Springer Netherlands.
- You, L. (2004). Toward computational systems biology. *Cell Biochemistry and Biophysics*, 40(2), 167-184.
- Yu, J., Zhang, L., Hwang, P. M., Rago, C., Kinzler, K. W., & Vogelstein, B. (1999). Identification and classification of p53-regulated genes. *Proceedings of the National Academy of Sciences*, 96(25), 14517-14522.
- Yuan, J. S., Galbraith, D. W., Dai, S. Y., Griffin, P., & Stewart, C. N. (2008). Plant systems biology comes of age. *Trends in Plant Science*, 13(4), 165-171.
- Zhao, Y., Lou, I. C., & Conolly, R. B. (2012). Computational modeling of signaling pathways mediating cell cycle checkpoint control and apoptotic responses to ionizing radiation-induced DNA damage. *Dose-response*, 10(2), 251-273.
- Zhou, K. (1995). Frequency-Weighted L_{∞} norm and optimal Hankel norm model reduction. *IEEE Transactions on Automatic Control*, 40:1687–1699.
- Zinovyev, A. (2014). Dealing with complexity of biological systems: from data to models. arXiv preprint arXiv:1404.1626.